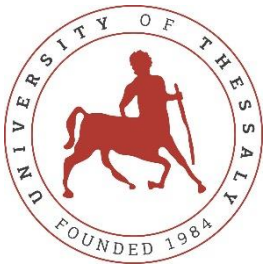

UNIVERSITY OF THESSALY

SCHOOL OF ENGINEERING

DEPARTMENT OF ELECTRICAL AND COMPUTER ENGINEERING

TRANSIENT STABILITY ANALYSIS OF A POWER SYSTEM WITH THE INTEGRATION OF WIND ENERGY

MSc Thesis

Tsantzalis Sofoklis

Supervisor: Bargiotas Dimitrios

Volos 2021

UNIVERSITY OF THESSALY

SCHOOL OF ENGINEERING

DEPARTMENT OF ELECTRICAL AND COMPUTER ENGINEERING

TRANSIENT STABILITY ANALYSIS OF A POWER SYSTEM WITH THE INTEGRATION OF WIND ENERGY

MSc Thesis

Tsantzalis Sofoklis

Supervisor: Bargiotas Dimitrios

Volos 2021

ΠΑΝΕΠΙΣΤΗΜΙΟ ΘΕΣΣΑΛΙΑΣ

ΠΟΛΥΤΕΧΝΙΚΗ ΣΧΟΛΗ

ΤΜΗΜΑ ΗΛΕΚΤΡΟΛΟΓΩΝ ΜΗΧΑΝΙΚΩΝ ΚΑΙ ΜΗΧΑΝΙΚΩΝ ΥΠΟΛΟΓΙΣΤΩΝ

ΑΝΑΛΥΣΗ ΣΥΣΤΗΜΑΤΟΣ ΗΛΕΚΤΡΙΚΗΣ ΕΝΕΡΓΕΙΑΣ ΜΕ ΤΗΝ ΠΑΡΟΥΣΙΑ ΑΝΕΜΟΓΕΝΝΗΤΡΙΑΣ

Μεταπτυχιακή Διπλωματική Εργασία

Τσαντζάλης Σοφοκλής

Επιβλέπων: Μπαργιώτας Δημήτριος

Βόλος 2021

Approved by the Examination Committee:

Supervisor	**Dimitrios Bargiotas** Associate Professor, Department of Electrical and Computer Engineering, University of Thessaly
Member	**Lefteris Tsoukalas** Professor, Department of Electrical and Computer Engineering, University of Thessaly
Member	**Aspasia Daskalopoulou** Assistant Professor, Department of Electrical and Computer Engineering, University of Thessaly

Date of approval: February 2021

Εγκρίνεται από την Τριμελή Εξεταστική Επιτροπή:

Επιβλέπων	**Μπαργιώτας Δημήτριος** Αναπληρωτής Καθηγητής, Τμήμα Ηλεκτρολόγων Μηχανικών και Μηχανικών Υπολογιστών, Πανεπιστήμιο Θεσσαλίας
Μέλος	**Τσουκαλάς Ελευθέριος** Καθηγητής, Τμήμα Ηλεκτρολόγων Μηχανικών και Μηχανικών Υπολογιστών, Πανεπιστήμιο Θεσσαλίας
Μέλος	**Δασκαλοπούλου Ασπασία** Επίκουρη Καθηγήτρια, Τμήμα Ηλεκτρολόγων Μηχανικών και Μηχανικών Υπολογιστών, Πανεπιστήμιο Θεσσαλίας

Ημερομηνία έγκρισης: Φεβρουάριος 2021

Acknowledgments

I would like to express my gratitude to the Examination Committee for guiding and contributing to the completion of this thesis.

First, my Supervisor, Dr. Dimitrios Bargiotas, with his immense knowledge in energy and power system stability, guided me to use appropriately the data and motivated me to preach the optimal result. Besides, he pushed me to handle the challenges that arose.

Second, I would like to thank Dr. Eleftherios Tsoukalas and Dr. Aspasia Daskalopoulou for the critical work in pointing out important things about our preliminary write-ups, which helped in the concise presentation of our work.

Finally, I would like to express my gratitude to all my professors in the Department of Electrical and Computer Engineering at the University of Thessaly, who gave me the necessary knowledge through the courses, and my family and friends for the unconditional support.

DISCLAIMER ON ACADEMIC ETHICS AND INTELLECTUAL PROPERTY RIGHTS

Being fully aware of the implications of copyright laws, I expressly state that this diploma thesis, as well as the electronic files and source codes developed or modified in the course of this thesis, are solely the product of my personal work and do not infringe any rights of intellectual property, personality and personal data of third parties, do not contain work / contributions of third parties for which the permission of the authors / beneficiaries is required and are not a product of partial or complete plagiarism, while the sources used are limited to the bibliographic references only and meet the rules of scientific citing. The 11 points where I have used ideas, text, files and / or sources of other authors are clearly mentioned in the text with the appropriate citation and the relevant complete reference is included in the bibliographic references section. I fully, individually and personally undertake all legal and administrative consequences that may arise in the event that it is proven, in the course of time, that this thesis or part of it does not belong to me because it is a product of plagiarism.

The declarant

Tsantzalis Sofoklis
Date: February 2021

ΥΠΕΥΘΥΝΗ ΔΗΛΩΣΗ ΠΕΡΙ ΑΚΑΔΗΜΑΪΚΗΣ ΔΕΟΝΤΟΛΟΓΙΑΣ ΚΑΙ ΠΝΕΥΜΑΤΙΚΩΝ ΔΙΚΑΙΩΜΑΤΩΝ

Με πλήρη επίγνωση των συνεπειών του νόμου περί πνευματικών δικαιωμάτων, δηλώνω ρητά ότι η παρούσα διπλωματική εργασία, καθώς και τα ηλεκτρονικά αρχεία και πηγαίοι κώδικες που αναπτύχθηκαν ή τροποποιήθηκαν στα πλαίσια αυτής της εργασίας, αποτελεί αποκλειστικά προϊόν προσωπικής μου εργασίας, δεν προσβάλλει κάθε μορφής δικαιώματα διανοητικής ιδιοκτησίας, προσωπικότητας και προσωπικών δεδομένων τρίτων, δεν περιέχει έργα/εισφορές τρίτων για τα οποία απαιτείται άδεια των δημιουργών/δικαιούχων και δεν είναι προϊόν μερικής ή ολικής αντιγραφής, οι πηγές δε που χρησιμοποιήθηκαν περιορίζονται στις βιβλιογραφικές αναφορές και μόνον και πληρούν τους κανόνες της επιστημονικής παράθεσης. Τα σημεία όπου έχω χρησιμοποιήσει ιδέες, κείμενο, αρχεία ή/και πηγές άλλων συγγραφέων, αναφέρονται ευδιάκριτα στο κείμενο με την κατάλληλη παραπομπή και η σχετική αναφορά περιλαμβάνεται στο τμήμα των βιβλιογραφικών αναφορών με πλήρη περιγραφή. Αναλαμβάνω πλήρως, ατομικά και προσωπικά, όλες τις νομικές και διοικητικές συνέπειες που δύναται να προκύψουν στην περίπτωση κατά την οποία αποδειχθεί, διαχρονικά, ότι η εργασία αυτή ή τμήμα της δεν μου ανήκει διότι είναι προϊόν λογοκλοπής.

Ο Δηλών

Τσαντζάλης Σοφοκλής
Ημερομηνία: Φεβρουάριος 2021

ABSTRACT

The environmental problems derived by the overuse of fossil fuels render essential energy production from new alternative sources, such as the wind. Harnessing wind energy requires low investments, is widely available, and eco-friendly. But the task of this energy's integration in the old and new grids is no easy task due to intermittencies and instabilities when a significant part of the load is supplied. This thesis aims to smoothly integrate wind energy in the IEEE 9 Bus System and study the remodeled system for its transient stability.

Firstly, this thesis explicates the concept of transient stability because it is essential for this study. Furthermore, there is a presentation of the IEEE 9 Bus System's components and dynamics. Moreover, using two types of fault, a symmetrical three-phase and an SLG, a transient analysis is made to calculate the critical fault clearing time (CFCT), the maximum duration of the fault for the system to maintain its synchronism. For the analysis of five diagrams, the generators' power angle with respect to the power angle of the swing bus, the real and reactive power, and the bus's voltage and frequency are studied. Additionally, an introduction to wind turbine technology is presented, and using a variable-speed wind turbine with full conversion (type 4), the integration of wind energy on the IEEE 9 Bus System is made. There are four scenarios of different wind integration and for each scenario, the CFCT is calculated, and the transient behavior is studied. Finally, there is a comparison of the four scenarios and future research suggestions. All the simulations are implemented and executed in the PSS/E software.

ΠΕΡΙΛΗΨΗ

Τα περιβαλλοντικά προβλήματα που προκύπτουν από την υπερκατανάλωση των ορυκτών καυσίμων καθιστούν αναγκαία τη στροφή σε νέες πηγές ενέργειας, όπως του ανέμου. Η εκμετάλλευση της αιολικής ενέργειας απαιτεί χαμηλά κόστη, είναι διαθέσιμη σε πολλές περιοχές και, φιλική στο περιβάλλον. Ωστόσο η ενσωμάτωση της στα υπάρχοντα και στα νέα συστήματα είναι δύσκολη, λόγω προβλημάτων αστάθειας στην προσπάθεια να καλύψει σε ένα δίκτυο σημαντικό μέρος του φορτίου. Γι’ αυτό το λόγο στόχος αυτής της διπλωματικής εργασίας είναι η ενσωμάτωση της αιολικής ενέργειας με ομαλό τρόπο στο σύστημα 9 ζυγών της IEEE και η μελέτη της μεταβατικής ευστάθειας.

Αρχικά, γίνεται μία αποσαφήνιση της έννοιας της ευστάθειας και κυρίως της μεταβατικής. Επιπροσθέτως, ακολουθεί μία παρουσίαση των στοιχείων και των δυναμικών δεδομένων του συστήματος των 9 ζυγών. Στη συνέχεια, με τη χρήση δύο τύπων σφαλμάτων, του συμμετρικού τριφασικού και του στερεού μονοφασικού υπολογίζεται ο κρίσιμος χρόνος εκκαθάρισης του σφάλματος και γίνεται μία ανάλυση μεταβατικής ευστάθειας. Για το λόγο αυτό χρησιμοποιούνται πέντε διαγράμματα, της γωνίας ισχύος των γεννητριών σε σχέση με τη γωνία ισχύος του ζυγού αναφοράς, της συχνότητας και τάσης των ζυγών και της πραγματικής και άεργους ισχύος των γεννητριών. Επιπλέον, γίνεται μια αναφορά στην τεχνολογία των ανεμογεννητριών (Α/Γ) και επιτυγχάνεται η ενσωμάτωση της αιολικής ενέργειας στο σύστημα 9 ζυγών με 4 διαφορετικούς τρόπους με τη χρήση μιας Α/Γ μεταβλητής ταχύτητας τύπου 4. Για κάθε περίπτωση υπολογίζεται ο κρίσιμος χρόνος εκκαθάρισης και μελετάται η μεταβατική συμπεριφορά του. Τέλος, γίνεται σύγκριση των περιπτώσεων αυτών και παρουσιάζονται προτάσεις για μελλοντική έρευνα. Αξίζει να αναφερθεί πως όλες οι προσομοιώσεις γίνονται στο PSS/E.

TABLE OF CONTENTS

LIST OF FIGURES

CHAPTER 2

CHAPTER 3

LIST OF TABLES

ABBREVIATIONS

PCC	**Point of Common Coupling**
DFIG	**Double Fed Inductive Generator**
SLG	**Solid Line- Ground**
CIGRE	**Conseil International des Grands Reseaux Electrique**
SMIB	**Single Machine Infinite Bus**
PSS/E	**Power System Simulation for Engineering**
LG	**Line-Ground**
LL	**Line-Line**
DLG	**Double Line-Ground**
AC	**Alternative Current**
CFCT	**Critical Fault Clearing Time**
pu	**Per-unit**
FACT	**Flexible AC Technology**

CHAPTER 1

INTRODUCTION

1.1 Background

The technological growth of the last decades has brought a huge revolution in everyday modern life. Huge amounts of electricity are spent to cover the new energy needs that appear. That has led to many problems with the most important to be fossil fuel depletion that directly affect people's health. For that reason, the shift to renewable energy is necessary. Renewable energy sources (RES) such as wind, solar and hydro are regarded as the best solutions to reduce carbon emission under the increase in power demand and load coverage. Many countries have used alternative energy sources and are still trying to benefit from their usage, even more, replacing the conventional way of producing energy using fossil fuels. With the most important being Germany, Denmark, and Spain, European countries have relied a lot upon exploiting renewable energy sources. Moreover, the traditional energy systems are centralized, and there is a need for the decentralization of these to have distributed energy production for more stability and financial reasons. For that, reliance on RES is necessary. One of the most significant and, simultaneously, most used is wind energy despite that wind energy penetration in modern and traditional grids has a few challenges. First of all, the wind nature is a bit unpredictable, with the possibility of forecast errors. That can create many problems in energy production and load coverage. Moreover, it is important to mention that wind energy and, in general, all the RES create problems in the grid's stability. The deviations from the frequency, small-signal stability, and voltage stability are a few issues. If the system has a 0.2 Hz divergence in frequency, the consequences can be severe. Also, there can be many oscillations that will completely desynchronize the grid in its frequency, which we will analyze in the next chapters. Finally, the inability to store large amounts of energy, combined with the large expenses RES have, can be a suspense factor in energy production. [1] [2] [3] [4]

1.2 Thesis Object

In this thesis, we study the effects of wind integration in four different scenarios in an existing power system. We will make a transient stability analysis, which is how the system returns to stability after a disturbance, small or large, which occurs in order to estimate the wind power penetration level. Also, the results of these four scenarios will be analyzed and compared to each other to see if the integration can be made and, if possible, in the smoothest way.

1.3 Literature Review

Wind integration in power systems is a trending issue and has attracted a lot of research from the academic community. The IEEE 9 Bus System, which will be used in our case, is a system that is used for that reason. In [5], there is performance research using governor and exciter control with the PowerWorld software. Reference [6] adds a wind farm at a bus of the point of common connection (PCC) in the IEEE9 system and studies the impact of the reactive power using the Matlab software. The same system is used in [7] for a transient stability analysis providing useful information about the generators' modeling using the ETAP software. Focusing on [8], there is transient stability on the IEEE9 Bus system and will be used for the analysis of the results in this thesis. In reference [4], there is a transient stability analysis of the IEEE 9 Bus System with an addition of 51 MW Double-Fed Inductive Generator (DFIG). In reference [9], there is a transient stability study on the IEEE9 Bus System and in the remodeled system with the replacement of generation 3 with a wind farm, which will be made in this thesis. In [10], there is a stability analysis using the PSS/E representing a Scandinavian system with wind power and recreating two disturbances, a nuclear generator loss, and a blackout in Sweden that were real. References [11] and [12] are evaluating wind turbines and their performances in built-in systems, providing tuning information. The results were used for the modeling and the analysis in this thesis. The DFIG wind turbine is also used for the transient stability analysis of a 6-bus system under faulty conditions in [13]. This is interesting because there will be a solid line ground (SLG) fault in this thesis. Another example of transient stability analysis using the reactive power,

voltage, and active power responses when wind turbines are added in the Kosovo Power System is used in [14]. Stability studies with wind power integration have been applied in many power systems such as the Moroccan in [15], where there is steady-state and dynamic analysis, a large-scale integration in the Danish power system in [16], and the offshore integration on the system of Taiwan in [17]. Helpful for results analysis, but without wind power presence, is the transient analysis on the Sarawak's System in Malaysia [18]. Similar work with the use of both PV and wind power is used in [19]. In the [20] reference, there is a type 4 wind turbine small-signal performance that will help analyze the results in this thesis because in the cases that will be mentioned in chapter 5, the same turbine is used. It is essential because it proves that the type 4 turbine creates a few damps. Aside from the IEEE 9 Bus System, the IEEE 14 Bus System is often used for academic purposes. A transient stability analysis without wind energy integration is used in [21], and in [22], the wind turbine is added with three different configurations. Two comparative stability analyses are happening in [23] and [24] using DFIG (Double-Fed Inductive Generator) wind turbines in the IEEE 14 Bus System.

1.4 Thesis Layout

This thesis's structure starts with a small introduction of wind energy integration challenges, the thesis object, and the similar work that the academic community has researched. In the second chapter, there will be a theoretical analysis of power stability. The types it consists of, with most important the transient stability, will be the primary purpose of this thesis. In the third chapter, there is an introduction to the PSS/E software that will implement the IEEE 9 Bus System simulations. Also, we will make a transient stability analysis of this system without the integration of wind energy. In the fourth chapter, there is an introduction to the wind turbines and a presentation of the turbine model that we will use for this thesis' simulations. Furthermore, in the fifth chapter, simulations for the four scenarios and the relative transient stability analyses are shown. Finally, the final chapter will include the conclusion and the future research possible activities.

CHAPTER 2

POWER SYSTEM STABILITY

2.1 Definition and Classification of Power System Stability

The definition of the Power System Stability by an IEEE/CIGRE Joint Task Force on Stability Terms and Definitions is “The ability of an electric power system, for a given initial operating condition, to regain a state operating equilibrium after being subjected to a physical disturbance, with most system variables bounded so that practically the entire system remains intact.” A power system consists of transmission lines, generators, loads that must be covered, and many other components that create instabilities. They are all constantly changing conditions when disturbances, small or large, happen. These disturbances can be an increase in load or faults. All these instabilities change the initial conditions and, therefore, creating equilibrium problems in the generation process. These problems indicate the grid's necessity to be stable and maintain its initial conditions and synchronism. There are three main classifications of power stability, the rotor angle, the voltage, and the frequency stability, as seen in Figure 2.1. Stability refers, mostly, to the maintenance of the synchronism of the synchronous plants after a disturbance, whether it occurs or not. But instability can be a voltage drop that will have a severe effect on the part of the system, as there can be no normal production or even a change in the load that needs to be covered. [10][25][26]

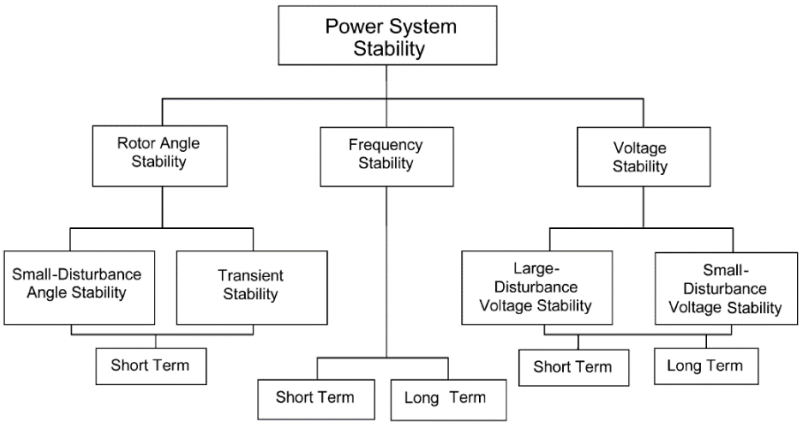

Figure 2. 1 Classification of Power System Stability

2.2 Voltage Stability

Voltage stability is the ability of a system to maintain all buses' voltage to acceptable levels after a disturbance occurs from an operation in the initial conditions. When there is voltage instability, the main trait is the voltage drop. Another result of voltage instability is the loss of load and the tripping of the lines. Moreover, a possible outcome can be the loss of synchronism. As shown in Figure 2.1, there are two types of voltage stability the large-disturbance or the small-disturbance. The small disturbances refer to small increment changes in load, stressed conditions in the generators, or high currents. The characteristics of these disturbances are that they are instant and last for a few seconds. The large-disturbance stability refers to the system's ability to maintain its voltage levels when large-scale disturbances occur, such as faults, generator loss, and circuit contingencies. The voltage collapse term can be used for these disturbances, as there is a complete blackout or abnormally low voltages. The duration of these varies from a few seconds to many minutes. [9][10][25]

2.3 Frequency Stability

The design of the power system has to maintain its initial operating conditions when a disturbance occurs. Aside from voltage, the system's other value that must preserve is the frequency. As stated in [25], frequency stability refers to a power system's ability to maintain steady frequency following a severe grid upset, resulting in a significant imbalance between generation and load. That depends on the restoration of the balance between generator and load with the minimum loss of load. An instability in frequency can have a severe effect like tripping loads or making generator units unable to produce. Many frequency instabilities occur in isolated islands system. Situations like this, where the generation cannot provide the necessary load, can be short-term and last a few seconds. On the other hand, when the duration is from a few seconds to many minutes, the instability is long-termed and severely affects the voltage magnitude. [9][25]

2.4 Rotor Angle Stability

The rotor angle stability is the synchronous generators' ability, connected in a power system, to maintain their synchronism after a disturbance occurs. This is possible due to the restoration of the balance in each synchronous machine's electromagnetic torque and mechanical torque. The instability can occur from the increased angular swing of one generator and loss of synchronism with the others. The rotor angle stability problem involves studying the electromechanical oscillations that occur in the rotor angle of a generator relative to another, mainly the swing bus. When there is a disturbance, the rotor angle can accelerate or decelerate, creating abnormalities in the generation and load coverage. [9][25]

Small signal stability refers to the ability of the system the ability of the power system to maintain its synchronism under small disturbances. The acceleration of the rotor angle from the small disturbances is short, and sometimes it permits the usage of the equations that describe a linear system. Small signal stability can be considered local and global. Local is when small oscillations exist in a generator in a part of the power system. Global refers to the fluctuations in many generators of the power system in relation to other generators. The global oscillations affect many areas, and because they can create problems, power system stabilizers and voltage regulators are a possible solution. [9][24]

2.5 Transient Stability

Transient Stability is the power system's ability to maintain synchronism within the machines after high transient disturbance such as short circuits on transmissions line. [9] There can be fatal results for the grid if large deviations are happening in the rotor angle. The transient stability studies usually last for 5 sec after the disturbance occurs, even though academic research can extend to 30 sec. Many researchers usually check the first or the second swing of the rotor angle diagram. If after the second swing the angle is decreasing, the system is considered to be stable. In Figure 2.2, an example features three

different rotor angle plots. Case 1 is a stable system, while cases 2 and 3 are plots of an unstable system from the first and second swings, respectivelly.[27]

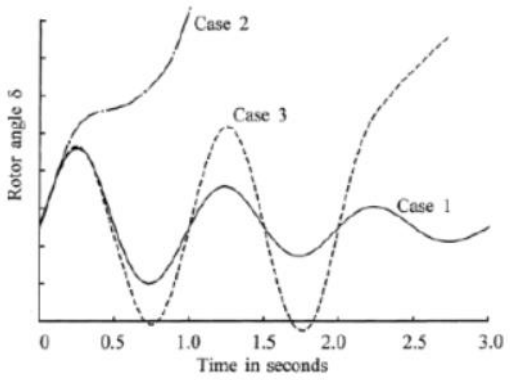

Figure 2. 2 Stable and Unstable Curves [26]

2.5.1 Concept of Transient Stability

To understand how the transient stability works and explain what was said above about torque and rotor angle, we will use the equal criterion area theorem and the swing equation, and the power angle curve. The analysis is obtained with the help of the reference [27]. The swing equation is:

$$\frac{2H}{w_0} \cdot \frac{d^2\delta}{dt^2} = \mathrm{Tm} - Tmax \sin\delta \quad (2.1)$$

where,

H is the inertia constant in MW * sec / MVA

w_0 is the rotor angle speed in rad/sec

t is time in sec

δ is the rotor angle in rad

Tm is the mechanical torque input in pu

Tmax is the mechanical torque output in pu

For the power and angle curve, it is necessary to use the single machine infinite bus (SMIB) with two circuits, as seen in Figure 2.3 and in its phase equivalent in Figure 2.4.

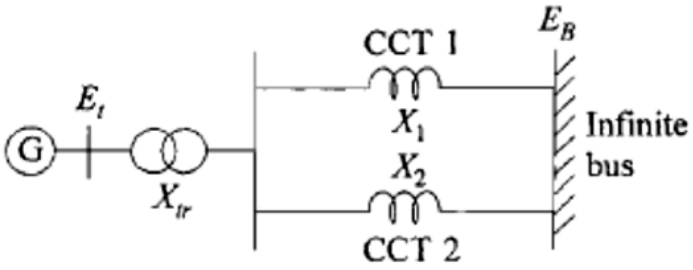

Figure 2. 3 SMIB with two circuits [27]

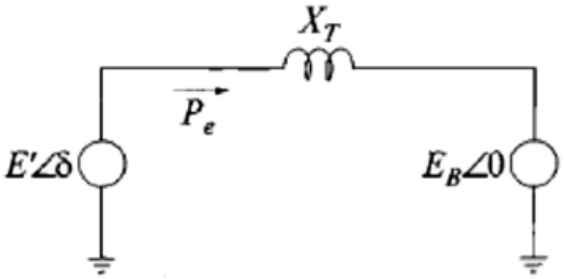

Figure 2. 4 Phase Equivalent [27]

The electrical power of the generator is given:

$$Pe = \frac{E'E_B}{X_T} \sin\delta = Pmax \sin\delta \quad (2.2)$$

The Pe is the electrical power output in pu, E' and E_B are voltages in pu, and δ is the rotor's angle in rad, and X_T is the reactance pu. This formula (2.2) shows the relationship between power and rotor angle. The max total power is given when δ is 90 degrees:

$$Pmax = \frac{E'E_B}{X_T} \quad (2.3)$$

This equation is the power angle relationship, and in Figure 2.5, it is presented in two cases. The first is when both circuits are online, and the second is when circuit 2 is off. From this figure, when there is only one circuit, the power plot decreases due to increased Thevenin impedance. The Pm is the mechanical power output of the system. The point of equilibrium for plot 1 is a, and for plot 2 is b. During a disturbance, the rotor angle's oscillation must be overlaid to rotor speed w_0, but the actual speed is less. Therefore, the generator speed

becomes w_0 and the torque is equal to the mechanical power. The new rotor angle swing equation becomes:

$$\frac{2H}{w_0} \cdot \frac{d^2\delta}{dt^2} = \mathrm{Pm} - Pmax \sin\delta \quad (2.4)$$

where,

H is the inertia constant in MW * sec / MVA

w_0 is the rotor angle speed in rad/sec

t is time in sec

δ is the rotor angle in rad

Pm is the mechanical input in pu

Pmax is the mechanical electrical output in pu

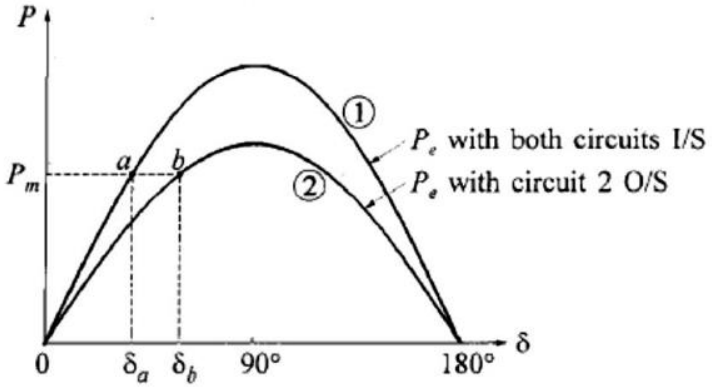

Figure 2. 5 Power Angle Plot of the SMIB [27]

In Figure 2.6, the power angle plot and the rotor angle time plots are shown. The system's transient behavior can be examined when a sudden increase in the mechanical input and the initial P_{m0} is increased to P_{m1}. The new equilibrium point becomes b from a as $P_e = P_{m1}$. Due to the inertia, the rotor cannot change instantly from δ_0 to δ_1. The mechanical power then surpasses the electrical, meaning that the accelerating torque causes the rotor to accelerate and reaches point b. Then the acceleration no longer exists, and the rotor speed is greater than the w_0, hence the rotor continues to increase. For δ values that are greater than δ_1, P_e is greater than P_{m1} and the rotor decelerates to meet the initial condition. After that, there are δ values that make P_e lower than P_{m1}, so the rotor accelerates again. For the

system to be stable and not lose synchronization, according to the equal square criterion the A1 and A2 areas must be equal. If not, there is desynchronization as can be seen in Figure 2.2. [27]

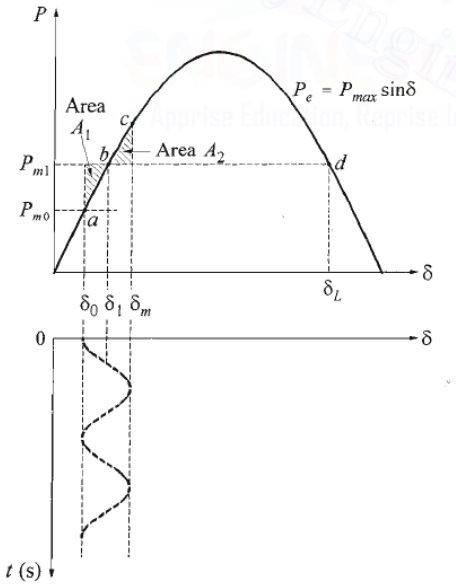

Figure 2. 6 Power-angle relationship and Rotor angle-time diagram [27]

2.5.2 Factors affecting the Transient Stability

In the previous section, it was presented the concept of transient stability with an example. Many factors affect the generation of transient stability. These are:

- The load that a generator is connected to and must cover it.
- When a fault happens, the output of the generator is changed. The impact of this depends on the type of the fault and the distance from the disturbance's location.
- The inertia of the generator.
- The internal voltage magnitude of the generator is a function of field excitation.
- Change in the impedances.
- Critical Fault Clearing Time (CFCT). CFCT is defined as the maximum time allowed to remove the disturbance without interrupting the system's performance. The

system will be stable if the disturbance can be cleared before the time allowed. If the clearance time is exceeded, the system loses its synchronization. [9] [28]

CHAPTER 3

THE IEEE 9 BUS SYSTEM

3.1 PSS/E Software

Power System Simulation for Engineering (PSS/E) is an integrated set of computer programs used by engineers to simulate power systems. It is provided by Siemens PTI and is well accepted by the engineering community. This software allows the calculation with phase vector and electromechanical simulations, and it is being used for steady-state (load flow) and dynamic condition simulation. PSS/E handles various power systems analysis calculations, such as power flow, balanced and unbalanced fault, network equivalent construction, and dynamic simulation.

Power or Load flow is a functional analysis that is important in this thesis. A power flow study makes the power system simpler using the per-unit system or the one-line diagram. That way, AC components, like reactive and active power or voltage, are easier to handle. This analysis enables the easier management of the system, its expansion, and its optimization.

Dynamic simulation is a function that this program offers that helps in stability studies. With the dynamic simulation, it is possible to find problems in the grid's operation, and it enables the snapshot function to check the system every moment for a few seconds. In this operation, it is possible to do things like apply a disturbance or disconnect buses and lines. For Dynamic simulation usage, it is necessary to input dynamic data for generators or wind turbines, like in this thesis. PSS/E provides models for both. It is worth mentioning that many wind turbine manufacturers offer models for wind turbines and their modeling values in the PSS/E.

Balanced and Unbalanced Faults Analysis is an operation of PSS/E that not only can be used together with dynamic simulation, like mentioned above but also in short circuits. This operation is beneficial for transient stability studies and the calculation of post-fault power system currents. The faults that are included are the three-phase symmetrical, the

line-ground, solid or not (SLG or LG respectively), the line-line fault (LL), and the double line ground (DLG).

To conclude, PSS/E provides great assistance for power system studying and designing and provides more functions that enable data input, output, operation with python programming, and data exchange with other programs like Microsoft Excel or PSCAD. [12][29][30]

3.2 The IEEE 9 Bus System

IEEE9 Bus System is a power system consisting of nine buses and three generators. It is the most common template of power systems used by researchers and power system designers for stability studies, new algorithm testing, and new technology creations. This system, along with IEEE 14 Bus system, is the most common template also for wind power integration testing, as we have seen in the first chapter. Figure 3.1 shows the system as designed in PSS/E with the inputs taken from [31]. The active generation, load data, and impedances are also visible. It is symmetrical, and it has three active generators that produce 319.6 MW, supplying a total load of 315 MW, 115MVAR, and transmission losses of 4.6 MW. The generation at bus 2 produces 52% (163 MW) of the system's total power while the generator at bus 3 85 MW. The generator is producing the rest in bus 1 (71.6 MW), the swing bus. As it is visible from Figure 3.1, there are three loads, one in bus 8 (100MW), one in bus 5 (125MW), and one in bus 6 (90MW). After the initial Power Flow on the IEEE9 Bus System, a number of quantities can be seen in Table 3.1, where the voltage in pu is shown, as well the active and reactive power of the generators and loads. The method used for the Power Flow is the Newton-Raphson because generally, it has some advantages over the Gauss-Seidel method. [4][9]

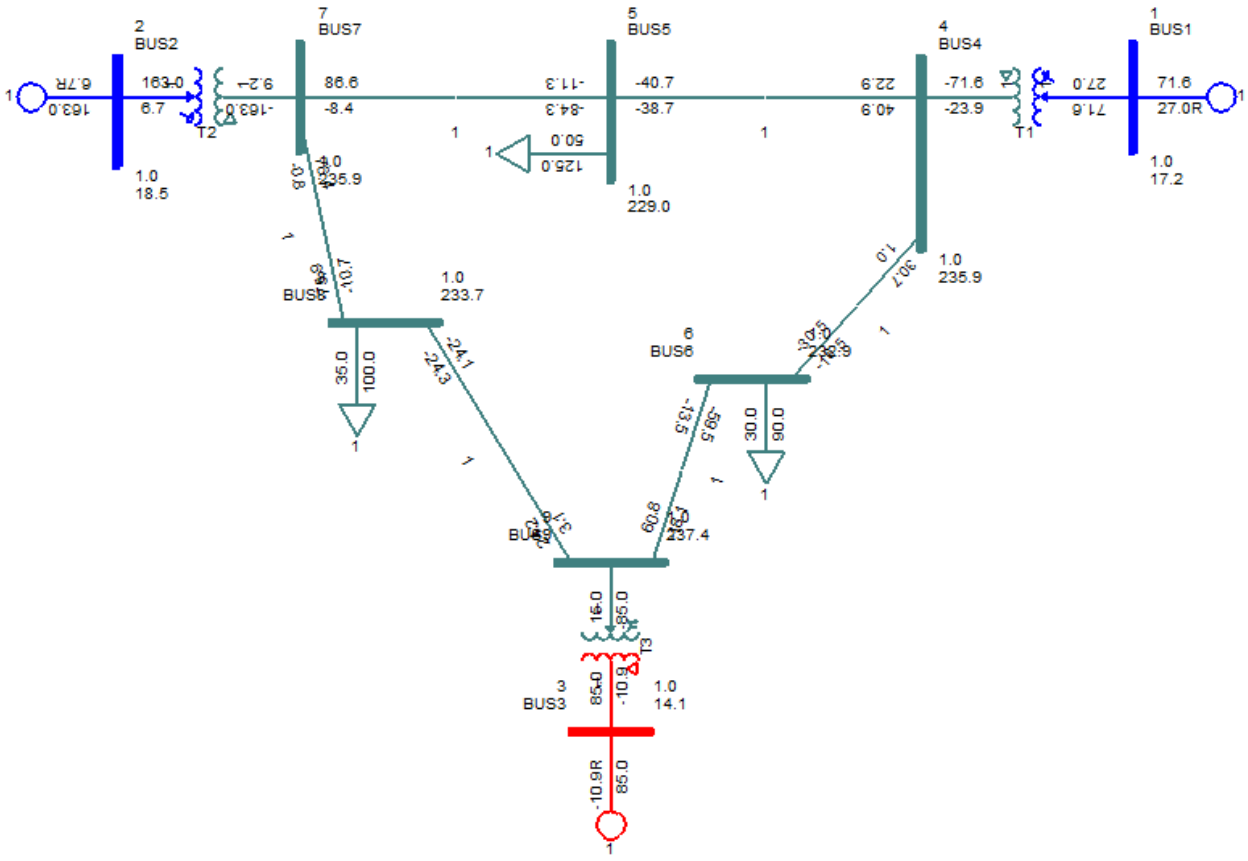

Figure 3. 1 IEEE9 bus system from PSS/E

Table 3. 1 IEEE9 bus system Power Flow

Bus No	Voltage (pu)	Angle (deg)	Pgen (MW)	Qgen (MVAR)	PL (MW)	QL (MVAR)
1	1.0400	0.00	71.6410	27.0459	0	0
2	1.0250	9.28	163.0000	6.6536	0	0
3	1.0250	4.66	85.0000	-10.8597	0	0
4	1.0258	-2.22	0	0	0	0
5	0.9956	-3.99	0	0	125	50
6	1.0127	-3.69	0	0	90	30
7	1.0258	3.72	0	0	0	0
8	1.0159	0.73	0	0	100	35
9	1.0324	1.97	0	0	0	0

3.3 Dynamic Modelling of the IEEE 9 Bus System

In this chapter, a dynamic simulation takes place in the IEEE9 Bus System without the wind turbines. So, it is first necessary to provide the parts of the synchronous generators, such as exciters and rotors. For the swing bus generator (bus 1), the rotor machine model is the synchronous GENSAL (Figure 3.2). The other two buses (2 and 3) have a different rotor machine model, the synchronous GENROU (Figure 3.3). The Generation 2 and 3 GENROU model have different values in some variables. Both GENROU and GENSAL machine models produce machine speed and rotor angle for transient stability observation. A vital part of the dynamic simulation is the exciter. The exciter contains a small generator that provides the stationary rotating magnetic field for the main generator. In this system, all three plants have the same type of exciter, the IEEET1 (Figure 3.4). Moreover, an important part of the dynamic simulation is the turbine governor, which regulates the rotational speed in response to changing load conditions. The model used is the IEESGO, and it can be seen in Figure 3.5. Finally, for the modeling, essential is the stabilizer, which is very useful for transient stability as it helps in the damp width reduction. The machine for the stabilizer used in the PSS/E is the PSS2A and is presented in Figure 3.6. [18][29][33]

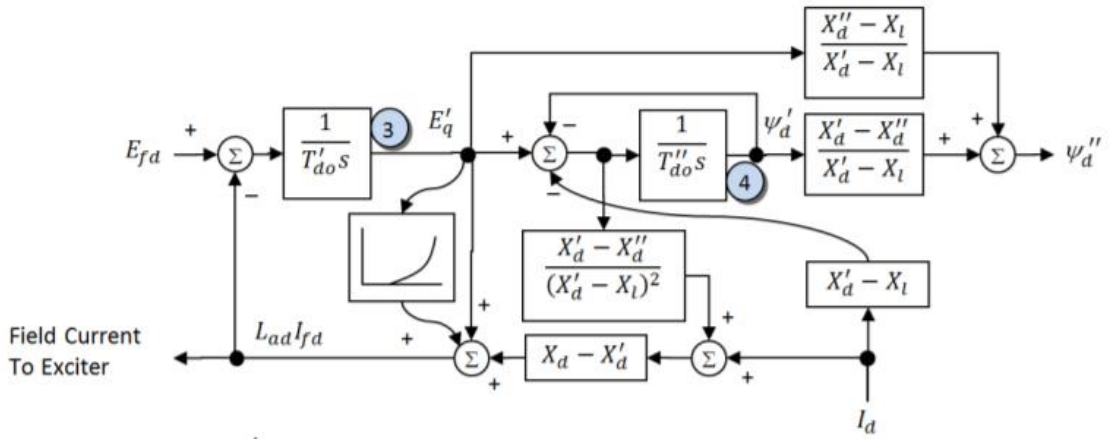

Figure 3. 2 GENSAL MODEL [32]

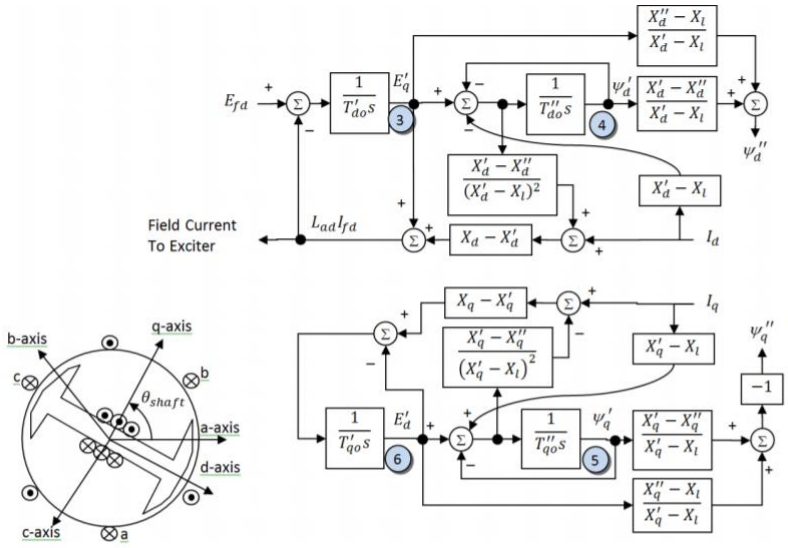

Figure 3. 3 GENROU MODEL [32]

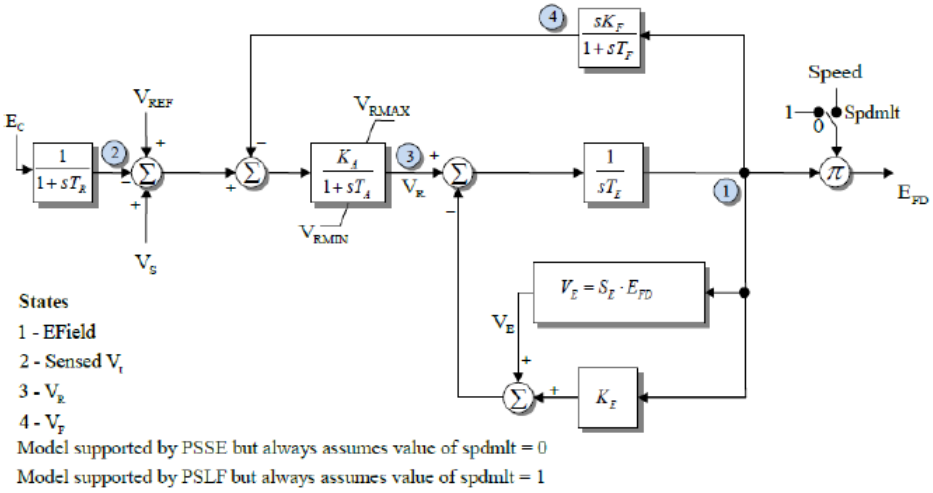

Figure 3. 4 IEEET1 MODEL [32]

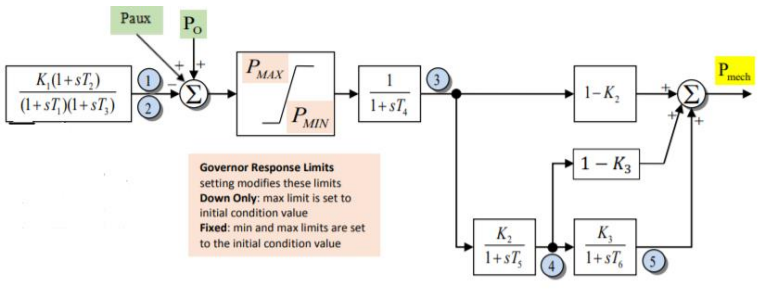

Figure 3. 5 IEESGO MODEL [32]

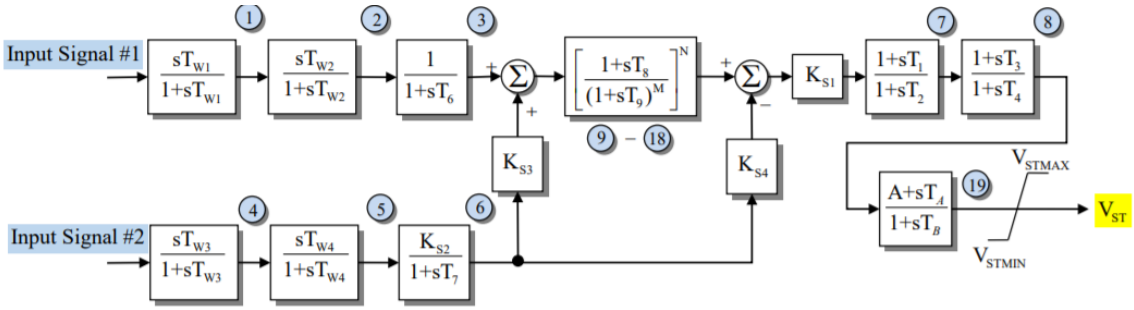

Figure 3. 6 PSS2A MODEL [32]

3.4 Dynamic Simulation of IEEE 9 Bus System

The simulation in the PSS/E must be done in a specific process, as shown in Figure 3.7. At first, PSS/E reads the network data the user inputs. These inputs are the plants, the loads, the transmission lines, and impedances. The next step is the power flow function that is mentioned in section 3.1. It is essential here to check if the network converges. If it does not, the initial inputs need to be changed. If it converges, then the next step is the convergence of the loads and the generator elements into dynamic data so that it is possible to do that type of analysis. After that, the PSS/E reads the dynamic data, which are the data in the previous section. In the next chapter, there will be renewable energy sources, so in these data, there will be the addition of wind turbine generators. The next step is setting the output channels so that the dynamic simulation results are visible. In this step, the channels are set to show relative power angle of generators with respect to swing bus power angle. After the setting, the data are initialized. If the initial conditions of the dynamic data are met and there is no error, then the simulation will proceed to the next step else the data must be changed. After that, there is a steady-state run for 1 sec and then the disturbance is applied for a specific ΔT (initial ΔT = 0.05 sec). Then the fault is cleared and the line next to the bus is tripped for 1 sec. The line that was tripped is connected after 1 second and the system runs until 12 sec. If the system is stable then the ΔT is increased by 0.05 and the dynamic data must be read again, else the diagrams from the channels are analyzed. [16]

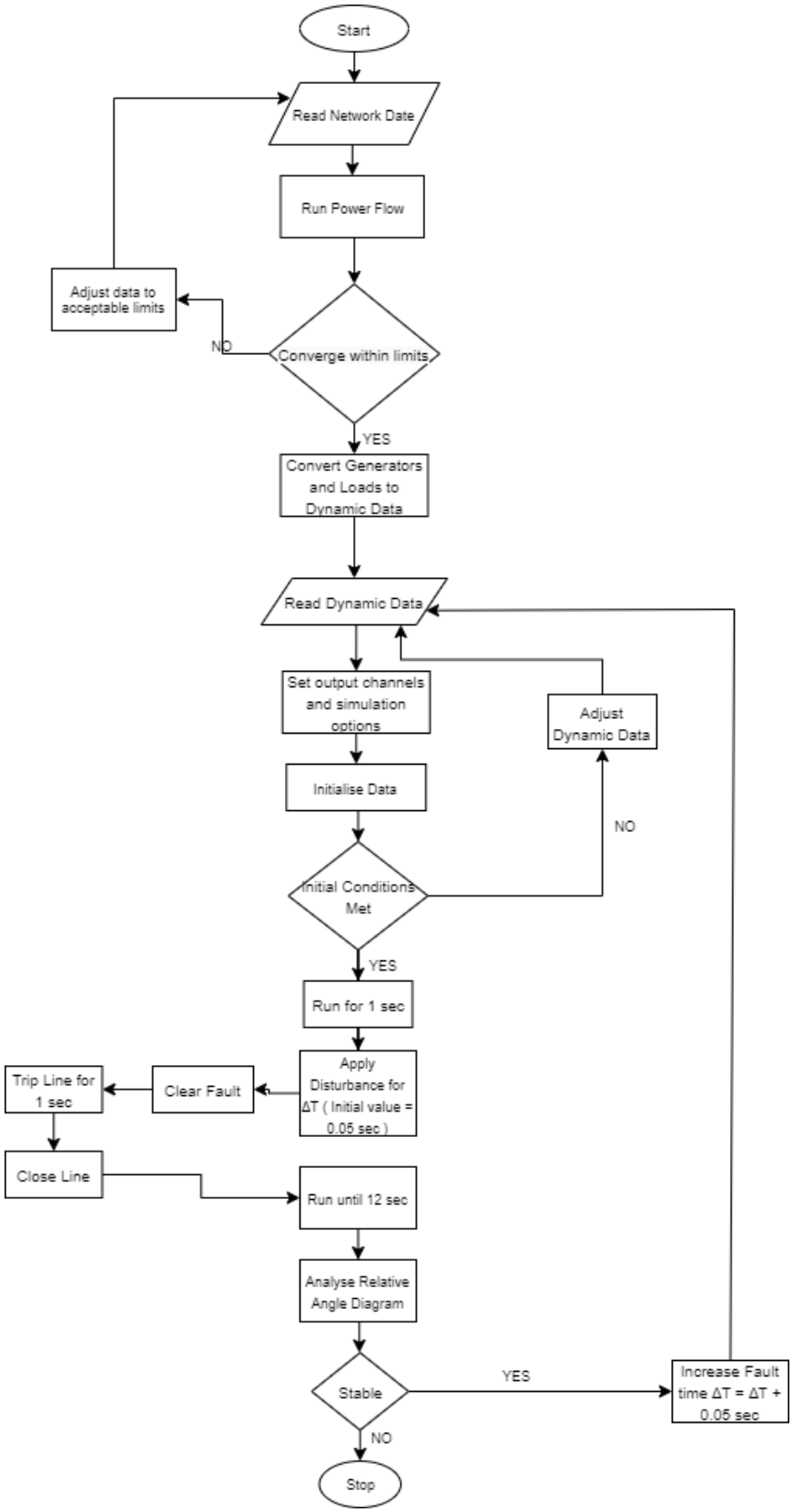

Figure 3. 7 Simulation Process

3.5 IEEE 9 Bus System Simulation Results

The IEEE9 Bus system in this section will be analyzed for the study of its transient stability. Two types of fault is going to be applied in 3 buses. The types of fault are the Three-phase symmetrical fault, and the SLG, and the buses that the faults will occur are the buses 2, 7, and 8. It is mentioned that there is a tripped line in the process so that the fault can be cleared without further problems. When the fault occurs in bus 2, the line that is tripped is line 2-7. When the fault happens in bus 7, the line 7-8 is tripped and, finally, when the disturbance is at bus 8 the line 8-7 is tripped. In this simulation 6 diagrams will be analyzed:

- The relative power angle of generator 2, generator 3, or both in relation to the power angle of bus 1 (swing bus) at the Critical Fault Clearing Time (CFCT) or simply critical time. In some cases, one generator is replaced so there is no point to include it.
- The active power of the 3 generators at the critical time.
- The reactive power of the 3 generators at the critical time.
- The frequency of all the buses at the critical time.
- The voltage of all the buses at the critical time.
- The relative power angle of the generators in relation to the power angle of the swing bus 1 for fault duration equals to CFTC increased by 0.05 sec and the appearance of desynchronization.

All simulations will be implemented in the PSS/E Software. In Figure 3.1 and Table 3.1 there are some load flow values of voltage (pu), active (MW), and reactive power (MVAR) but in this simulation, these results will be presented in pu. The base for real power (P) and reactive power (Q) is 100 MW and 100 MVAR so in Table 3.2 the values after the power flow are shown so that the diagrams are understandable, and the transient stability analysis is easier to be made.

Table 3. 2 Active and Reactive power generation in pu after Power Flow

GENERATOR	Active Power (pu)	Reactive Power (pu)
BUS 1 (Swing Bus)	0.715	0.27046
BUS 2	1.63	0.065
BUS 3	0.85	-0.12

3.5.1 Faults at Bus 2 of the IEEE 9 Bus System

The first simulation in this thesis takes place in the IEEE9 bus system for faults at bus 2. We check for desynchronization of the relative power angles of generations 2 and 3 in relation to the swing bus power angle. The system, in the beginning, is running at a steady-state for 1 sec. Then, the fault is applied. The time the fault is applied is different between buses 2,7, and 8. The disturbance is cleared at the calculated CFCT so that the system keeps its synchronization. After that, line 2-7 is tripped, and after 1 second it is connected again. The generator at bus 2 has an output of 163 MW, so it is expected for the fault to be quite severe as it is happening next to that bus.

3.5.1.1 Three-phase Symmetrical Fault at Bus 2 of the IEEE 9 Bus System

After the analysis, the CFCT is calculated to be 0.25 sec, which is the duration of the fault. That way, the system is able to maintain its stability. The simulation process is presented in Table 3.3 and indicates that the fault must be cleared at 1.25 sec. Simultaneously, the line 2-7 is tripped, and after 1 sec at 2.25 sec it is connected again until 12 sec when the simulation ends. Figures 3.8 - 3.12 present the generators' relative power angle with respect to the power angle of the swing bus, the frequency of the buses, the active and reactive power of the generators, the voltage of the buses, respectively, when the duration of the fault is 0.25 sec. Figure 3.13 shows the relative power angle with respect to the generator's power angle when the fault lasts for 0.3 sec, 0.05 sec longer than the CFCT. The system can be quite vulnerable when a three-phase symmetrical fault occurs.

Table 3. 3 IEEE9 three-phase symmetrical Fault at Bus2

Action	Time (sec)
Steady-state	0.00
Apply Fault	1.00
Clear Fault	1.25
Trip Line	1.25
Connect Line	2.25
Power Flow	12.00

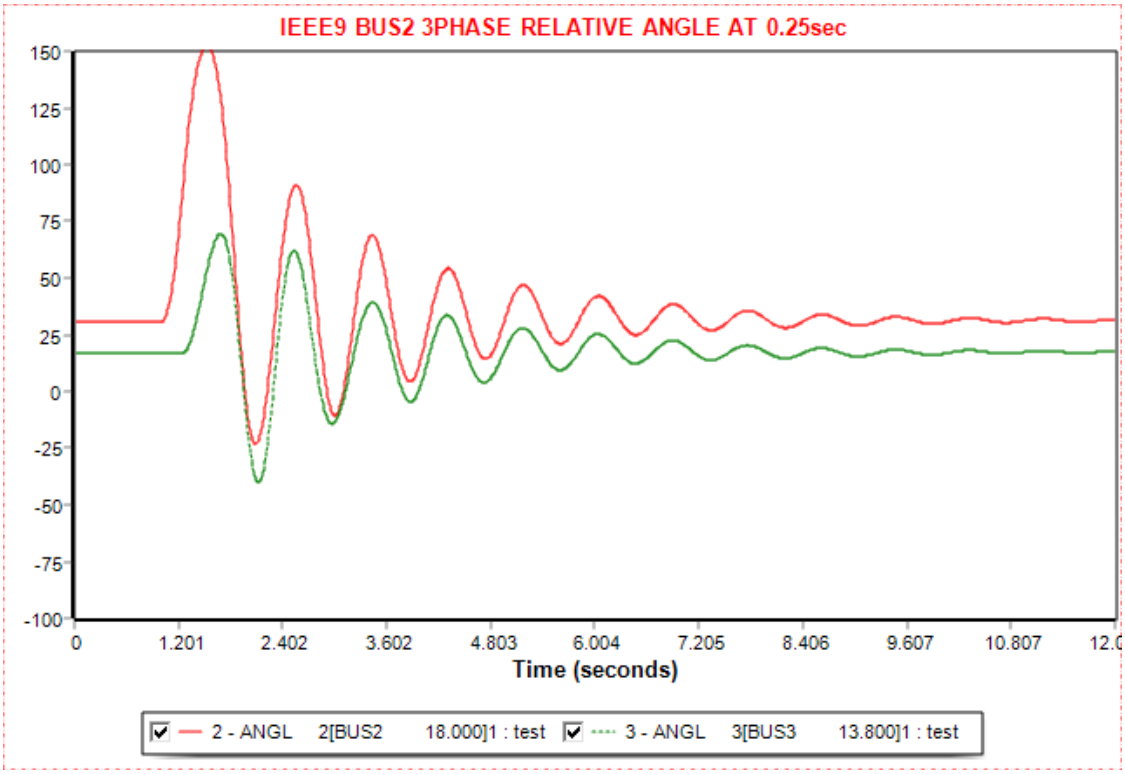

Figure 3. 8 Relative power angle plots of three-phase symmetrical fault when it is cleared at 1.25 sec at IEEE9 bus system

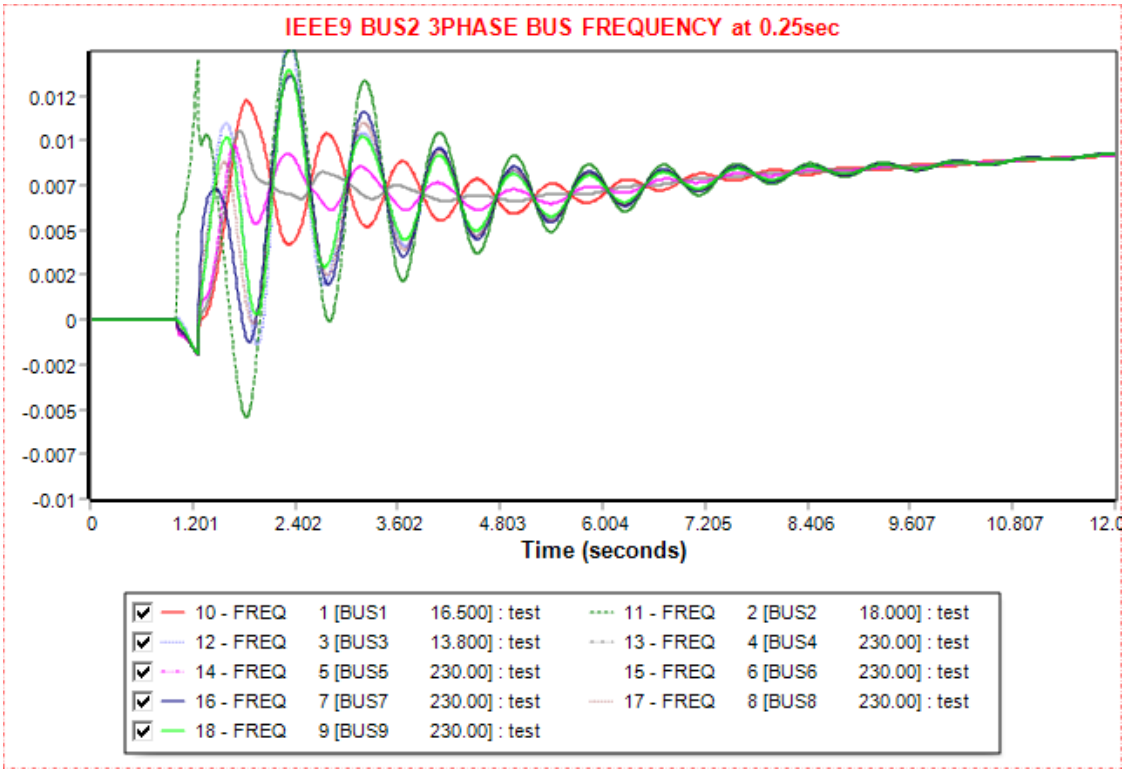

Figure 3. 9 Frequency plots of three-phase symmetrical fault at bus 2 when it is cleared at 1.25 sec at IEEE9 bus system

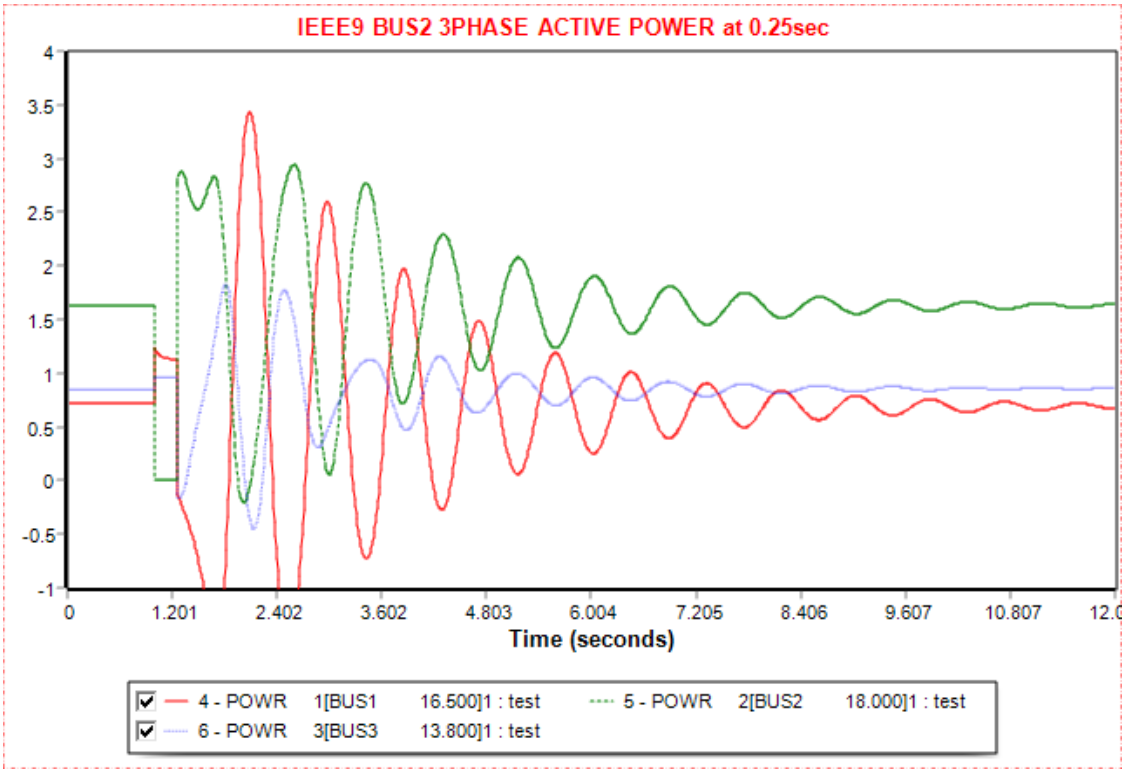

Figure 3. 10 Active Power plots of three-phase symmetrical fault at bus 2 when it is cleared at 1.25 sec at IEEE9 bus system

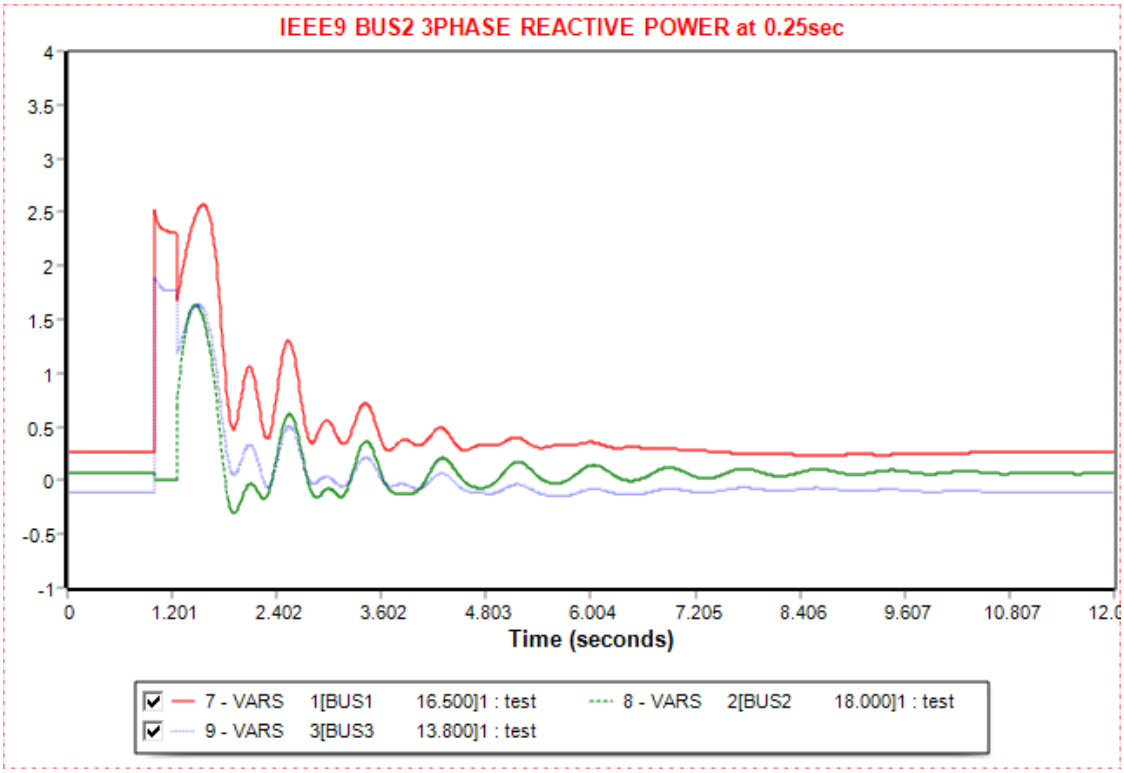

Figure 3. 11 Reactive Power plots of three-phase symmetrical fault at bus 2 when it is cleared at 1.25 sec at IEEE9 bus system

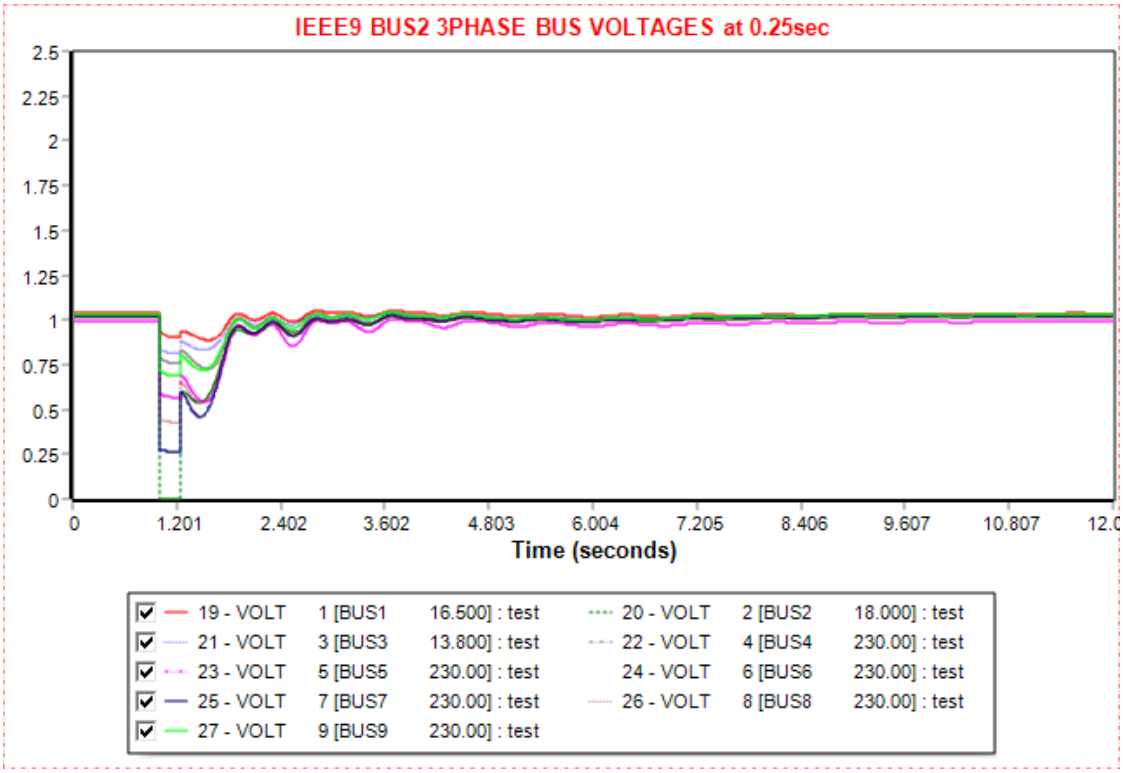

Figure 3. 12 Voltage plots of three-phase symmetrical fault at bus 2 when it is cleared at 1.25 sec at IEEE9 bus system

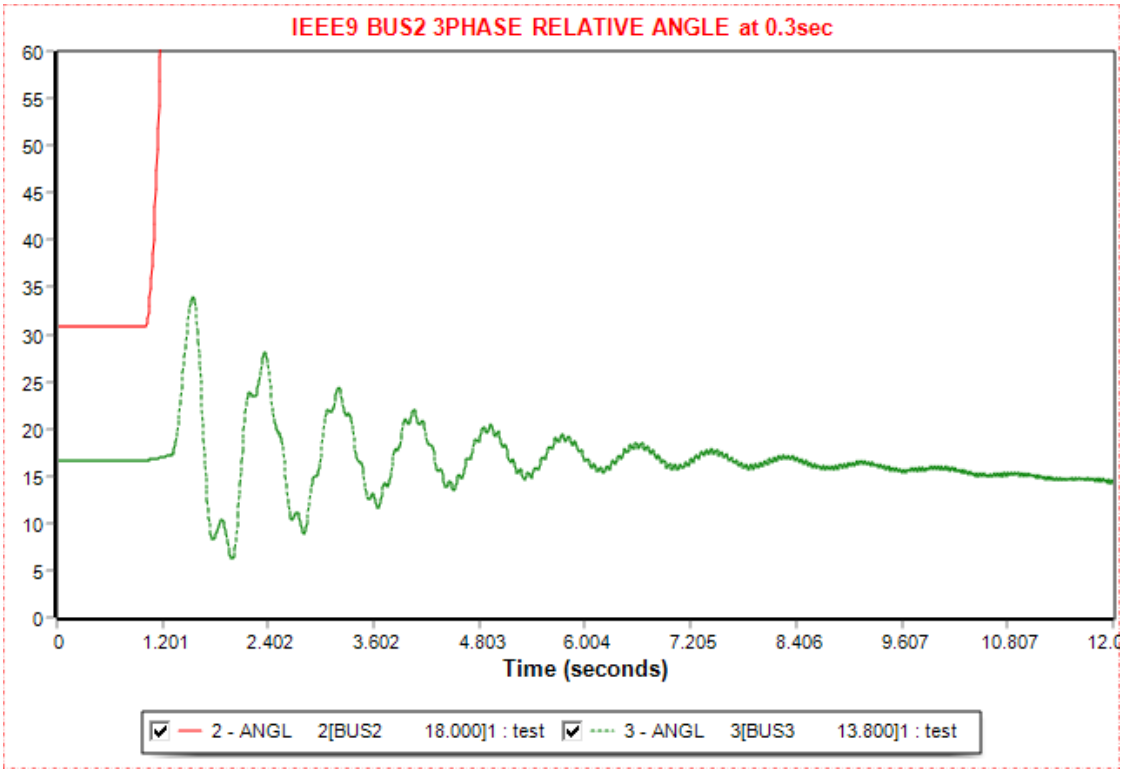

Figure 3. 13 Relative power angle plots of three-phase symmetrical fault at bus 2 when it is cleared at 1.3 sec at IEEE9 bus system

3.5.1.2 SLG Fault at Bus 2 of the IEEE 9 Bus System

This simulation is similar to the one in section 3.5.1.1 but with a different type of fault: SLG. The system maintains its stability and endures the fault so there is no CFCT for this case. The disturbance is cleared at 0.5 seconds to see the transient behavior of the system. Firstly, there is a steady-state analysis for 1 sec. Then an SLG occurs and is removed at 1.5 sec. Immediately, line 2-7 is tripped for 1 sec until 2.5 sec. Then it is connected again, and the simulation proceeds until 12 sec. This is shown in Table 3.4. Figures 3.14 - 3.18 present the generators' relative power angle with respect to the power angle of the swing bus, the frequency of the buses, the active and reactive power of the generators, the voltage of the buses, respectively, when the duration of the fault is 0.5 sec.

Table 3. 4 IEEE9 SLG Fault at Bus2

Action	Time (sec)
Steady-state	0.00
Apply Fault	1.00
Clear Fault	1.5
Trip Line	1.5
Connect Line	2.5
Power Flow	12.00

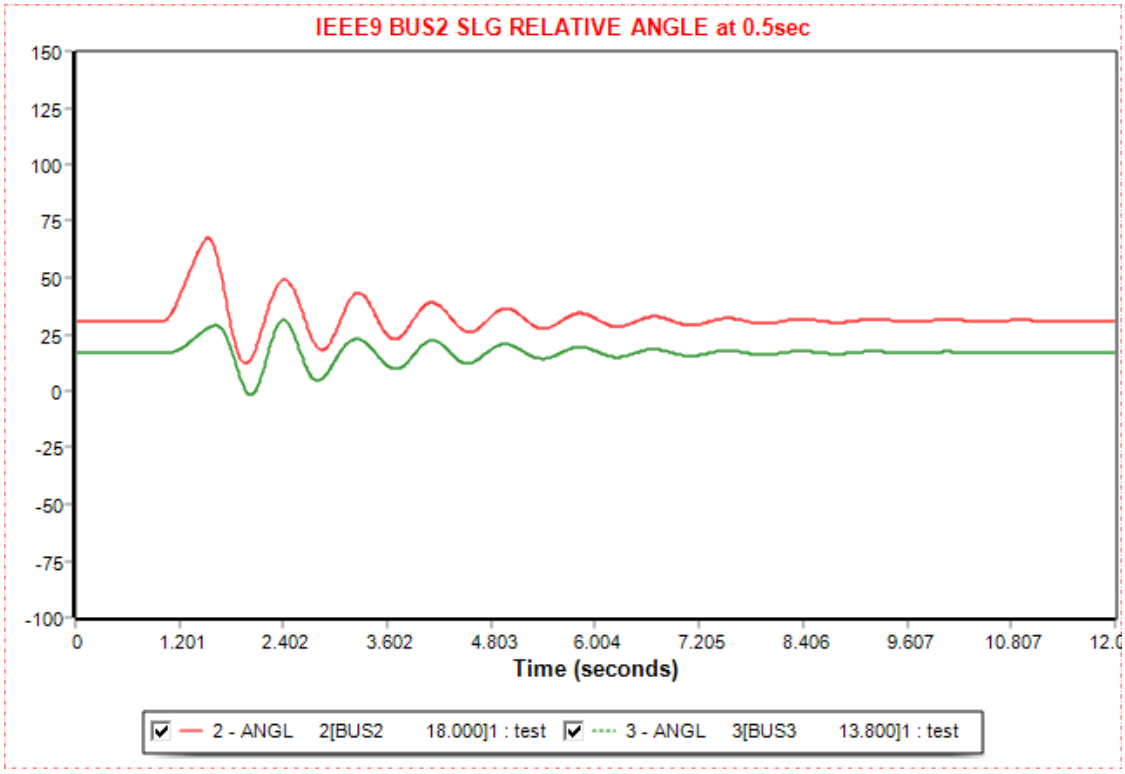

Figure 3. 14 Relative power angle plots of SLG fault at bus 2 when it is cleared at 1.5 sec at IEEE9 bus system

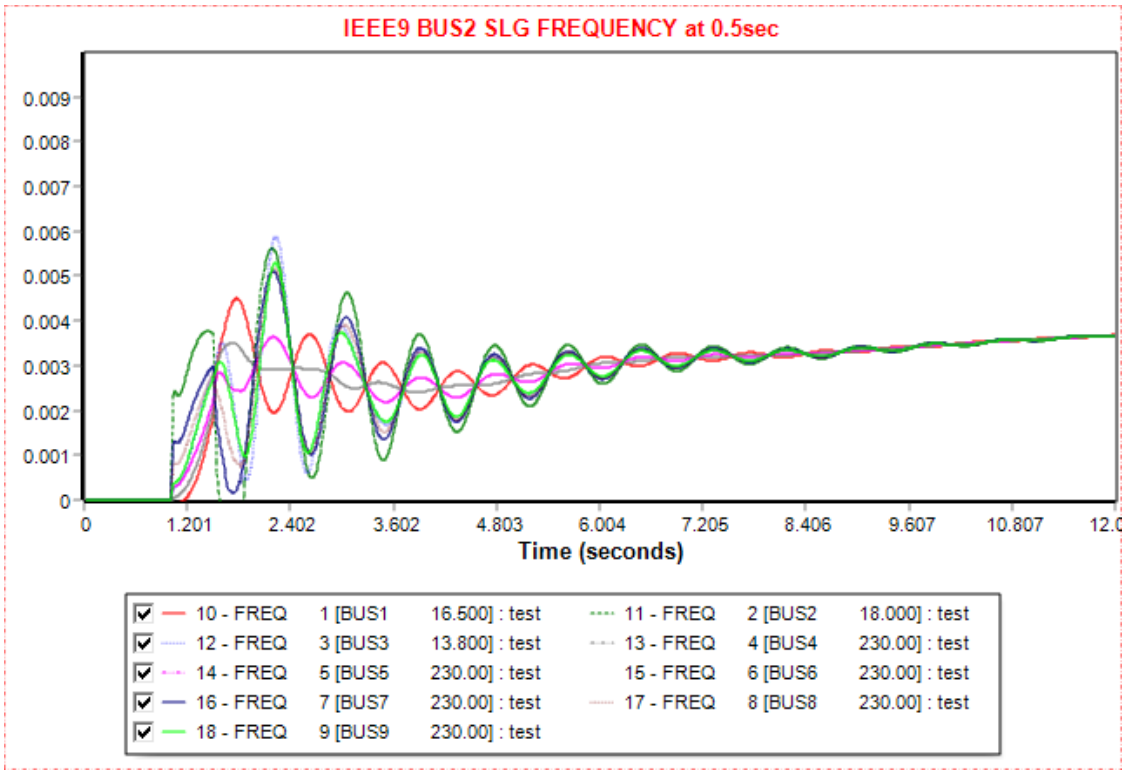

Figure 3. 15 Frequency plots of SLG fault at bus 2 when it is cleared at 1.5 sec at IEEE9 bus system

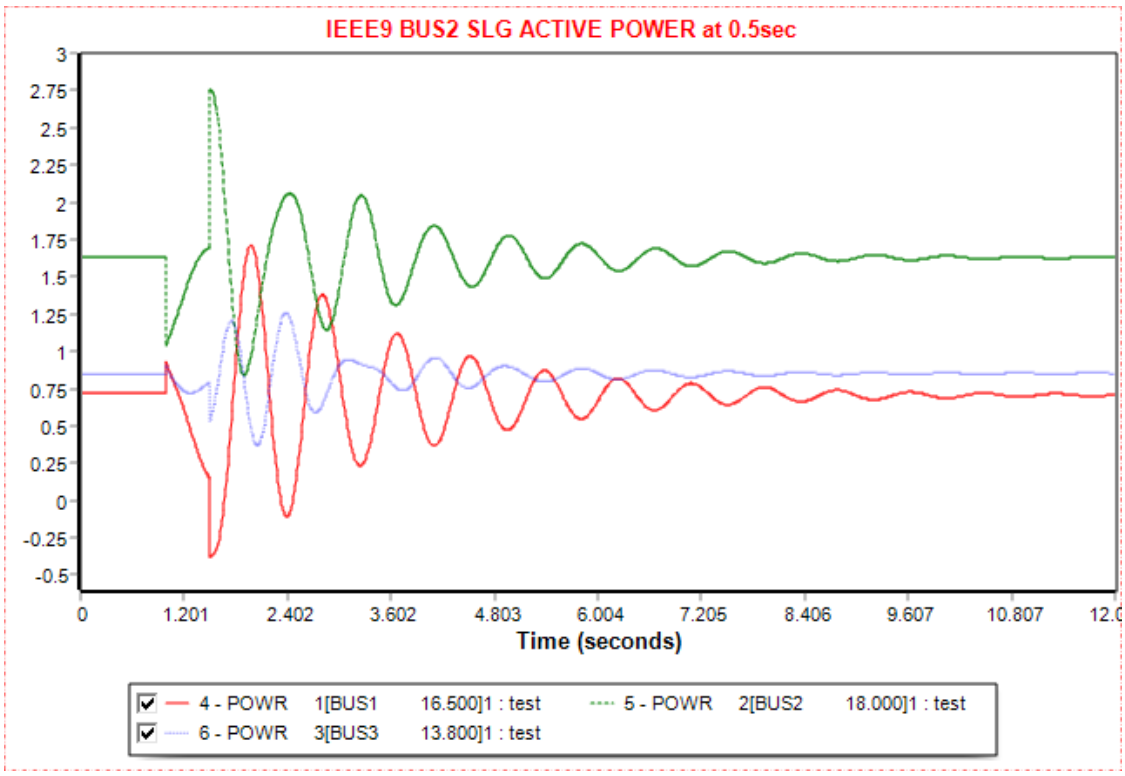

Figure 3. 16 Active Power plots of SLG fault at bus 2 when it is cleared at 1.5 sec at IEEE9 bus system

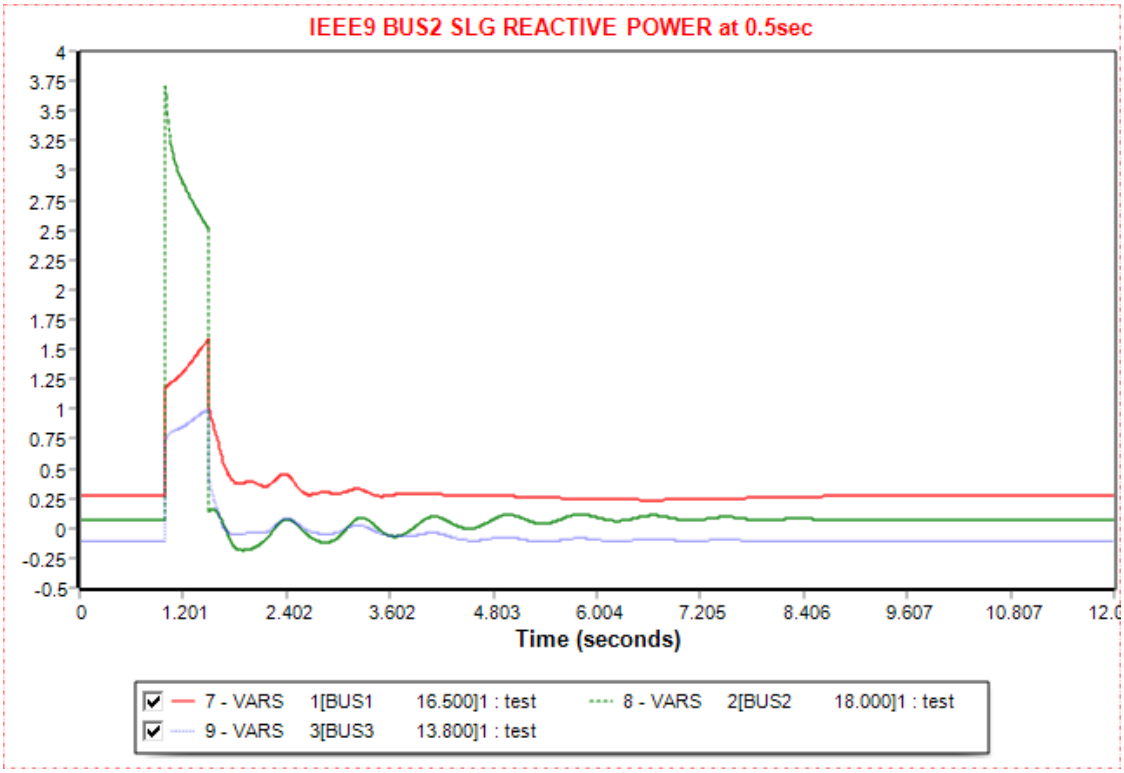

Figure 3. 17 Reactive Power plots of SLG fault at bus 2 when it is cleared at 1.5 sec at IEEE9 bus system

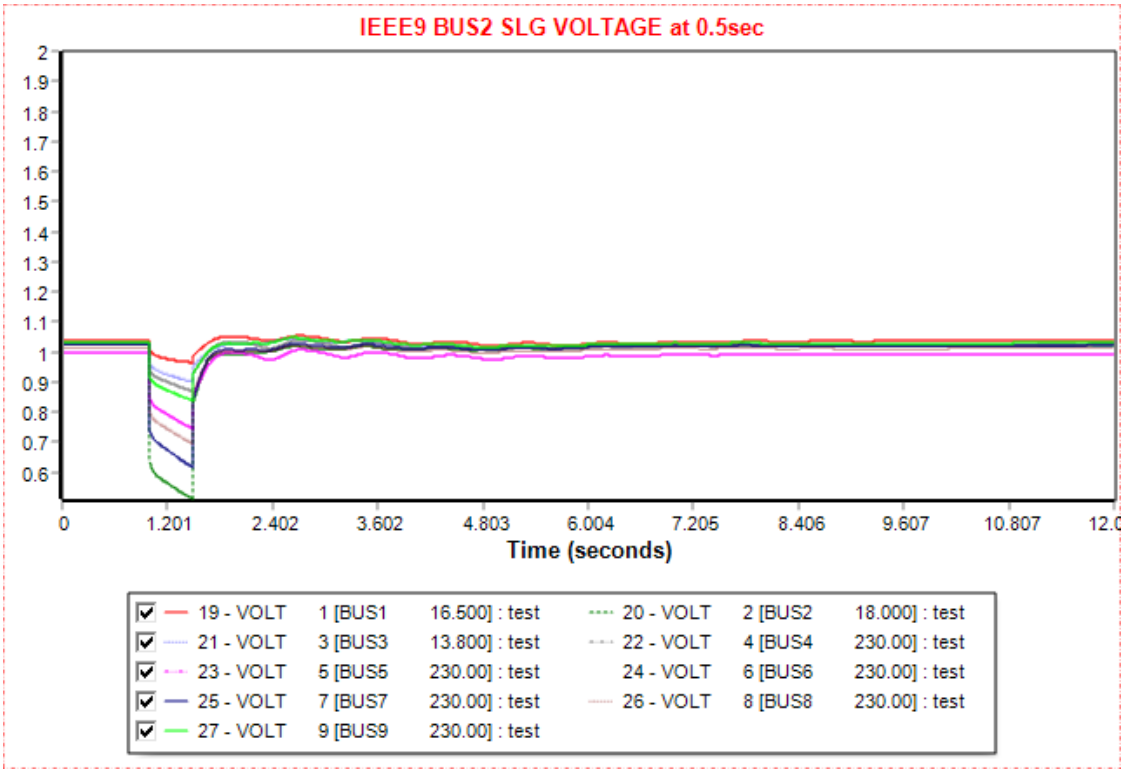

Figure 3. 18 Voltage plots of SLG fault at bus 2 when it is cleared at 1.5 sec at IEEE9 bus system

3.5.2 Faults at Bus 7 of the IEEE 9 Bus System

Bus 7 is the bus next to bus 2 of the power system. It does not have a load and it is interesting to be studied for transient stability. For all the disturbances that happen, line 7-8 is tripped and after 1 sec it is connected again.

3.5.2.1 Three-phase Symmetrical Fault at Bus 7 of the IEEE 9 Bus System

From the simulation, the CFCT is 0.25 sec, which is the maximum duration of the fault. The simulation process is presented in Table 3.5 and indicates that the fault must be cleared at 1.25 sec. Simultaneously, the line 7-8 is tripped, and after 1 sec, at 2.25 sec, it is connected again until 12 sec when the simulation ends. Figures 3.19 - 3.23 present the generators' relative power angle with respect to the power angle of the swing bus, the frequency of the buses, the active and reactive power of the generators, the voltage of the buses, respectively, when the duration of the fault is 0.25 sec. Figure 3.24 shows the relative power angle with respect to the generator's power angle when the fault lasts for 0.3 sec, 0.05 sec longer than the CFCT.

Table 3. 5 IEEE9 three-phase symmetrical Fault at Bus7

Action	**Time (sec)**
Steady-state	0.00
Apply Fault	1.00
Clear Fault	1.25
Trip Line	1.25
Connect Line	2.25
Power Flow	12.00

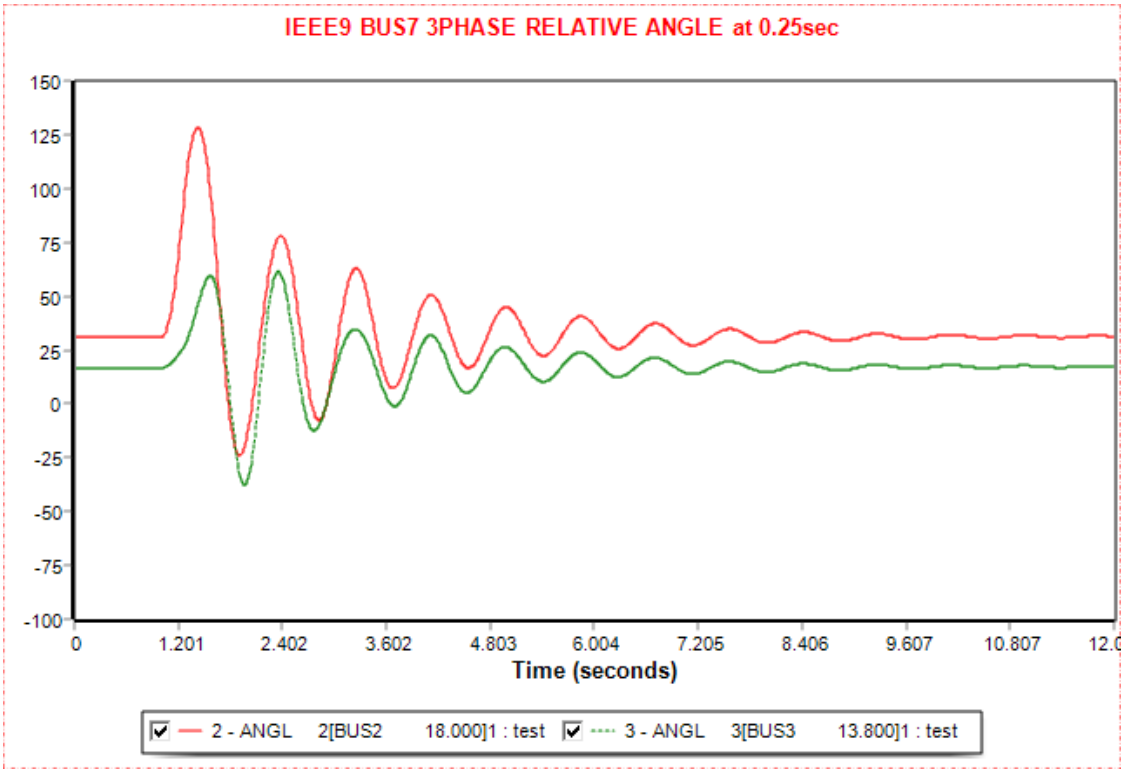

Figure 3. 19 Relative power angle plots of three-phase symmetrical fault at bus 7 when it is cleared at 1.25 sec at IEEE9 bus system

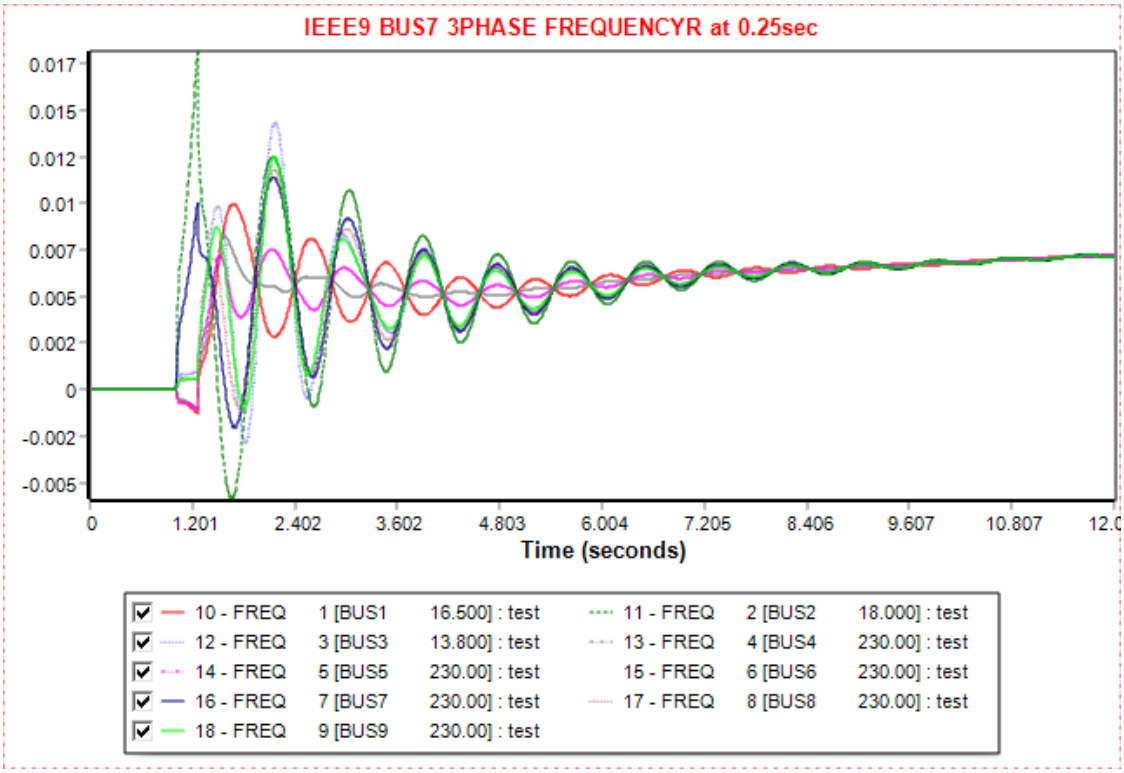

Figure 3. 20 Frequency plots of three-phase symmetrical fault at bus 7 when it is cleared at 1.25 sec at IEEE9 bus system

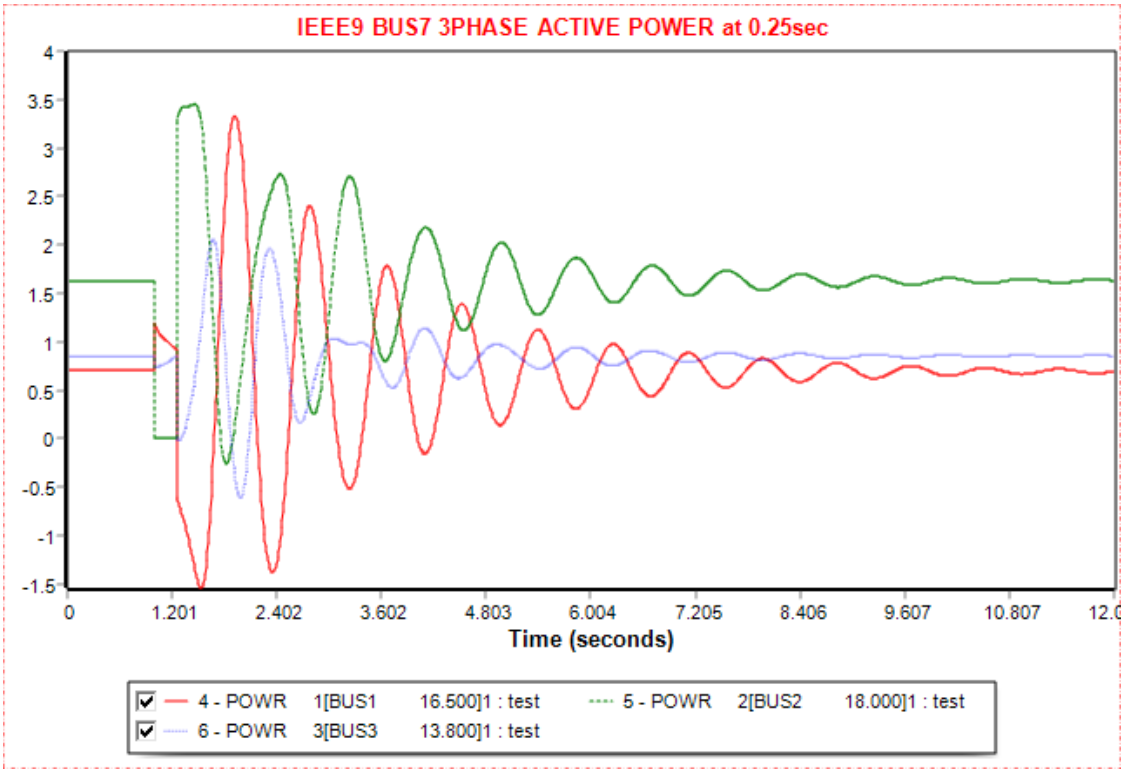

Figure 3. 21 Active Power plots of three-phase symmetrical fault at bus 7 when it is cleared at 1.25 sec at IEEE9 bus system

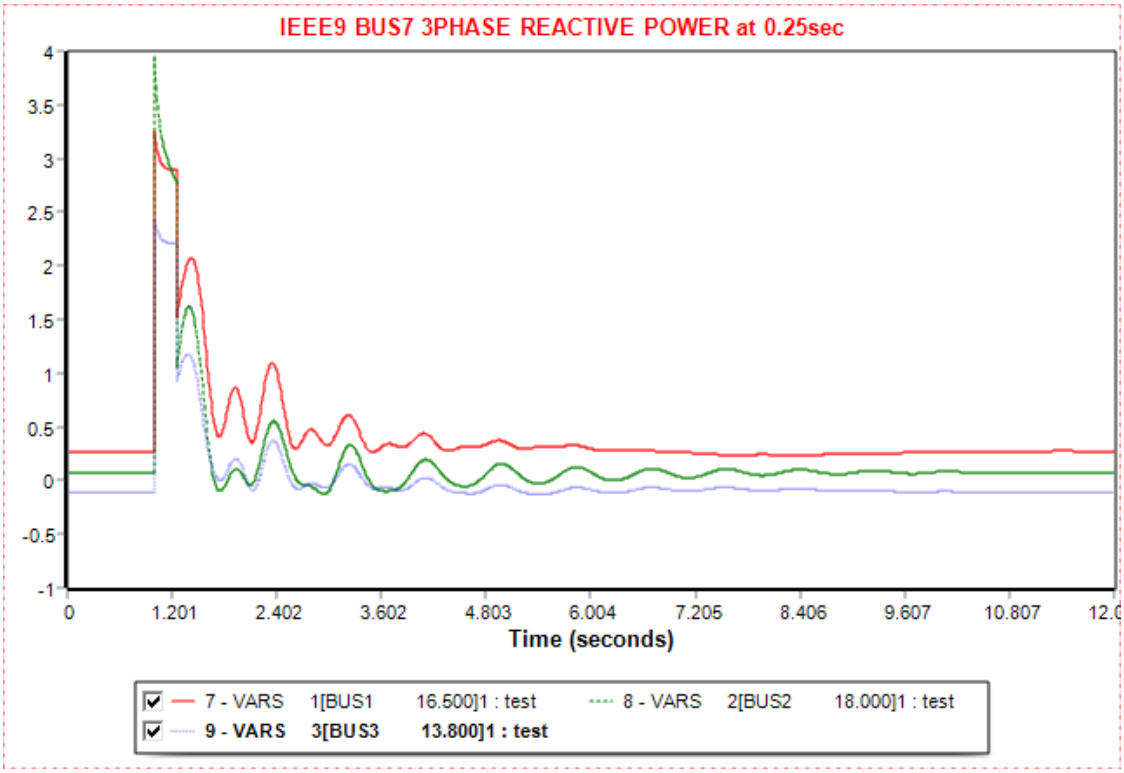

Figure 3. 22 Reactive Power plots of three-phase symmetrical fault at bus 7 when it is cleared at 1.25 sec at IEEE9 bus system

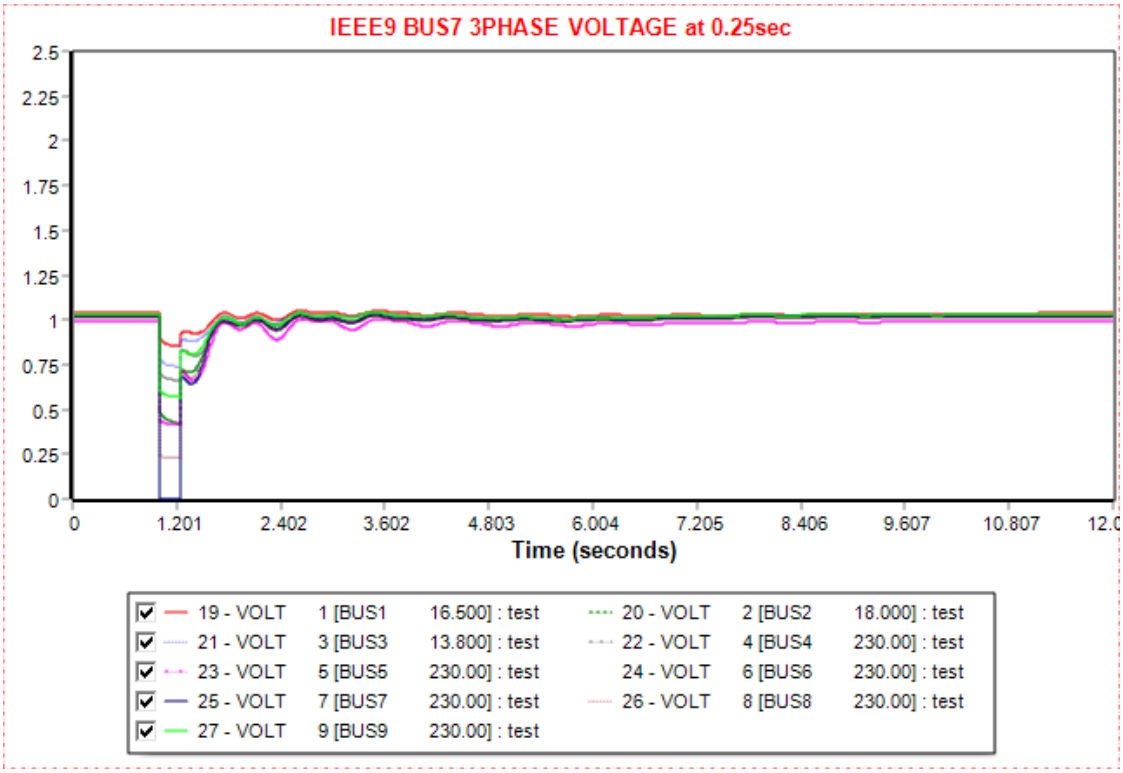

Figure 3. 23 Voltage plots of three-phase symmetrical fault at bus 7 when it is cleared at 1.25 sec at IEEE9 bus system

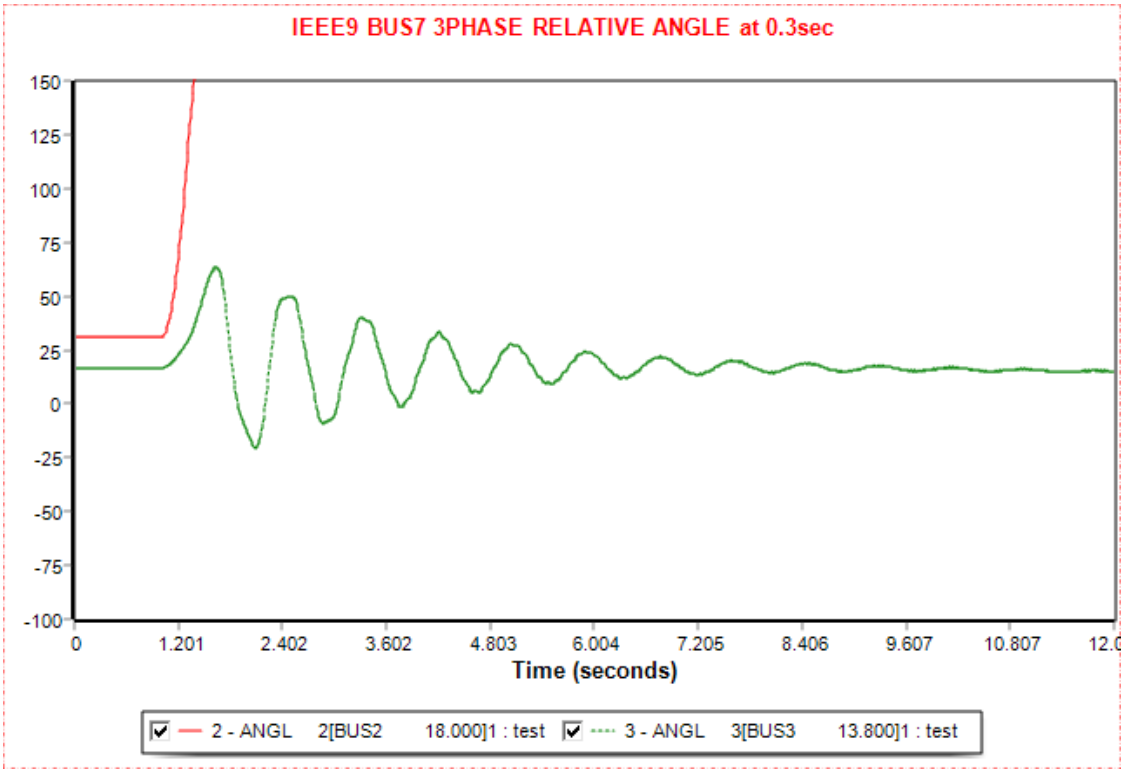

Figure 3. 24 Relative power angle plots of three-phase symmetrical fault at bus 7 when it is cleared at 1.3 sec at IEEE9 bus system

3.5.2.2 SLG Fault at Bus 7 of the IEEE 9 Bus System

The simulation of this section involves the same system that was used in 3.5.1.2. The system withstands the fault, and there is no CFCT. In order to see the transient behavior of the system, we present the results for a duration of the fault for 0.5 sec. In the beginning, the system is subjected to a steady-state run for 1 sec and then the disturbance occurs. After 0.5 sec the SLG is cleared and the line 7-8 is tripped. At 2.5 sec, the line is connected, and the simulation ends in 12 sec. This is shown in Table 3.6. Figures 3.25 - 3.29 present the generators' relative power angle with respect to the power angle of the swing bus, the frequency of the buses, the active and reactive power of the generators, the voltage of the buses, respectively, when the duration of the fault is 0.5 sec.

Table 3. 6 IEEE9 SLG Fault at Bus 7

Action	**Time (sec)**
Steady-state	0.00
Apply Fault	1.00
Clear Fault	1.5
Trip Line	1.5
Connect Line	2.5
Power Flow	12.00

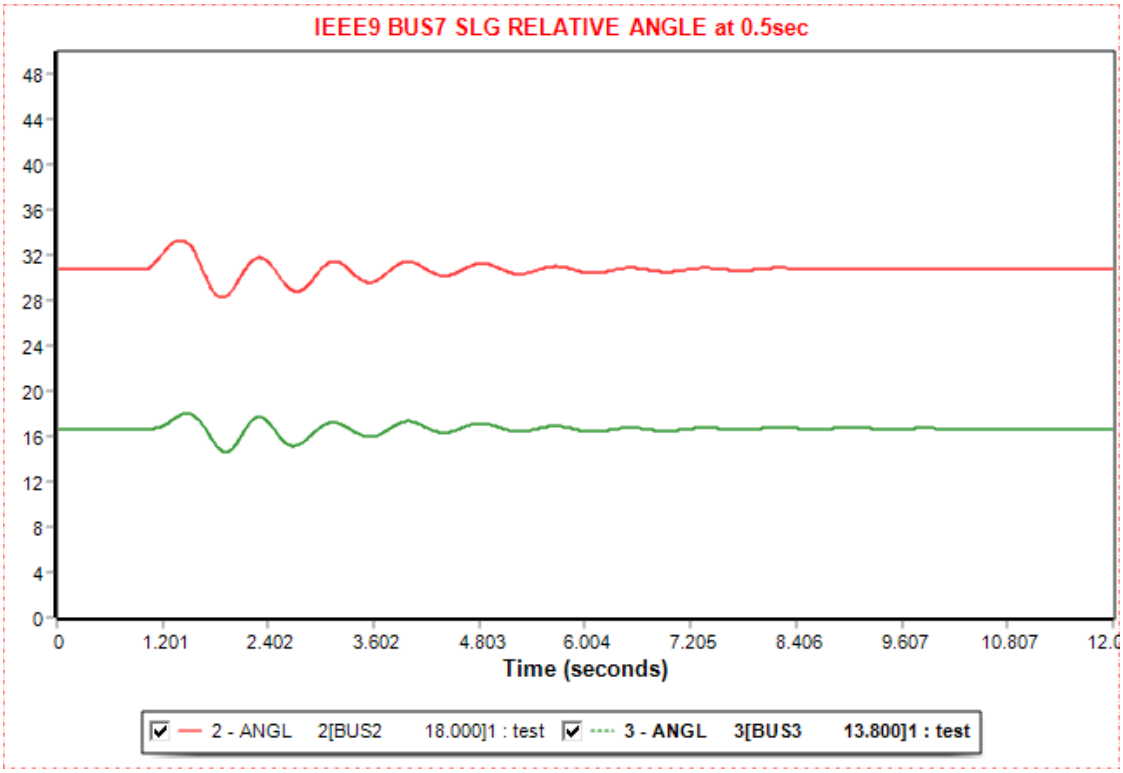

Figure 3. 25 Relative power angle plots of SLG fault at bus 7 when it is cleared at 1.5 sec at IEEE9 bus system

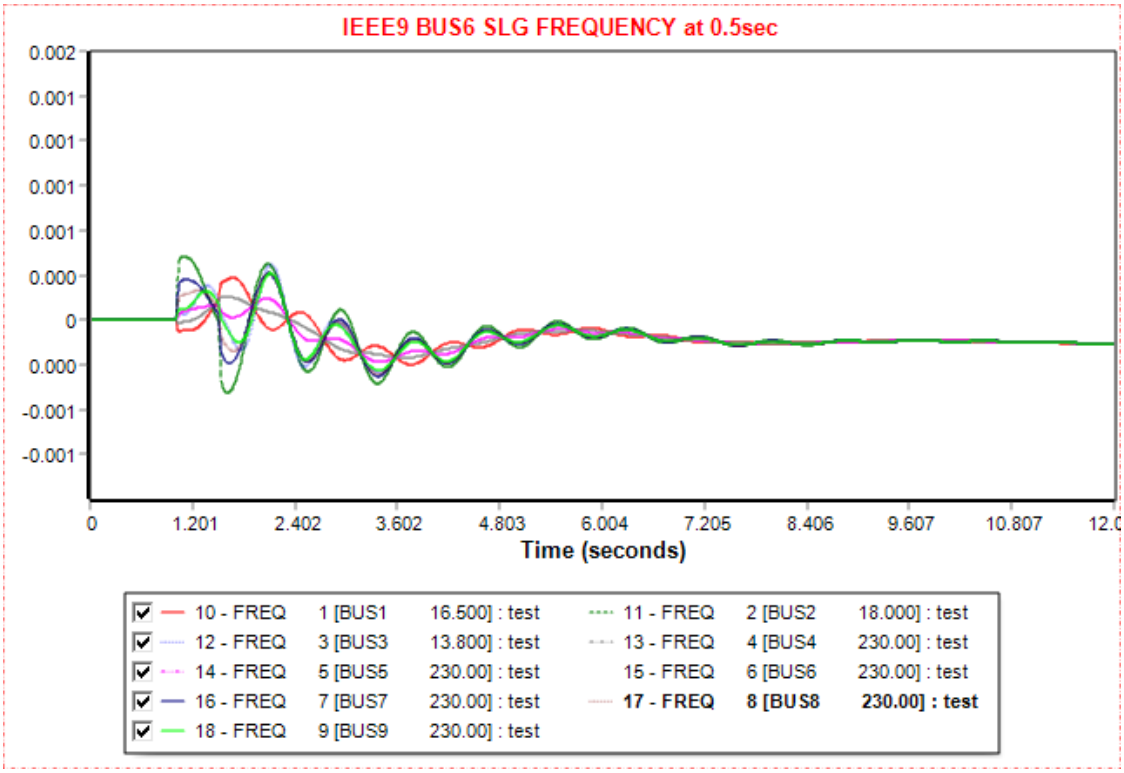

Figure 3. 26 Frequency plots of SLG fault at bus 7 when it is cleared at 1.5 sec at IEEE9 bus system

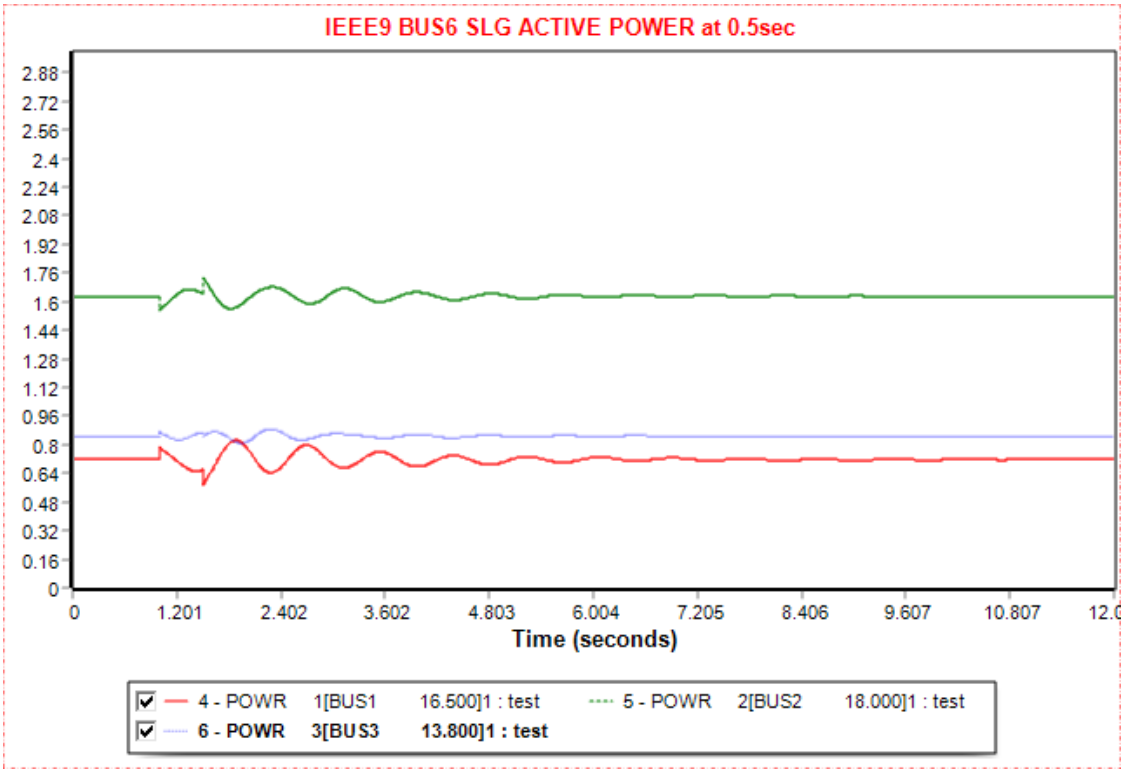

Figure 3. 27 Active Power plots of SLG fault at bus 7 when it is cleared at 1.5 sec at IEEE9 bus system

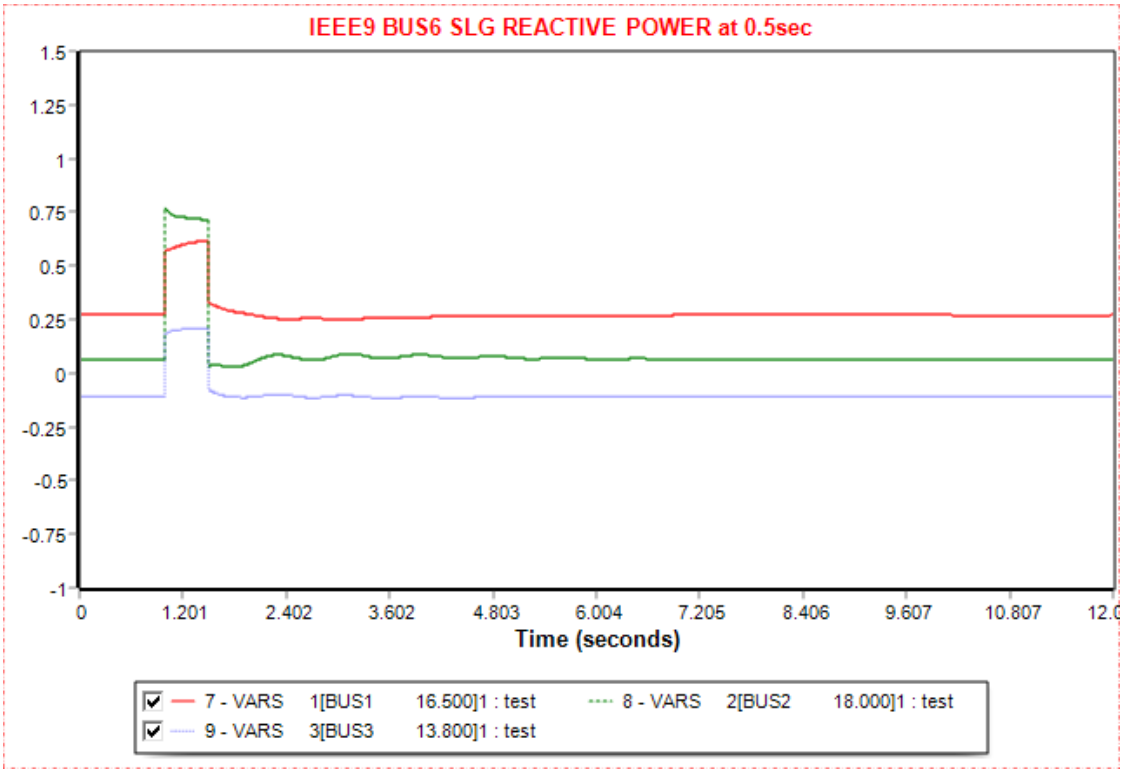

Figure 3. 28 Reactive Power plots of SLG fault at bus 7 when it is cleared at 1.5 sec at IEEE9 bus system

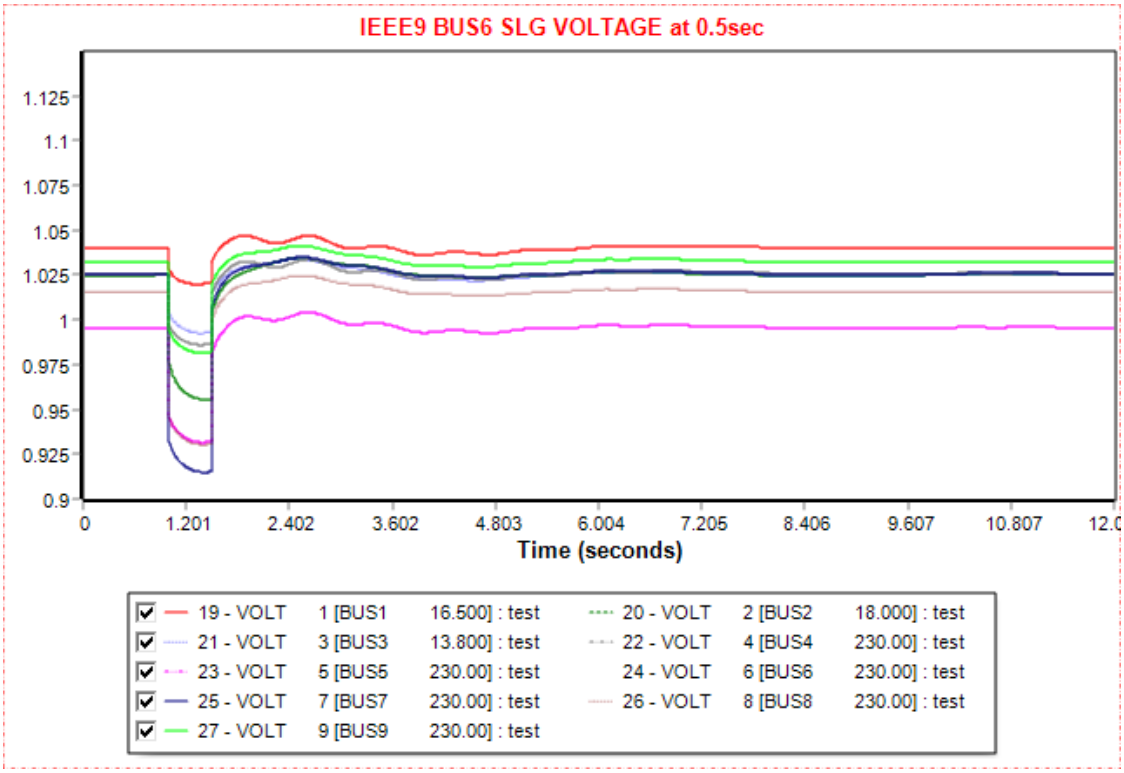

Figure 3. 29 Voltage plots of SLG fault at bus 7 when it is cleared at 1.5 sec at IEEE9 bus system

3.5.3 Faults at Bus 8 of the IEEE 9 Bus System

Bus 8 is one of the central buses of the IEEE9 bus system. It is a different case than the other buses that were examined because it has a load of 100MW. The other buses that were examined were not connected with a load and were generator buses or, simply, connection buses. The process of the simulation is the same that was used in the previous sections. The line that is tripped is line 8-7 where the fault happens in bus 8.

3.5.3.1 Three-phase Symmetrical Fault at Bus 8 of the IEEE 9 Bus System

In the standard IEEE9 bus system, the three-phase symmetrical fault is proven severe if it is cleared at a time greater than 0.5 sec. The process involves a load flow for 1 sec when the disturbance is applied at bus 8. The critical time is 0.5 sec, so the fault is cleared at 1.5 sec and at the same time the line 7-8 is tripped. At 2.5 sec the line 7-8 is connected to the system, and the simulation continues until 12 sec. The timesteps of this

process can be seen in Table 3.7. Figures 3.30 - 3.34 present the generators' relative power angle with respect to the power angle of the swing bus, the frequency of the buses, the active and reactive power of the generators, and the buses' voltage, respectively, when the duration of the fault is 0.5 sec. Figure 3.35 shows the relative power angle of the generator in bus 2 with respect to the power angle of the swing bus when the fault lasts for 0.55 sec, 0.05 sec longer than the CFCT. The more central the bus is, the more tolerance it has towards a fault.

Table 3. 7 IEEE9 Three-phase symmetrical Fault at Bus8

Action	**Time (sec)**
Steady-state	0.00
Apply Fault	1.00
Clear Fault	1.5
Trip Line	1.5
Connect Line	2.5
Power Flow	12.00

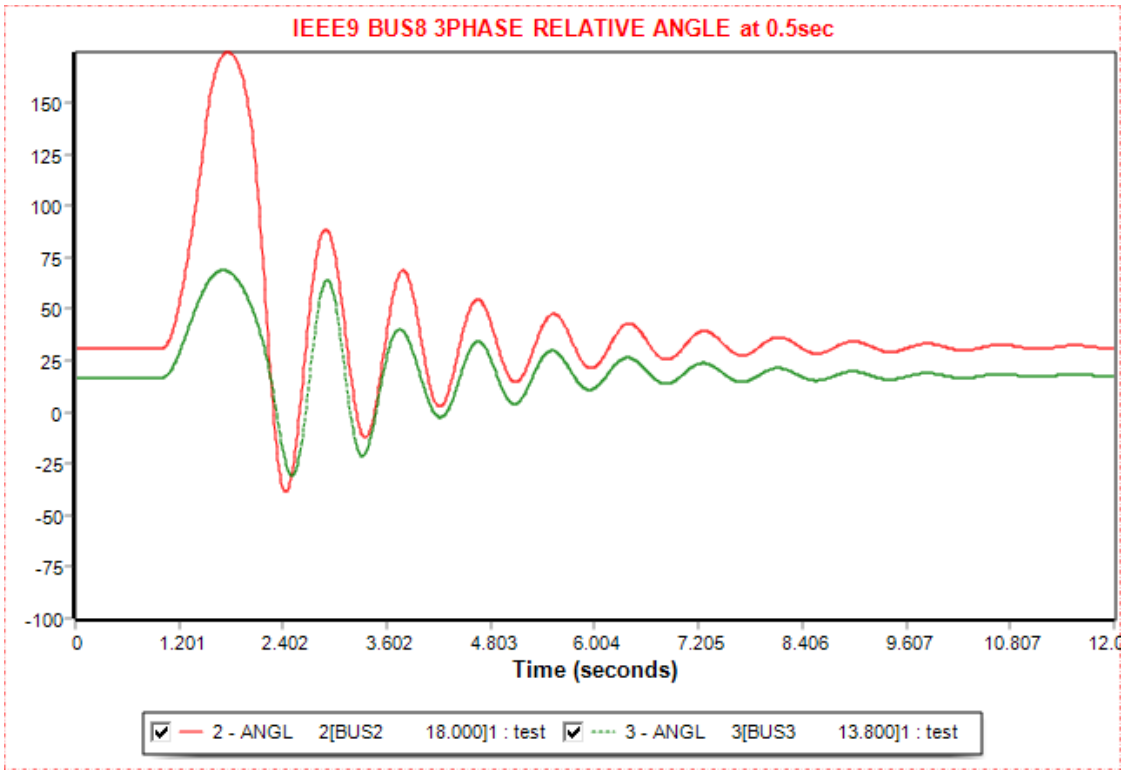

Figure 3. 30 Relative power angle plots of three-phase symmetrical fault at bus 8 when it is cleared at 1.5 sec at IEEE9 bus system

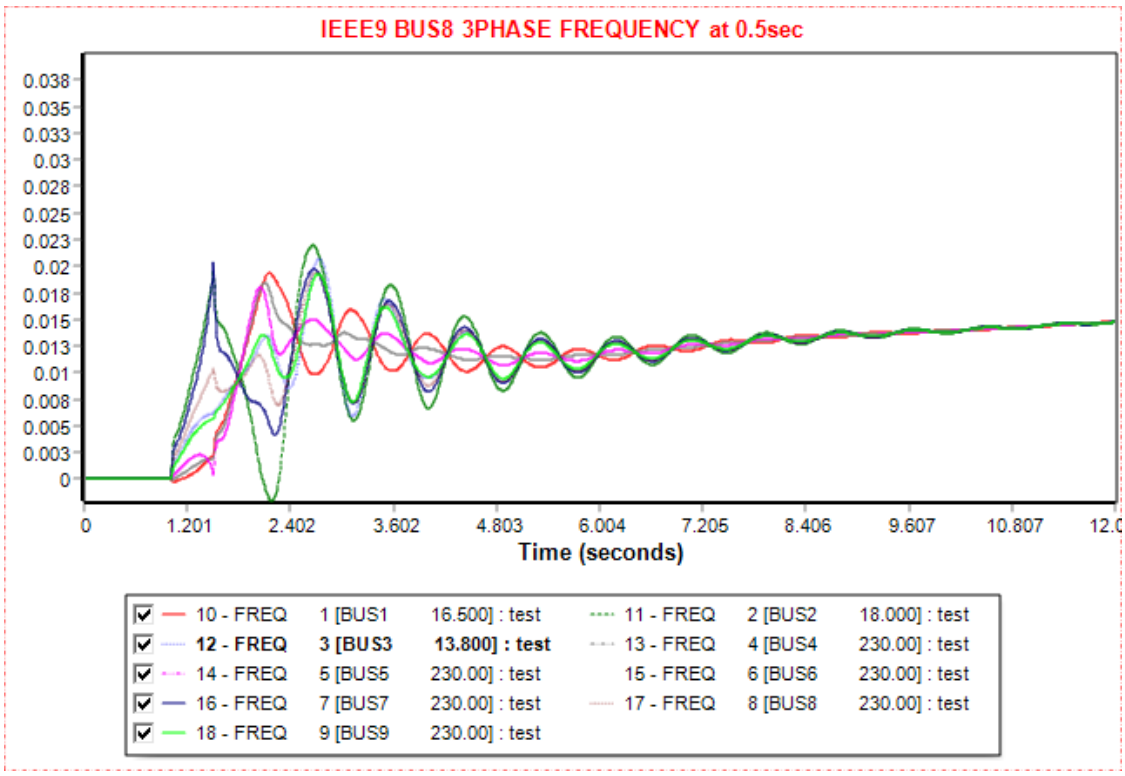

Figure 3. 31 Frequency plots of three-phase symmetrical fault at bus 8 when it is cleared at 1.5 sec at IEEE9 bus system

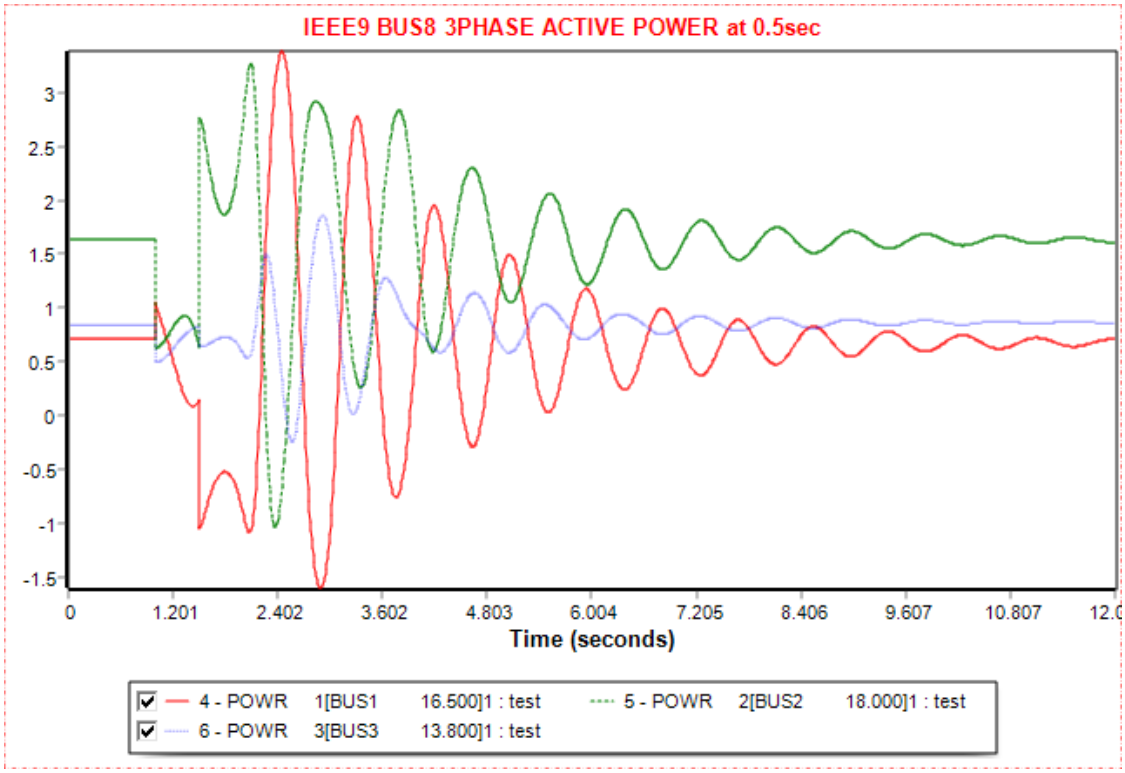

Figure 3. 32 Active Power plots of three-phase symmetrical fault at bus 2 when it is cleared at 1.5 sec at IEEE9 bus system

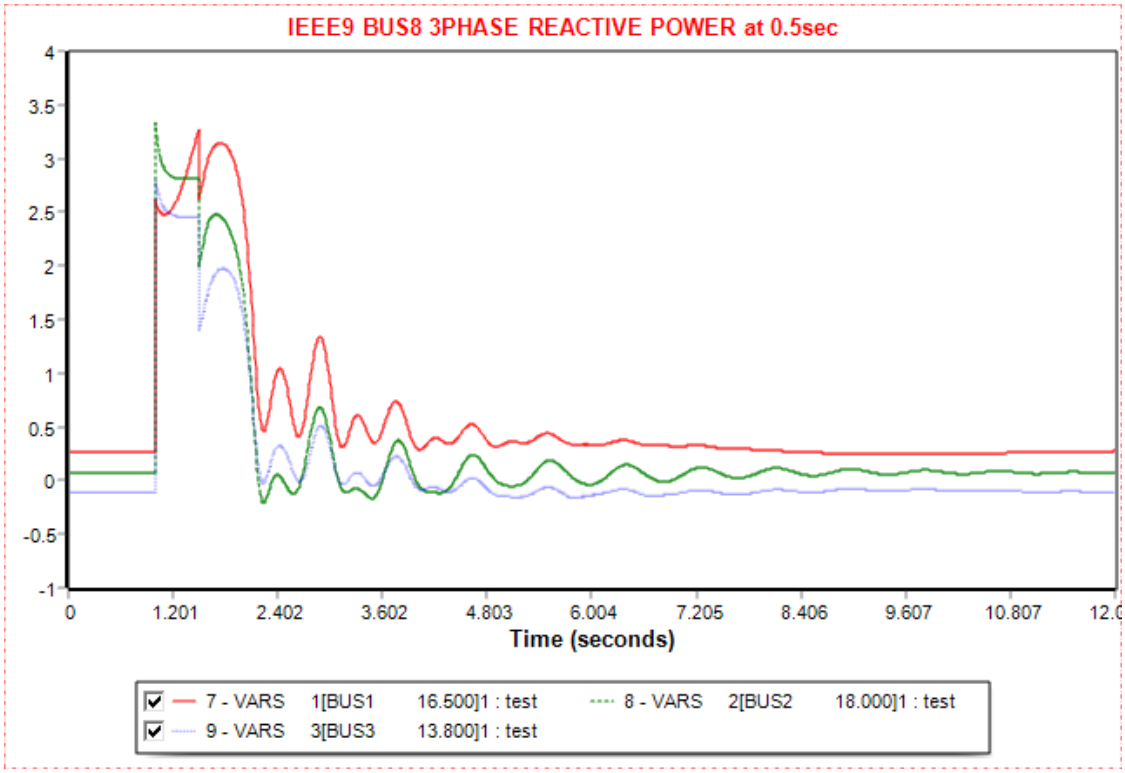

Figure 3. 33 Reactive Power plots of three-phase symmetrical fault at bus 8 when it is cleared at 1.5 sec at IEEE9 bus system

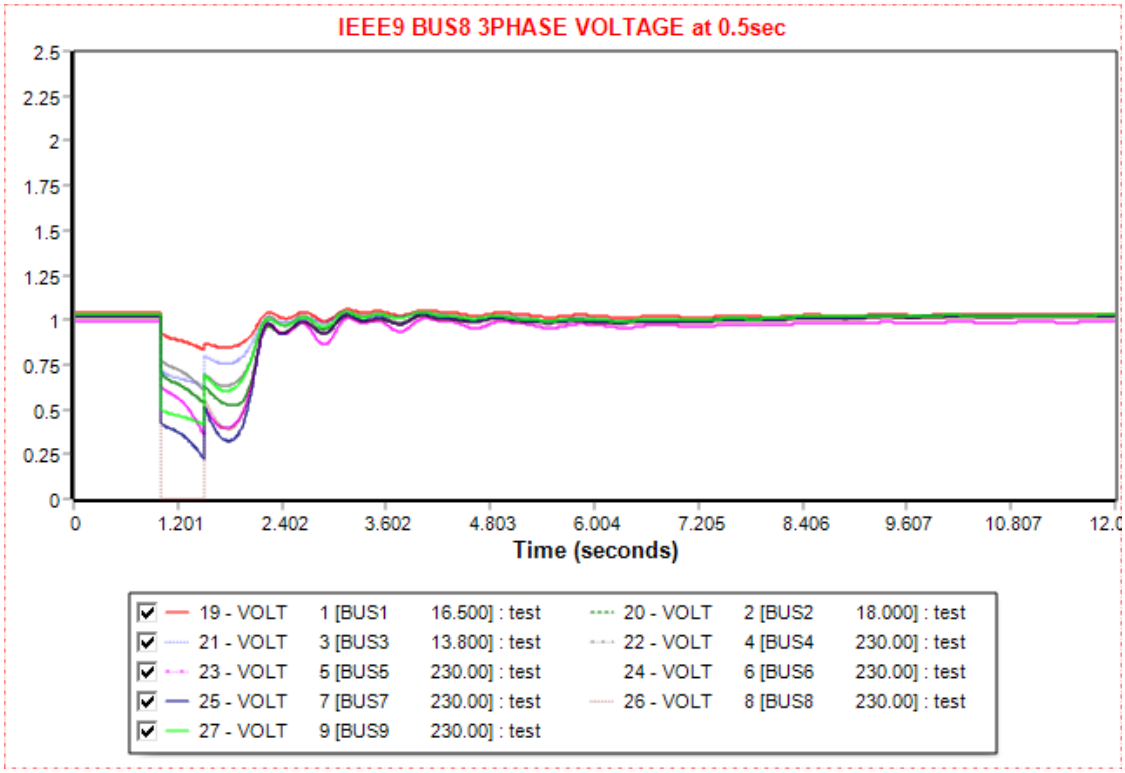

Figure 3. 34 Voltage plots of three-phase symmetrical fault at bus 8 when it is cleared at 1.5 sec at IEEE9 bus system

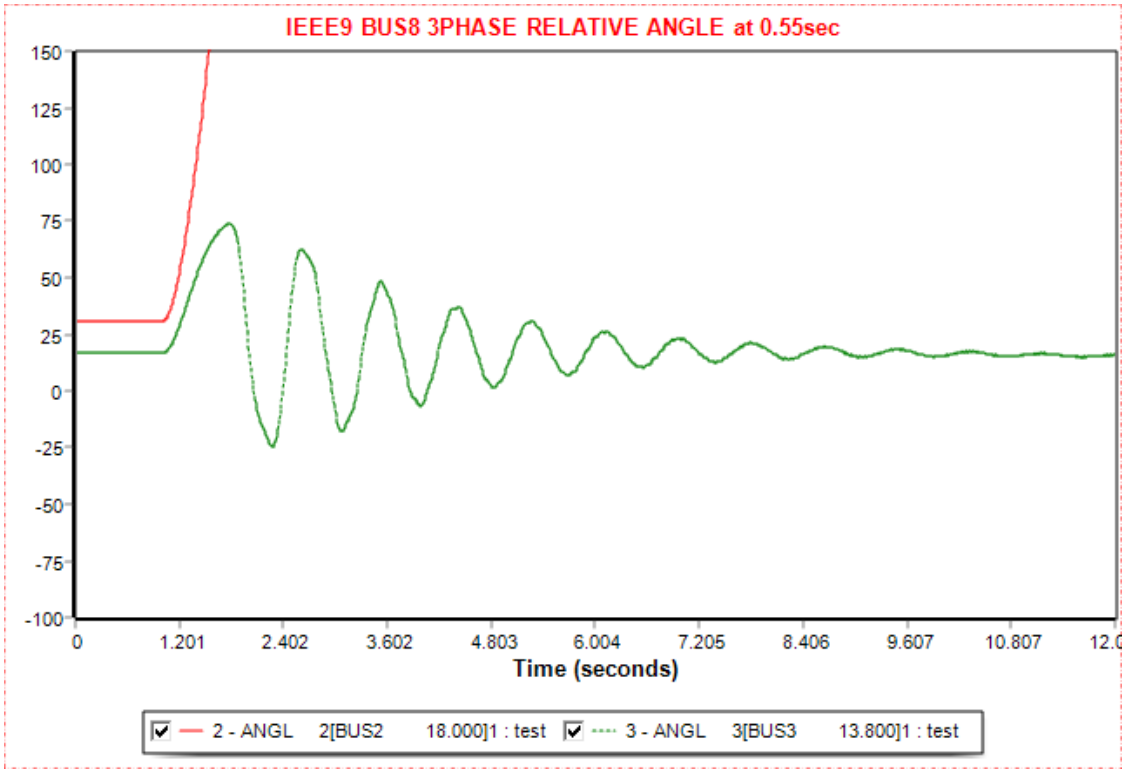

Figure 3. 35 Relative power angle plots of three-phase symmetrical fault at bus 8 when it is cleared at 1.55 sec at IEEE9 bus system

3.5.3.2 SLG Fault at Bus 8 of the IEEE 9 Bus System

When an SLG fault occurs in bus 8 of the remodeled system, the system can sustain it. In this simulation, the disturbance will be cleared at 0.5 sec, since there is no critical time, for purpose of presenting the transient stability behavior of the system. As shown in Table 3.8, an SLG is applied at 1 sec for 0.5 sec. Then the line 8-7 is opened so that the fault can be cleared internally, and after 1 sec, at 2.5 sec, the line is connected. The system then runs until 12 sec. Figures 3.36 - 3.40 present the generator connected in bus 2 relative power angle with respect to the power angle of the swing bus, the frequency of the buses, the active and reactive power of the generators, the voltage of the buses, respectively when the duration of the fault is 0.5 sec. The SLG has a lower impact than the three-phase symmetrical, also in this case.

Table 3. 8 IEEE9 SLG Fault at Bus8

Action	**Time (sec)**
Steady-state	0.00
Apply Fault	1.00
Clear Fault	1.5
Trip Line	1.5
Connect Line	2.5
Power Flow	12.00

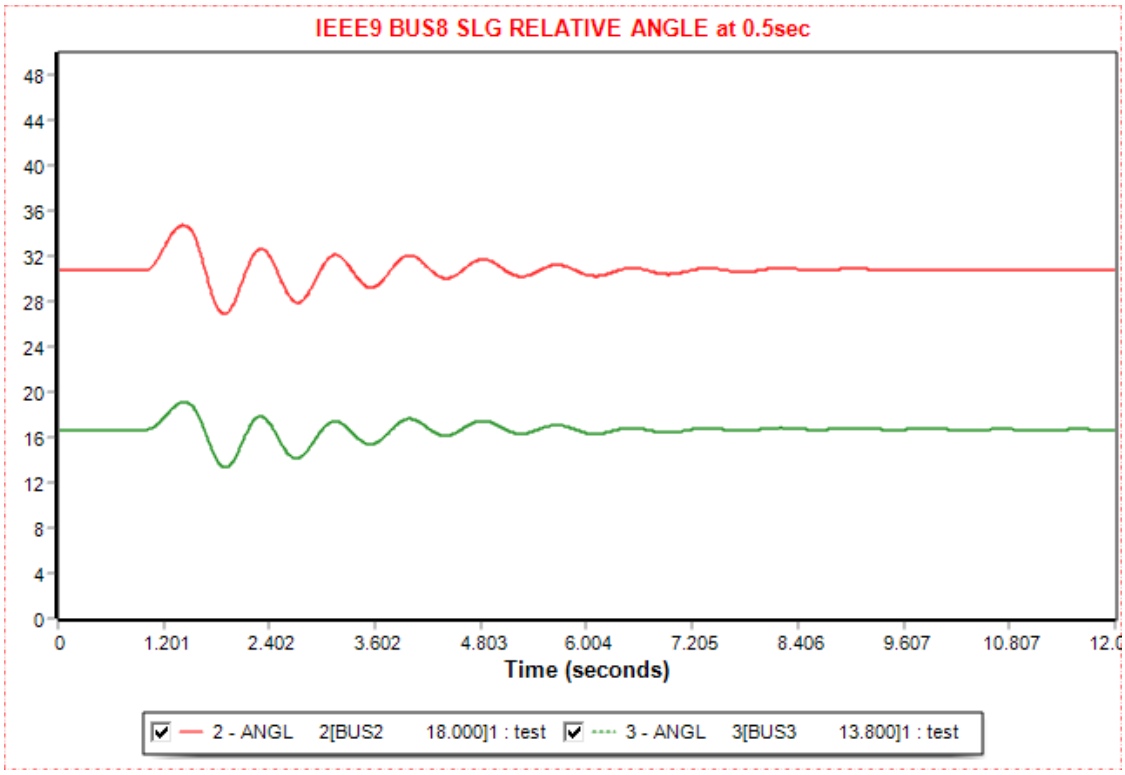

Figure 3. 36 Relative power angle plots of SLG fault at bus 8 when it is cleared at 1.5 sec at IEEE9 bus system

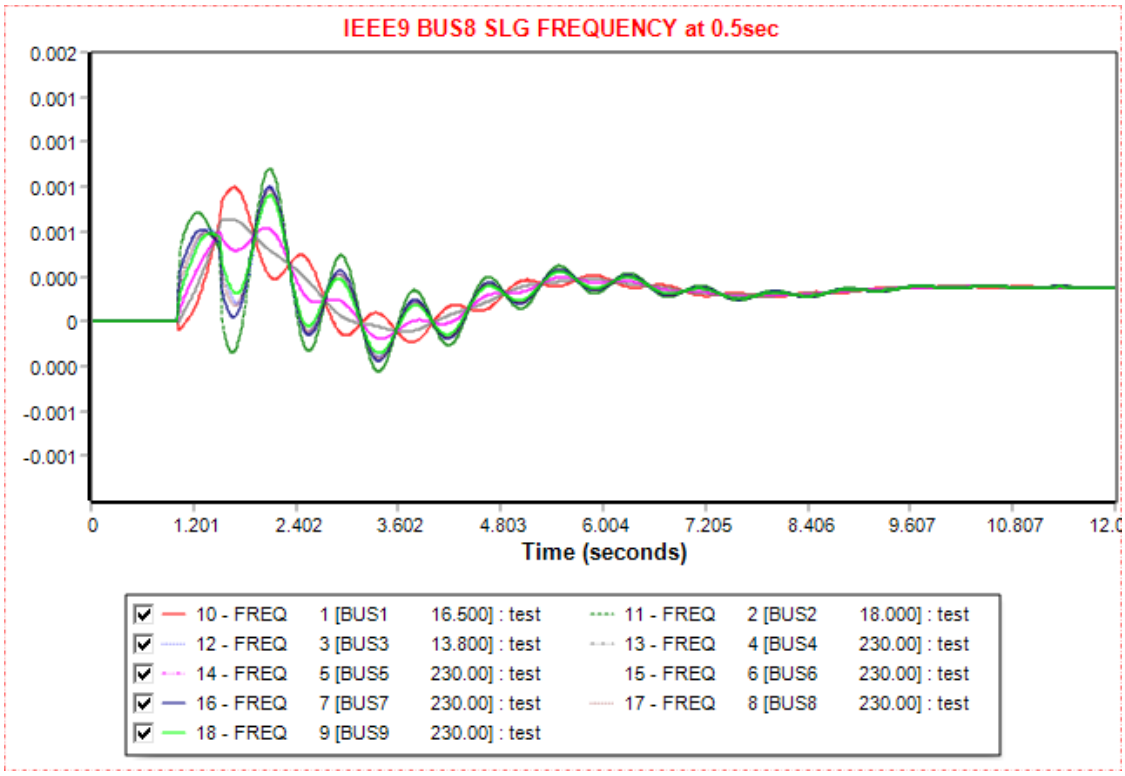

Figure 3. 37 Frequency plots of SLG fault at bus 8 when it is cleared at 1.5 sec at IEEE9 bus system

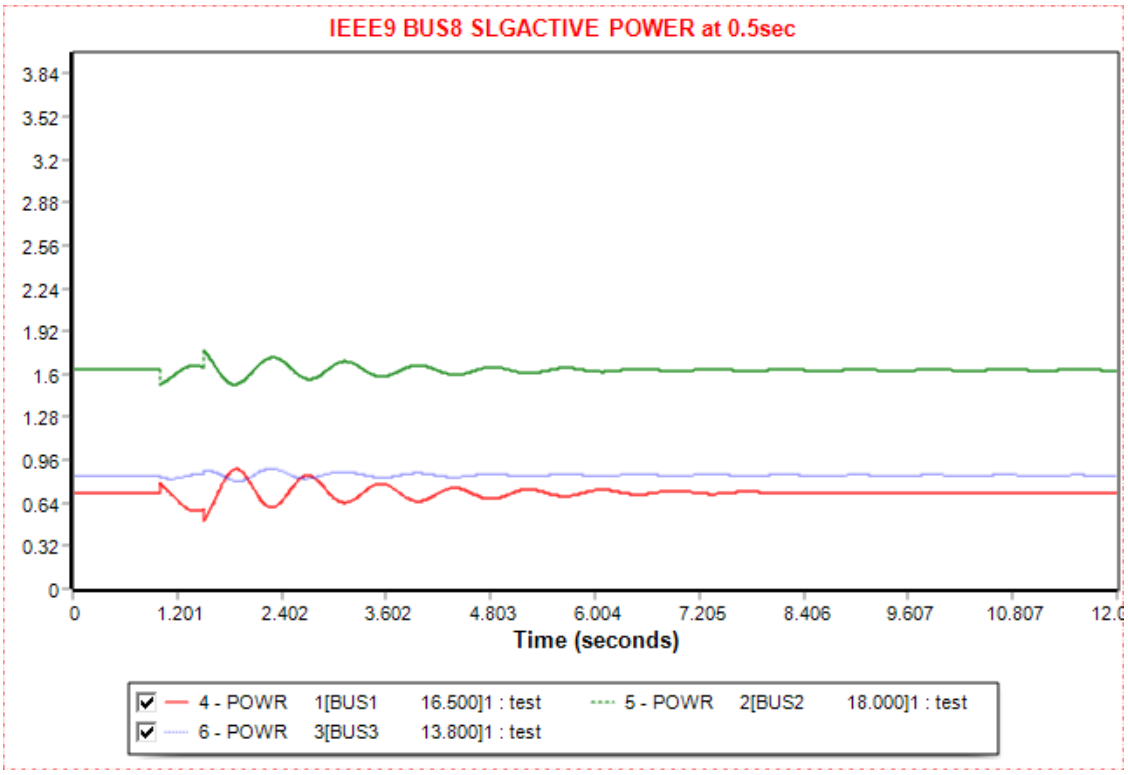

Figure 3. 38 Active Power plots of SLG fault at bus 8 when it is cleared at 1.5 sec at IEEE9 bus system

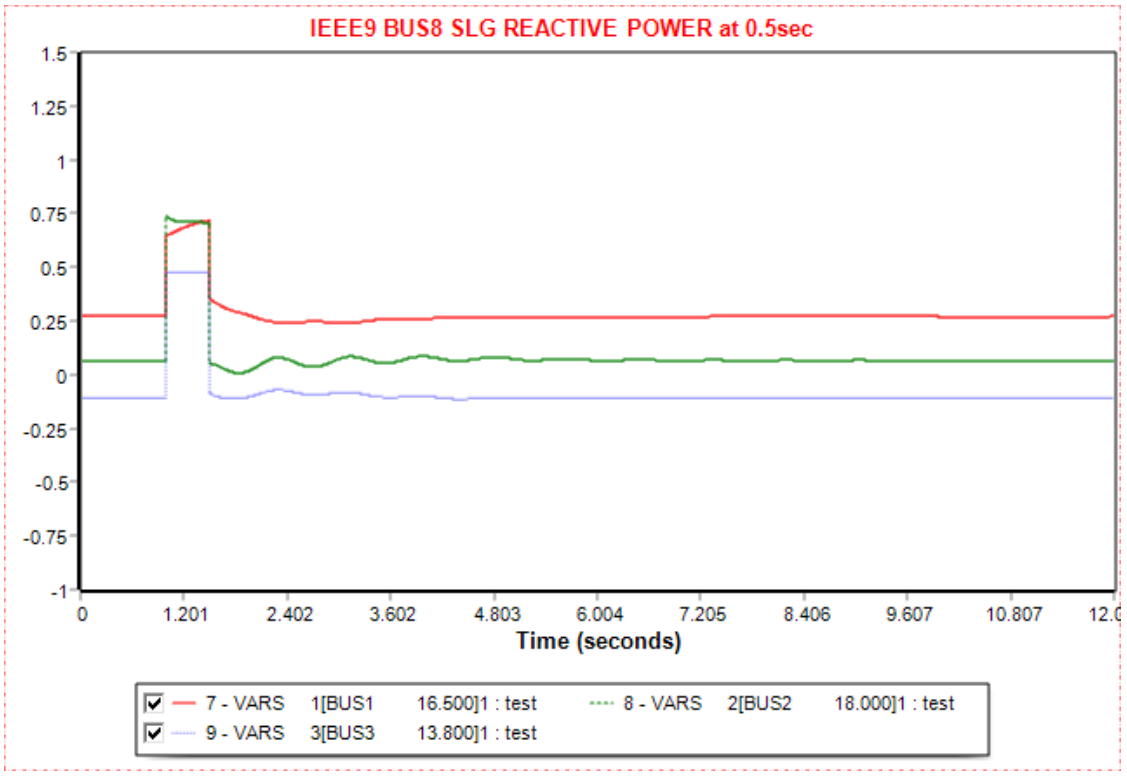

Figure 3. 39 Reactive Power plots of SLG fault at bus 8 when it is cleared at 1.5 sec at IEEE9 bus system

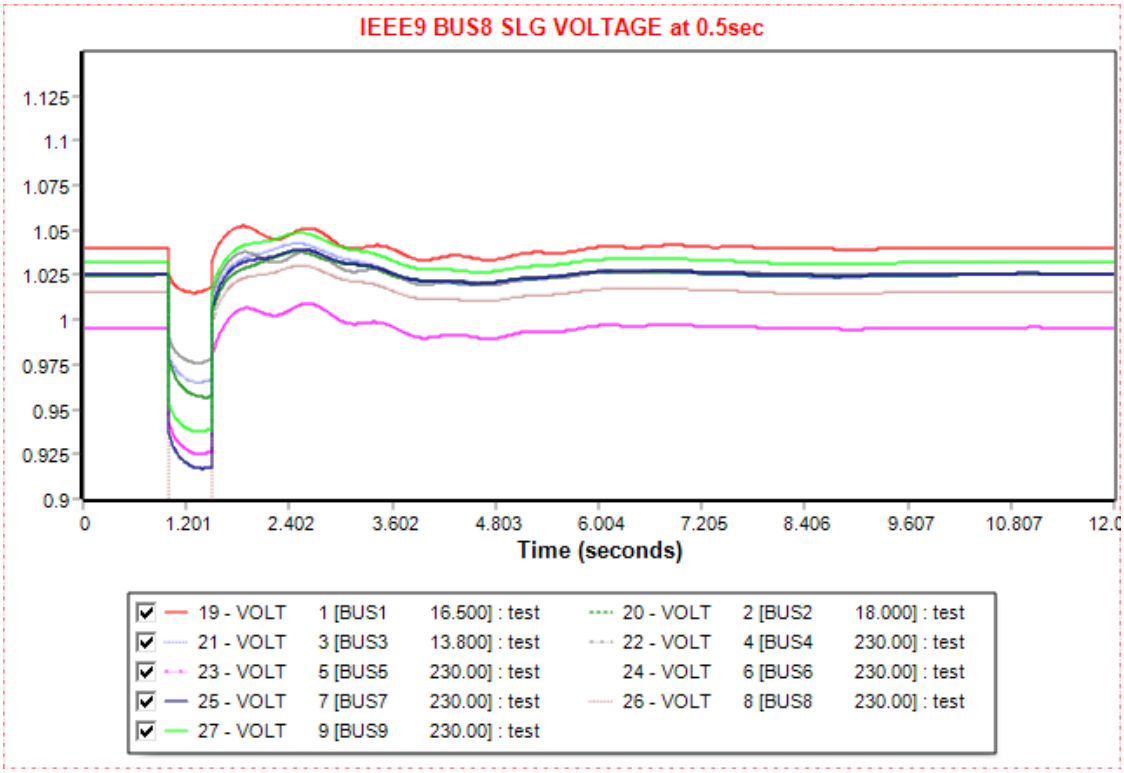

Figure 3. 40 Voltage plots of SLG fault at bus 8 when it is cleared at 1.5 sec at IEEE9 bus system

3.6 Diagram Analysis for the IEEE 9 Bus System

This section presents an analysis of the diagrams of the IEEE 9 Bus System simulation. In the relative power angle diagrams that have three-phase symmetrical faults at buses 2, 7 and 8 where the synchronization is not lost (Figures 3.8, 3.19, 3.30), the two generators' power angle with respect to the swing bus power angle are illustrated. The first swing of the generator 2 power angle is greater than of the generator 3. The upper and lower limits of the swings for plant 2 are around -25 degrees to 160 and for 3 around -30 to 75. It can be observed that the closer to the generator the fault is, the greater the oscillation limits are, justifying the smaller swings of generator 3 angle. Moreover, the different values of the generator modeling is a cause for this. After 4 sec of the fault occurrence, the system starts to become stable reaching the initial conditions. In Figures 3.13, 3.24, and 3.35 the generator 2 power-angle is completely desynchronized as it has exceeded the time necessary for the stability maintenance, and the power-angle increases exponentially. When the SLG fault occurs, the system has similar behavior like three-phase

symmetrical, but the oscillation swings are smaller around 20 to 40 degrees, as presented in Figures 3.14, 3.25, and 3.36. The main reason is because the SLG is weaker than the three-phase symmetrical.

The frequency diagrams between the three-phase symmetrical fault (Figures 3.9, 3.20, 3.31) and the SLG fault (Figures 3.15, 3.26, 3.37) are quite similar in the way they proceed through the simulation. They start to oscillate when the fault occurs, but after 4 sec they return to stability a little higher than the initial value, varying from 0.005 Hz to 0.01 Hz. In the three-phase diagrams the longer the fault is applied at a bus, the less impact it has in the frequency. That is the reason bus 2 has higher frequency width. The three-phase symmetrical limits of the oscillation are maxed around 0.2 Hz at the time of the impact. For SLG, it is from 0.01 Hz minimum and maximum around 0.006 Hz.

The active power plot diagrams refer to the three generators of the system. The three-phase symmetrical fault diagrams (Figure 3.10, 3.21, 3.32) and the SLG diagrams (Figure 3.16, 3.27, 3.38) have similar behavior but differ in the limits the real power reaches. The fluctuations in three-phase diagrams are greater comparing them to the SLG ones. Bus 2, which harbors a 163 MW generator has the biggest upper limit and along with generator at bus 3, it starts by increasing drastically after the fault is applied unlike the swing bus (red plot). The swing bus plot has the greatest fluctuation width than the other two. The closer the fault to the generator is, the bigger the damps can be. In the SLG the oscillations are very small, proving the impact of the SLG to be milder than the three-phase symmetrical except for Bus 2 (Figure 3.16) where the fault is happening at the generator bus and directly affects it.

The reactive power diagrams like the active power refer only to the three generator buses. Like the other diagrams, the three-phase symmetrical (Figure 3.11, 3.22, 3.33) and the SLG (Figure 3.17, 3.28, 3.39) have similar plot lines but the fluctuations of the reactive power are different. When the fault occurs, the reactive power's increase is greater than of the other two generators. After comparing them, generator 2 has bigger increase than generator 3. After 3 sec post-fault, the reactive powers start to stabilize in their initial values. The sudden increase is due to the excitation of the generators. In Figures 3.11, 3.22, and 3.33, the three-phase symmetrical diagrams, and the 3.17, the SLG fault at bus 2 diagram, the total increase in the reactive power can be around 4 pu, while in the other two Figures around 0.5 pu.

The voltage diagrams refer to all the buses, like the frequency diagrams. The voltages in the three-phase symmetrical fault diagrams (Figure 3.12, 3.23, 3.34) and the SLG voltage diagrams (Figure 3.18, 3.29, 3.40) have a similar behavior in all diagrams. The initial value is 1 pu and after the fault is applied, all voltages decrease. The closer the fault is to a bus, the larger the sudden decrease is. In Figure 3.12, where the fault is three-phase symmetrical and it happens at bus 2, the bus 2 voltage reaches 0 pu. The same thing happens in bus 7 voltage in Figure 3.23 and bus 8 voltage in Figure 3.34. The lowest limit is 0 pu in three-phase symmetricals while in the SLG case is around 0.9 pu for both bus 7 and bus 8 (Figure 3.29, 3.40) and 0.5 for bus 2 case (Figure 3.18). The larger decrease in SLG fault at bus 2 is because the generator that is inspected for desynchronization is the one that is connected in bus 2. After the fault all voltages gradually increase to their initial state. [4][5][7][8][15][18]

CHAPTER 4

WIND TURBINE GENERATOR TECHNOLOGY AND MODELLING

4.1 Basic Configuration of Wind Turbines

In this thesis, wind turbines will be placed on the IEEE 9 Bus System for transient stability analysis of an integrated wind energy power system. For that reason, an analysis of the wind turbines, and their usage in the PSSE, must be made. The wind turbines can be separated based on their axis's configuration, in HAWT (Horizontal axis wind turbine) and VAWT (Vertical axis wind turbine). Figure 4.1 presents these two types of wind turbines. [33] HAWT is the most popular type of wind turbine for wind energy covering a percentage of 99%. This type of wind turbine has an advantage over vertical rotor placement. Placing the entire rotor at the top of the pillar can provide higher wind speeds than placing it in low heights, and in advance, more kinetic energy. Moreover, HAWT has the advantage of better pitch blades, improved power capture, and structural performance. Also, they have longer usage, and thus they are more economically beneficial. One advantage VAWT has over HAWT is that they make less noise.[9][34][35]

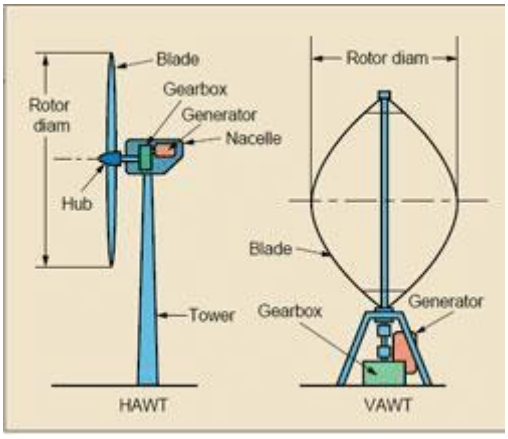

Figure 4.1 HAWT and VAWT [34]

4.2 Components of Wind Turbines

The components of the wind turbines are the pillar, the nacelle, and the rotor. Inside the nacelle, the generator is connected to the high-speed shaft, driven by the gearbox. There is also the controller and the low-speed shaft in this structure that gives the rational speed for the high-speed shaft. The low-speed shaft is connected to the rotor, which is a part of the blades that help produce kinetic energy. Under the nacelle, the yaw control system helps to turn the nacelle in the direction of the wind so that the produced energy can be maximized. The components of a HAWT with three blades can be seen in Figure 4.2. Depending on the usage of the wind turbine, many parts can present differences. HAWT can be upwind or downwind, considering the position of the rotor. This configuration changes the way the yaw control system is placed. Another different configuration of the components refers to the pitch. It can be variable or fixed, resulting in the blades rotating or not in their initial axis. While the fixed pitch is less expensive, they are not widely used because they cannot control loads as variable pitch and aerodynamic torque. [9][35]

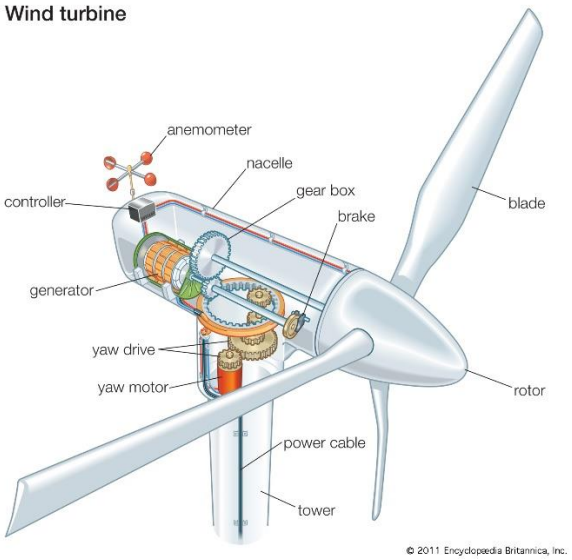

Figure 4. 2 Components of HAWT [36]

4.3 Wind Turbine Generator Types

The wind turbine generator (WTG) is the most crucial part of the wind turbine. Depending on the needs, it can be synchronous or asynchronous, but nowadays, in most cases, the asynchronous setting is most wanted because it has benefits in the maintenance of the synchronization within the grid. Wind turbine generators can have a variable or fixed speed. Based on that, there are four types of WTG (Figure 4.3) according to Western Electricity Coordinating Council (WECC):

- Type 1: Fixed-Speed Wind Turbines
- Type 2: Variable-Speed wind turbine with variable rotor resistance
- Type 3: Variable-Speed wind turbine with a double fed inductive generator (DFIG)
- Type 4: Variable-Speed wind turbine with full converter

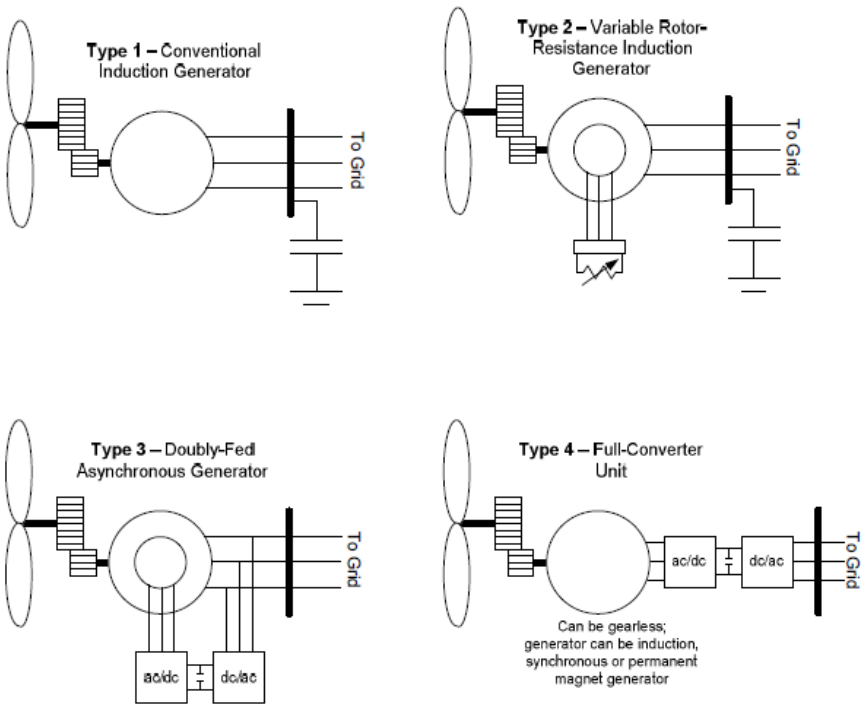

Figure 4. 3 The four types of WTG

4.3.1 Fixed-Speed Wind Turbine

A fixed-speed wind turbine is the first type of WTG. These turbines rotate at a standard speed determined by the frequency of the grid, the gear ratio, and the pole pairs of generators. That fact makes this type of WTG synchronous to the grid. As seen in Figure 4.3, this set requires a capacitor so that it does not take reactive power from the grid. They operate at a fixed speed, so there is no control, and they can easily destabilize a weak grid. This type of wind turbine causes great fluctuations in the initial voltage at the power flow, and after a fault, it tends to be unstable. For maintaining grid stability, often FACTS devices are used.[9]

4.3.2 Variable-Speed wind turbine with variable rotor resistance

Variable-Speed wind turbine with variable rotor resistance is the second type of wind turbine. The first type is unable to control speed and generator output, and the second type answers this problem. As stated in [34], variable resistance is integrated into the rotor of the wound rotor induction generator through slip rings using external resistors and power electronic devices and is directly connected to the grid. The second type of wind turbine requires reactive power from the grid, which is why it has a capacitor. The variable speed is attained in this type by altering the resistance of the rotor. [9]

4.3.3 Variable-Speed wind turbine with DFIG

DFIG wind turbine generator is an evolution of the second type of wind turbine generator. The third type's main advantage over the second is that its rotor and stator are directly connected with the AC-DC-AC converter, and thus it has better control and does not absorb reactive power from the grid. The power electronics added rectify the supplied voltage and, after a conversion, it is provided to the rotor for excitation. DFIG is one of the most popular wind turbine generators and is widely used, along with type 4, for academic purposes. [9][37][38]

4.3.4 Variable-Speed wind turbine with Full Conversion

The fourth type of WTG is, in contrast to the third, directly connected to the grid. This gives many possibilities for using the generator as it can be used as a permanent magnet synchronous generator and synchronous or asynchronous wound rotor induction generator. In most cases, it is used like the DFIG, but it has the advantage of using the full rated power in contrast to the latter, where there is a 20-30% decrease. In the modeling that is provided by the WECC and is used in many power system simulators, such as the PSS/E that this thesis uses, these two generators have one main difference, that the model takes as inputs both reactive and active current commands. That is because the converter control model delivers the active and reactive power to the system. This will be easier to understand in the next section, where the type 4 second-generation model is presented. Finally, another important fact that must be referenced is that type 3 DFIG is not preferred for unbalanced disturbances, and that is a reason a type 4 WTG is used.[9][37][38]

4.4 Wind Turbine Generator Modelling in PSS/E

In this thesis, the system of chapter 3, the IEEE9 Bus System, is remodeled and modified to study how it reacts after a three-phase symmetrical and a line phase fault occurs. For the simulation, the PSS/E supports all four models, and the one that we use is the second generation of type 4. As mentioned in the previous section, this model uses the converter to deliver the active and reactive current to the grid. The controller structure is like the type 3 second generation and uses logic to determine the current limits. The objective is not to exceed these limits. The control that is selected for this study is using reactive power, making the wind turbine used as a wound rotor inductive generator. In Figure 4.4, the overall structure of the wind turbine generator can be seen. Every wind turbine of the farm is around 2.5 MW total installed capacity. [37][38][39]

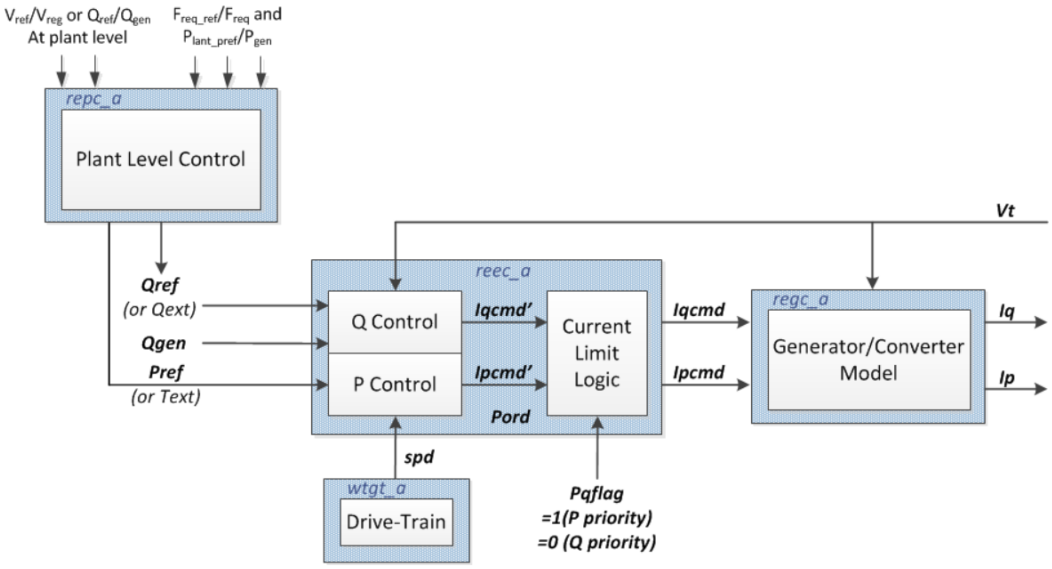

Figure 4. 4 Overall Structure of the WTG Type 4 (Phase ii)

The overall structure of Type 4 second-generation wind turbine generator can be used in PSS/E and consists of 4 main parts as is presented by WECC in source [40]:

1. The renewable energy generator/converter model (*regc_a*), which has inputs of real (*Ipcmd*) and reactive (*Iqcmd*) current command and outputs of real (*Ip*) and reactive (*Iq*) current injection into the grid model. The parameters and their structure can be seen in Figure 4.5.

2. The renewable energy electrical controls model (*reec_a*), which has inputs of real power reference (*Pref*) that can be externally controlled, reactive power reference (*Qref*) that can be externally controlled, and feedback of the reactive power generated (*Qgen*). The outputs of this model are the real (*Ipcmd*) and reactive (*Iqcmd*) current command. The parameters and their structure can be seen in Figure 4.6.

3. The emulation of the wind turbine generator driven-train (*wtgt_a*) for simulating drive-train oscillations. The output of this model is speed (*spd*). In this case, speed is assumed to be a vector spd = [ω_t ω_g], where ω_t is the turbine speed and ω_g the generator speed. The parameters and their structure can be seen in Figure 4.7.

4. A simple renewable energy plant controller (*repc_a*), which has inputs of either voltage reference (*Vref*) and measured/regulated voltage (*Vreg*) at the plant level,

or reactive power reference (*Qref*) and measured (*Qgen*) at the plant level. The output of the repc_a model is a reactive power command that connects to *Qref* on the reec_a model. Note: presently this plant controller can control only one aggregated WTG model representing a single plant with the same type of WTG. The parameters and their structure can be seen in Figure 4.8. It is important to say that the DFIG type 3 WTG uses these 4 parts also in PSS/E. [40]

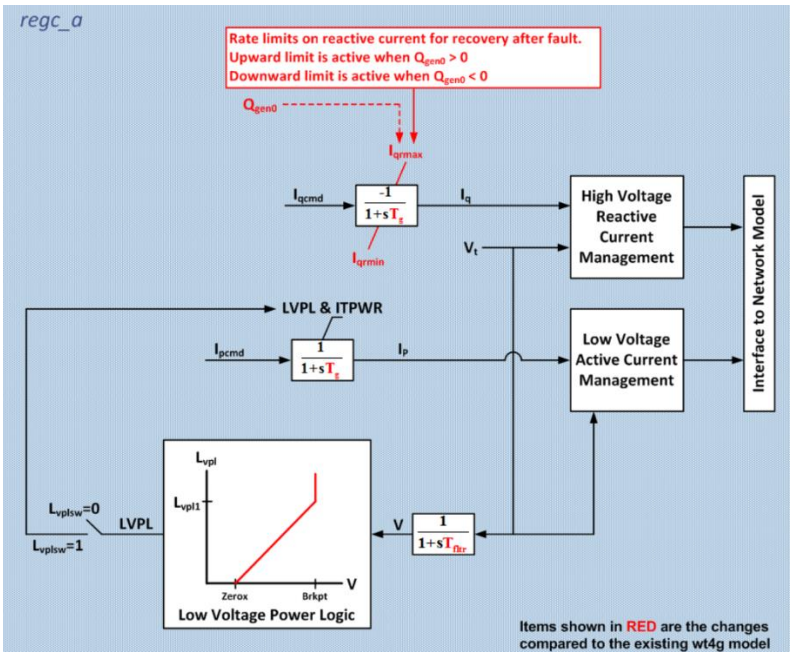

Figure 4. 5 REGC_A

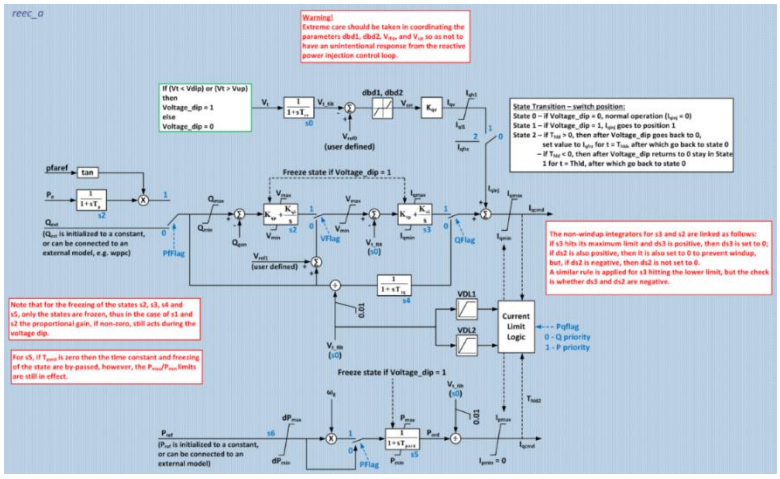

Figure 4. 6 REEC_A

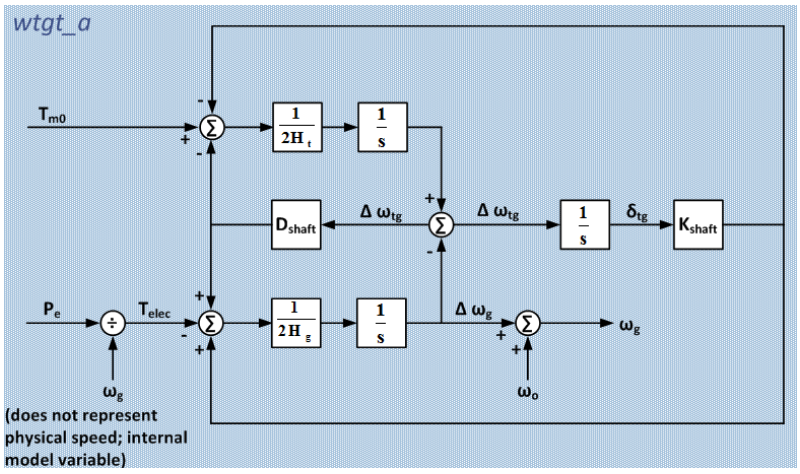

Figure 4. 7 WTGT_A

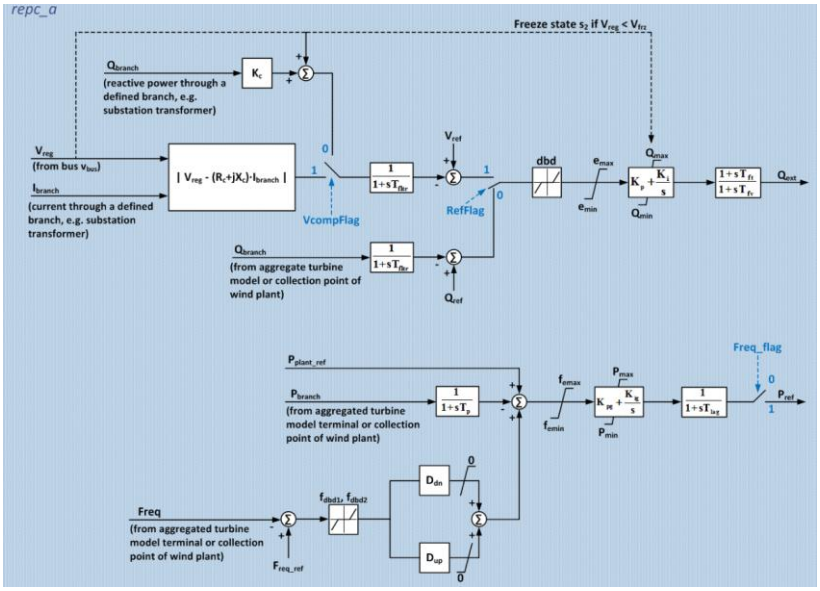

Figure 4. 8 REPC_A

CHAPTER 5

WIND POWER SIMULATION RESULTS

An induction WTG type 4 presented in the previous chapter is used to integrate wind energy in the IEEE9 Bus System. The inductive wind turbine is illustrated in Figure 5.1. In this chapter, four scenarios expand the initial analysis in chapter 3. For each scenario, a transient stability analysis is made to examine how the system operates after a disturbance. Moreover, for all the simulations, the CFCT is calculated. The wind turbine's insertion was made using the Siemens Guide for second-generation wind turbines [38] as reference. The four scenarios that remodel the standard IEEE 9 Bus System are:

SCENARIO 1: IEEE9 Bus System Wind Power Remodeled with the Replacement of Generator 3.

SCENARIO 2: IEEE9 Bus System Wind Power Remodeled with the Partial Replacement (50%) of Generator 3.

SCENARIO 3: IEEE9 Bus System Wind Power Remodeled with the Partial Replacement (50%) of Generator 3 and the Addition of the other 50% at bus 8.

SCENARIO 4: IEEE9 Bus System Wind Power Remodeled with the Partial Replacement (50%) of Generator 2 and the Addition of the other 50% at bus 8.

The simulations are implemented in PSS/E software, and the process is the same as in the initial simulation in section 3.4. First, the PSS/E reads the remodeled IEEE9 Bus System data (impedances, loads, transmission line data, etc.) followed by a power flow. If, after the power flow, the network converges, then the generators and the data are converted to be used as dynamic data, else the network data must be corrected. The next step is the dynamic data reading and the output channels' setting to illustrate the diagrams. Then, the system is initialized, and if the dynamic data are acceptable and there is no error, the simulation begins. There is a steady-state run for 1 sec, and then the disturbance occurs. After a certain amount of time, the fault is cleared, and a line is tripped. 1 sec later, the line is connected, and the system runs until 12 sec. That way, depending on the system synchronization, the critical fault clearing time can be calculated. As was mentioned in

chapter 3, there are two types of faults, a three-phase symmetrical and an SLG, at buses 2, 7, and 8. When the fault occurs at bus 2, line 2-7 is tripped. When it is applied at bus 7, line 7-8 is tripped, and when the fault occurs at bus 8, line 8-7 is opened. The wind turbine model benefits system stability, and for that reason, it makes some faults, especially SLG, not severe for the grid. In these cases, the fault will have a duration of 0.5 sec. Just like the initial transient stability analysis, there are five or six diagrams that are going to be analyzed:

- The relative power angle of generator connected at bus 2 or 3 with respect to the power angle of bus 1 (swing bus), when the fault is cleared at the critical time.
- The active power of the generators at the critical time.
- The reactive power of the generators at the critical time.
- The frequency of all the buses at the critical time.
- The voltage of all the buses at the critical time.
- The relative power angle of the generators in relation to the power angle of the swing bus 1 for fault duration equals to CFTC increased by 0.05 sec and the appearance of desynchronization.

For the reactive and active power components of the grid, the base is 100MVAR and 100MW. Before the diagram presentation of each case, there is a table that shows the plants' initial real and reactive power.

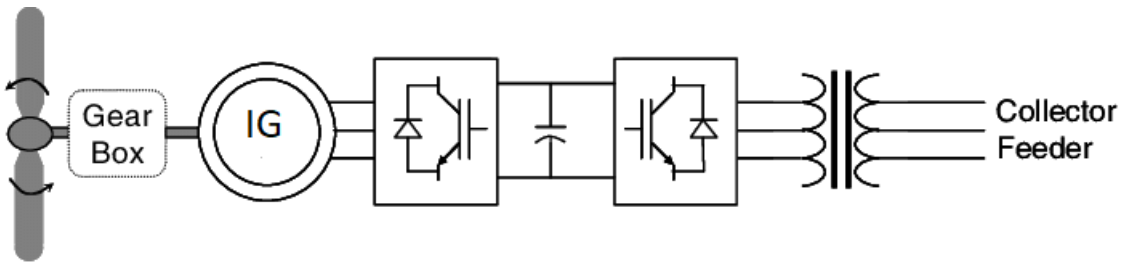

Figure 5. 1 Induction Wind Turbine Generator Type 4

5.1 SCENARIO 1: IEEE9 Bus System Wind Power Remodeled with the Replacement of Generator 3

In the IEEE9 Bus System Wind Power Remodeled with the Replacement of Generator 3, the generator connected to bus 2 remains, and the 85.5 MW generator connected to bus 3 is replaced with a wind farm that produces the same amount of power. In Figure 5.2, the remodeled system designed in PSS/E is presented. In Table 5.1, the initial power flow of the active and reactive power is presented with a base of 100MVA. The wind farm's real and reactive power is 0.85 pu, or 85 MW, and 0 pu, respectively, which is desired.

Table 5. 1 Active and Reactive power generation of the IEEE9 Bus System Wind Power Remodeled with the Replacement of Generator 3

GENERATOR	Active Power (pu)	Reactive Power (pu)
BUS 1 (Swing Bus)	0.715	0.20651
BUS 2	1.63	0.007
BUS 3 (Wind Power)	0.85	0

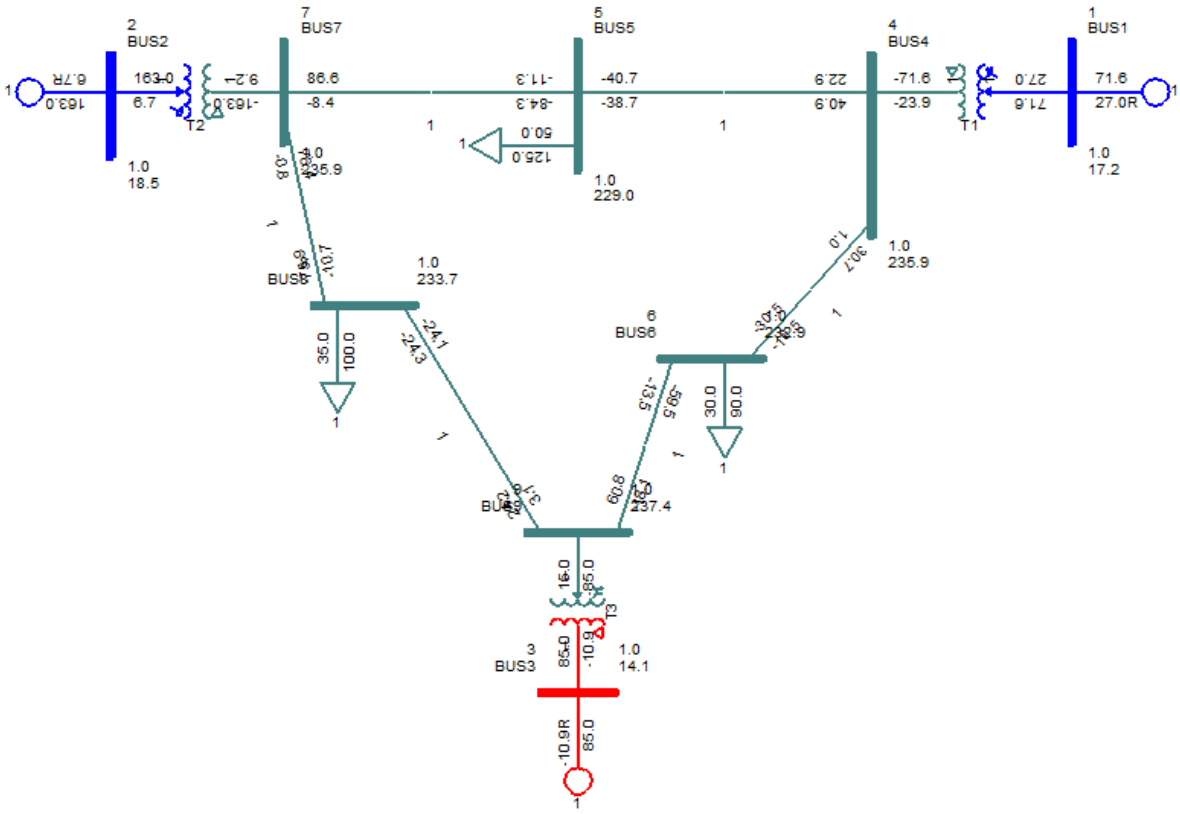

Figure 5. 2 IEEE9 Bus System Wind Power Remodeled with the Replacement of Generator 3

5.1.1 Faults at Bus 2 of the IEEE9 Bus System Wind Power Remodeled with the Replacement of Generator 3

The disturbance is expected to be more severe for the network as a wind farm replaces a synchronous generator. Moreover, a possible outcome of the plots is oscillations due to the wind turbine model.

5.1.1.1 Three-phase Symmetrical Fault at Bus 2 of the IEEE9 Bus System Wind Power Remodeled with the Replacement of Generator 3

The CFCT was calculated to be 0.2 sec from the simulation, meaning the duration of the three-phase symmetrical is 0.2 sec for the system stability. In the beginning, the system is for 1 sec in steady-state condition, and then a three-phase symmetrical fault is applied. Next step is the clearance of the fault at 1.2 sec and the concurrent opening of line 2-7. After 1 sec, at 2.2 sec, line 2-7 is reclosed again, and the system continues the load flowing

until 12 sec. All the process is presented in Table 5.2. Figures 5.3-5.7 illustrate the power angle of generator 2 with respect to the power angle of the swing bus, the buses frequency, the real and active power of the generators, including the one producing wind power, and the buses voltage when the fault is cleared at CFCT. Figure 5.8 shows the loss of synchronization of the power angle of generator 2 with respect to the power angle of the swing bus when the fault is cleared 0.05 sec after the CFCT.

Table 5. 2 IEEE9 Bus System Wind Power Remodeled with the Replacement of Generator 3 Three-phase symmetrical Fault at Bus 2

Action	**Time (sec)**
Steady-state	0.00
Apply Fault	1.00
Clear Fault	1.2
Trip Line	1.2
Connect Line	2.2
Power Flow	12.00

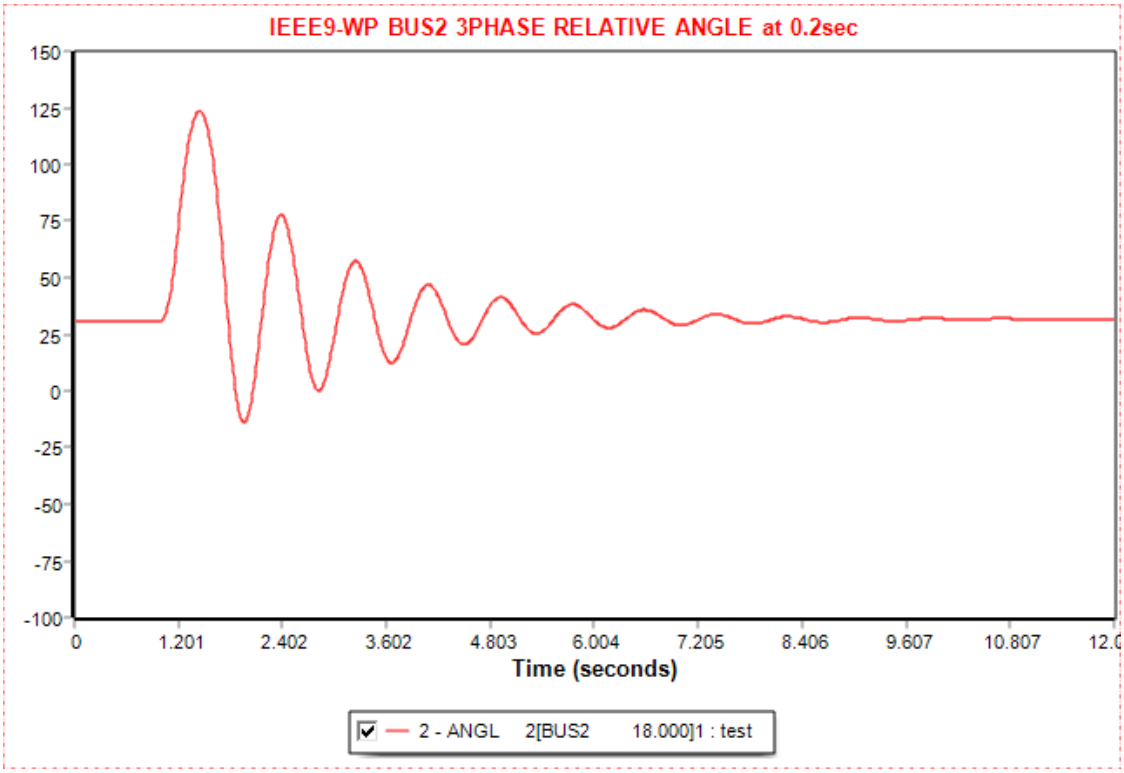

Figure 5. 3 Relative power angle plots of three-phase symmetrical fault at bus 2 when it is cleared at 1.2 sec at IEEE9 Bus System Wind Power Remodeled with the Replacement of Generator 3

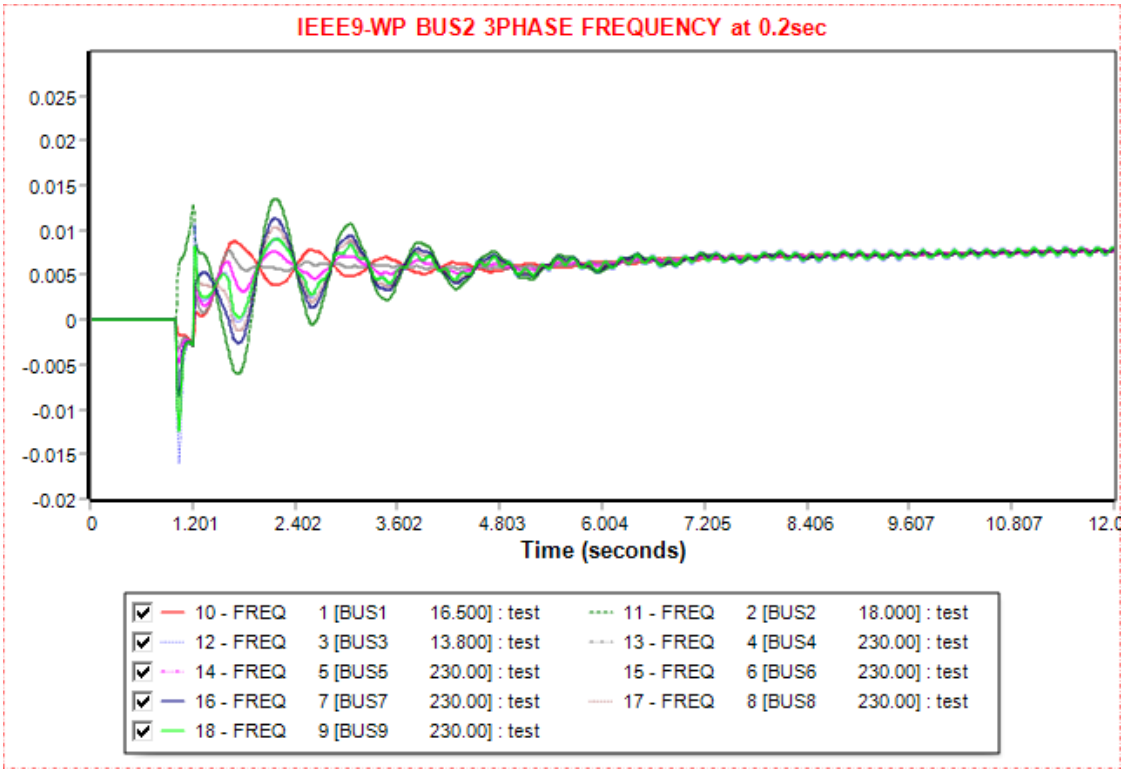

Figure 5. 4 Frequency plots of three-phase symmetrical fault at bus 2 when it is cleared at 1.2 sec at IEEE9 Bus System Wind Power Remodeled with the Replacement of Generator 3

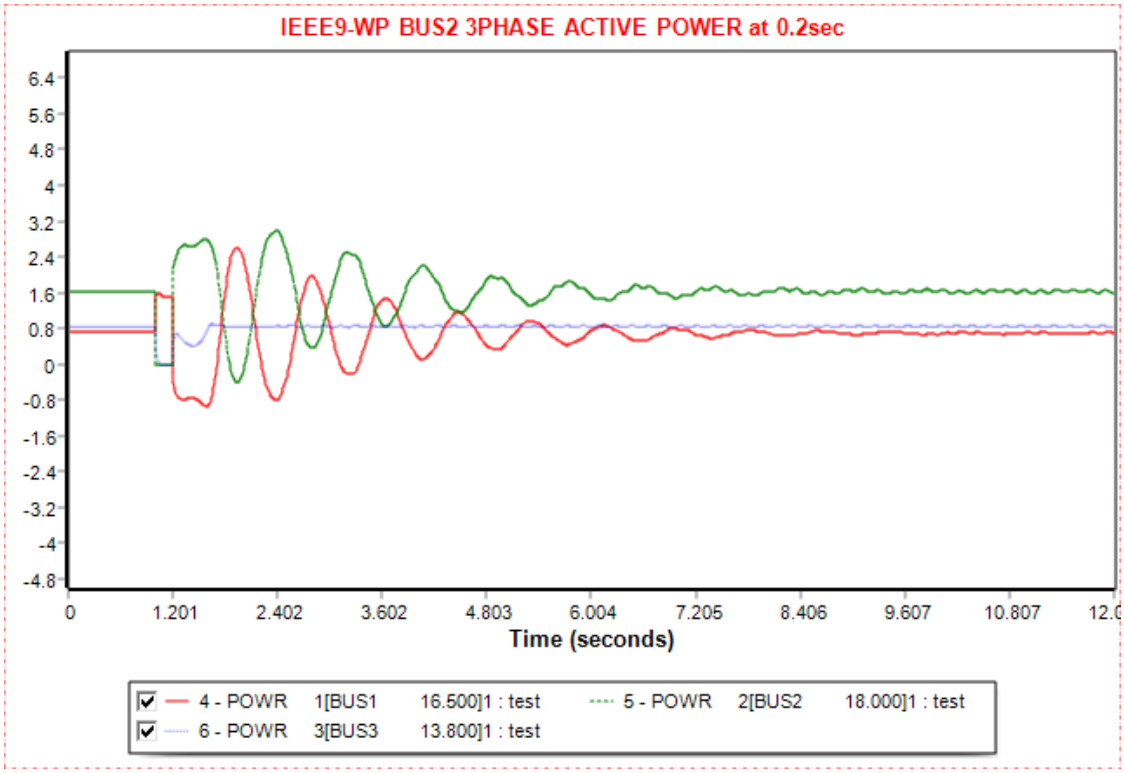

Figure 5. 5 Active Power plots of three-phase symmetrical fault at bus 2 when it is cleared at 1.2 sec at IEEE9 Bus System Wind Power Remodeled with the Replacement of Generator 3

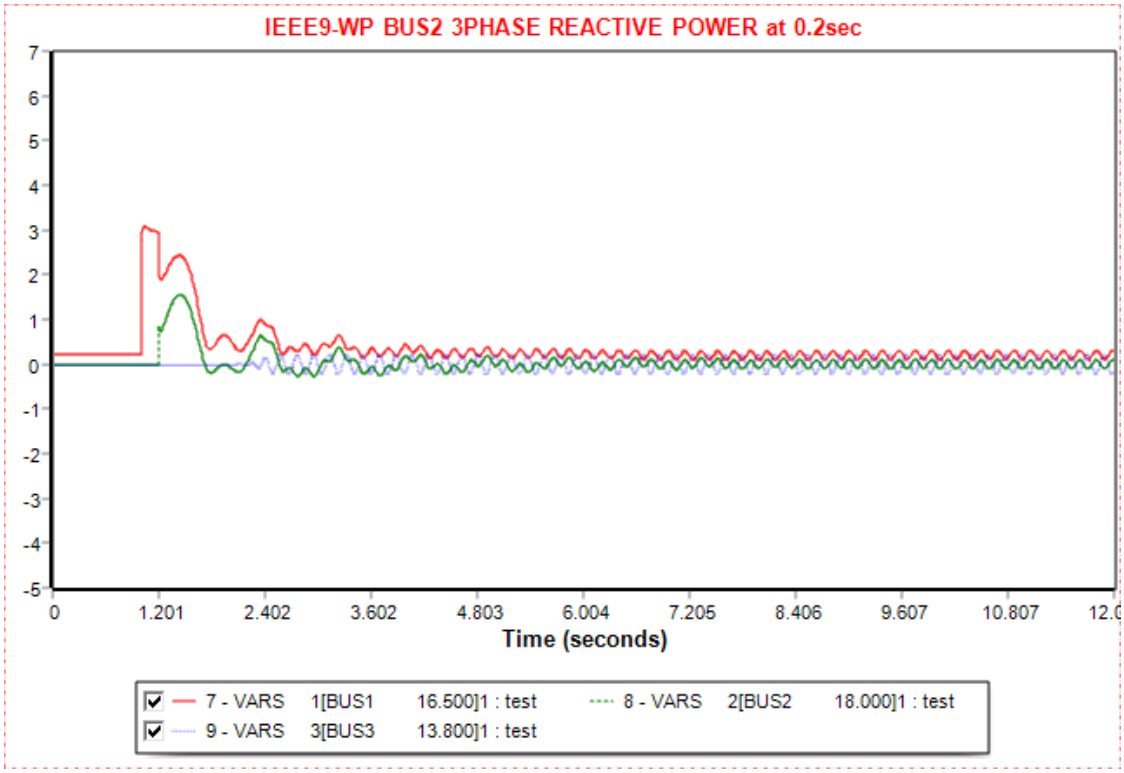

Figure 5. 6 Reactive Power plots of three-phase symmetrical fault at bus 2 when it is cleared at 1.2 sec at IEEE9 Bus System Wind Power Remodeled with the Replacement of Generator 3

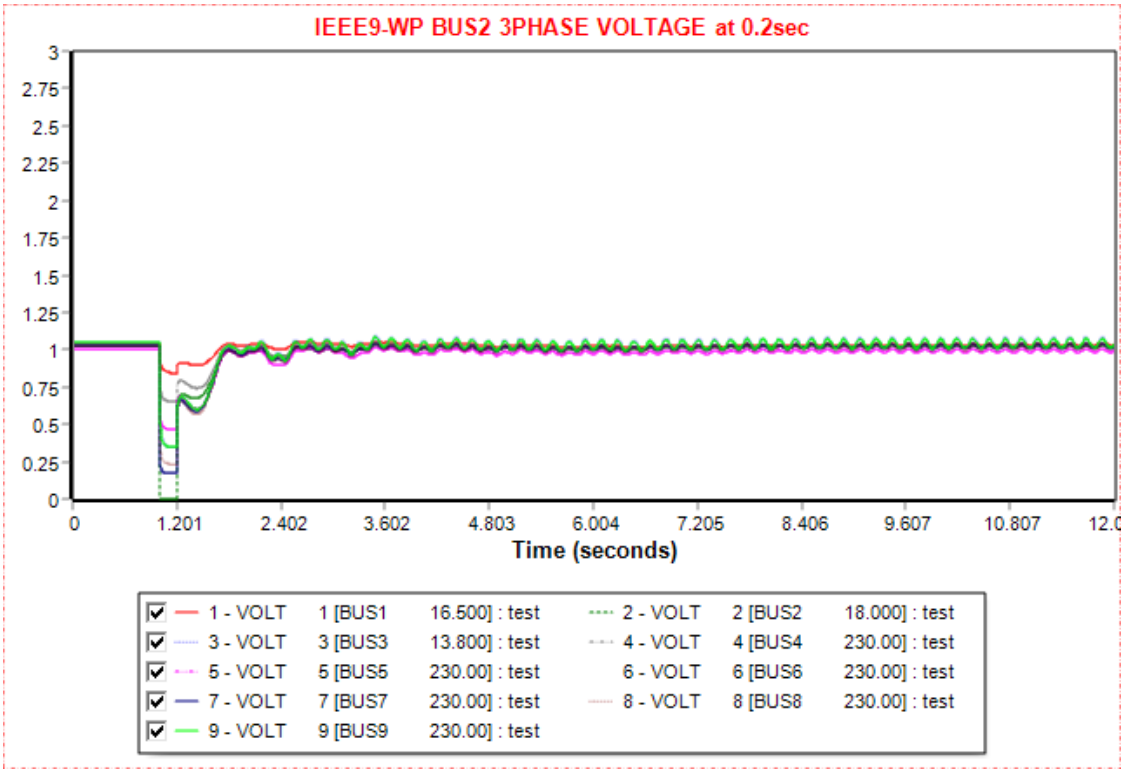

Figure 5. 7 Voltage plots of three-phase symmetrical fault at bus 2 when it is cleared at 1.2 sec at IEEE9 Bus System Wind Power Remodeled with the Replacement of Generator 3

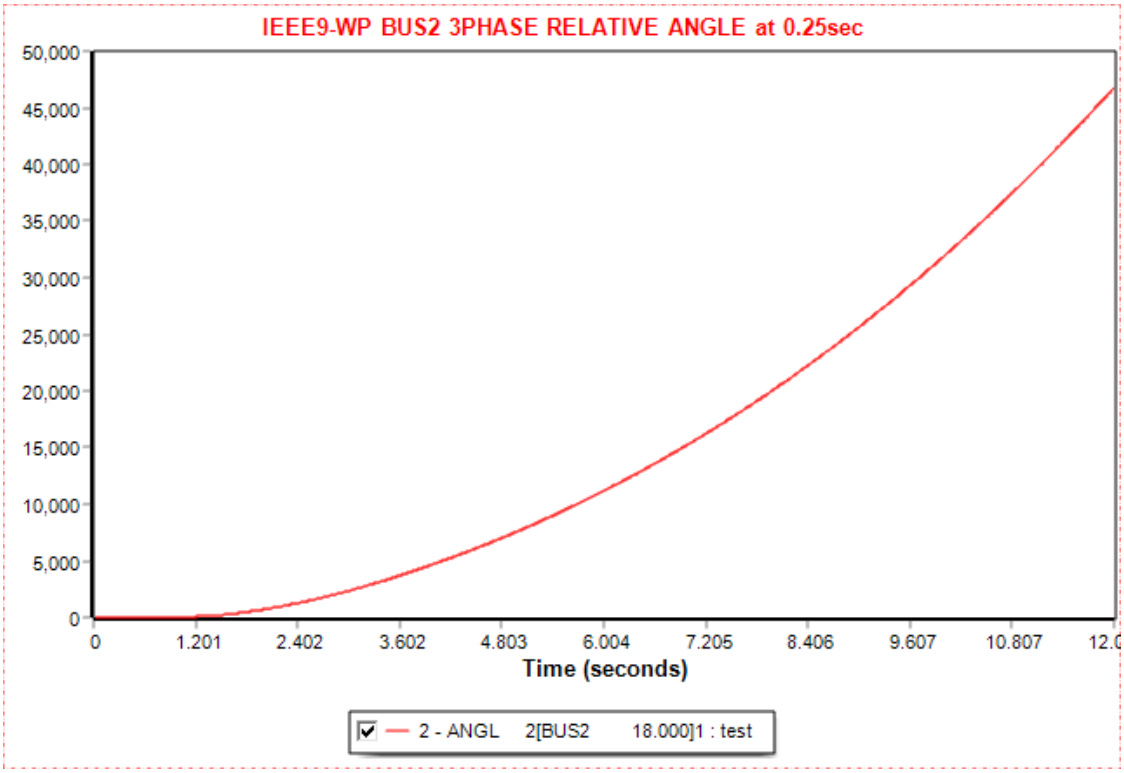

Figure 5. 8 Relative power angle plots of three-phase symmetrical fault at bus 2 when it is cleared at 1.25 sec at IEEE9 Bus System Wind Power Remodeled with the Replacement of Generator 3

5.1.1.2 SLG Fault at Bus 2 of the IEEE9 Bus System Wind Power Remodeled with the Replacement of Generator 3

The situation is similar as in section 5.1.1.1, with the type of the fault being SLG instead of balanced three-phase. In contrast to the 0.2 sec, in this simulation, the CFCT is 0.9 sec. After the load-flow for 1 sec, an SLG fault is applied for 0.9 sec at bus 2. At the same time, for the clearance of the fault the line 2-7 is tripped and at 1.9 sec, is connected again in the system. As shown in Table 5.3, the simulation lasts for 12 sec. Figures 5.9-5.13 illustrate the power angle of generator 2 with respect to the power angle of the swing bus, the buses frequency, the real and active power of the generators, including the one producing wind power, and the buses voltage when the fault is cleared at CFCT. Figure 5.14 shows the loss of synchronization of the power angle of generator 2 with respect to the power angle of the swing bus when the fault is cleared 0.05 sec after the CFCT. Judging from the CFCT, the SLG fault compared to the three-phase is milder but has an impact as the rotor excitation is considerable.

Table 5. 3 IEEE9 Bus System Wind Power Remodeled with the Replacement of Generator 3 Three-phase symmetrical Fault at Bus 2

Action	**Time (sec)**
Steady-state	0.00
Apply Fault	1.00
Clear Fault	1.9
Trip Line	1.9
Connect Line	2.9
Power Flow	12.00

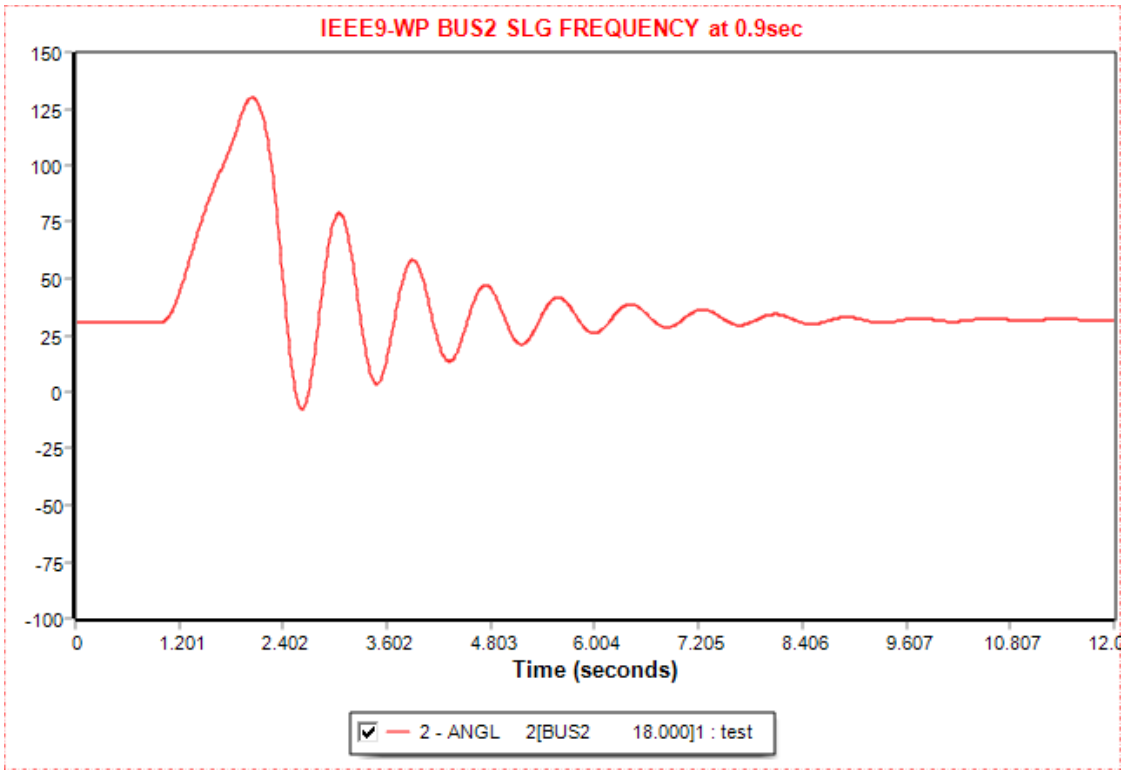

Figure 5. 9 Relative power angle plots of SLG fault at bus 2 when it is cleared at 1.9 sec at IEEE9 Bus System Wind Power Remodeled with the Replacement of Generator 3

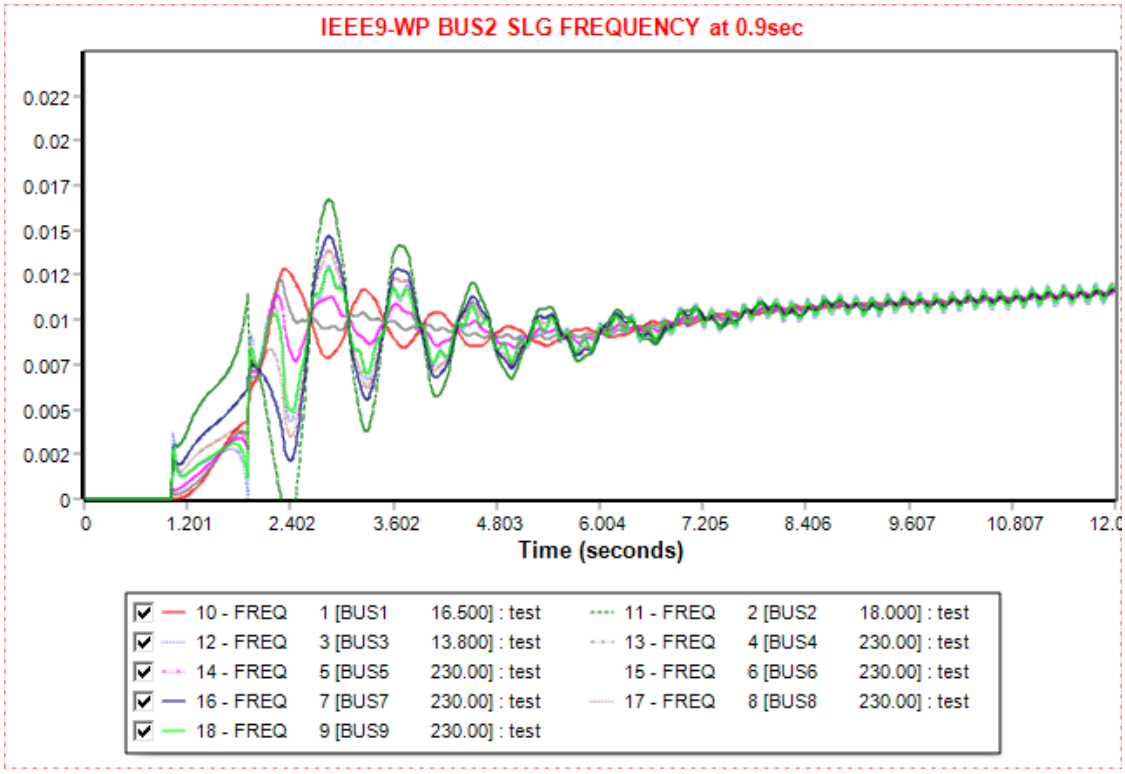

Figure 5. 10 Frequency plots of SLG fault at bus 2 when it is cleared at 1.9 sec at IEEE9 Bus System Wind Power Remodeled with the Replacement of Generator 3

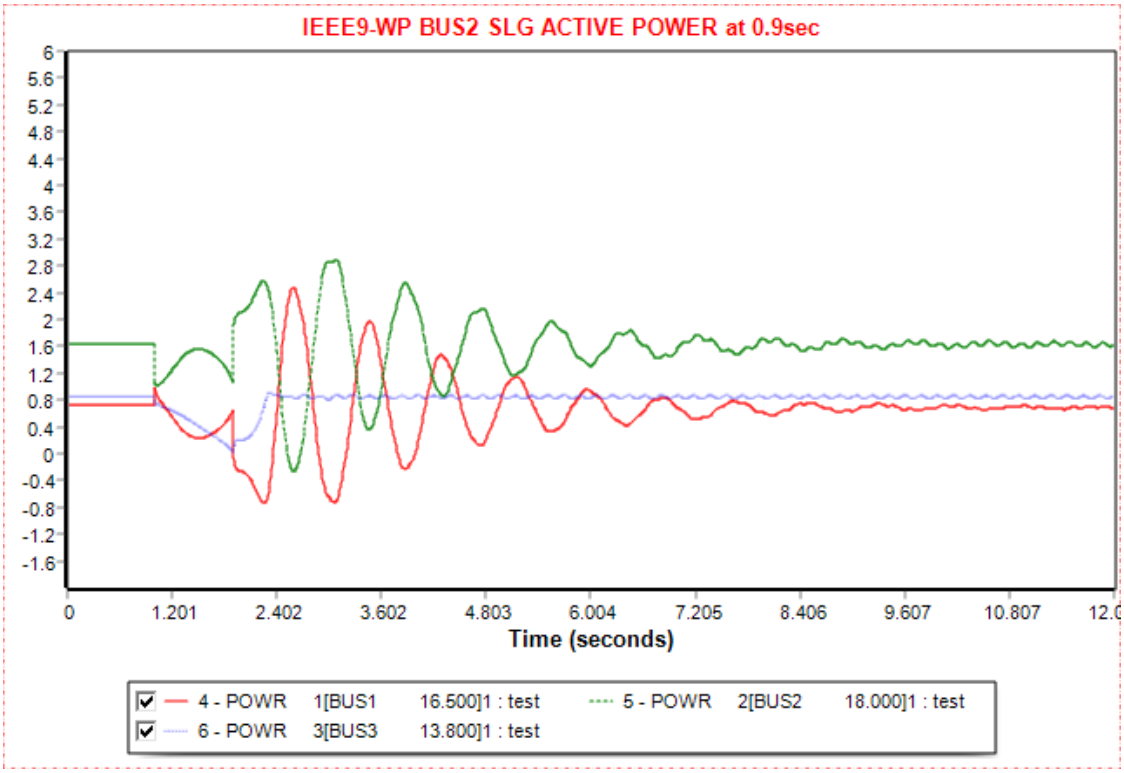

Figure 5. 11 Active Power plots of SLG fault at bus 2 when it is cleared at 1.9 sec at IEEE9 Bus System Wind Power Remodeled with the Replacement of Generator 3

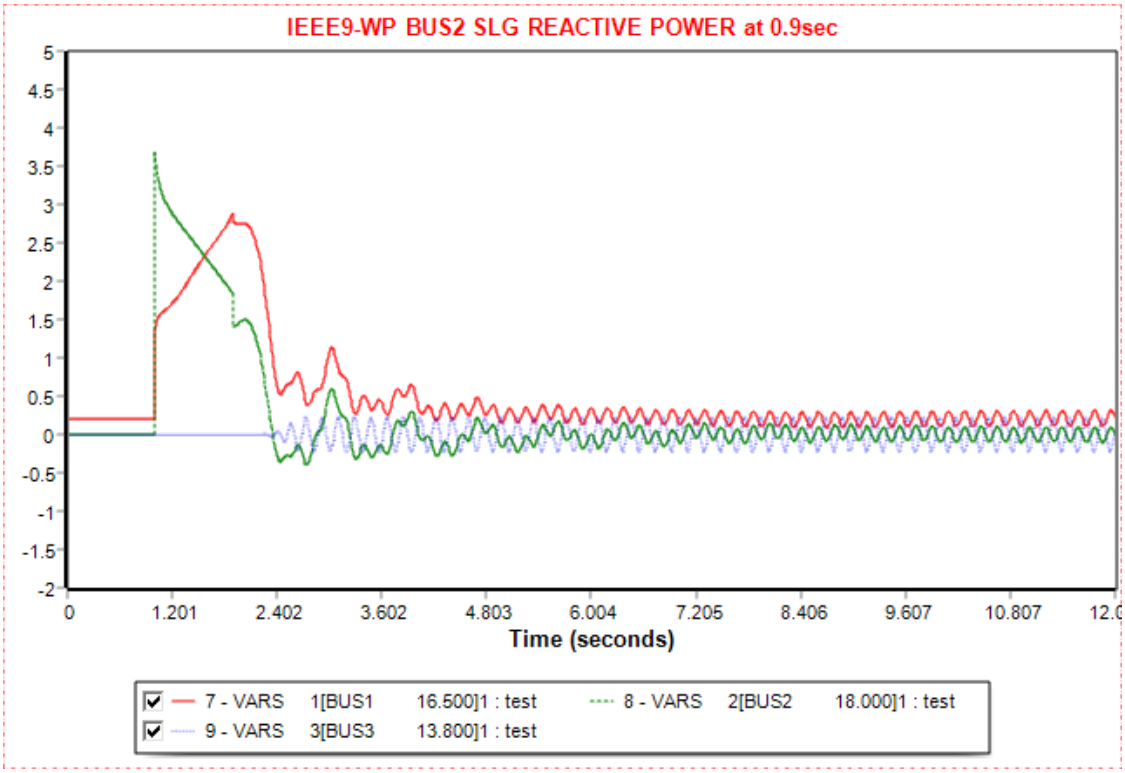

Figure 5. 12 Reactive Power plots of SLG fault at bus 2 when it is cleared at 1.9 sec at IEEE9 Bus System Wind Power Remodeled with the Replacement of Generator 3

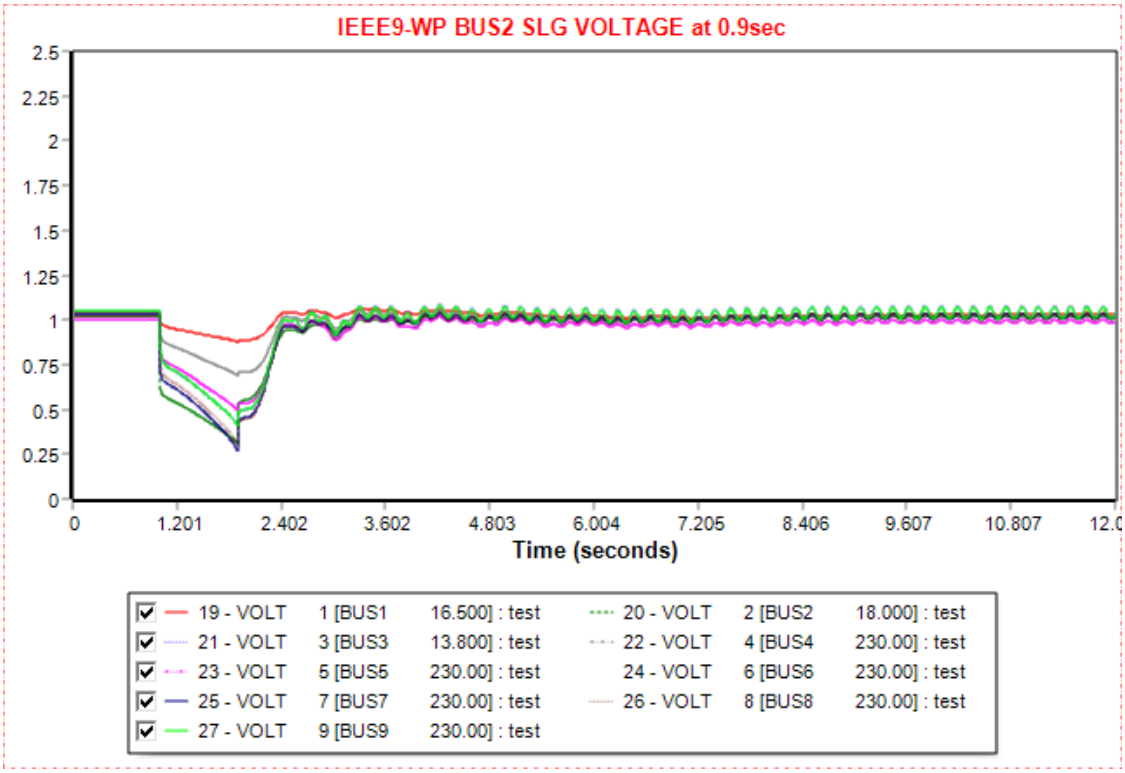

Figure 5. 13 Voltage plots of SLG fault at bus 2 when it is cleared at 1.9 sec at IEEE9 Bus System Wind Power Remodeled with the Replacement of Generator 3

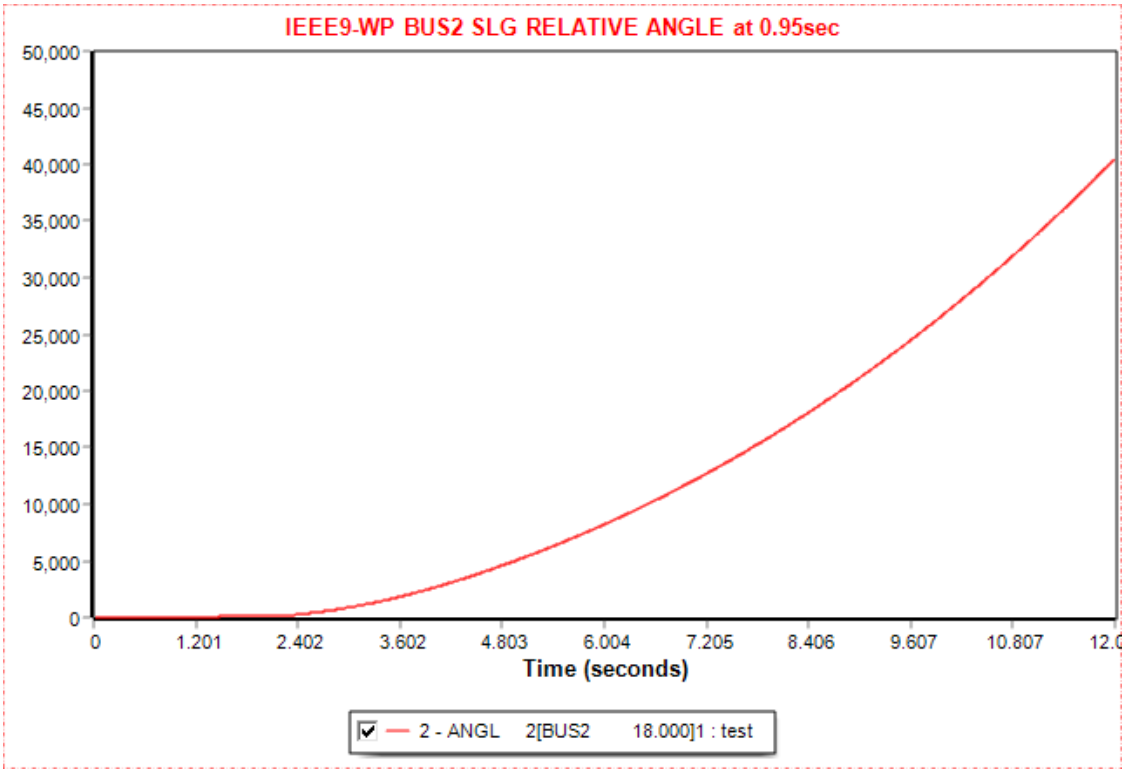

Figure 5. 14 Relative power angle plots of SLG fault at bus 2 when it is cleared at 1.95 sec at IEEE9 Bus System Wind Power Remodeled with the Replacement of Generator 3

5.1.2 Faults at Bus 7 of the IEEE9 Bus System Wind Power Remodeled with the Replacement of Generator 3

Bus 7 is neither a generator bus nor has a load. It is expected in this simulation the faults to have less impact than in bus 2.

5.1.2.1 Three-phase Symmetrical Fault at Bus 7 of the IEEE9 Bus System Wind Power Remodeled with the Replacement of Generator 3

The network's standard operation is ensured if the three-phase symmetrical fault should not exceed 0.2 sec, which is the CFCT. There is an initial power flow for 1 sec, and then the disturbance is applied for 0.2 sec. Simultaneously, for the fault clearance the line 7-8 is tripped and after 1 sec, at 2.2 sec, it is connected to the network. As seen from Table 5.4, the simulation lasts for 12 sec. Figures 5.15-5.19 present the power angle of generator 2 with respect to the power angle of the swing bus, the buses frequency, the real and active power of the generators, including the one producing wind power, and the buses voltage when the fault is cleared at CFCT. Figure 5.20 shows the loss of synchronization of the power angle of generator 2 with respect to the power angle of the swing bus when the fault is cleared 0.05 sec after the CFCT. Comparing the CFCTs of this simulation and the one in 5.1.1.1, they are expected to be the same due to their distance with generator 2.

Table 5. 4 IEEE9 Bus System Wind Power Remodeled with the Replacement of Generator 3 Three-phase symmetrical Fault at Bus 7

Action	Time (sec)
Steady-state	0.00
Apply Fault	1.00
Clear Fault	1.2
Trip Line	1.2
Connect Line	2.2
Power Flow	12.00

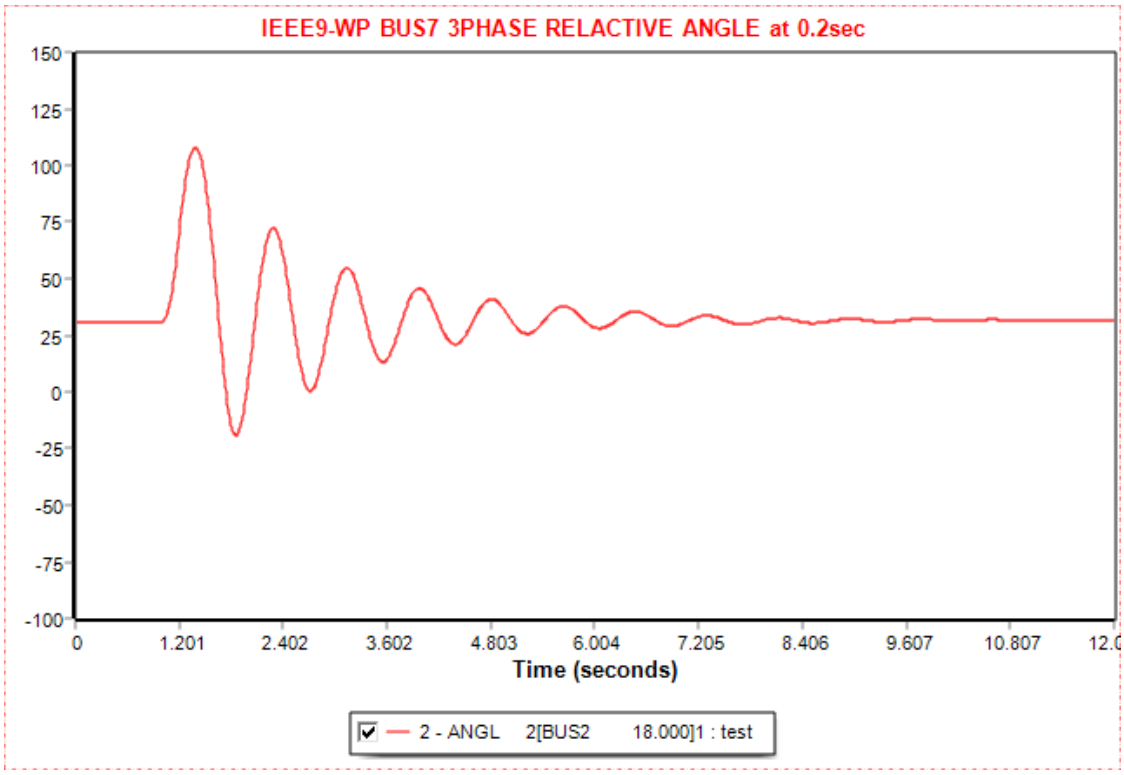

Figure 5. 15 Relative power angle plots of three-phase symmetrical fault at bus 7 when it is cleared at 1.2 sec at IEEE9 Bus System Wind Power Remodeled with the Replacement of Generator 3

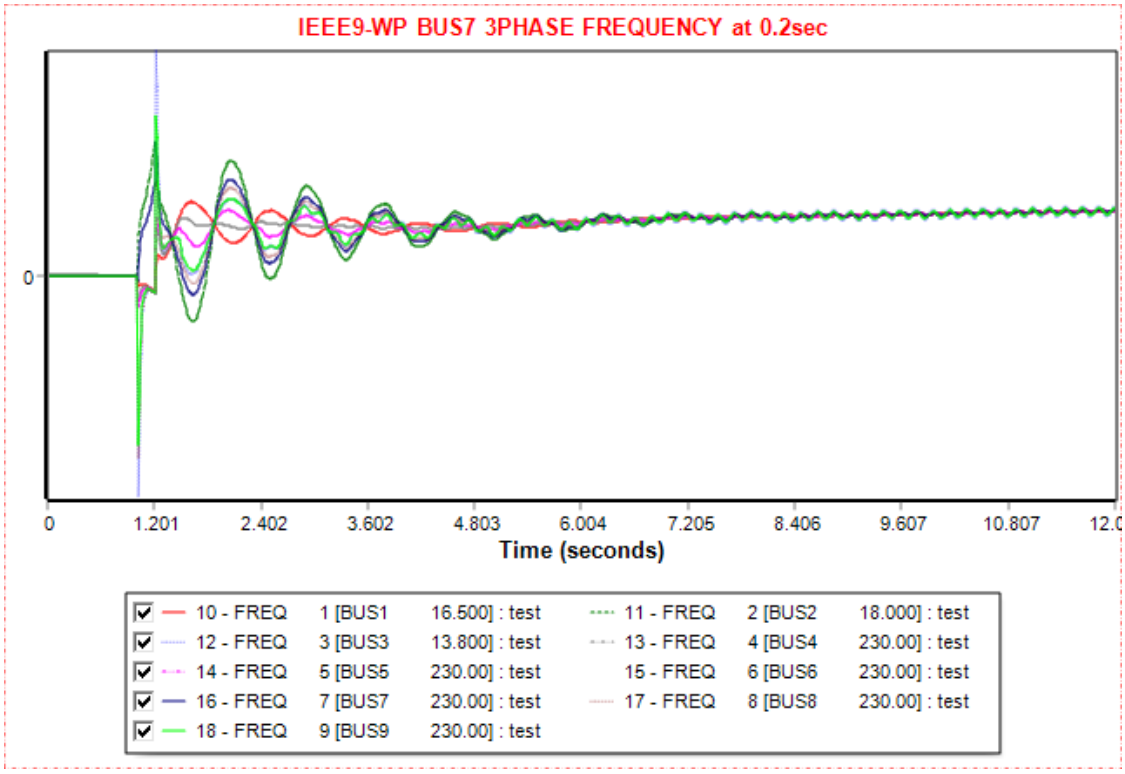

Figure 5. 16 Frequency plots of three-phase symmetrical fault at bus 7 when it is cleared at 1.2 sec at IEEE9 Bus System Wind Power Remodeled with the Replacement of Generator 3

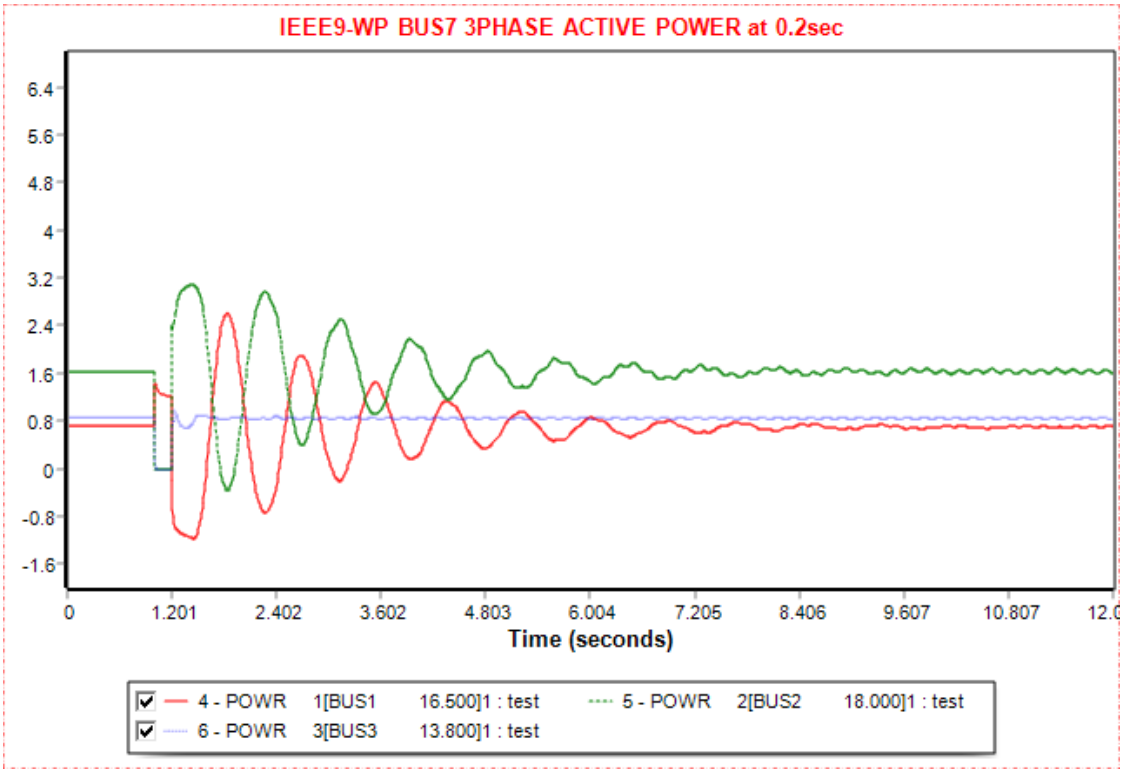

Figure 5. 17 Active power plots of three-phase symmetrical fault at bus 7 when it is cleared at 1.2 sec at IEEE9 Bus System Wind Power Remodeled with the Replacement of Generator 3

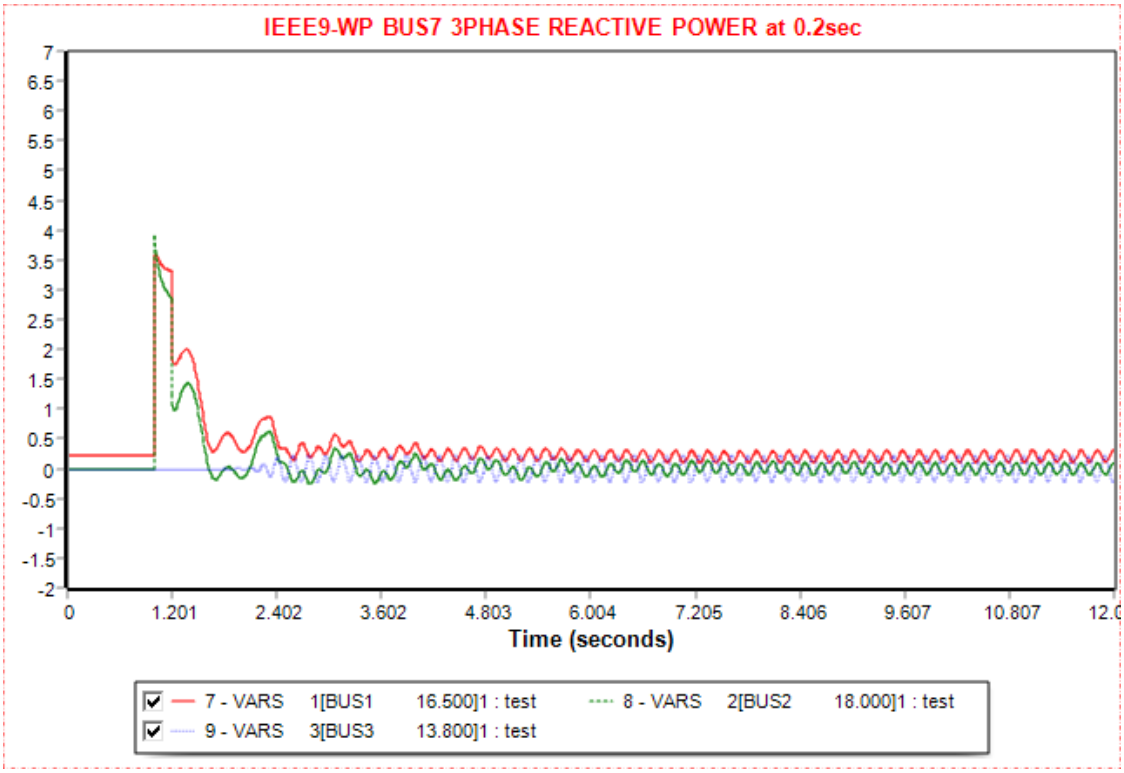

Figure 5. 18 Reactive power plots of three-phase symmetrical fault at bus 7 when it is cleared at 1.2 sec at IEEE9 Bus System Wind Power Remodeled with the Replacement of Generator 3

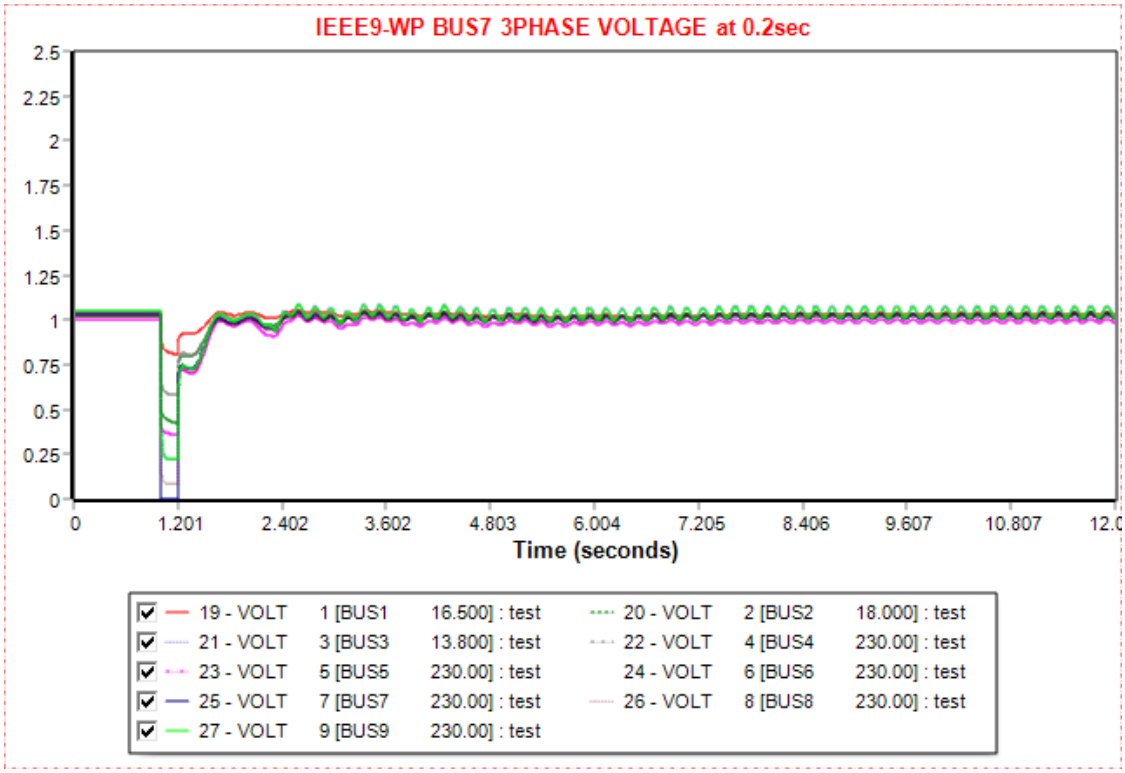

Figure 5. 19 Voltage plots of three-phase symmetrical fault at bus 7 when it is cleared at 1.2 sec at IEEE9 Bus System Wind Power Remodeled with the Replacement of Generator 3

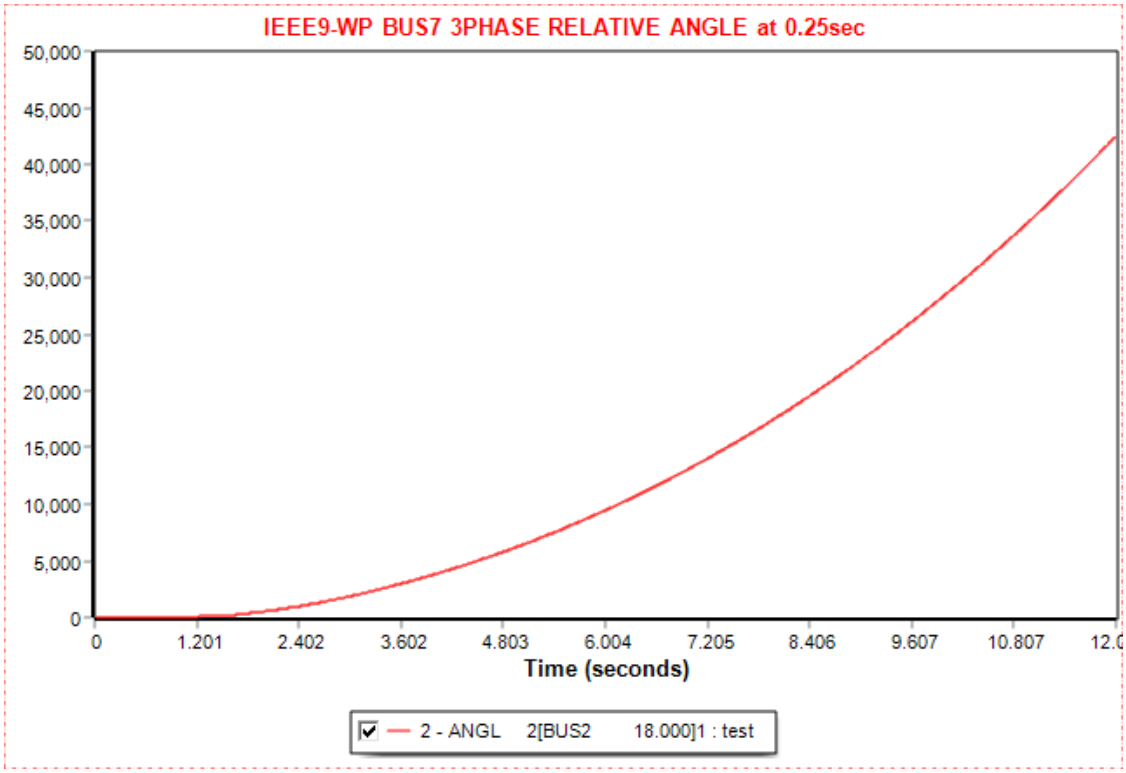

Figure 5. 20 Relative power angle plots of three-phase symmetrical fault at bus 7 when it is cleared at 1.25 sec at IEEE9 Bus System Wind Power Remodeled with the Replacement of Generator 3

5.1.2.2 SLG Fault at Bus 7 of the IEEE9 Bus System Wind Power Remodeled with the Replacement of Generator 3

The network can maintain its stability despite the duration of the SLG fault. The fault is cleared at 0.5 sec to study the transient behavior of the system, as there is no CFCT. Firstly, there is an initial power flow for 1 sec and then the disturbance is applied for 0.5 sec. Simultaneously, for the fault clearance the line 7-8 is tripped and after 1 sec, at 2.5 sec, it is connected to the network. As seen from Table 5.4 the simulation lasts for 12 sec. Figures 5.21-5.25 present the power angle of generator 2 with respect to the power angle of the swing bus, the buses frequency, the real and active power of the generators, including the one producing wind power, and the buses voltage when the fault is cleared at 0.5 sec. In contrast to the SLG at bus 2, the fault has less impact as there is distance from the generator at bus 2.

Table 5. 5 IEEE9 Bus System Wind Power Remodeled with the Replacement of Generator 3 SLG Fault at Bus

Action	**Time (sec)**
Steady-state	0.00
Apply Fault	1.00
Clear Fault	1.5
Trip Line	1.5
Connect Line	2.5
Power Flow	12.00

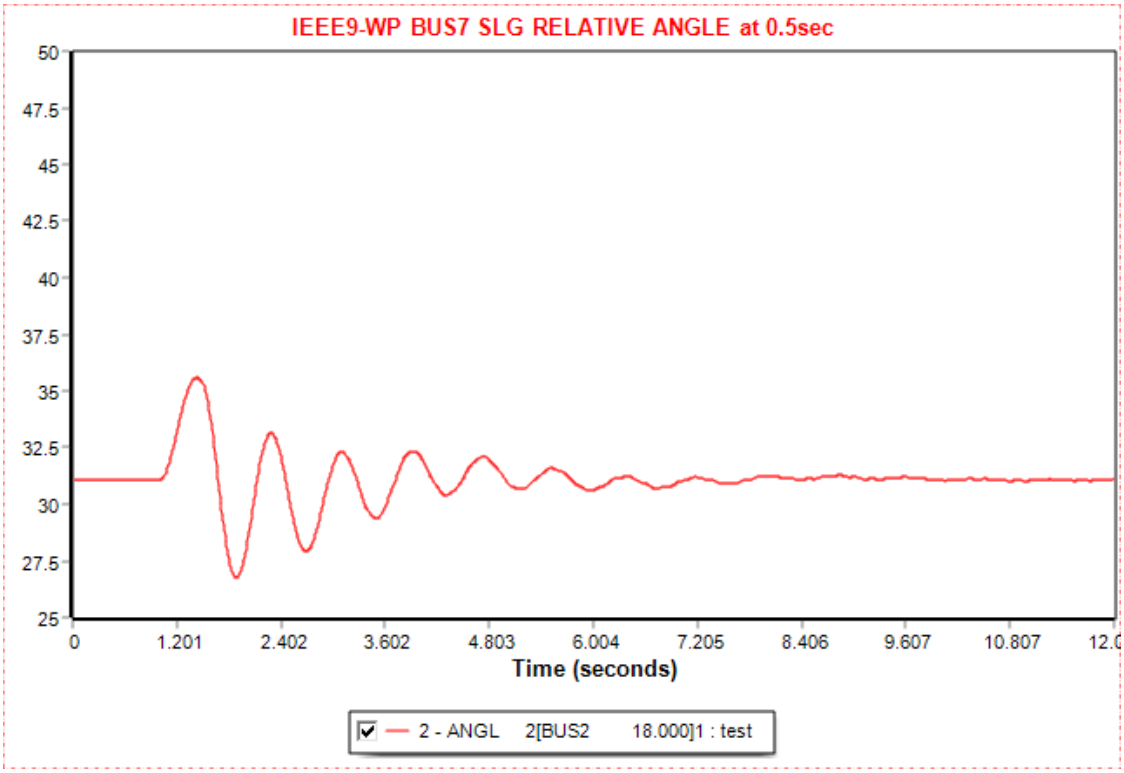

Figure 5. 21 Relative power angle plots of SLG fault at bus 7 when it is cleared at 1.5 sec at IEEE9 Bus System Wind Power Remodeled with the Replacement of Generator 3

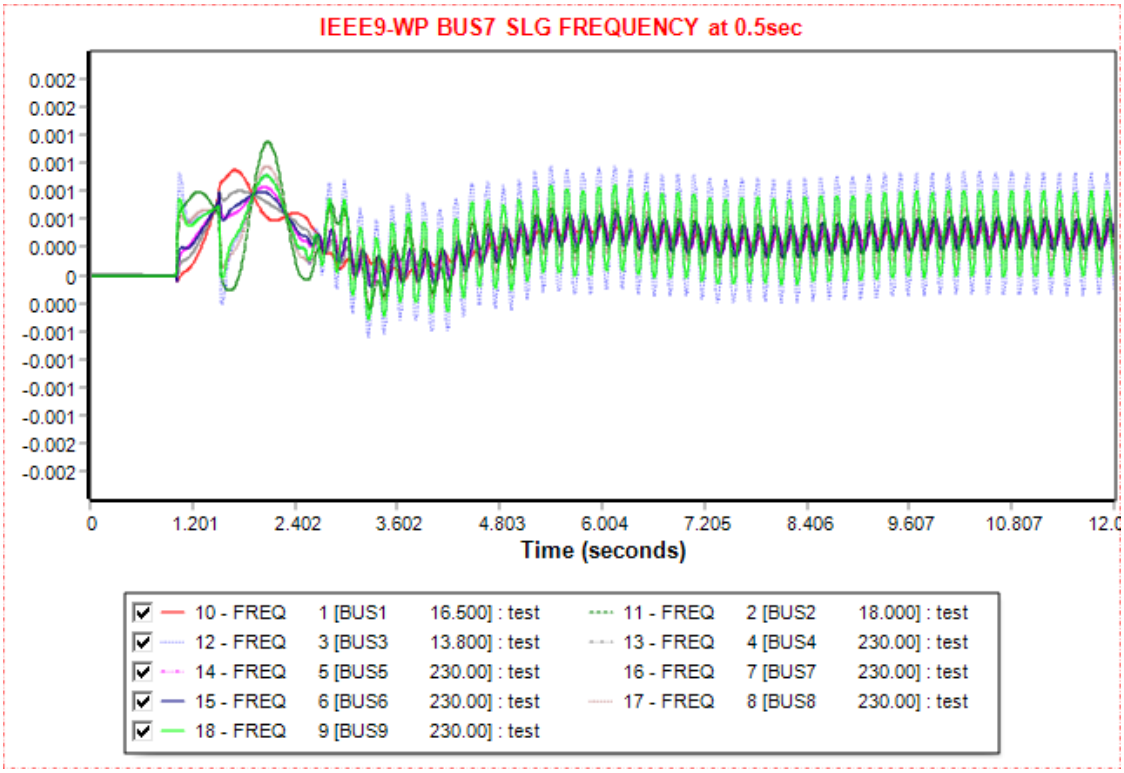

Figure 5. 22 Frequency plots of SLG fault at bus 7 when it is cleared at 1.5 sec at IEEE9 Bus System Wind Power Remodeled with the Replacement of Generator 3

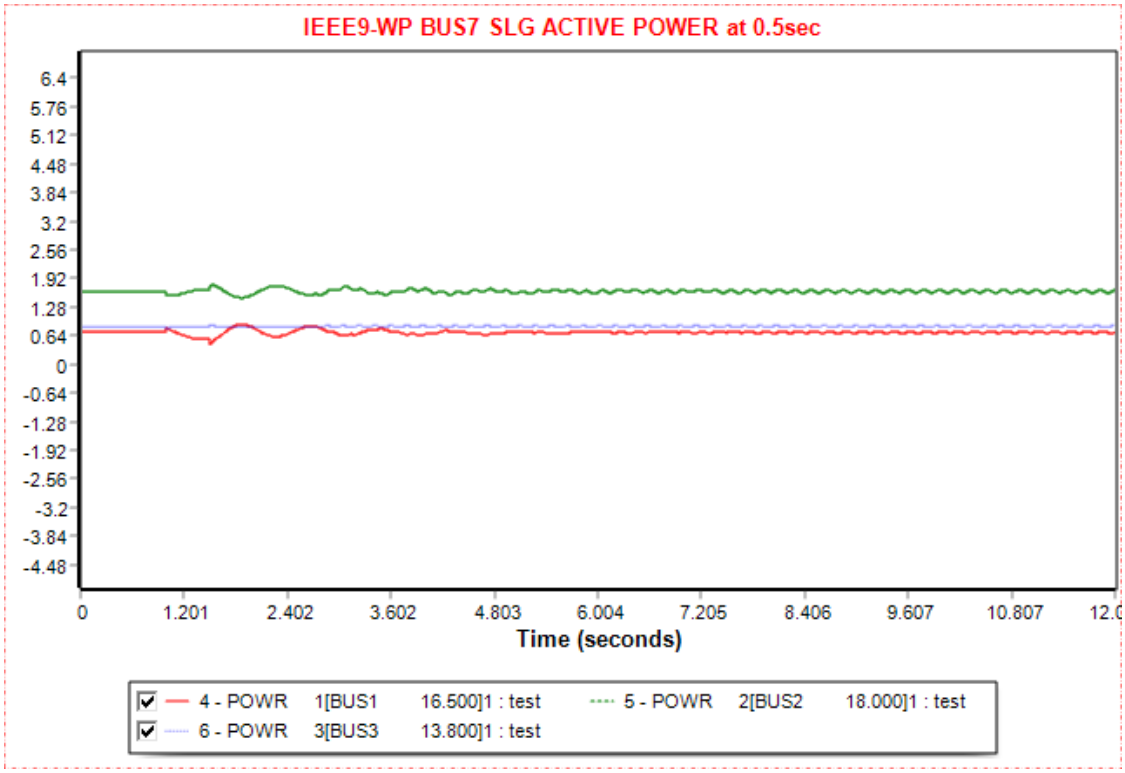

Figure 5. 23 Active Power plots of SLG fault at bus 7 when it is cleared at 1.5 sec at IEEE9 Bus System Wind Power Remodeled with the Replacement of Generator 3

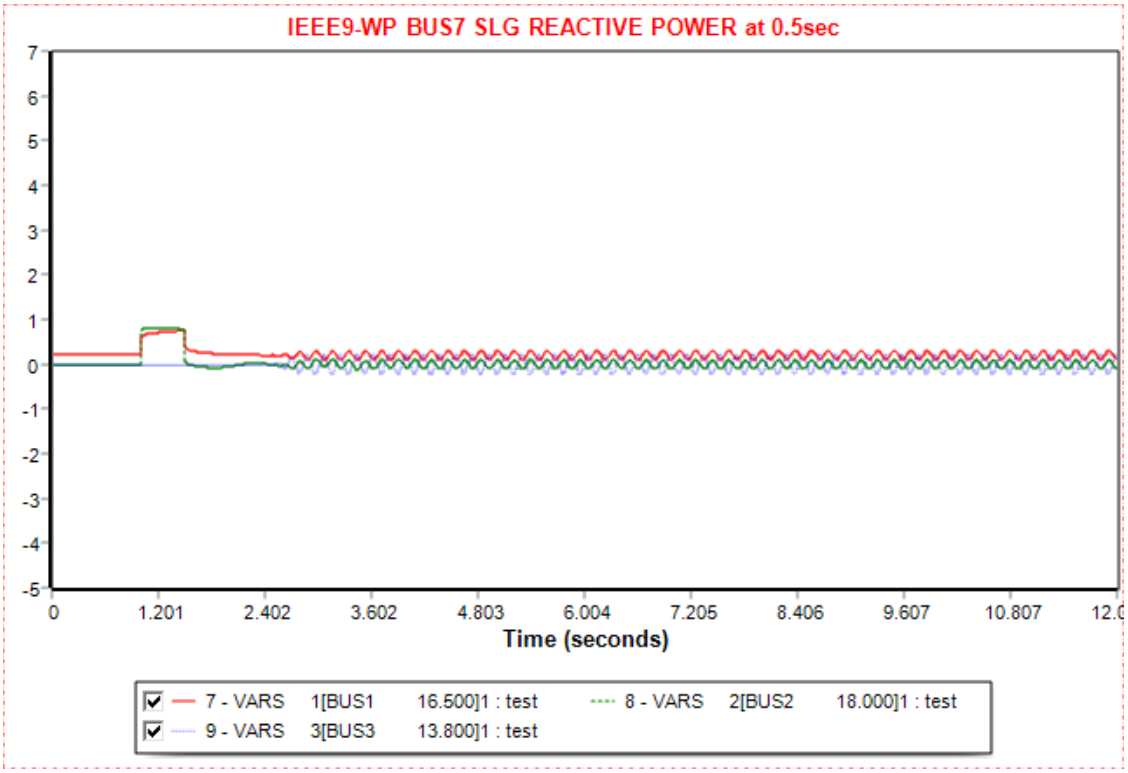

Figure 5. 24 Reactive Power plots of SLG fault at bus 7 when it is cleared at 1.5 sec at IEEE9 Bus System Wind Power Remodeled with the Replacement of Generator 3

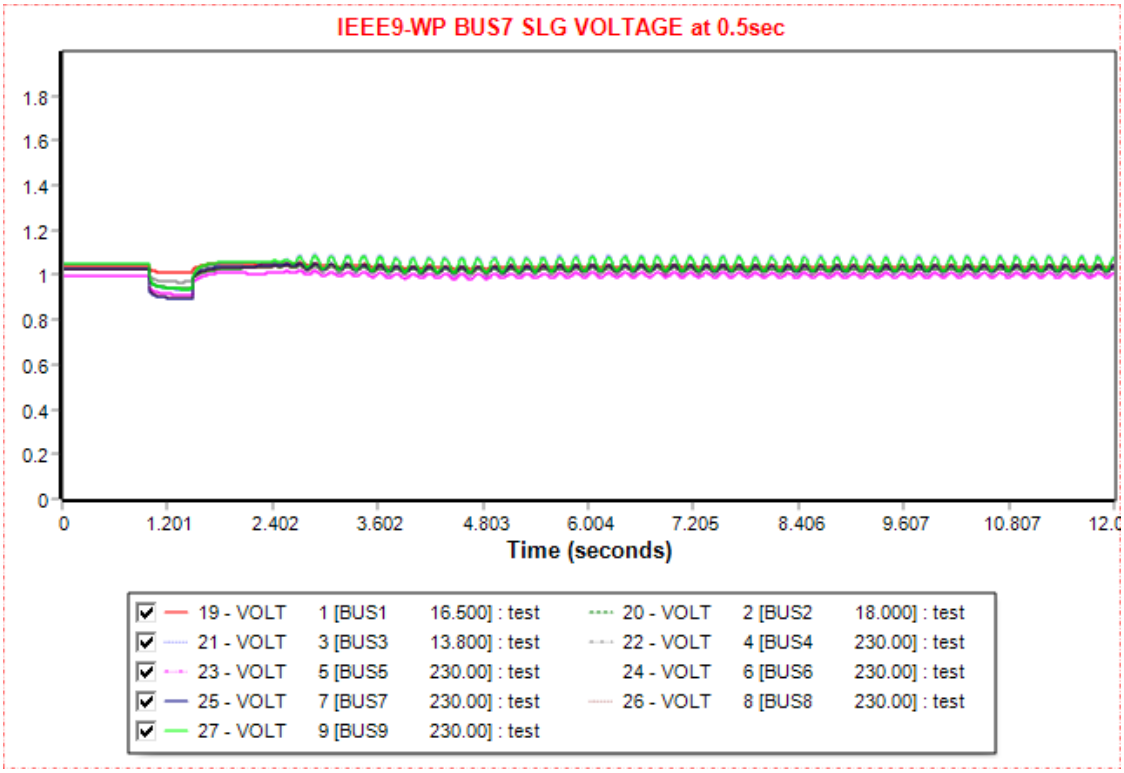

Figure 5. 25 Voltage plots of SLG fault at bus 7 when it is cleared at 1.5 sec at IEEE9 Bus System Wind Power Remodeled with the Replacement of Generator 3

5.1.3 Faults at Bus 8 of the IEEE9 Bus System Wind Power Remodeled with the Replacement of Generator 3

Bus 8 is connected to a 100 MW load. Despite the existence of the same wind turbine, the CFCT may be greater than buses 7 or 2 because bus 8 is a central one and the generator that is inspected for loss of synchronization is the one linked in bus 2, making the fault distance longer.

5.1.3.1 Three-phase Symmetrical Fault at Bus 8 of the IEEE9 Bus System Wind Power Remodeled with the Replacement of Generator 3

The network's standard operation is ensured if the three-phase symmetrical fault should not exceed 0.35 sec, which is the CFCT. There is an initial power flow for 1 sec, and then the disturbance is applied for 0.35 sec. Simultaneously, for the fault clearance the line 7-8 is tripped and after 1 sec, at 2.35 sec, it is connected to the network. As seen from Table

5.4, the simulation lasts for 12 sec. Figures 5.15-5.19 present the power angle of generator 2 with respect to the power angle of the swing bus, the buses frequency, the real and active power of the generators, including the one producing wind power, and the buses voltage when the fault is cleared at CFCT. Figure 5.20 shows the loss of synchronization of the power angle of generator 2 with respect to the power angle of the swing bus when the fault is cleared 0.05 sec after the CFCT. Comparing the CFCTs of this simulation and the one in 5.1.1.1, they are expected to be the same due to their distance with generator 2.

Table 5. 6 IEEE9 Bus System Wind Power Remodeled with the Replacement of Generator 3 Three-phase symmetrical Fault at Bus 8

Action	**Time (sec)**
Steady-state	0.00
Apply Fault	1.00
Clear Fault	1.35
Trip Line	1.35
Connect Line	2.35
Power Flow	12.00

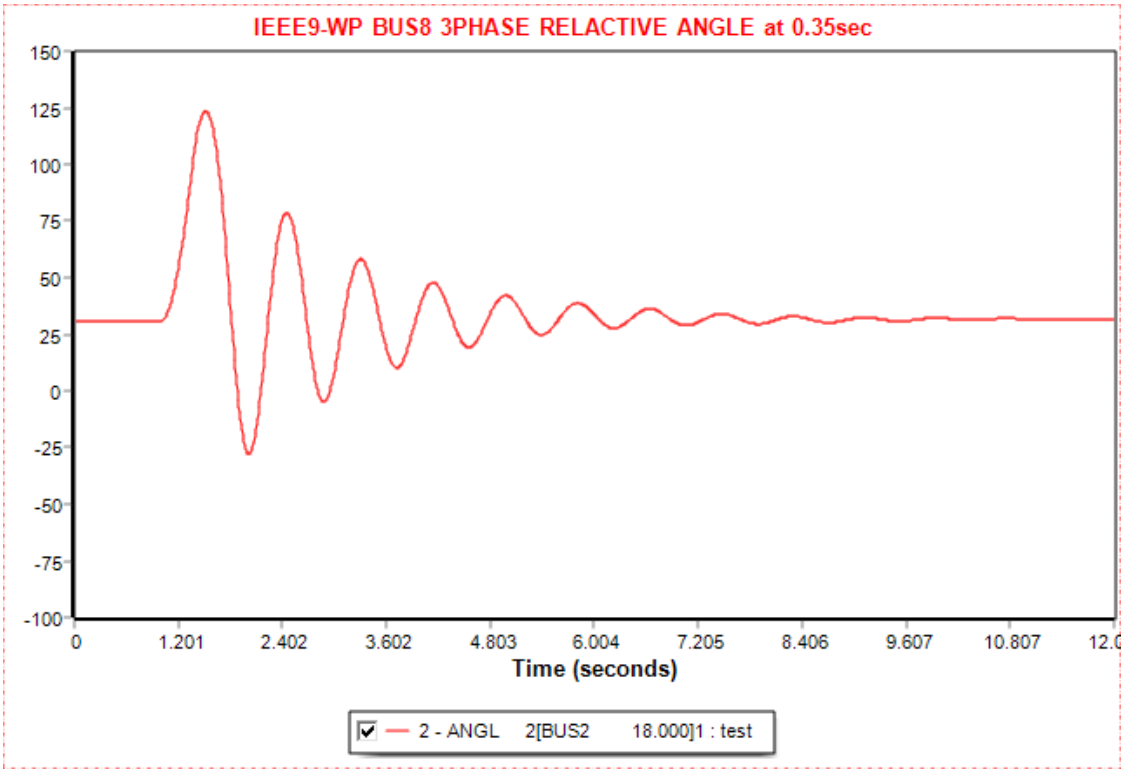

Figure 5. 26 Relative power angle plots of three-phase symmetrical fault at bus8 when it is cleared at 1.35 sec at IEEE9 Bus System Wind Power Remodeled with the Replacement of Generator 3

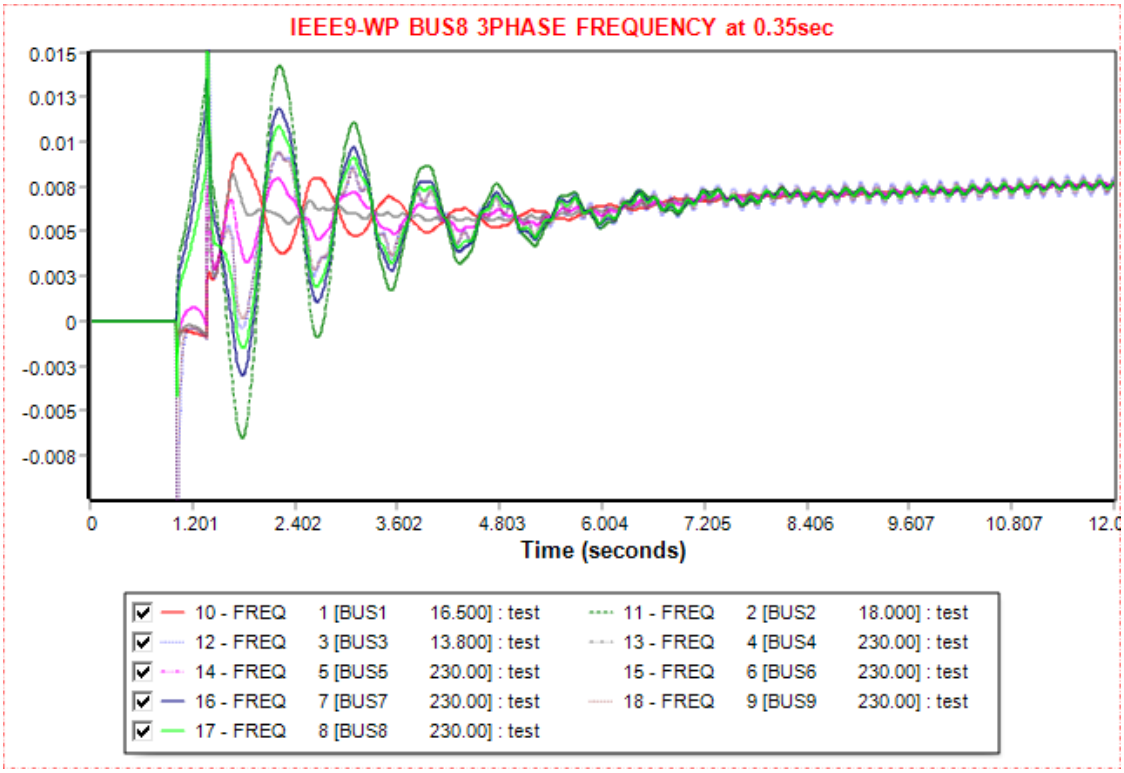

Figure 5. 27 Frequency plots of three-phase symmetrical fault at bus 8 when it is cleared at 1.35 sec at IEEE9 Bus System Wind Power Remodeled with the Replacement of Generator 3

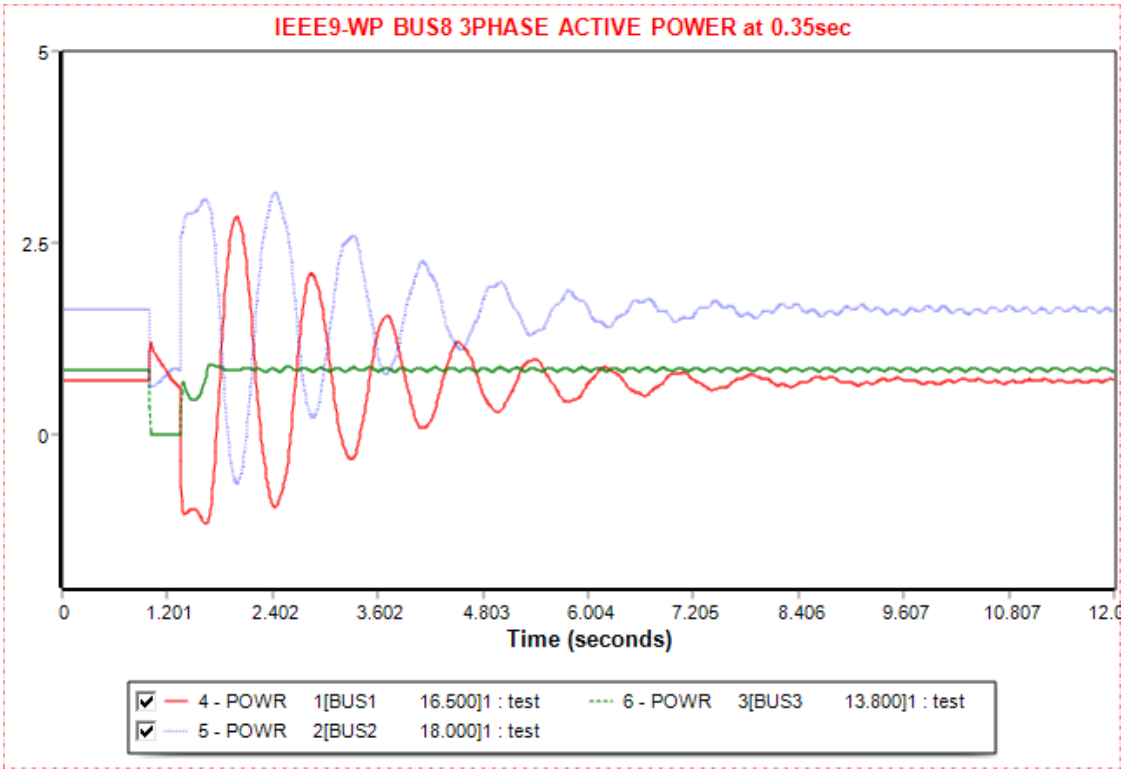

Figure 5. 28 Active Power plots of three-phase symmetrical fault at bus8 when it is cleared at 1.35 sec at IEEE9 Bus System Wind Power Remodeled with the Replacement of Generator 3

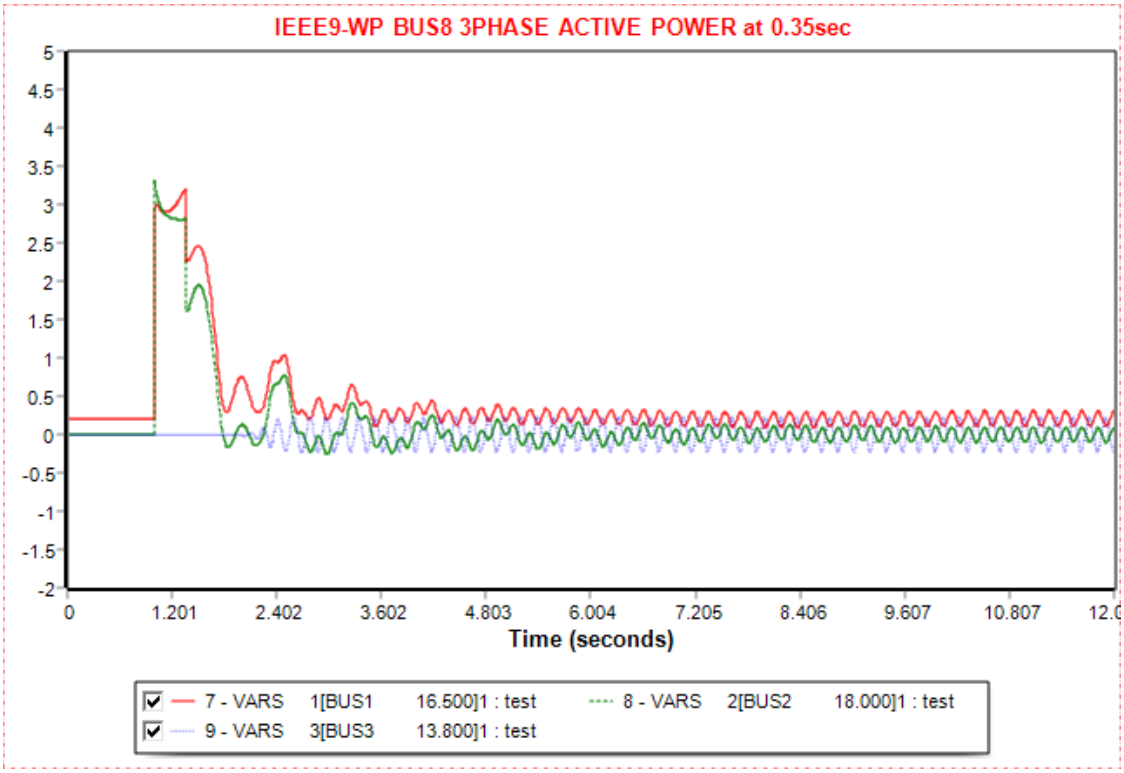

Figure 5. 29 Reactive Power plots of three-phase symmetrical fault at bus8 when it is cleared at 1.35 sec at IEEE9 Bus System Wind Power Remodeled with the Replacement of Generator 3

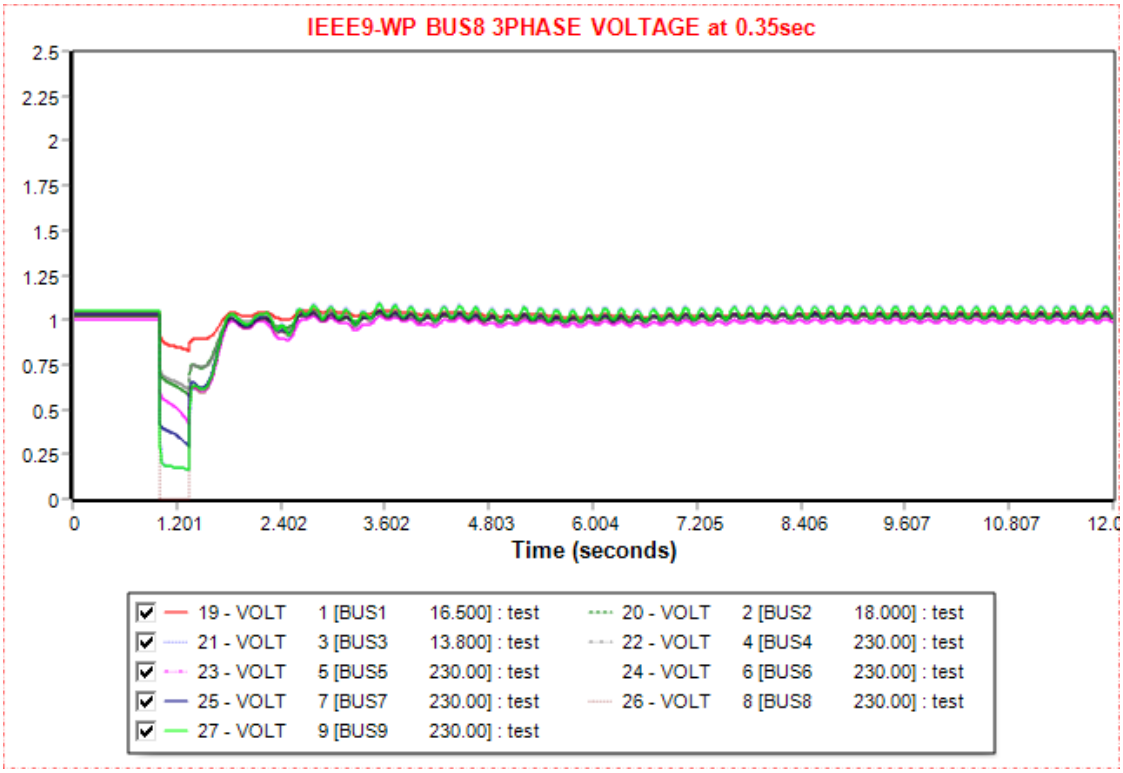

Figure 5. 30 Voltage plots of three-phase symmetrical fault at bus8 when it is cleared at 1.35 sec at IEEE9 Bus System Wind Power Remodeled with the Replacement of Generator 3

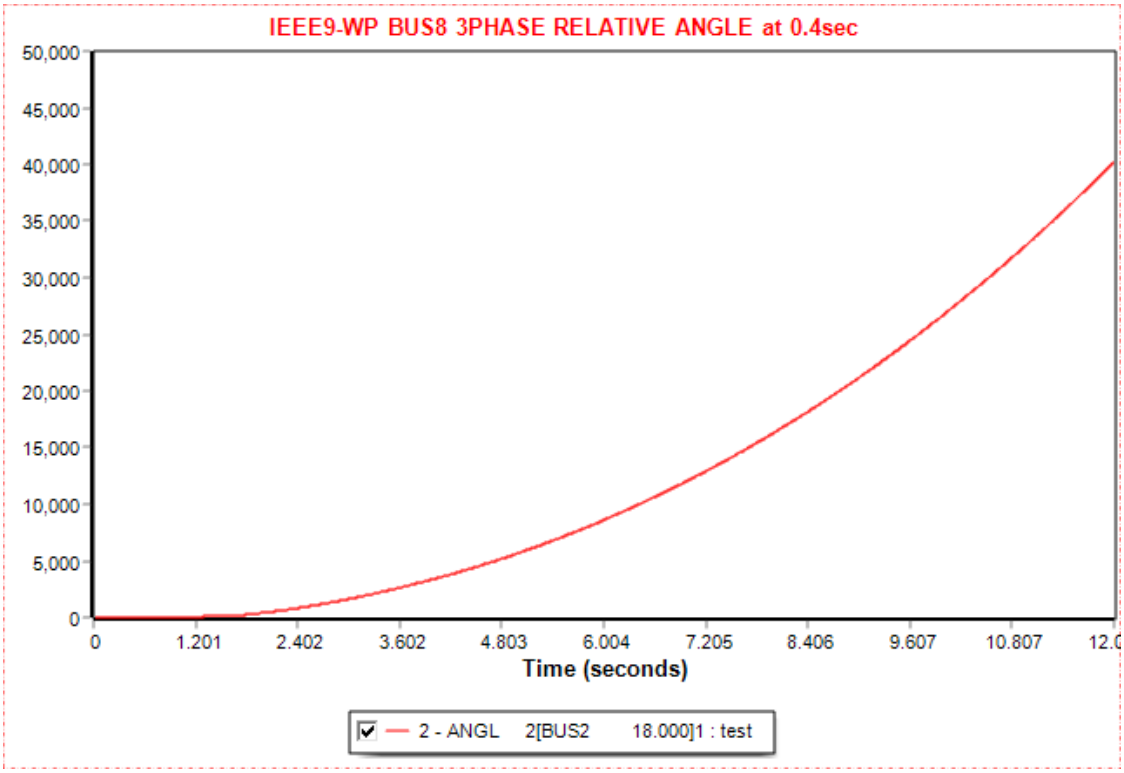

Figure 5. 31 Relative power angle plots of three-phase symmetrical fault at bus8 when it is cleared at 1.4 sec at IEEE9 Bus System Wind Power Remodeled with the Replacement of Generator 3

5.1.3.2 SLG Fault at Bus 8 of the IEEE9 Bus System Wind Power Remodeled with the Replacement of Generator 3

The network can maintain its stability despite the duration of the SLG fault. The fault is cleared at 0.5 sec to study the transient behavior of the system, as there is no CFCT. Firstly, there is an initial power flow for 1 sec, and then the disturbance is applied for 0.5 sec. Simultaneously, for the fault clearance the line 7-8 is tripped and after 1 sec, at 2.5 sec, it is connected to the network. As seen from Table 5.4, the simulation lasts for 12 sec. Figures 5.21-5.25 present the power angle of generator 2 with respect to the power angle of the swing bus, the buses frequency, the real and active power of the generators, including the one producing wind power, and the buses voltage when the fault is cleared at 0.5 sec. In contrast to the SLG at bus 2, the fault has less impact as there is distance from the generator at bus 2.

Table 5. 7 IEEE9 Bus System Wind Power Remodeled with the Replacement of Generator 3 SLG Fault at Bus 8

Action	Time (sec)
Steady-state	0.00
Apply Fault	1.00
Clear Fault	1.5
Trip Line	1.5
Connect Line	2.5
Power Flow	12.00

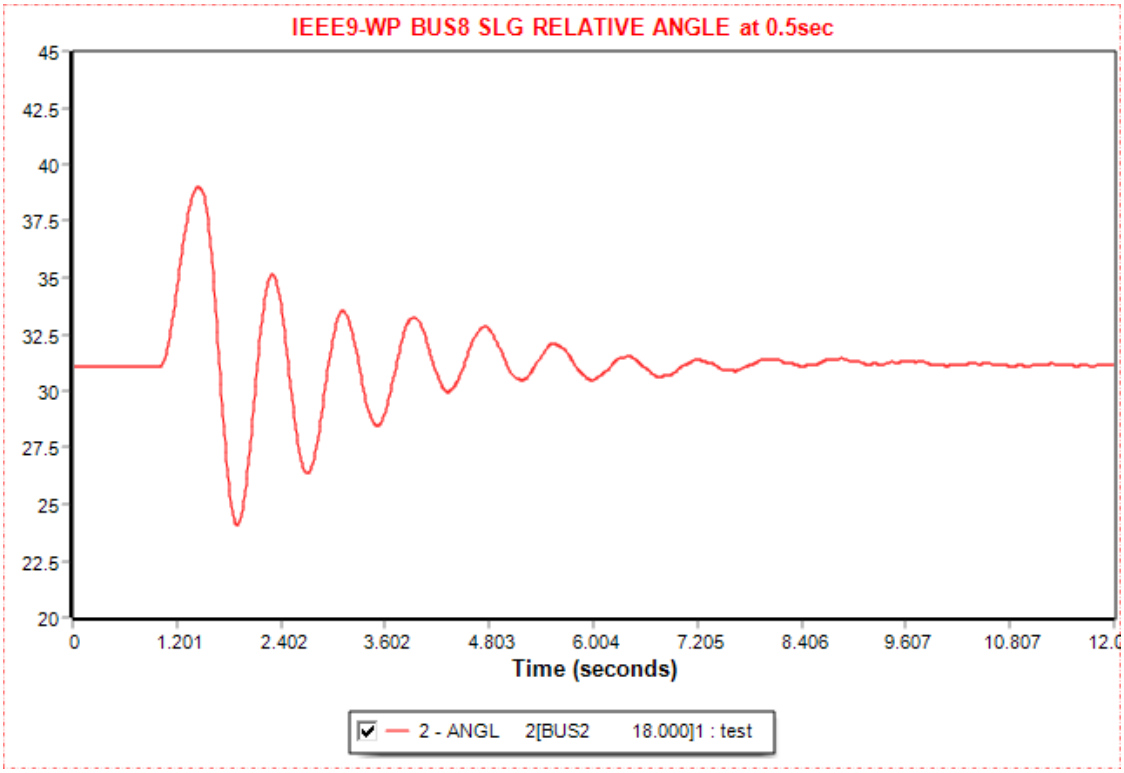

Figure 5. 32 Relative power angle plots of SLG fault at bus 8 when it is cleared at 1.5 sec at IEEE9 Bus System Wind Power Remodeled with the Replacement of Generator 3

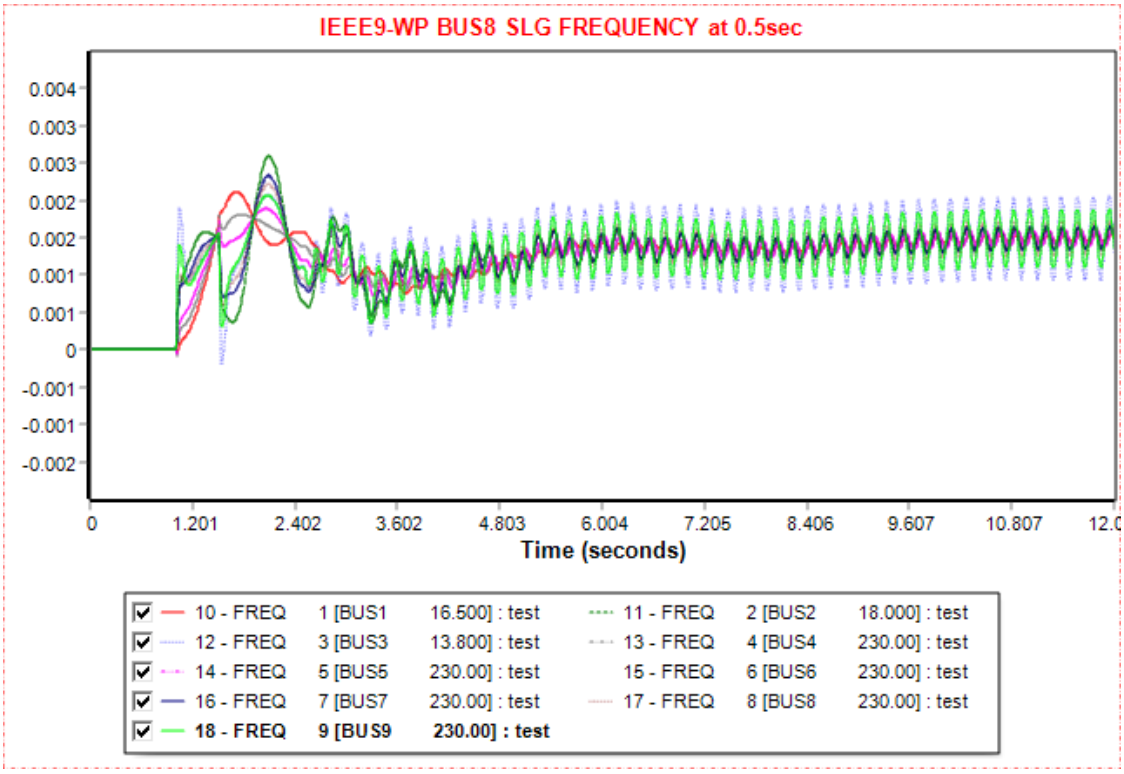

Figure 5. 33 Frequency plots of SLG fault at bus 8 when it is cleared at 1.5 sec at IEEE9 Bus System Wind Power Remodeled with the Replacement of Generator 3

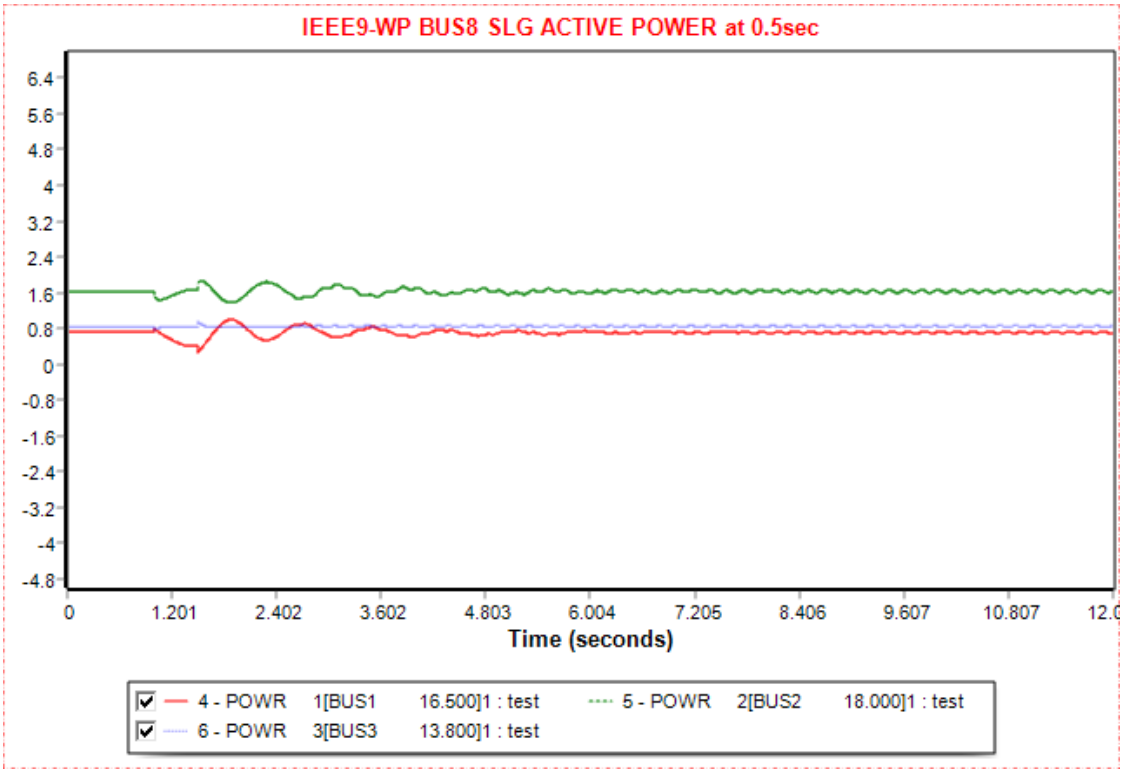

Figure 5. 34 Active Power plots of SLG fault at bus 8 when it is cleared at 1.5 sec at IEEE9 Bus System Wind Power Remodeled with the Replacement of Generator 3

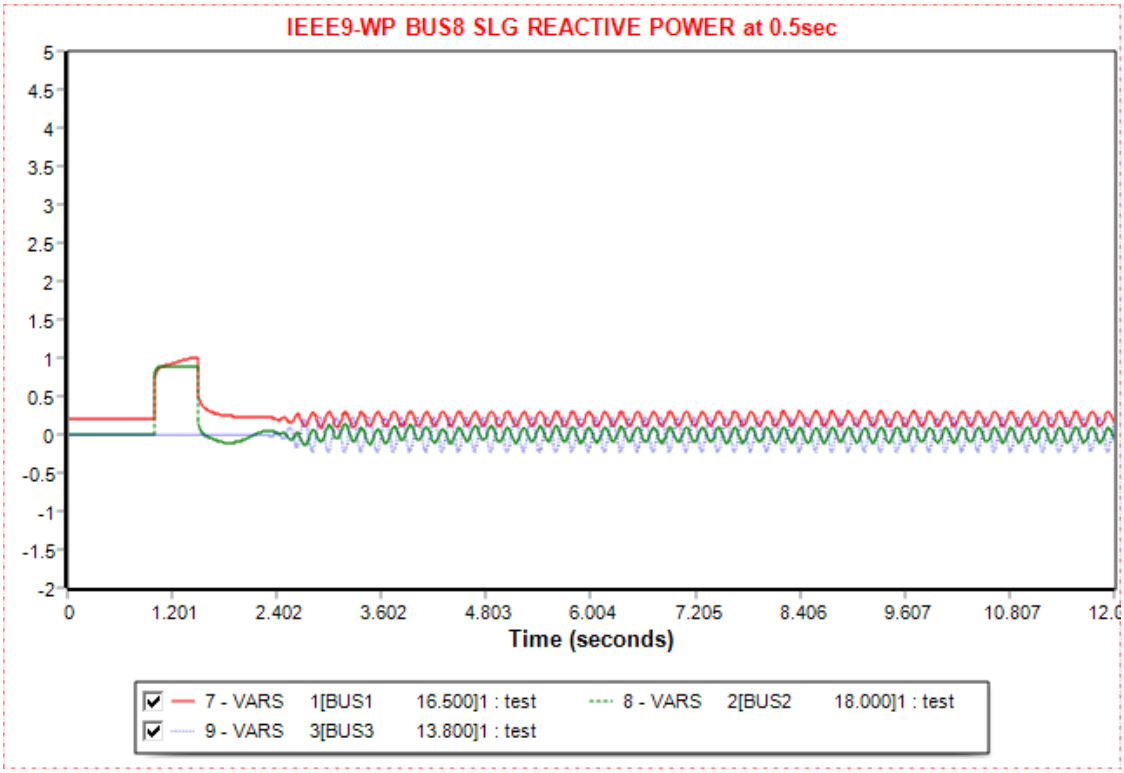

Figure 5. 35 Reactive Power Angle plots of SLG fault at bus 8 when it is cleared at 1.5 sec at IEEE9 Bus System Wind Power Remodeled with the Replacement of Generator 3

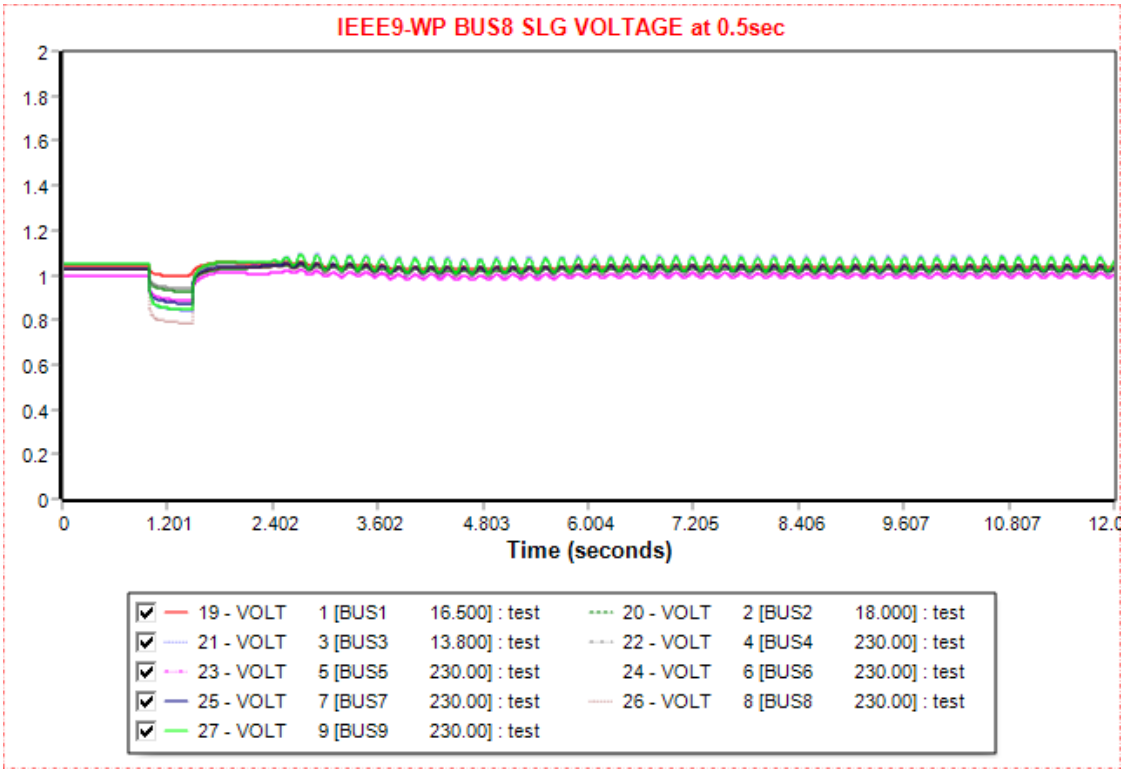

Figure 5. 36 Voltage plots of SLG fault at bus 8 when it is cleared at 1.5 sec at IEEE9 Bus System Wind Power Remodeled with the Replacement of Generator 3

5.1.4 Diagram Analysis of the IEEE9 Bus System Wind Power Remodeled with the Replacement of Generator 3

In all the Figures presenting the buses' frequency, the generators' real and active power, including the one producing wind power, and the buses' voltage when the fault is cleared at CFCT, there is a significant similarity. Four seconds after the clearance of the fault, there are small damps in stabilizing the network. This is due to the wind turbine model and the structure of the power system.

The relative power angle diagrams with respect to the swing bus's power angle are similar for the three-phase symmetrical cases (Figure 5.3, 5.15, 5.26). The plot of the generator connected to bus 2, after the fault occurs, increases and reaches 125 degrees, following a decrease at around -25 degrees. Something similar is happening in the SLG diagram when the fault occurs at a bus. The absolute difference between the upper and the lower limit is around 100 degrees (Figure 5.9). In the other two SLG diagrams (Figure 5.21, 5.32), the angle's oscillation width is approximately 15 degrees, proving the

disturbance's lower impact. In the desynchronization diagrams, the power angle increases exponentially as the critical fault clearing time is surpassed, destabilizing the system.

In the frequency diagrams, there is a similar plot in all three-phase symmetrical (Figure 5.4, 5.16, 5.27) and the SLG (5.10, 5.22, 5.33). After the fault, the frequencies are decreasing, followed by a rapid increase in their values. Even though it is about to be stabilized, some fluctuations happen mainly in the generator buses' frequencies. It is worth mentioning that the largest width of the oscillations is around 0.03 Hz for the three-phase symmetrical cases in the first swing, 0.017 Hz for Figure 5.10, where there is an SLG in bus 2 and 0.003 in the other two SLG plots. The wind turbine has a similar reaction to the other generators.

Similar behavior appears for all three-phase symmetrical active power plots (Figure 5.5, 5.17, 5.28) and in the SLG (5.11, 5.23, 5.34). Even though the fluctuations are similar, the values are different. In the three-phase symmetrical diagrams and the SLG at bus 2, the initial oscillations' width due to the fault is around 2.5 to 4 pu, since the values are -0.8 pu and 3.2 pu meaning -80 MW to 320 MW, mainly for generation 2. In the other SLG diagrams, the divergence from the initial value is smaller. There is a slight initial decrease for the wind turbine in all graphs due to the rotor acceleration following a recovery around 0.8 pu with small damps.

The reactive power diagrams like the active power refer only to the three generator buses. Like the other diagrams, the three-phase symmetrical (Figure 5.6, 5.18, 5.29) and the SLG (5.12, 5.24, 5.35) have similar plots, but the limits are different. When the fault occurs, the swing bus and generator 2's reactive power rises to stabilize the system from the disturbance and then gradually recovers. The wind turbine does not have any difference because it operates with around 0 pu reactive power. Then after 3 sec, the reactive power plots start to stabilize with few oscillations. In Figures 5.6, 5.18, and 5.29, the three-phase symmetrical diagrams, and the 5.12, the SLG fault at bus 2 diagram, the total increase in the reactive power reaches 4 pu, while in the other two graphs, Figure 5.24 and 5.35, it is around 1 pu.

Similar is the depiction of the voltage plots in the diagrams, the three-phase symmetrical (Figure 5.7, 5.19, 5.30) and the SLG (5.13, 5.25, 5.36). The voltages decrease instantly and then recover again in the initial 1 pu. The only different thing is the total pu

of the voltage decrease in each plot. The longer the distance of the fault is, the less is the voltage decrease. For the wind turbine, in all the three-phase symmetrical cases and SLG at bus 2, the decrease is around 0.25 pu, while in the other two SLG faults, the lower limit of bus 3 is a little lower than 1 pu. [4][6][9-17][19][20][22][23][38][41]

5.2 SCENARIO 2: IEEE9 Bus System Wind Power Remodeled with the Partial Replacement (50%) of Generator 3

This scenario shows many similarities with scenario at 5.1 but has one difference, the total capacity of the wind farm is 42.5 MW instead of 85 MW, meaning the wind turbine has the 50% of the generator's total capacity. Specifically, in the IEEE9 Bus system generator 1 remains as the swing bus, generator 2 remains as it is and generator 3 is replaced by a wind farm producing 42.5 MW. The modeling and the way the wind farm is connected are the same as in 5.1. In Figure 5.37, the system created in PSS/E is presented. In Table 5.8 the real and reactive power of the system is presented. The swing bus generator's active power is increased because it is essential for the system to cover the load.

Table 5. 8 Active and Reactive power generation of the IEEE9 Bus System Wind Power Remodeled with the Partial Replacement (50%) of Generator 3

GENERATOR	Active Power (pu)	Reactive Power (pu)
BUS 1 (Swing Bus)	0.92	0.27
BUS 2	1.63	0.09
BUS 3 (Wind Power)	0.425	0

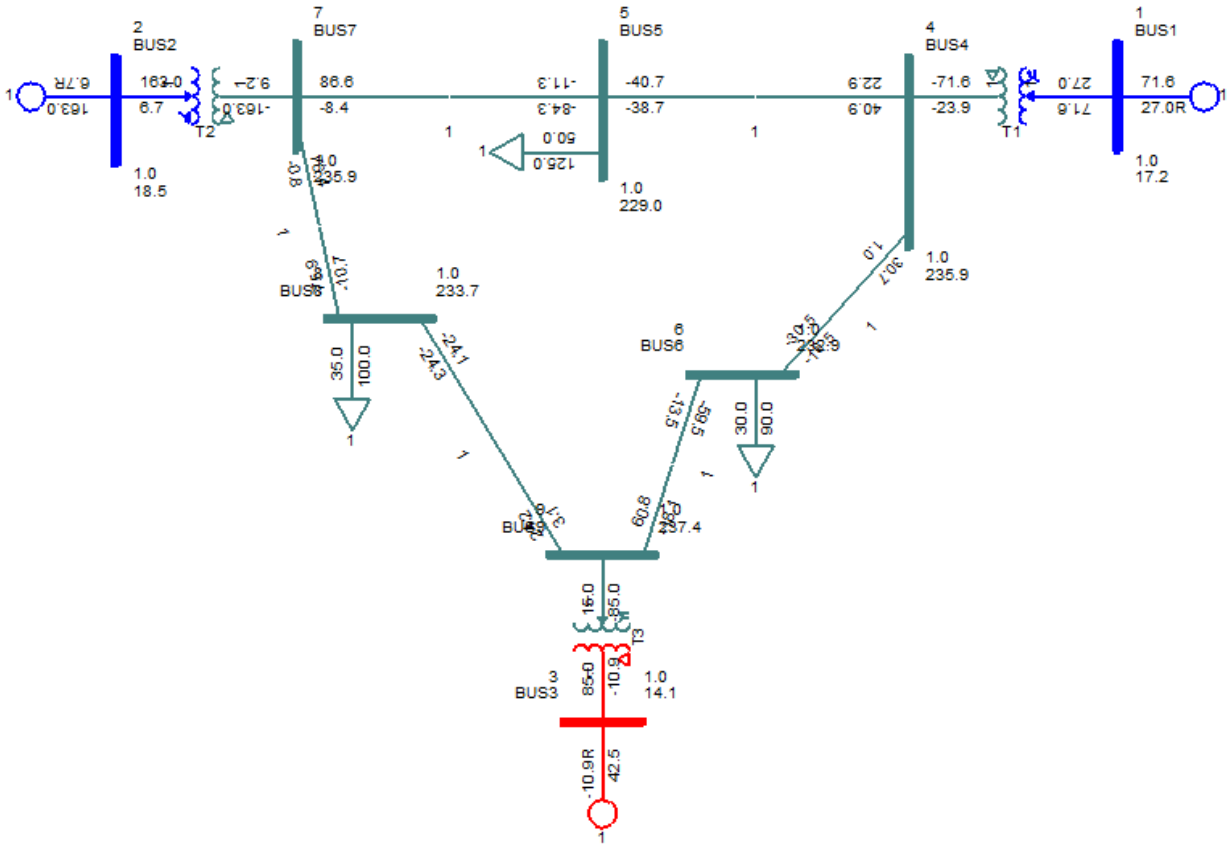

Figure 5. 37 IEEE9 Bus System Wind Power Remodeled with the Partial Replacement (50%) of Generator 3

5.2.1 Faults at Bus 2 of the IEEE9 Bus System Wind Power Remodeled with the Partial Replacement (50%) of Generator 3

The situation in bus 2 is the same as in the scenario where generator 3 was replaced by the wind farm. In both three-phase symmetrical and SLG, after the fault is cleared the line that is tripped is the 2-7. After 1 sec it is again connected, and the simulation runs until 12 sec.

5.2.1.1 Three-phase Symmetrical Fault at Bus 2 of the IEEE9 Bus System Wind Power Remodeled with the Partial Replacement (50%) of Generator 3

The CFCT was calculated to be 0.2 sec from the simulation, meaning the three-phase symmetrical fault duration is 0.2 sec for the system stability. Initially, the system is for 1 sec

in a steady-state condition, and then a three-phase symmetrical fault is applied. Then the fault is cleared at 1.2 sec and concurrently line 2-7 is tripped. After 1 sec, at 2.2 sec, line 2-7 is reclosed, and the system continues the load flowing until 12 sec. All the process is presented in Table 5.9. Figures 5.38-5.42 illustrate the power angle of generator 2 with respect to the power angle of the swing bus, the buses frequency, the real and active power of the generators, including the one producing wind power, and the buses voltage when the fault is cleared at CFCT. Figure 5.43 shows the loss of synchronization of the power angle of generator 2 with respect to the power angle of the swing bus when the fault is cleared 0.05 sec after the CFCT.

Table 5. 9 IEEE9 Bus Wind Power Remodeled with 50% Replacement Three-phase symmetrical Fault at Bus 2

Action	**Time (sec)**
Steady State	0.00
Apply Fault	1.00
Clear Fault	1.2
Trip Line	1.2
Connect Line	2.2
Power Flow	12.00

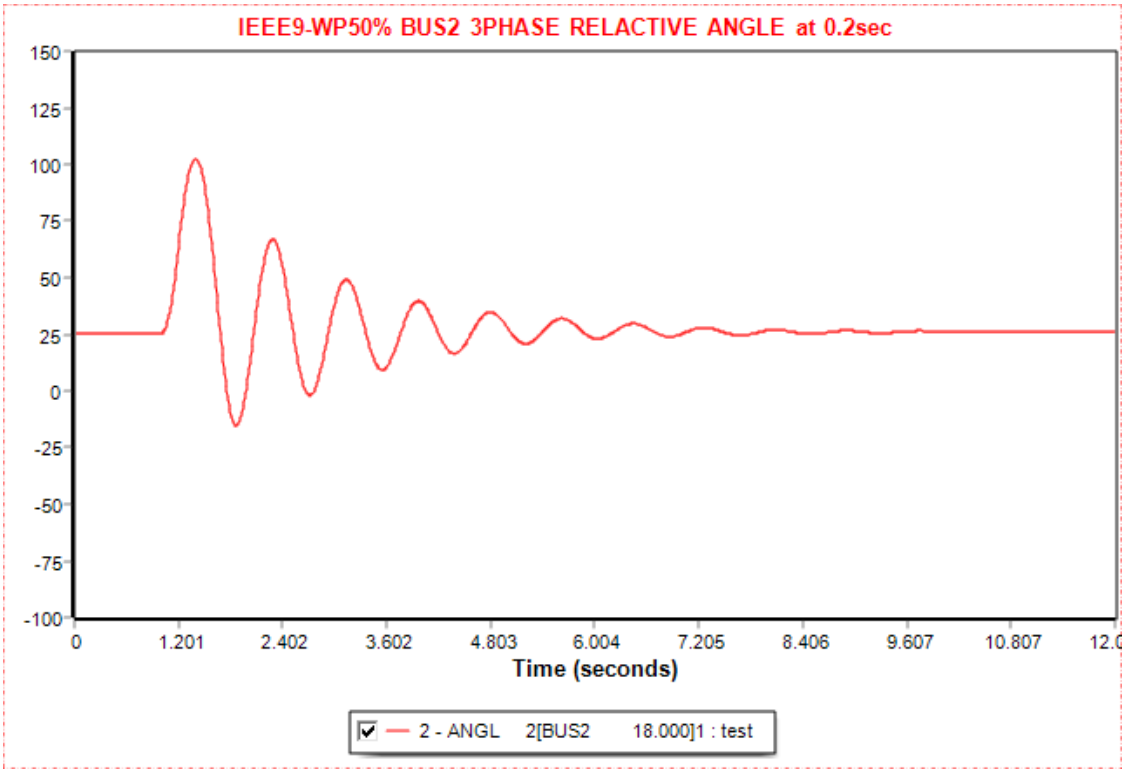

Figure 5. 38 Relative power angle plots of three-phase symmetrical fault at bus 2 when it is cleared at 1.2 sec at IEEE9 Wind Power Remodeled bus system with 50% Replacement

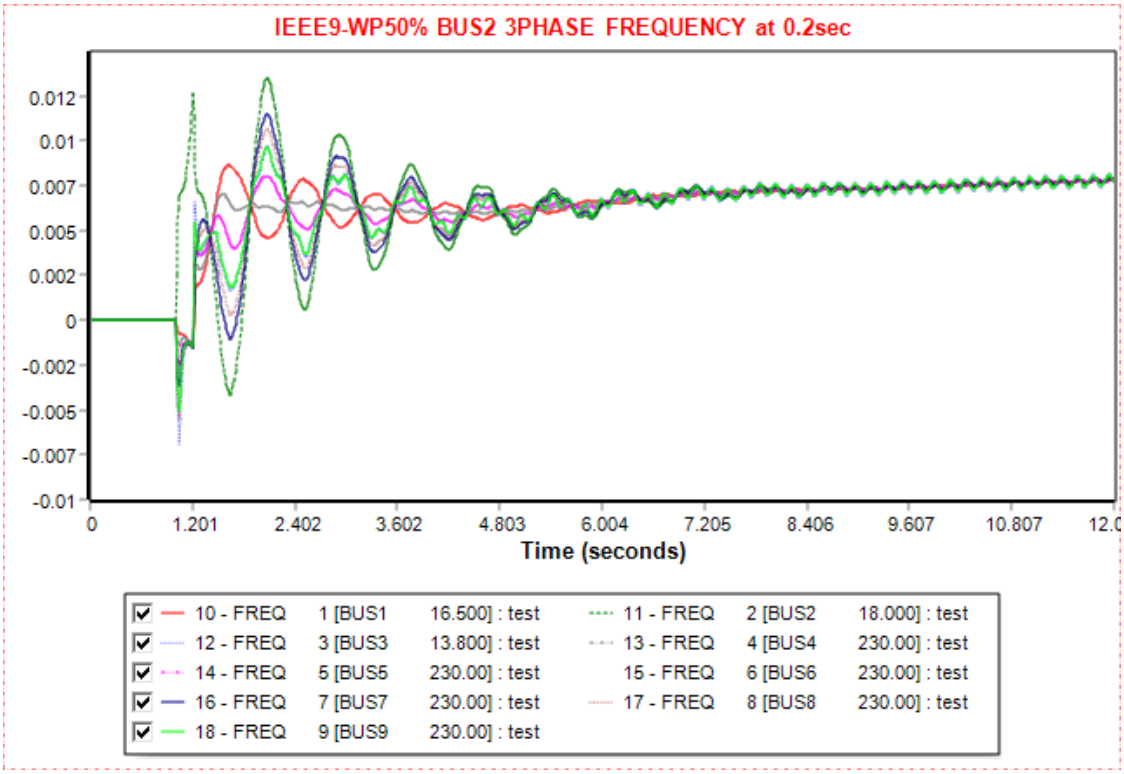

Figure 5. 39 Frequency plots of three-phase symmetrical fault at bus 2 when it is cleared at 1.2 sec at IEEE9 Wind Power Remodeled bus system with 50% Replacement

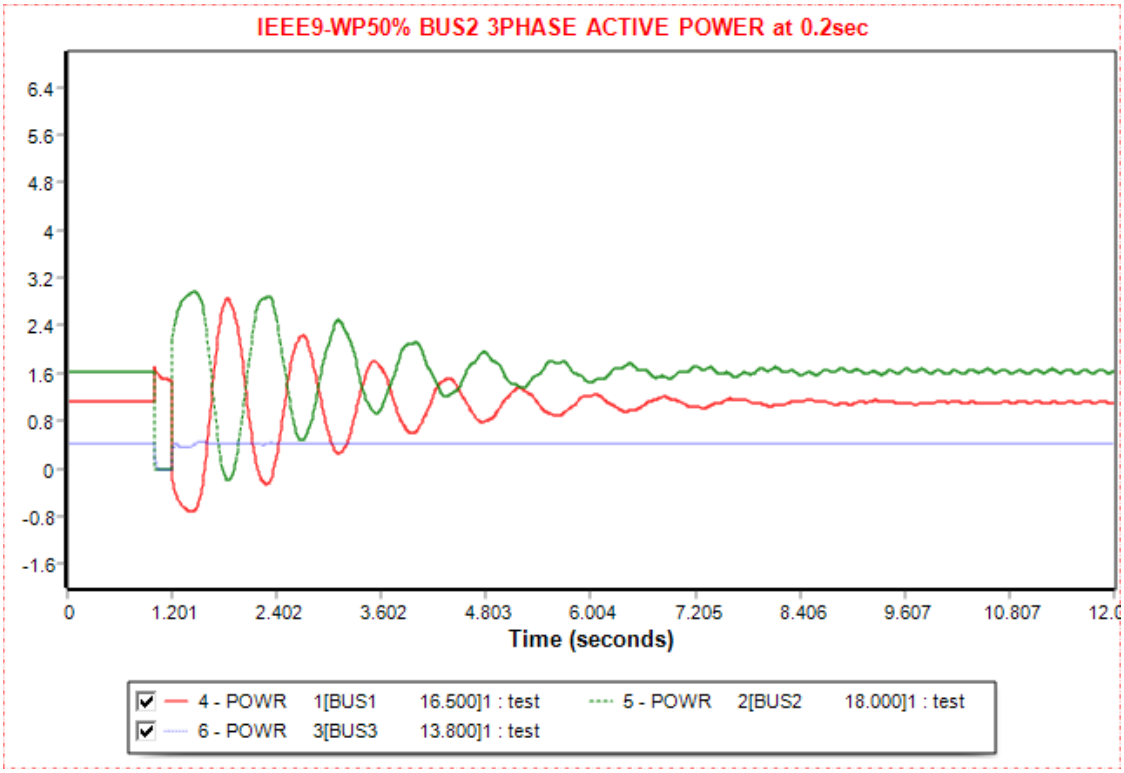

Figure 5. 40 Active Power plots of three-phase symmetrical fault at bus 2 when it is cleared at 1.2 sec at IEEE9 Wind Power Remodeled bus system with 50% Replacement

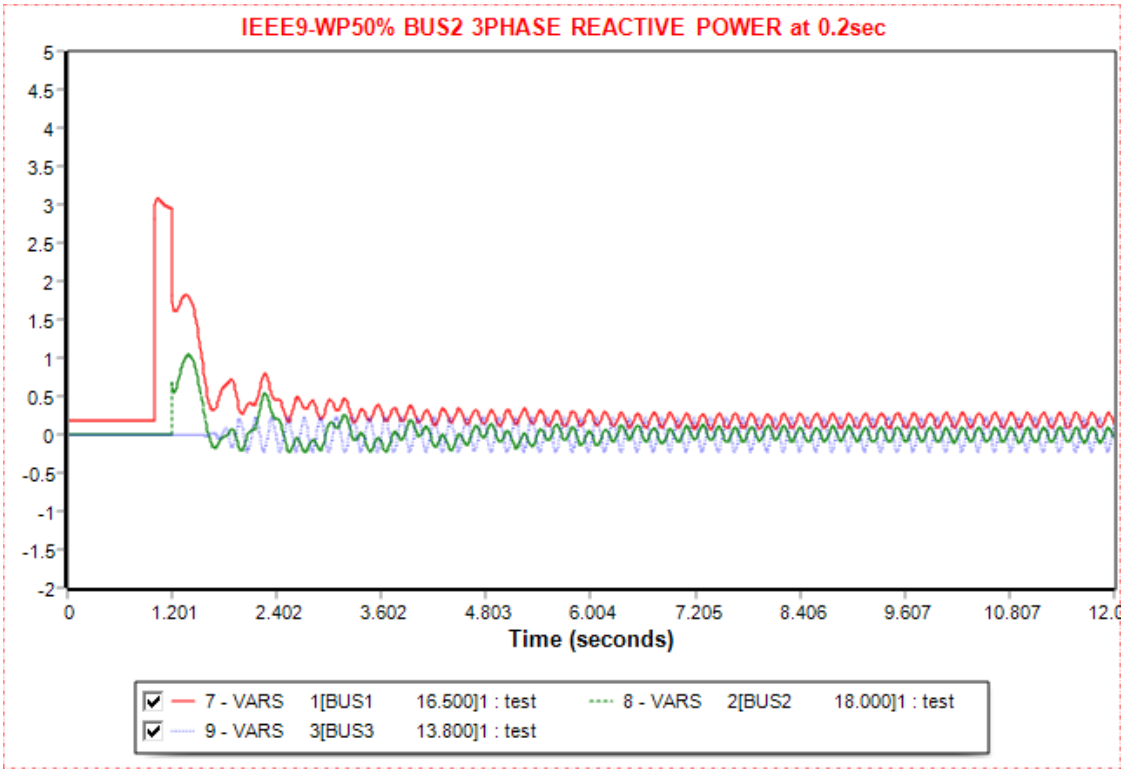

Figure 5. 41 Reactive Power plots of three-phase symmetrical fault at bus 2 when it is cleared at 1.2 sec at IEEE9 Wind Power Remodeled bus system with 50% Replacement

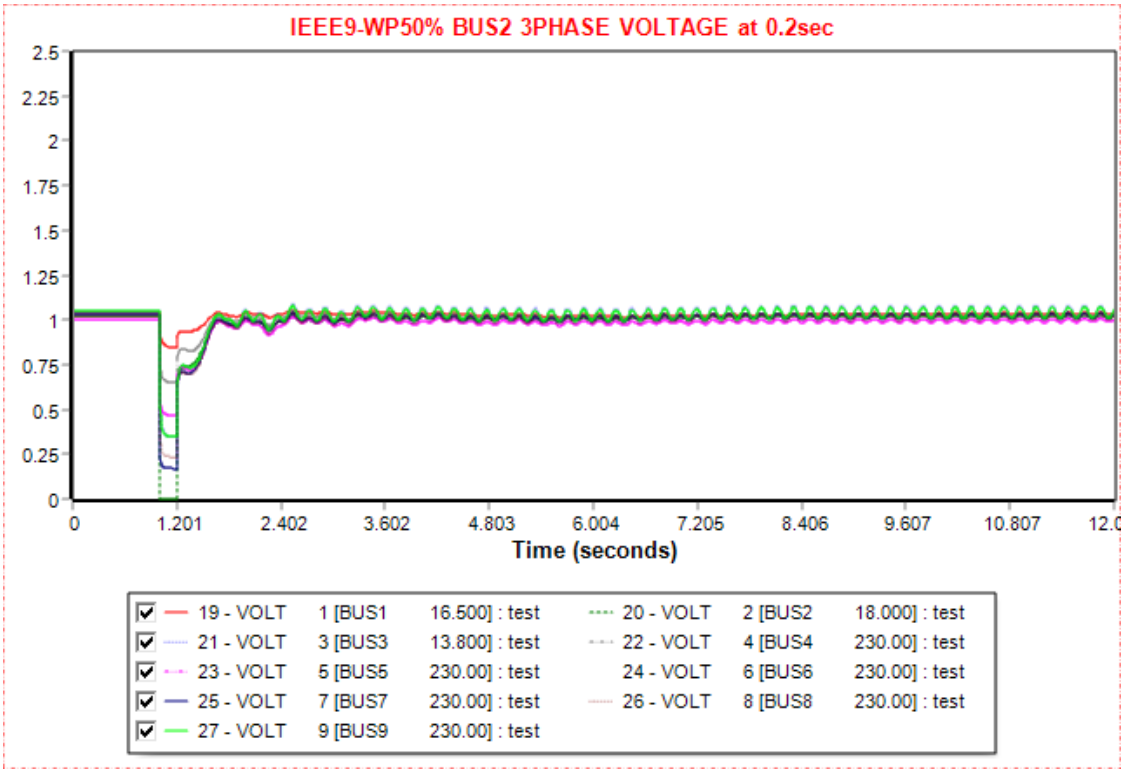

Figure 5. 42 Voltage plots of three-phase symmetrical fault at bus 2 when it is cleared at 1.2 sec at IEEE9 Wind Power Remodeled bus system with 50% Replacement

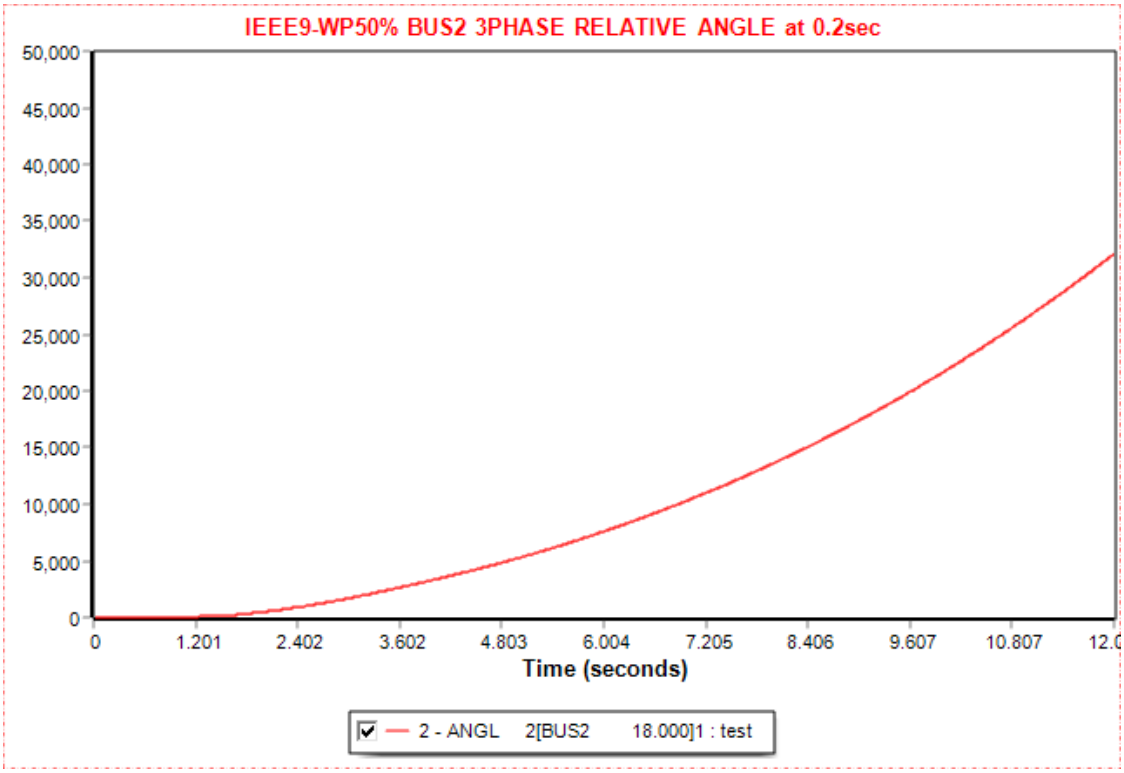

Figure 5. 43 Relative power angle plots of three-phase symmetrical fault at bus 2 when it is cleared at 1.25 sec at IEEE9 Wind Power Remodeled bus system with 50% Replacement

5.2.1.2 SLG Fault at Bus 2 of the IEEE9 Bus System Wind Power Remodeled with the Partial Replacement (50%) of Generator 3

This case is like 5.2.1.2 with the only difference being the type of fault, which is SLG. The clearing time of the fault is 1.75 sec which proves that the decrease of the MW affects the clearing time compared to the 0.9 sec of the SLG fault in section 5.1.1.2. In Table 5.10 below, the simulation steps are being presented, where the fault is applied at 1 sec and is cleared after 1.75 sec. Line 2-7 is tripped and after 1 sec it is connected again until 12 sec. Figures 5.44-5.48 present the power angle of generator 2 with respect to the power angle of the swing bus, the buses frequency, the real and active power of the generators, including the one producing wind power, and the buses voltage when the fault is cleared at CFCT. In Figure 5.49 shows the loss of synchronization of the power angle of generator 2 with respect to the power angle of the swing bus when the fault is cleared 0.05 sec after the CFCT, at 1.8 sec. It is visible that this SLG fault in Figure 5.44 the rotor angle tends to desynchronize due to the large duration of the fault but when it is cleared it is not severe.

Table 5. 10 IEEE9 Wind Power Remodeled bus system with 50% Replacement SLG Fault at Bus 2

Action	**Time (sec)**
Steady State	0.00
Apply Fault	1.00
Clear Fault	2.75
Trip Line	2.75
Connect Line	3.75
Power Flow	12.00

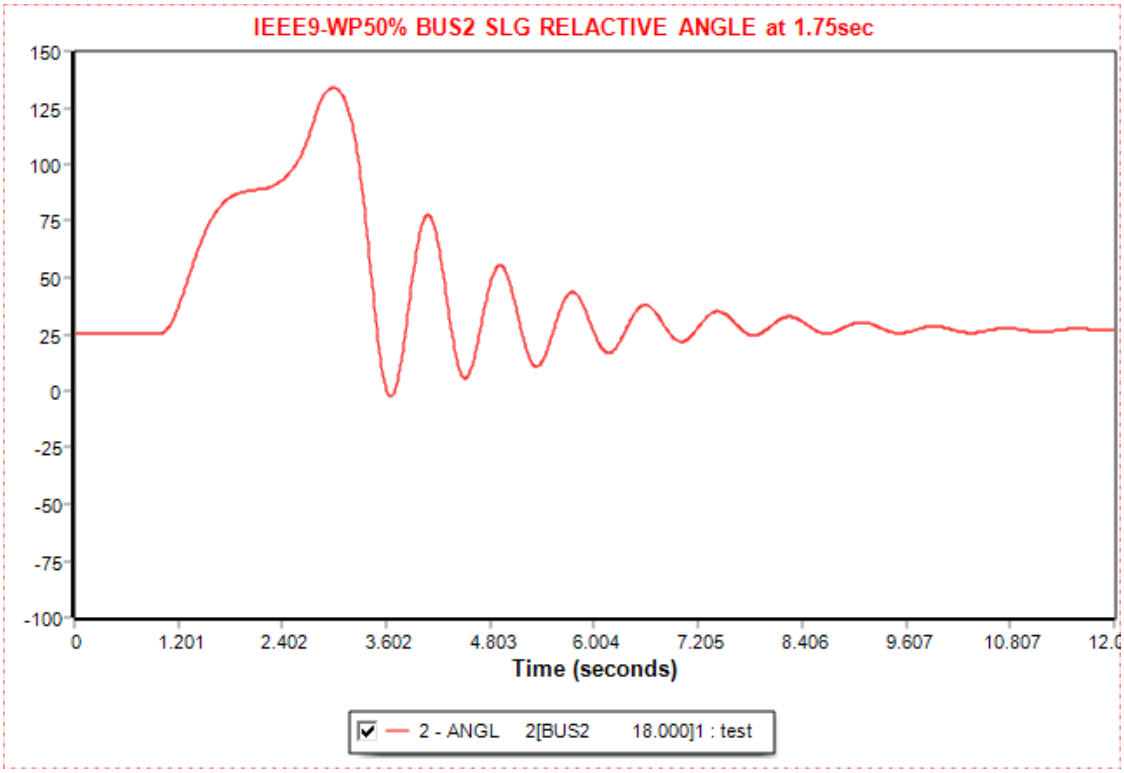

Figure 5. 44 Relative power angle plots of SLG fault at bus 2 when it is cleared at 2.75 sec at IEEE9 Wind Power Remodeled bus system with 50% Replacement

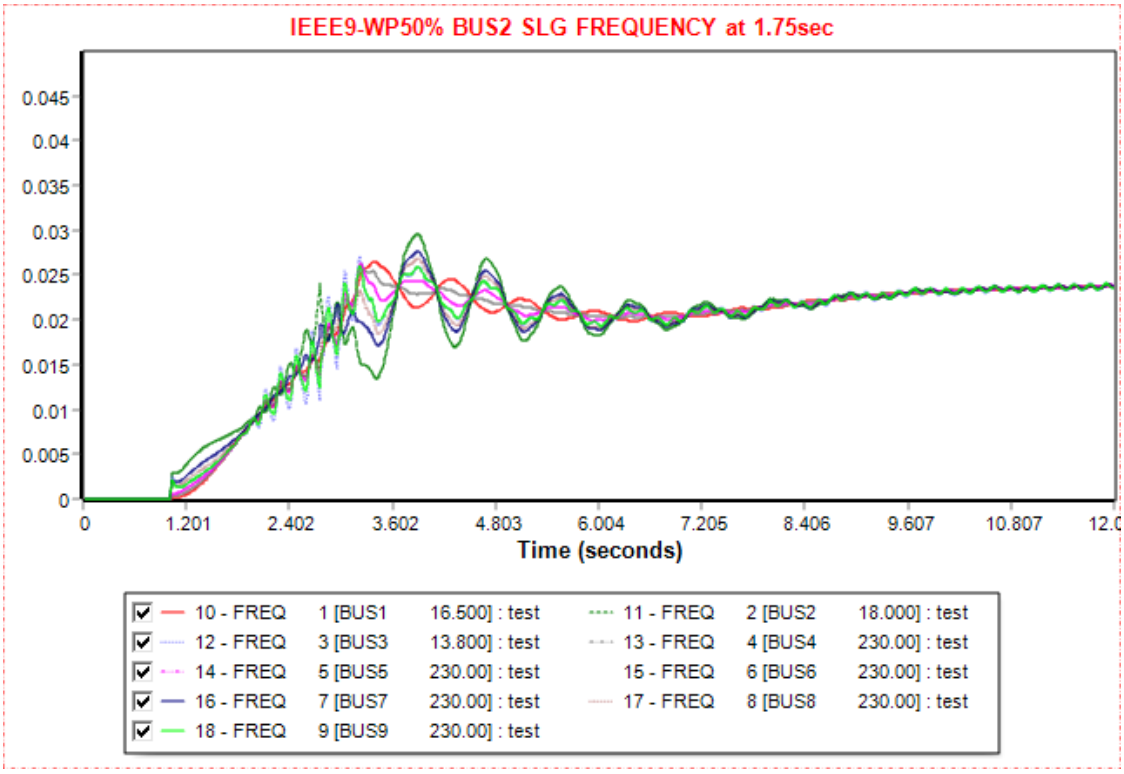

Figure 5. 45 Frequency plots of SLG fault at bus 2 when it is cleared at 2.75 sec at IEEE9 Wind Power Remodeled bus system with 50% Replacement

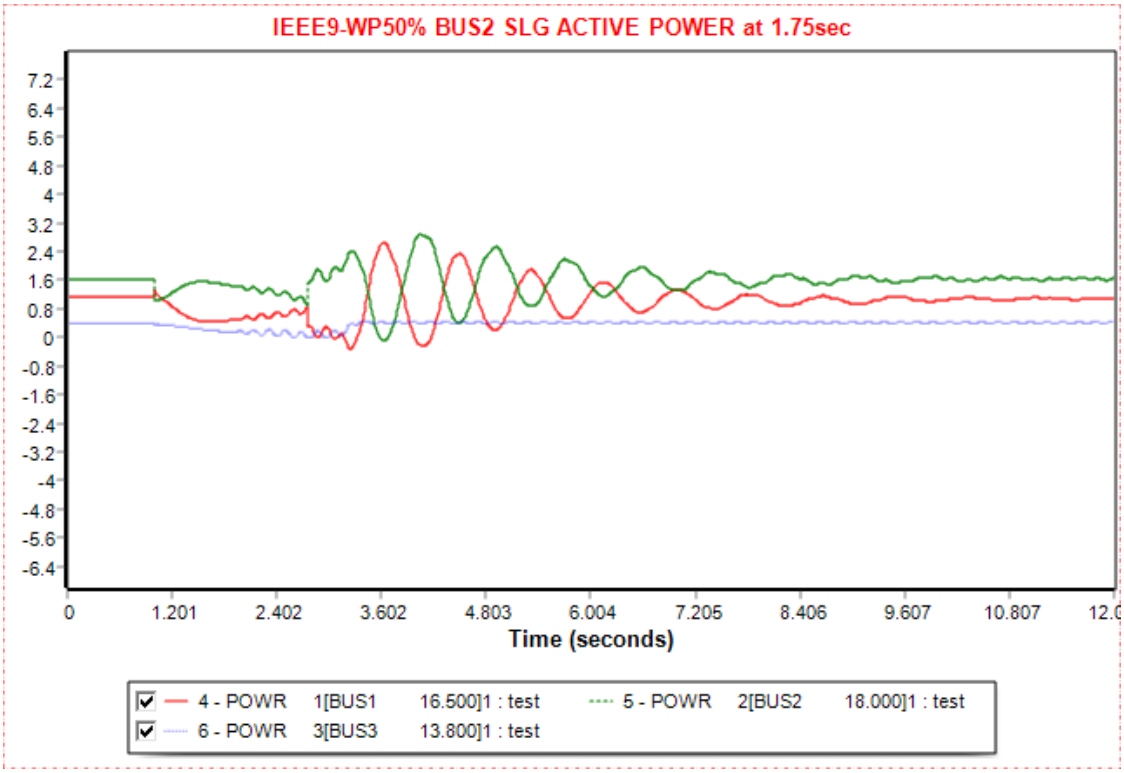

Figure 5. 46 Active Power plots of SLG fault at bus 2 when it is cleared at 2.75 sec at IEEE9 Wind Power Remodeled bus system with 50% Replacement

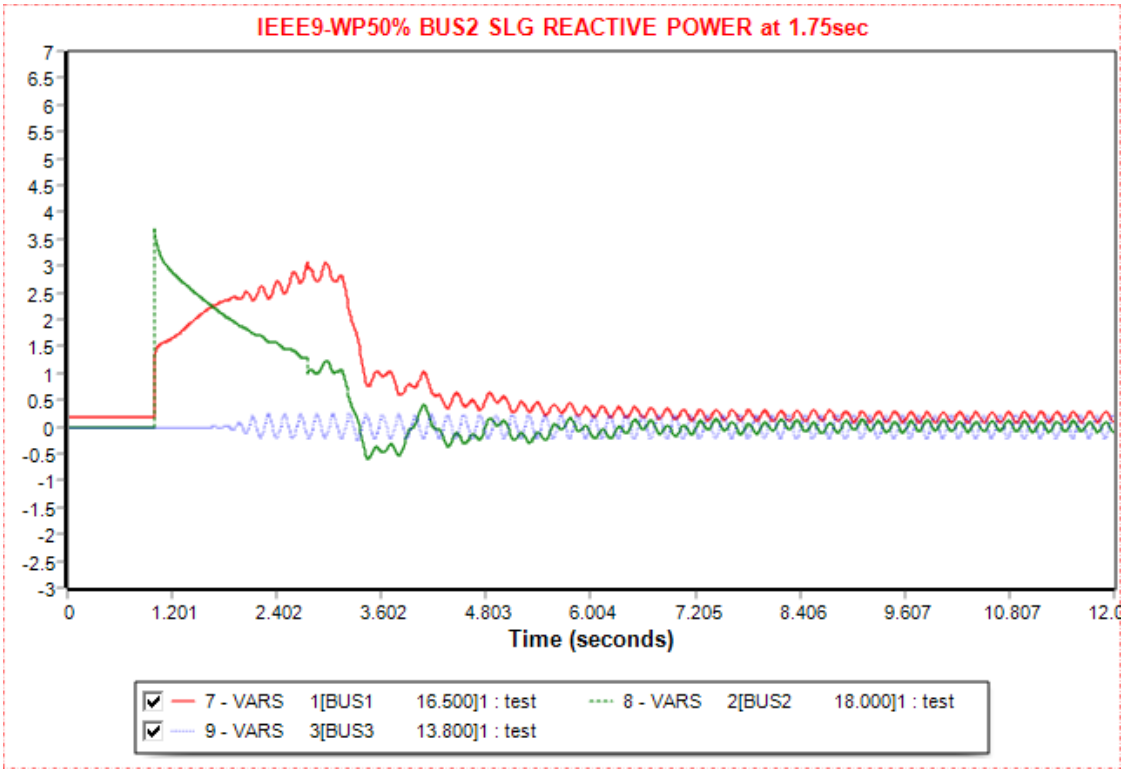

Figure 5. 47 Reactive Power plots of SLG fault at bus 2 when it is cleared at 2.75 sec at IEEE9 Wind Power Remodeled bus system with 50% Replacement

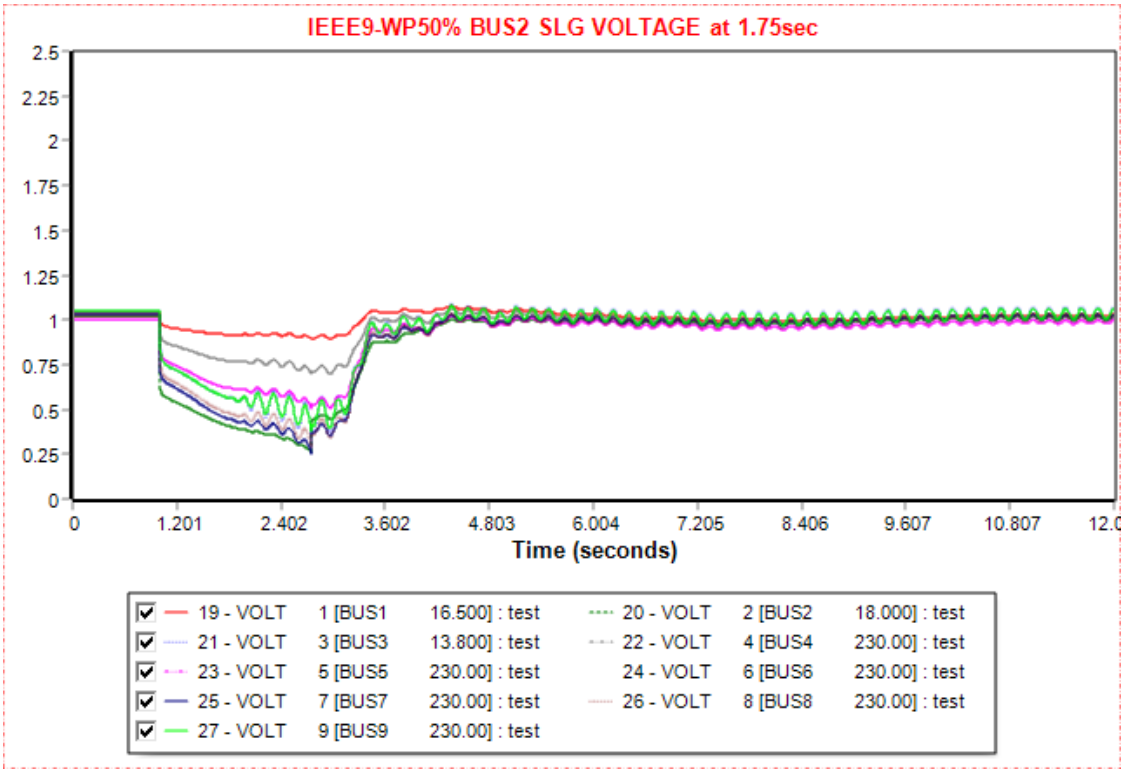

Figure 5. 48 Voltage plots of SLG fault at bus 2 when it is cleared at 2.75 sec at IEEE9 Wind Power Remodeled bus system with 50% Replacement

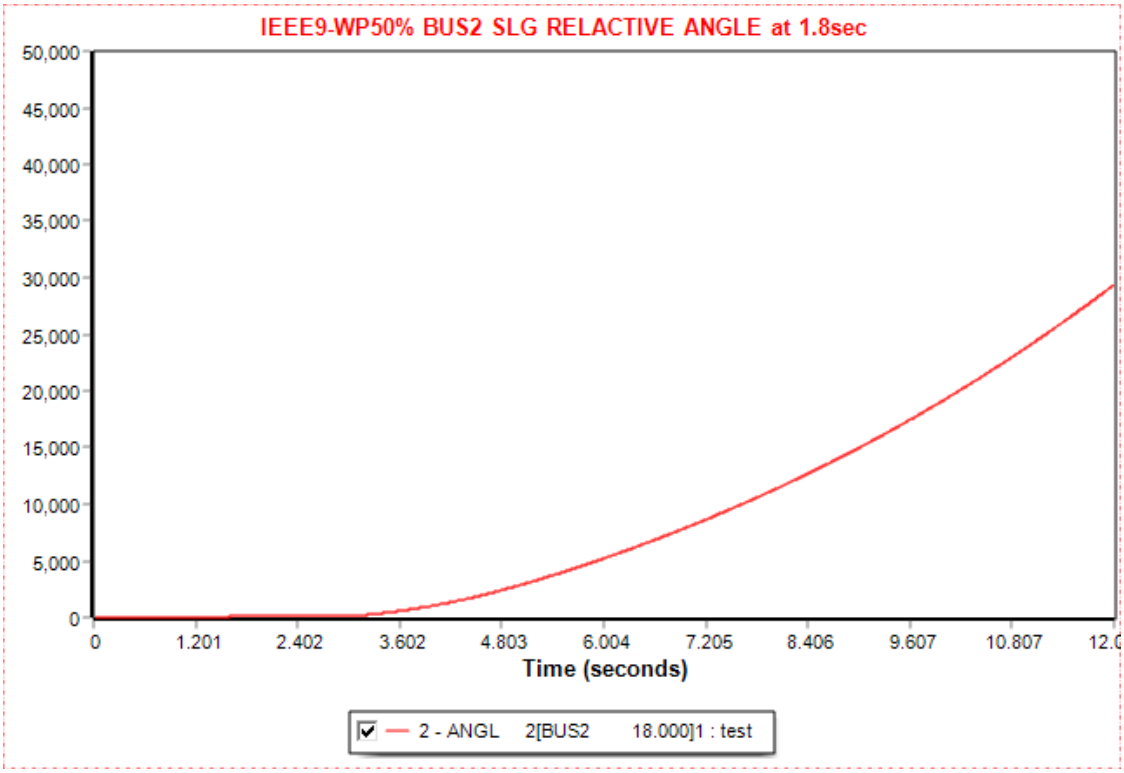

Figure 5. 49 Relative power angle plots of SLG fault at bus 2 when it is cleared at 2.8 sec at IEEE9 Wind Power Remodeled bus system with 50% Replacement

5.2.2 Faults at Bus 7 of the IEEE9 Bus System Wind Power Remodeled with the Partial Replacement (50%) of Generator 3

In the following sections, the fault location is bus 7, which is next to generating bus 2. The simulation is the same as section 5.2.1, with the only difference being the bus that the disturbance occurs.

5.2.2.1 Three-phase Symmetrical Fault at Bus 7 of the Wind Power 50% of a Generator Remodeled System

The critical time that the fault must be cleared is calculated to be 0.25 sec, the same as the IEEE9 system. That means after 0.25 sec of the fault occurrence, the disturbance must be removed for the system to maintain its stability. After the clearance, line 8-7 is tripped, and after 1 sec it is connected again until 12 sec. The process can be seen in Table 5.11. Figures 5.50-5.54 present the power angle of generator 2 with respect to the power angle of the swing bus, the buses frequency, the real and active power of the generators, including the one producing wind power, and the buses voltage when the fault is cleared at CFCT. Figure 5.55 shows the relative power angle when the system is desynchronized at 0.3 sec, 0.05 sec after the critical fault clearing time.

Table 5. 11 IEEE9 Wind Power Remodeled bus system with 50% Replacement Three-phase symmetrical Fault at Bus 7

Action	Time (sec)
Steady State	0.00
Apply Fault	1.00
Clear Fault	1.25
Trip Line	1.25
Connect Line	2.25
Power Flow	12.00

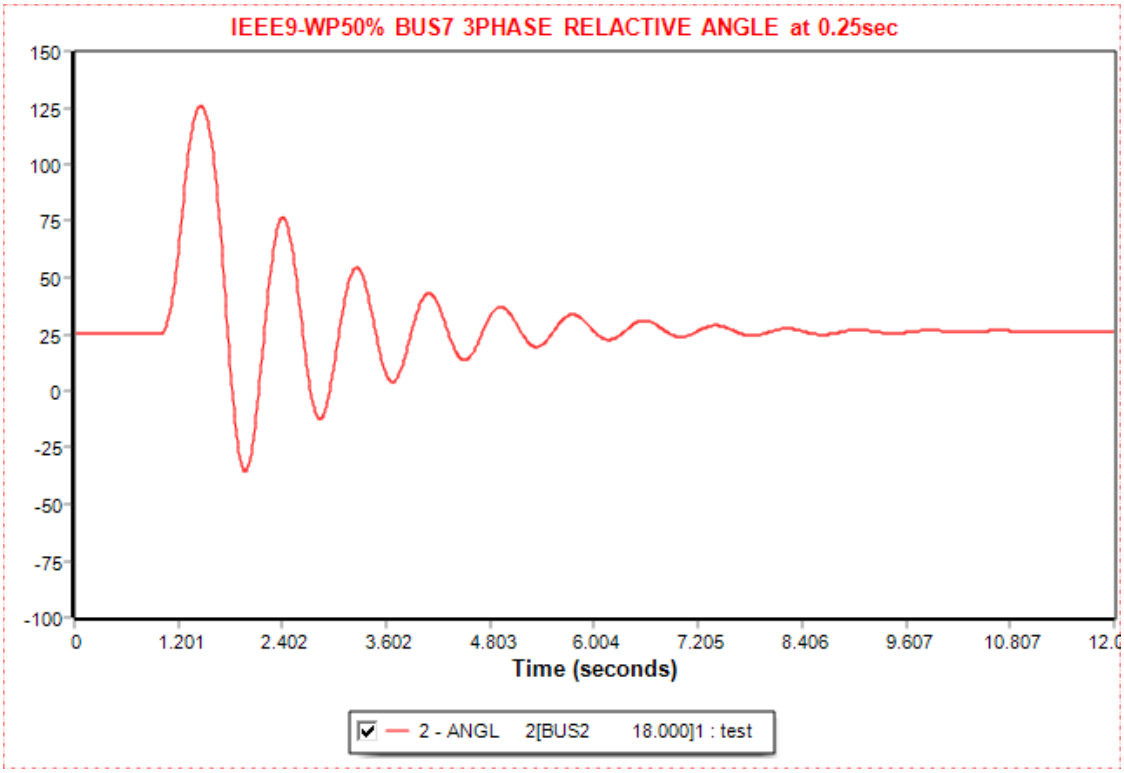

Figure 5. 50 Relative power angle plots of three-phase symmetrical fault at bus 7 when it is cleared at 1.25 sec at IEEE9 Wind Power Remodeled bus system with 50% Replacement

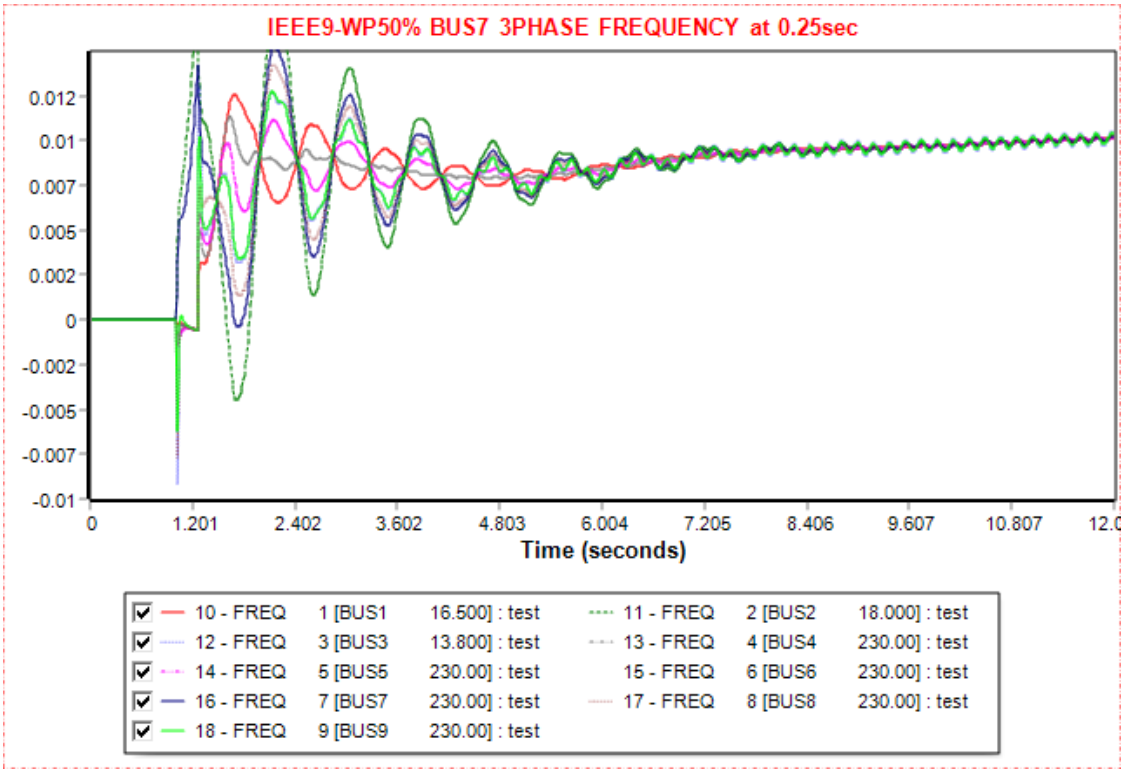

Figure 5. 51 Frequency plots of three-phase symmetrical fault at bus 7 when it is cleared at 1.25 sec at IEEE9 Wind Power Remodeled bus system with 50% Replacement

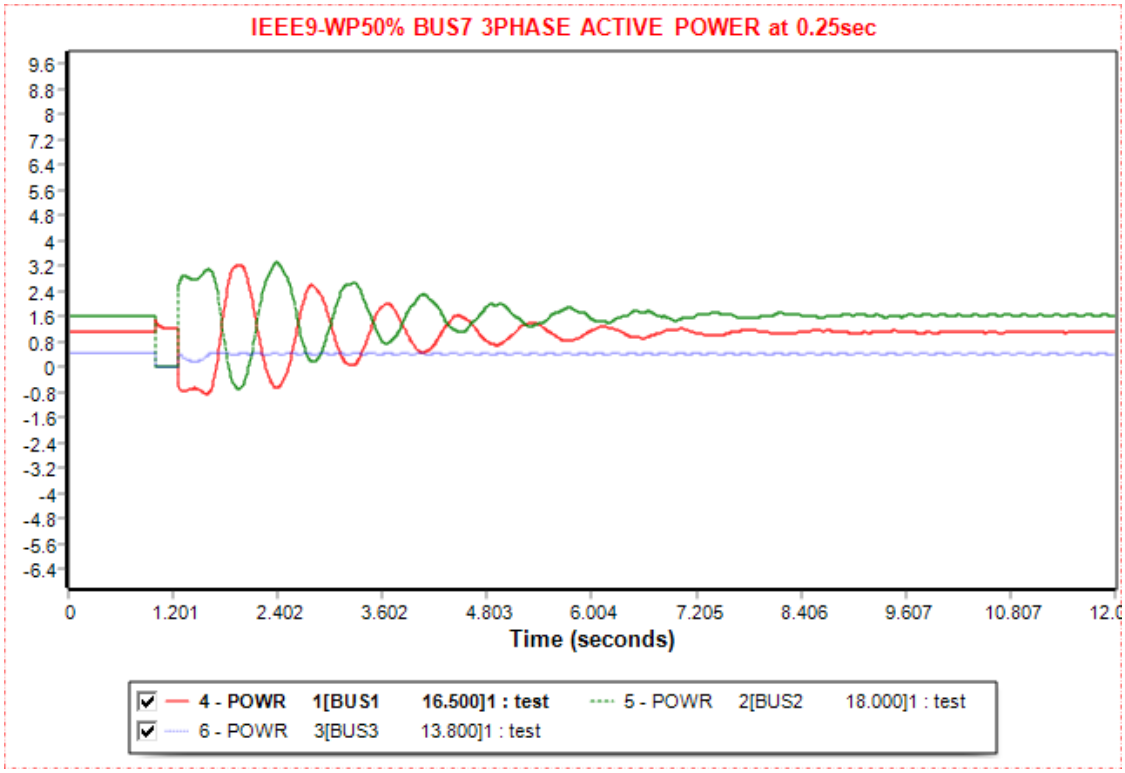

Figure 5. 52 Active Power plots of three-phase symmetrical fault at bus 7 when it is cleared at 1.25 sec at IEEE9 Wind Power Remodeled bus system with 50% Replacement

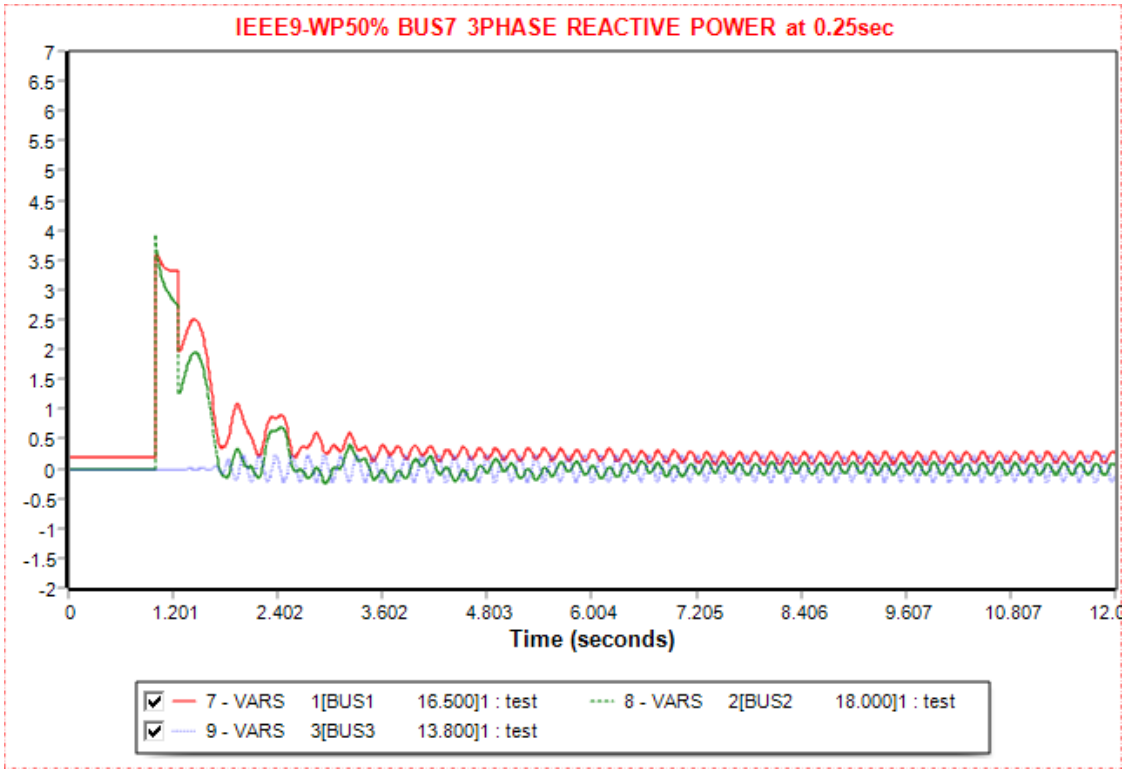

Figure 5. 53 Reactive Power plots of three-phase symmetrical fault at bus 7 when it is cleared at 1.25 sec at IEEE9 Wind Power Remodeled bus system with 50% Replacement

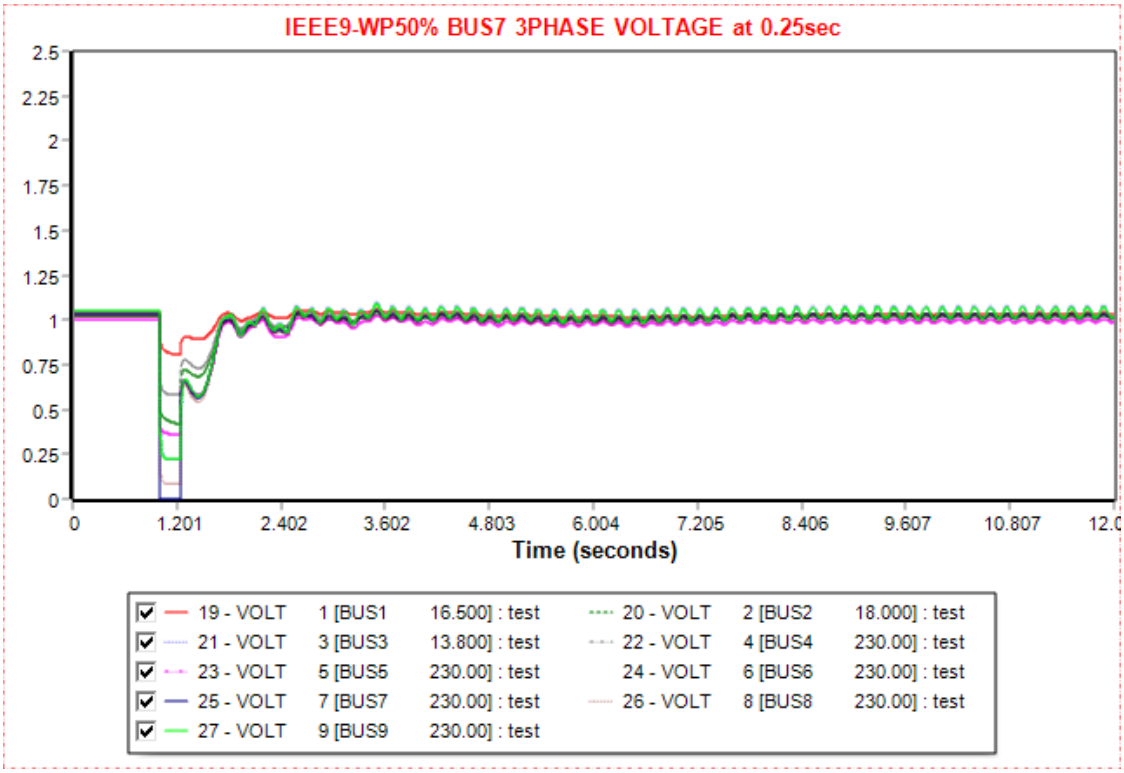

Figure 5. 54 Voltage plots of three-phase symmetrical fault at bus 7 when it is cleared at 1.25 sec at IEEE9 Wind Power Remodeled bus system with 50% Replacement

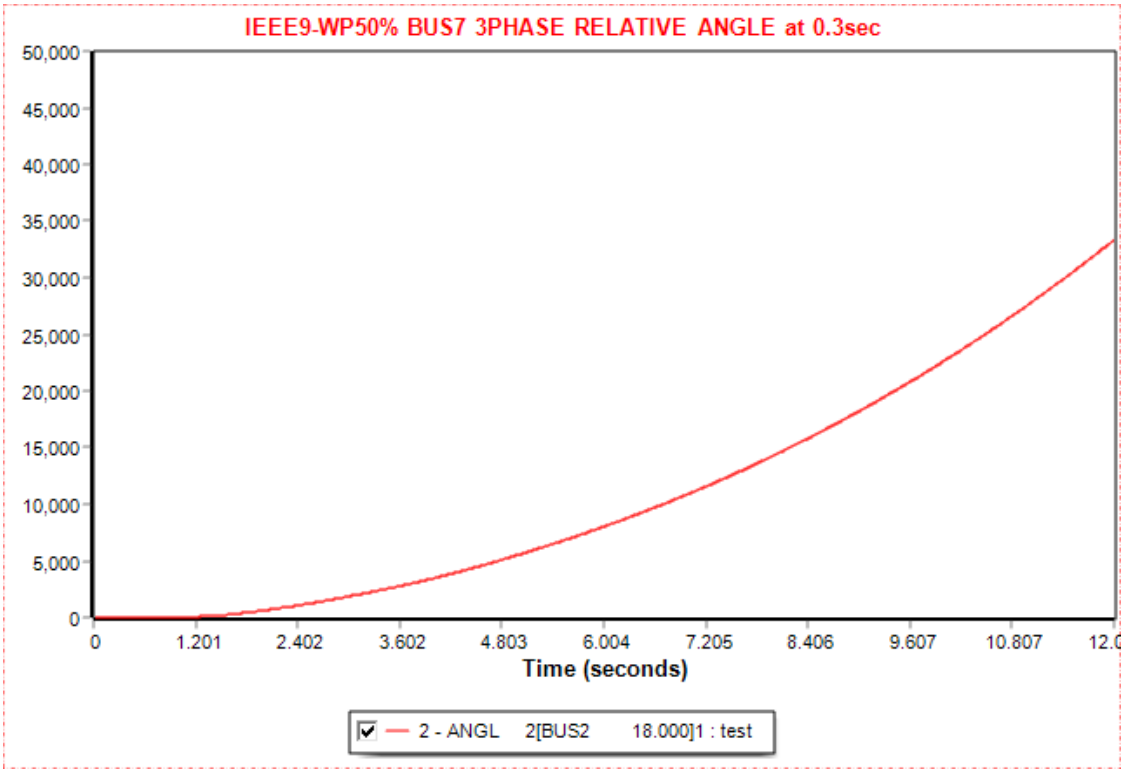

Figure 5. 55 Relative power angle plots of three-phase symmetrical fault at bus 7 when it is cleared at 1.3 sec at IEEE9 Wind Power Remodeled bus system with 50% Replacement

5.2.2.2 SLG Fault at Bus 7 of the IEEE9 Bus System Wind Power Remodeled with the Partial Replacement (50%) of Generator 3

In this simulation, the fault is an SLG, and the network can remain stable despite the duration of the fault. Like in other sections, since there is no CFCT, the duration of the fault is 0.5 sec in order to see the transient behavior of the system. Firstly, there is an initial power flow for 1 sec, and then the disturbance is applied for 0.5 sec. Simultaneously, for the fault clearance, line 7-8 is tripped, and after 1 sec, at 2.5 sec, it is connected to the network. As seen from Table 5.12, the simulation lasts for 12 sec. Figures 5.56-5.60 present the power angle of generator 2 with respect to the power angle of the swing bus, the buses frequency, the real and active power of the generators, including the one producing wind power, and the buses voltage when the fault is cleared at 0.5 sec. The limits of the plants' excitation are not at the same level as in the previous section where the fault was severe. This proves that the SLG is fatal for the system when it is not applied in the inspected generator bus.

Table 5. 12 IEEE9 Wind Power Remodeled bus system with 50% Replacement SLG Fault at Bus 7

Action	**Time (sec)**
Steady State	0.00
Apply Fault	1.00
Clear Fault	1.5
Trip Line	1.5
Connect Line	2.5
Power Flow	12.00

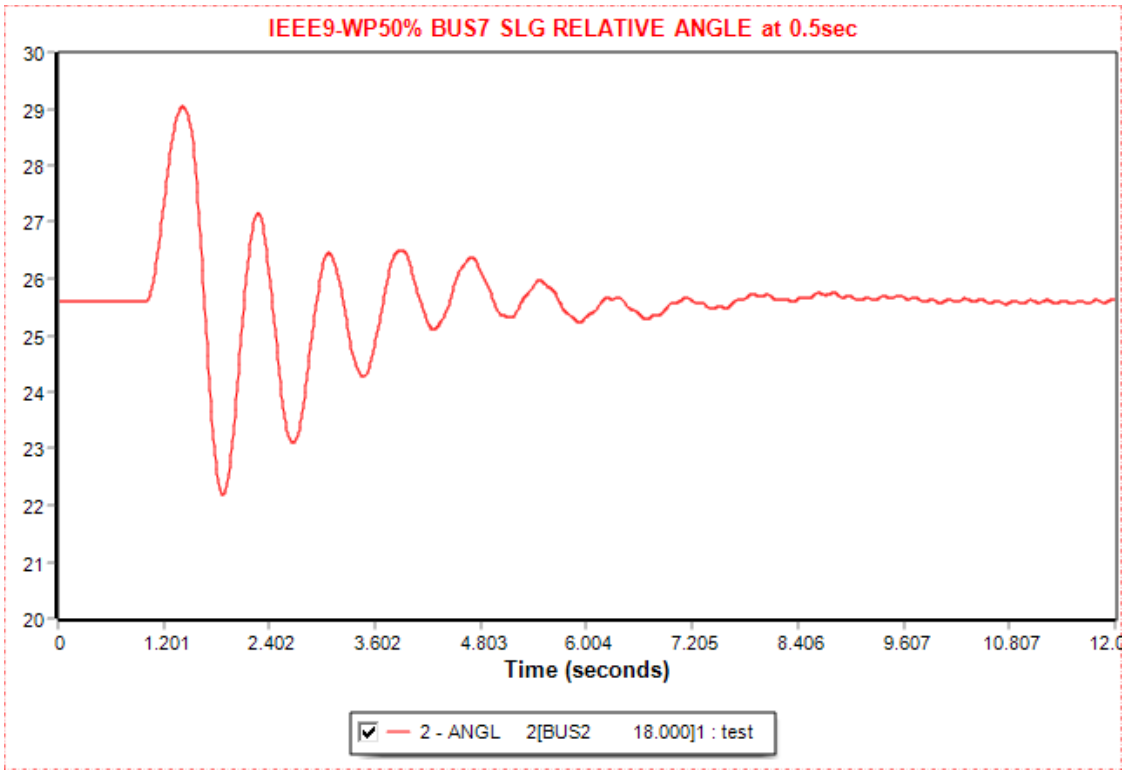

Figure 5. 56 Relative power angle plots of SLG fault at bus 7 when it is cleared at 1.5 sec at IEEE9 Wind Power Remodeled bus system with 50% Replacement

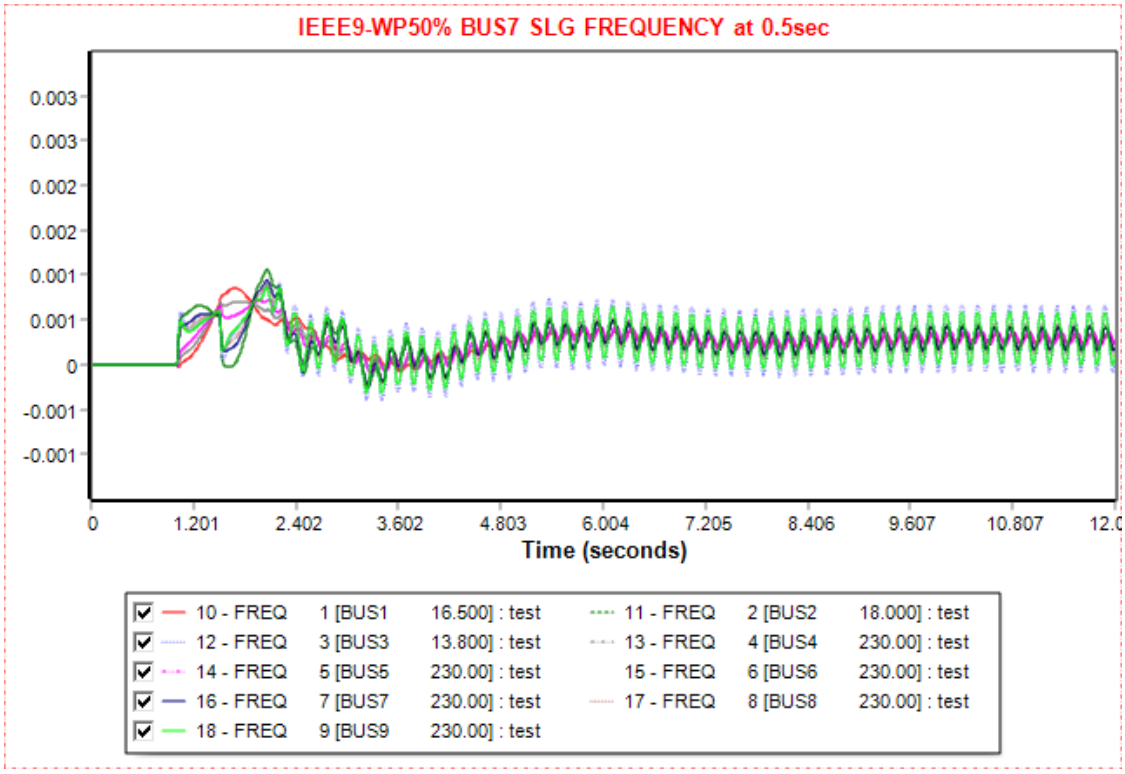

Figure 5. 57 Frequency plots of SLG fault at bus 7 when it is cleared at 1.5 sec at IEEE9 Wind Power Remodeled bus system with 50% Replacement

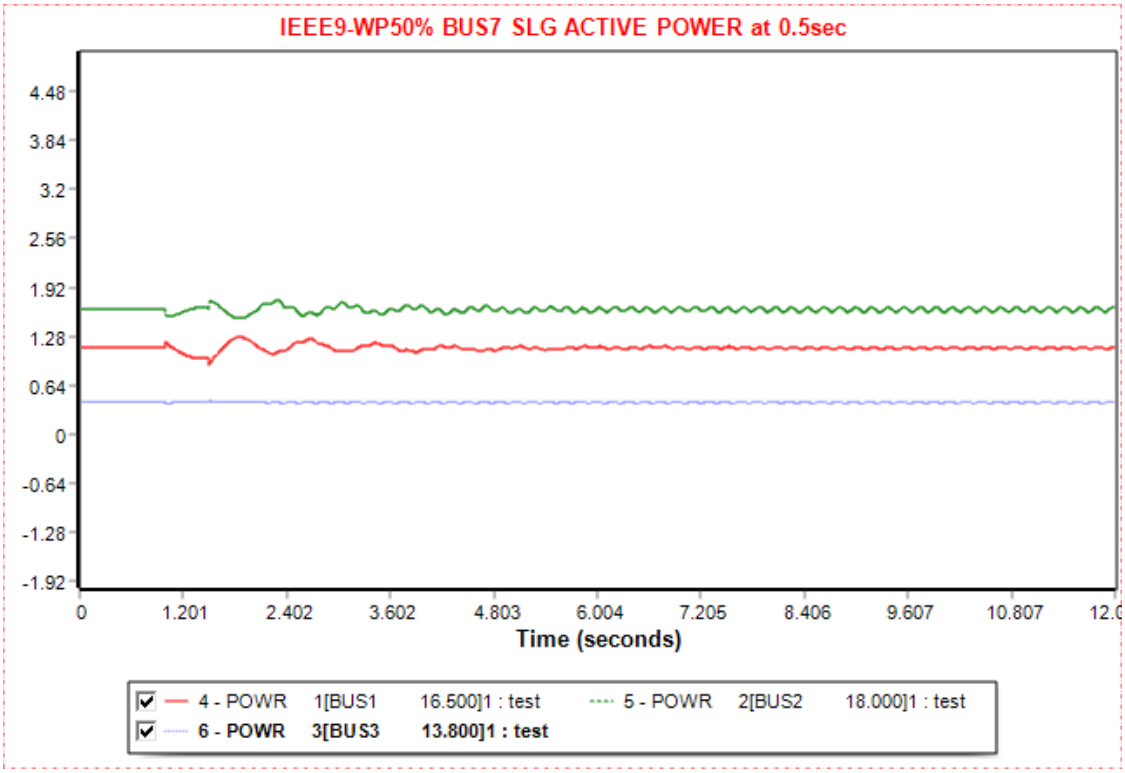

Figure 5. 58 Active Power plots of SLG fault at bus 7 when it is cleared at 1.5 sec at IEEE9 Wind Power Remodeled bus system with 50% Replacement

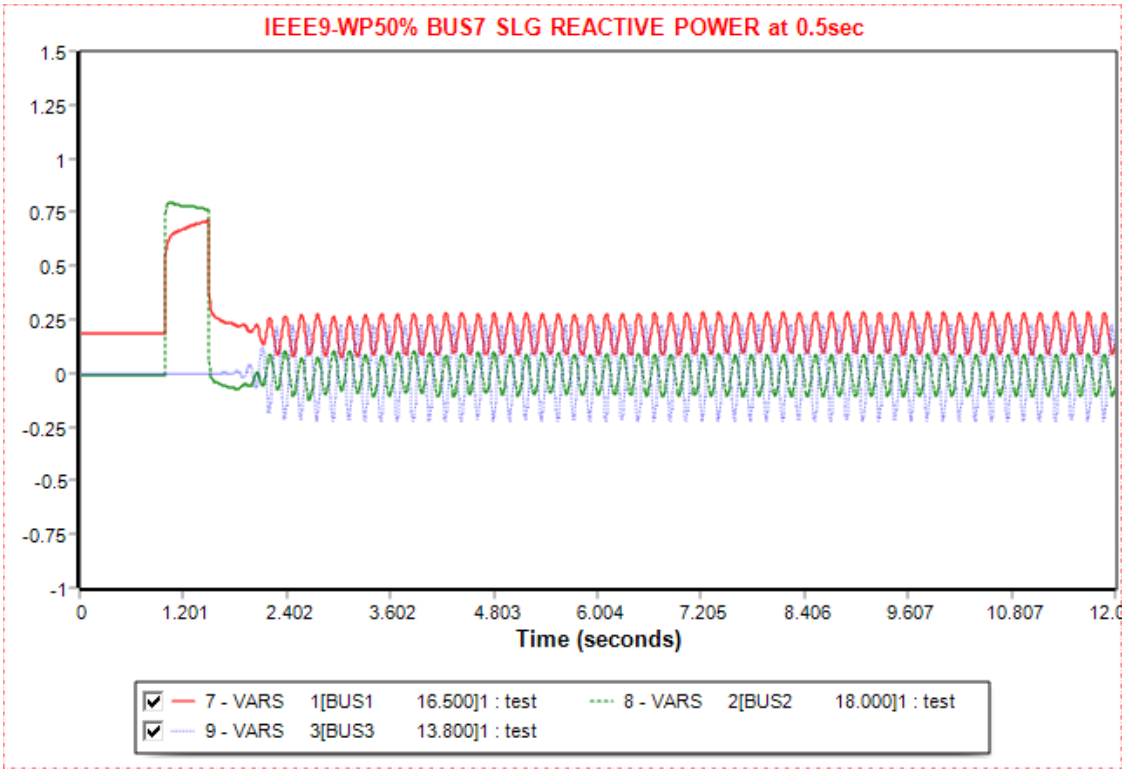

Figure 5. 59 Reactive Power plots of SLG fault at bus 7 when it is cleared at 1.5 sec at IEEE9 Wind Power Remodeled bus system with 50% Replacement

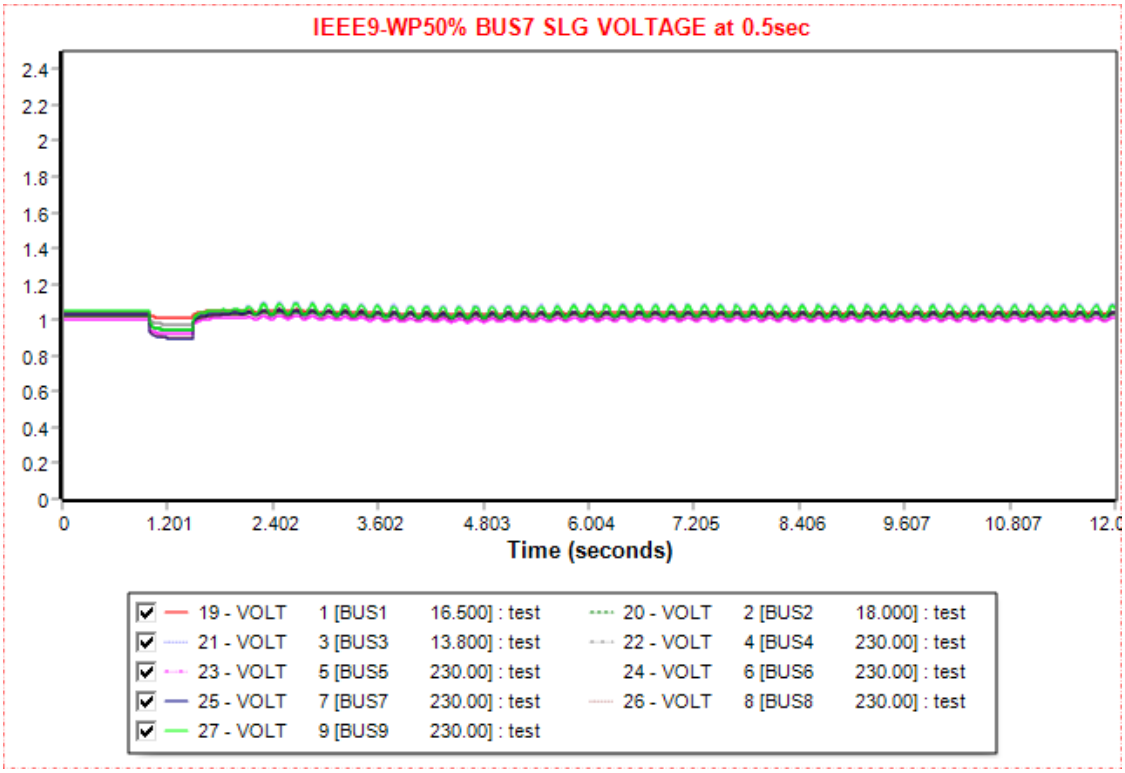

Figure 5. 60 Voltage plots of SLG fault at bus 7 when it is cleared at 1.5 sec at IEEE9 Wind Power Remodeled bus system with 50% Replacement

5.2.3 Faults at Bus 8 of the IEEE9 Bus System Wind Power Remodeled with the Partial Replacement (50%) of Generator 3

In the following sections, the fault location is bus 8, which is connected to a 100 MW load. The CFCT is expected to be greater than in other sections of this scenario due to the longer distance from generator to bus 2.

5.2.3.1 Three-phase Symmetrical at Bus 8 of the IEEE9 Bus System Wind Power Remodeled with the Partial Replacement (50%) of Generator 3

In the 50% Remodeled IEEE9 bus system, the three-phase symmetrical fault is proven severe if it is cleared at a time greater than 0.4 sec. The simulation process involves an initial load flow for 1 sec when the three-phase symmetrical fault is applied at bus 8. The critical time is 0.4 sec, so the fault is cleared at 1.4 sec and at the same time the line 8-7 is tripped. At 2.4 sec the line 7-8 is connected to the system, and the simulation continues

until 12 sec (Table 5.13). Figures 5.61-5.65 illustrate the power angle of generator 2 with respect to the power angle of the swing bus, the buses frequency, the real and active power of the generators, including the one producing wind power, and the buses voltage when the fault is cleared at CFCT. Figure 5.66 shows the loss of synchronization of the power angle of generator 2 with respect to the power angle of the swing bus when the fault is cleared 0.05 sec after the CFCT. The more central the bus is, the more tolerance it has towards a fault as the clearing time is lower than the other two buses. Despite that, the three-phase symmetrical fault's impact is strong for the grid as there are high limits in the excitation, around 4 pu, in both active and reactive power. Also, the bus 8 voltage is reaching 0 pu when the fault happens.

Table 5. 13 IEEE9 Wind Power Remodeled bus system with 50% Replacement Three-phase symmetrical Fault at Bus 8

Action	**Time (sec)**
Steady State	0.00
Apply Fault	1.00
Clear Fault	1.4
Trip Line	1.4
Connect Line	2.4
Power Flow	12.00

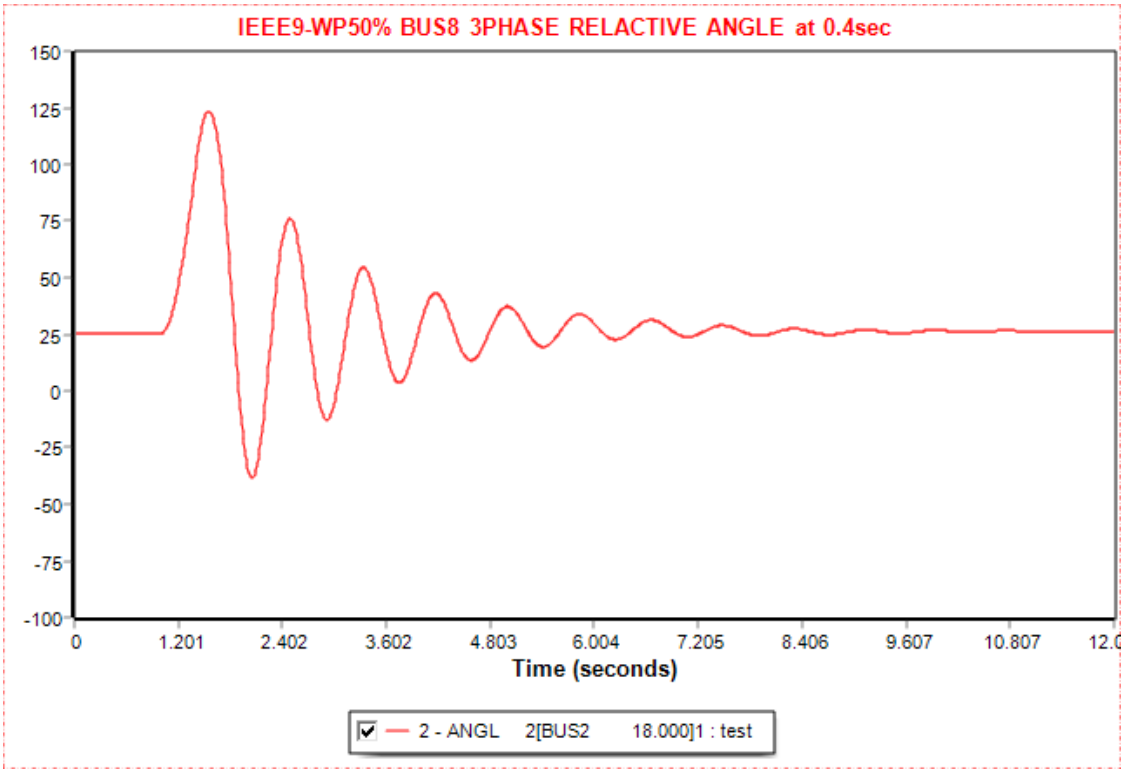

Figure 5. 61 Relative power angle plots of three-phase symmetrical fault at bus 8 when it is cleared at 1.4 sec at IEEE9 Wind Power Remodeled bus system with 50% Replacement

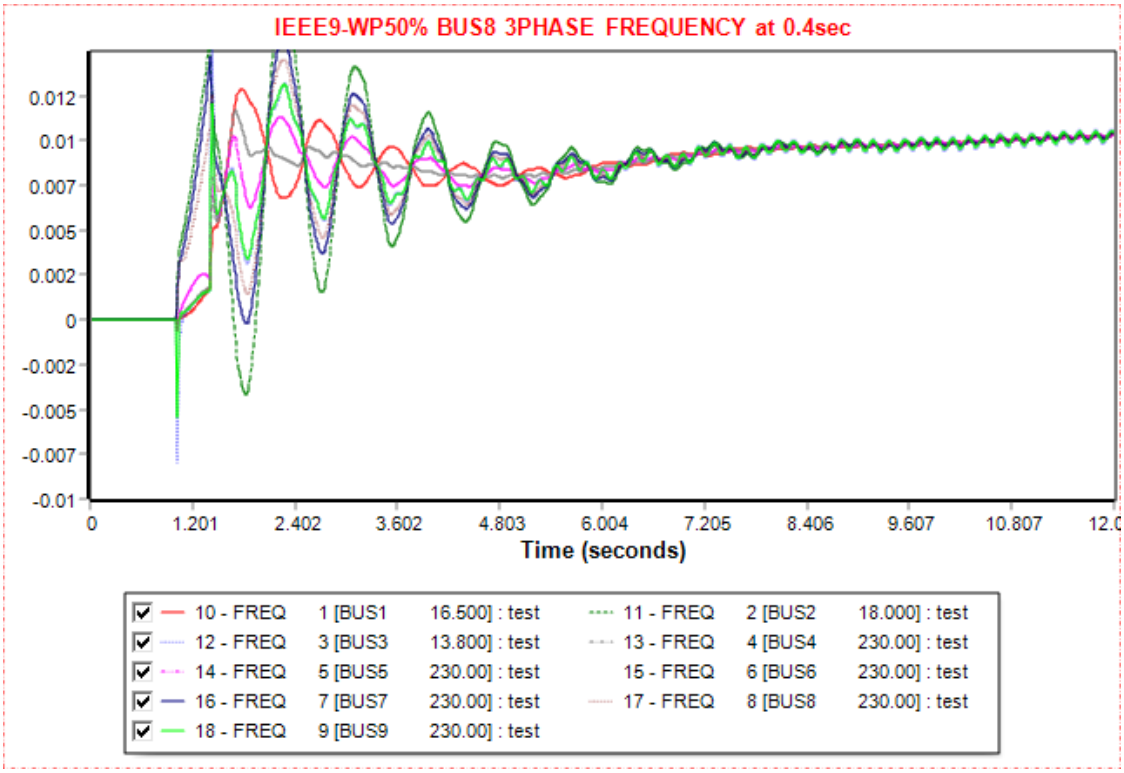

Figure 5. 62 Frequency plots of three-phase symmetrical fault at bus 8 when it is cleared at 1.4 sec at IEEE9 Wind Power Remodeled bus system with 50% Replacement

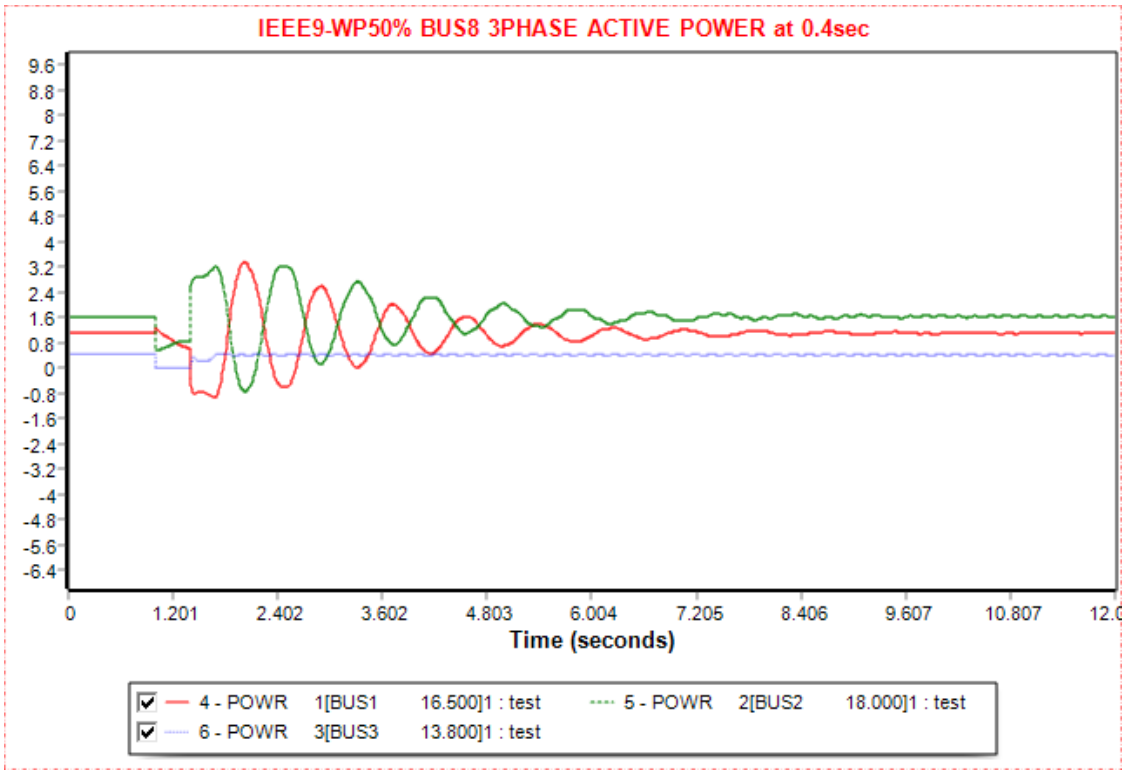

Figure 5. 63 Active Power plots of three-phase symmetrical fault at bus 8 when it is cleared at 1.4 sec at IEEE9 Wind Power Remodeled bus system with 50% Replacement

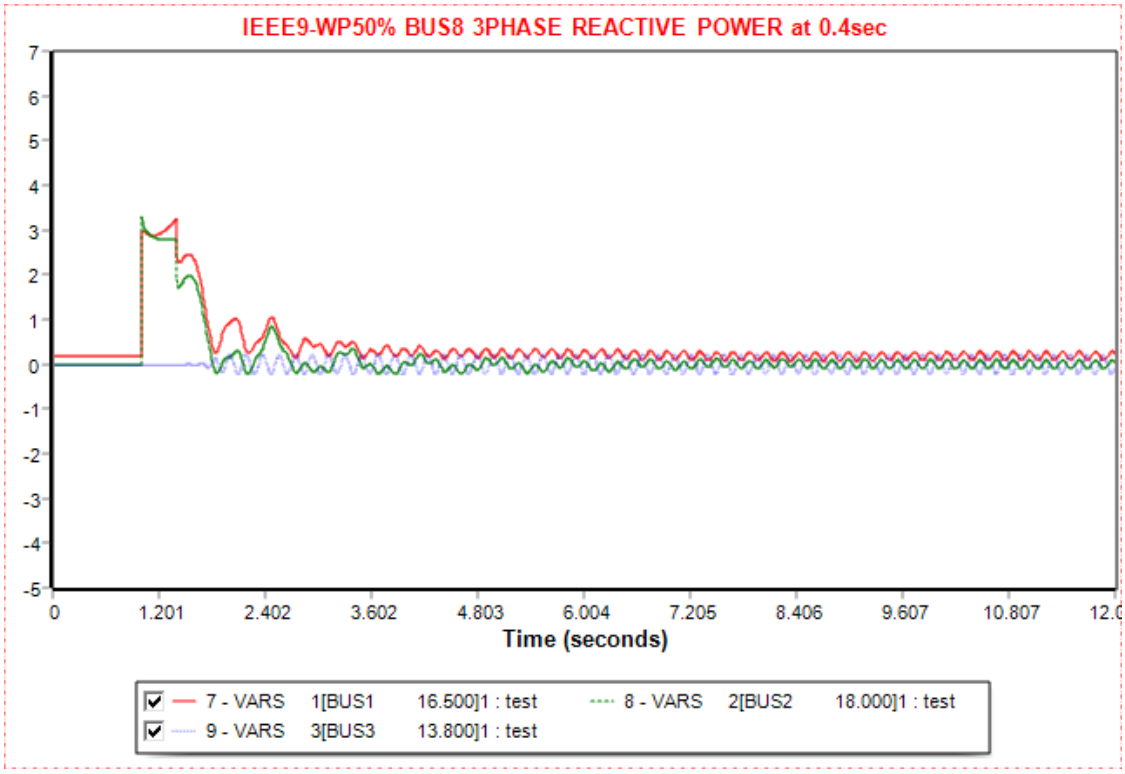

Figure 5. 64 Reactive Power plots of three-phase symmetrical fault at bus 8 when it is cleared at 1.4 sec at IEEE9 Wind Power Remodeled bus system with 50% Replacement

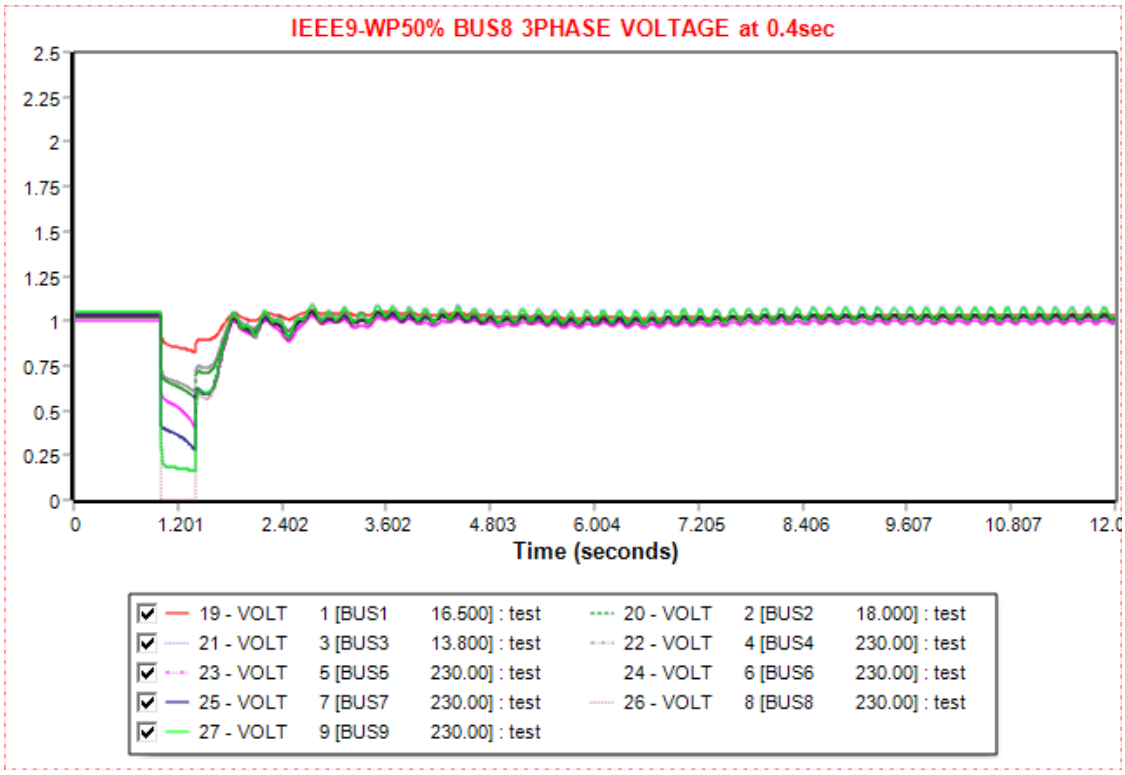

Figure 5. 65 Voltage plots of three-phase symmetrical fault at bus 8 when it is cleared at 1.4 sec at IEEE9 Wind Power Remodeled bus system with 50% Replacement

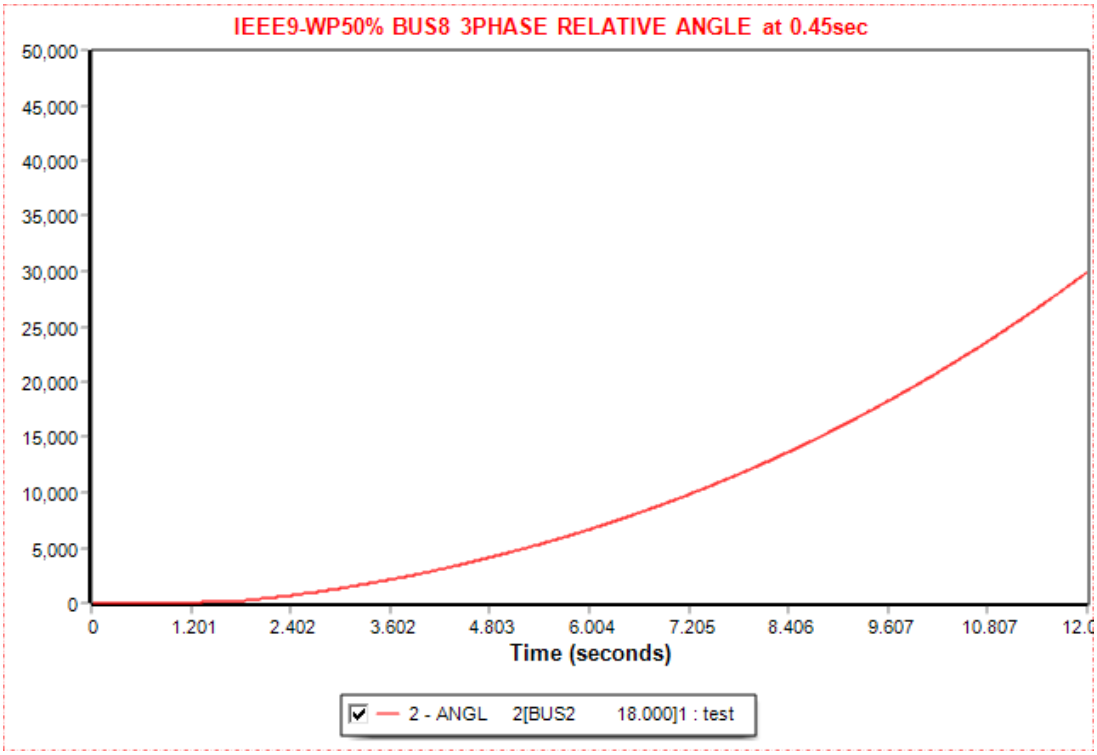

Figure 5. 66 Relative power angle plots of three-phase symmetrical fault at bus 8 when it is cleared at 1.45 sec at IEEE9 Wind Power Remodeled bus system with 50% Replacement

5.2.3.2 SLG Fault at Bus 8 of the IEEE9 Bus System Wind Power Remodeled with the Partial Replacement (50%) of Generator 3

There is no CFCT since the fault is not severe, so its duration is 0.5 sec in order to see the transient behavior of the system. Firstly, there is an initial power flow for 1 sec, and then the disturbance is applied for 0.5 sec. Simultaneously, for the fault clearance the line 7-8 is tripped and after 1 sec, at 2.5 sec, it is connected to the network. As seen from Table 5.4, the simulation lasts for 12 sec. Figures 5.67-5.71 present the power angle of generator 2 with respect to the power angle of the swing bus, the buses frequency, the real and active power of the generators, including the one producing wind power, and the buses voltage when the fault is cleared at 0.5 sec. The impact of this fault is not as strong as a three-phase symmetrical or an SLG at bus 2 as the fluctuations are around 1 pu in both reactive and active power compared to the 4 pu in the situations mentioned. The same applies to the angle plots, where in this simulation, the total width is around 15 degrees in contrast to 120-150 of the other cases. Due to the wind turbine model, there are a few oscillations in this case too.

Table 5. 14 IEEE9 Wind Power Remodeled bus system with 50% Replacement SLG Fault at Bus 8

Action	Time (sec)
Steady State	0.00
Apply Fault	1.00
Clear Fault	1.5
Trip Line	1.5
Connect Line	2.5
Power Flow	12.00

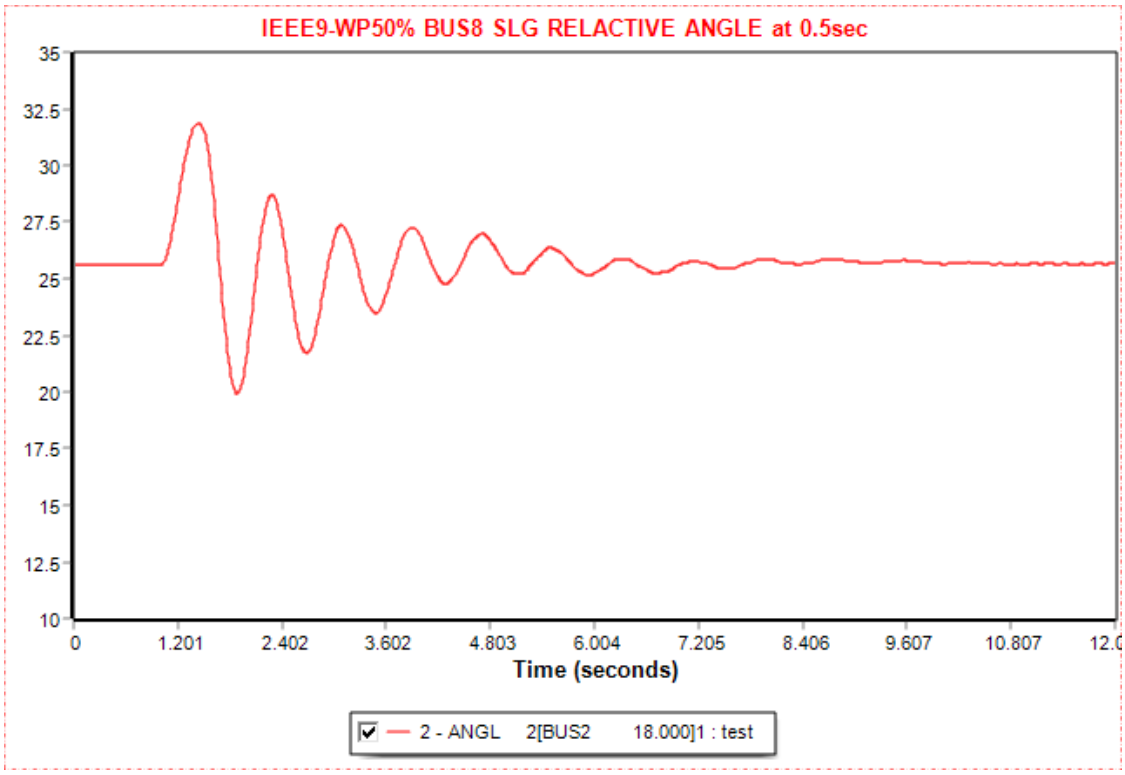

Figure 5. 67 Relative power angle plots of SLG fault at bus 8 when it is cleared at 1.5 sec at IEEE9 Wind Power Remodeled bus system with 50% Replacement

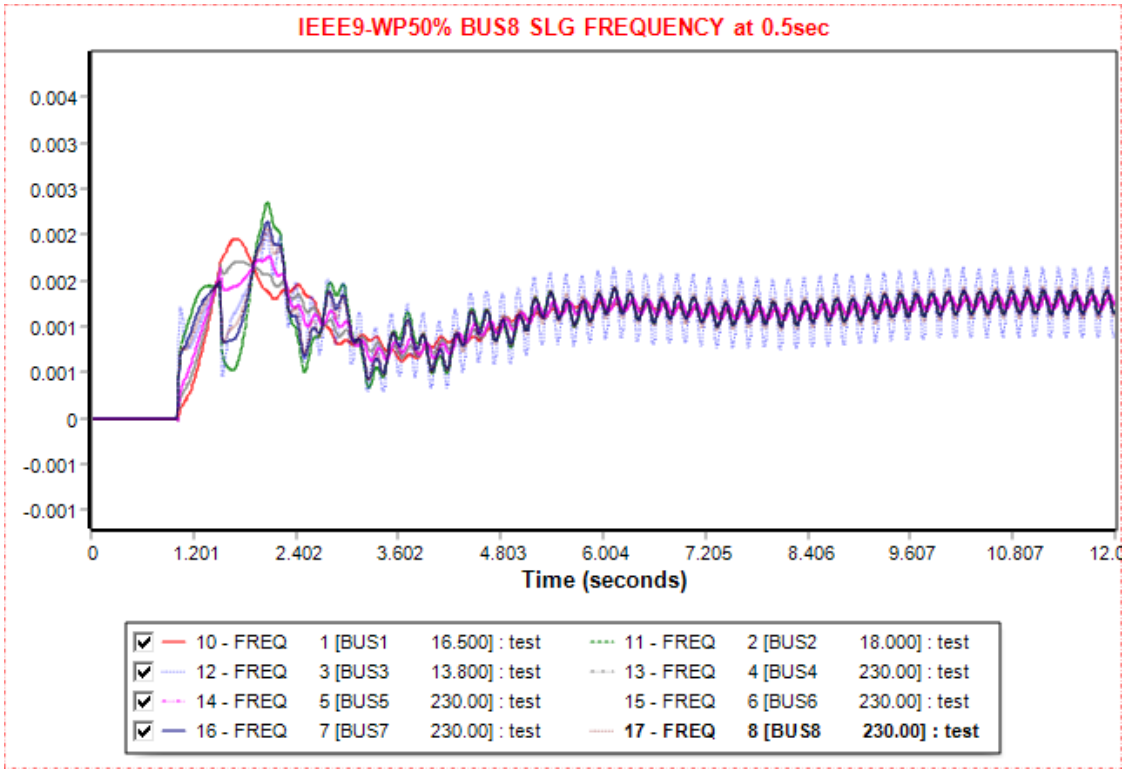

Figure 5. 68 Frequency plots of SLG fault at bus 8 when it is cleared at 1.5 sec at IEEE9 Wind Power Remodeled bus system with 50% Replacement

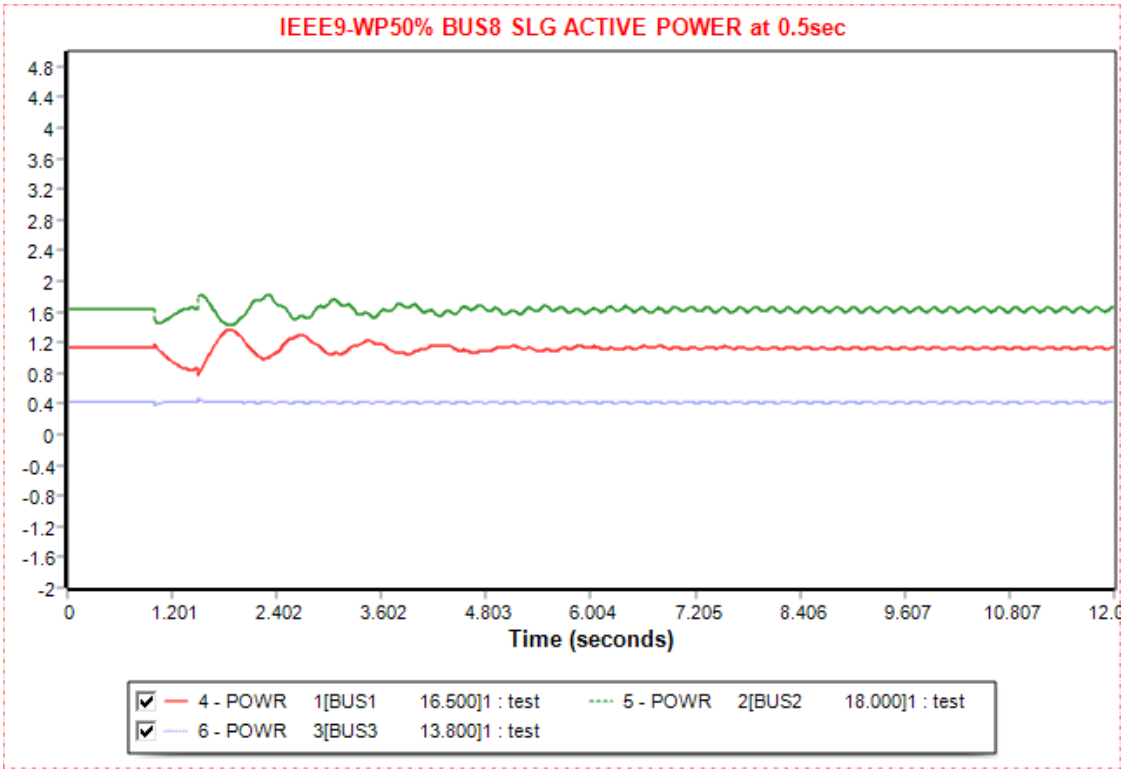

Figure 5. 69 Active Power plots of SLG fault at bus 8 when it is cleared at 1.5 sec at IEEE9 Wind Power Remodeled bus system with 50% Replacement

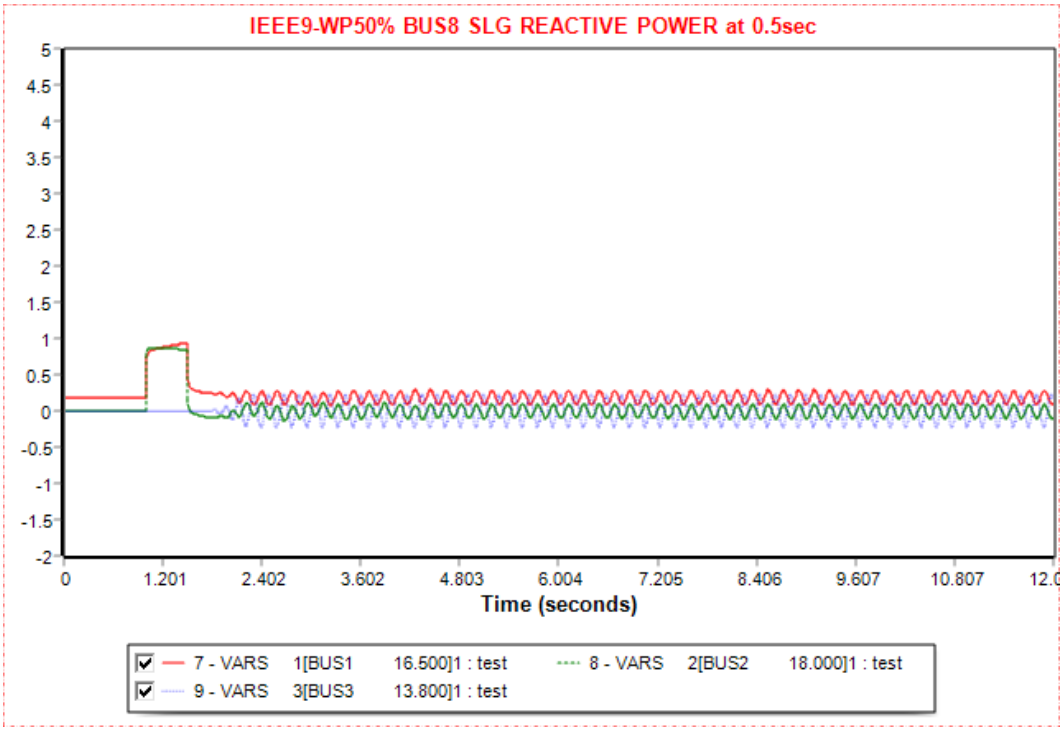

Figure 5. 70 Reactive Power plots of SLG fault at bus 8 when it is cleared at 1.5 sec at IEEE9 Wind Power Remodeled bus system with 50% Replacement

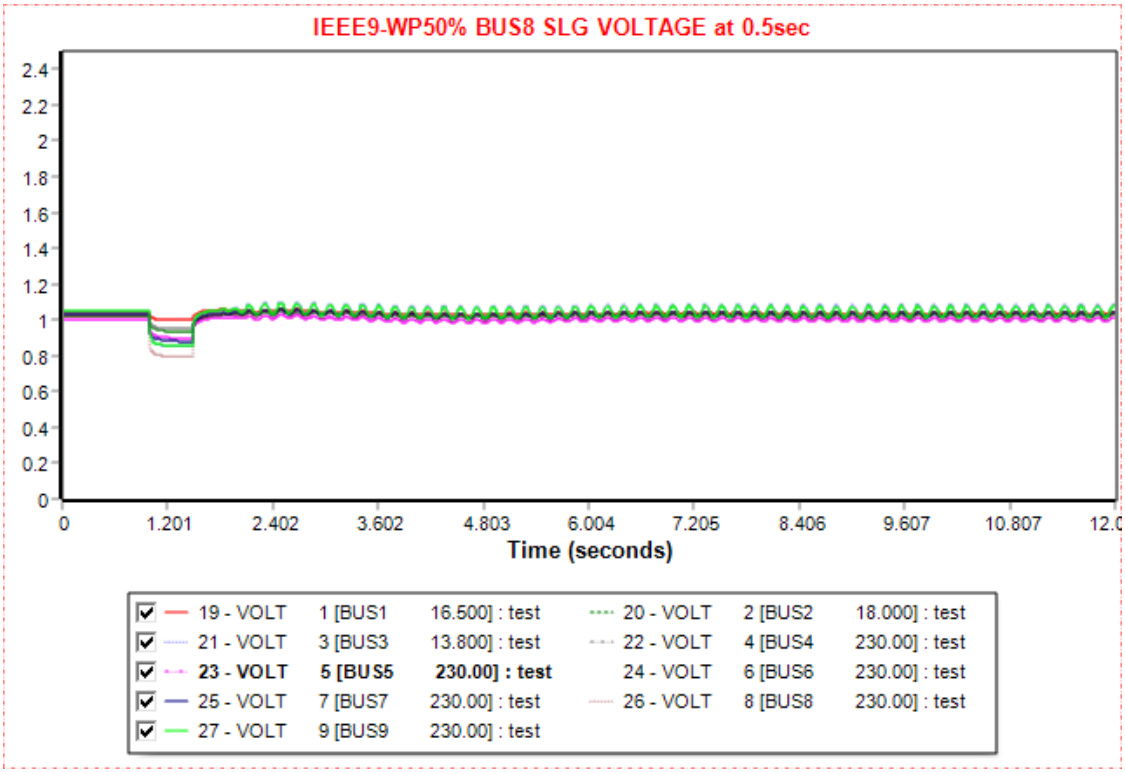

Figure 5. 71 Relative power angle plots of SLG fault at bus 8 when it is cleared at 1.5 sec at IEEE9 Wind Power Remodeled bus system with 50% Replacement

5.2.4 Diagram Analysis of the IEEE9 Bus System Wind Power Remodeled with the Partial Replacement (50%) of Generator 3

The first diagram presented in each case is a relative power angle with respect to the power angle of the swing bus. In the IEEE 9 Bus system with generator 3 replaced by 50% of the total capacity by wind energy, the power angle has the same fluctuations between the three-phase symmetrical faults (Figure 5.38, 5.50, 5.61). The generator 2 angle with respect to the swing bus power angle, at the beginning of the fault, increases and reaches up to 150 degrees and then goes down to -25 degrees in order to maintain stability. Similar behavior can be seen in the SLG diagram when the fault occurs at bus 2, where the angle reaches up to 125 degrees, proving that the SLG fault at a generator bus can have severe results (Figure 5.44). In the other two SLG Figures, the power angle goes up to 32.5 to 35 degrees and decreases to 20, meaning the SLG is not severe to the system. (Figure 5.56, 5.67). In the desynchronization diagrams, the fault cannot be sustained, and the generator 2 power angle increases exponentially.

In the frequency diagrams, there is a similar way the plots are in both three-phase symmetrical faults (Figure 5.39, 5.51, 5.62) and SLG (Figure 5.45, 5.56, 5.67). In the three-phase balanced, the 0 Hz initial frequency deviation is around 0.07 to 0.01 Hz, and after 4 sec during stabilization, a few small width oscillations exist. The buses that have the most deviations during the fault are connected to the wind turbine, bus 3, and the bus next to it, the bus 9. Similar results can be seen in the SLG at bus 2 (Figure 5.45), where there is a substantial deviation, which may derive from the considerable duration of the fault as the clearing time is 1.75 sec. In the other two SLG diagrams, the deviation is minimal and around 0.001 Hz.

The active plot diagrams are also similar in the three-phase symmetrical cases (Figure 5.40, 5.52, 5.63) and the SLG at bus 2 (Figure 5.46). There are oscillations but what is noticed is that the wind turbine plot is barely affected by the fault, and the fluctuations have a small width. Even smaller impacts have the other two SLG (Figure 5.57, 5.68), where the deviation from the initial active power value is smaller and is around 20 MW. In all diagrams, the swing bus active power is higher around 0.91 pu, and that is because the 41.5 MW of the wind farm can not produce the necessary power for the system's total load.

The reactive power diagrams, like the active power, refer only to the three generator buses. Like the other graphs, the three-phase symmetrical (Figure 5.41, 5.53, 5.64) and the SLG (5.47, 5.58, 5.69) have similar plots to the first case. That is because in both cases, the modeling of the wind farm is the same. In all the diagrams, when the fault happens in the two synchronous generators, the reactive power increases to stabilize the fault and then decreases. After 4 seconds, the system is stabilized, and only a few small oscillations exist due to the wind turbine. It is worth mentioning that bus 3 reactive power is not increasing and remains at around 0 pu when the fault occurs.

The voltage diagrams are similar in both three-phase symmetrical (Figure 5.42, 5.54, 5.65) and the SLG (5.48, 5.59, 5.70). When the fault occurs, there is a sudden decrease in the voltages, and after 4 sec, they tend to reach 1 pu. In the three-phase symmetrical fault cases and the SLG at bus 2 (Figure 5.48), the bus's decrease where the fault is happening reaches 0 pu. The wind farm voltage is around 0.75 pu during the fault. In the SLG diagrams at bus 7 and 8 (Figure 5.59, 5.70), the decrease is small, and the voltage is around 0.9 pu. [4][6][9-17][19][20][22][23][38][41]

5.3 SCENARIO 3: IEEE9 Bus System Wind Power Remodeled with the Partial Replacement (50%) of Generator 3 and the Addition of the other 50% at bus 8

This scenario is different than the previous ones. Here, bus 3 is partially replaced at 50% by a wind farm with a capacity of 42.5MW, and the other 50% is added as a new wind farm at bus 10 connected to bus 8. In this scenario, the distributed generation by wind energy is examined. The generator in bus 2 is examined for the loss of synchronization since generator 1 is in the swing bus and the others are asynchronous wind generators. In the diagrams, there one more plot, which is bus 10 because the creation of this bus was necessary for the addition of a wind farm at bus 8. The remodeled system created in PSS/E can be seen in Figure 5.72. Table 5.15 presents the initial power flow of the active and reactive power of the generators. With the base of 100MVA, the wind turbines appear to be operating correctly.

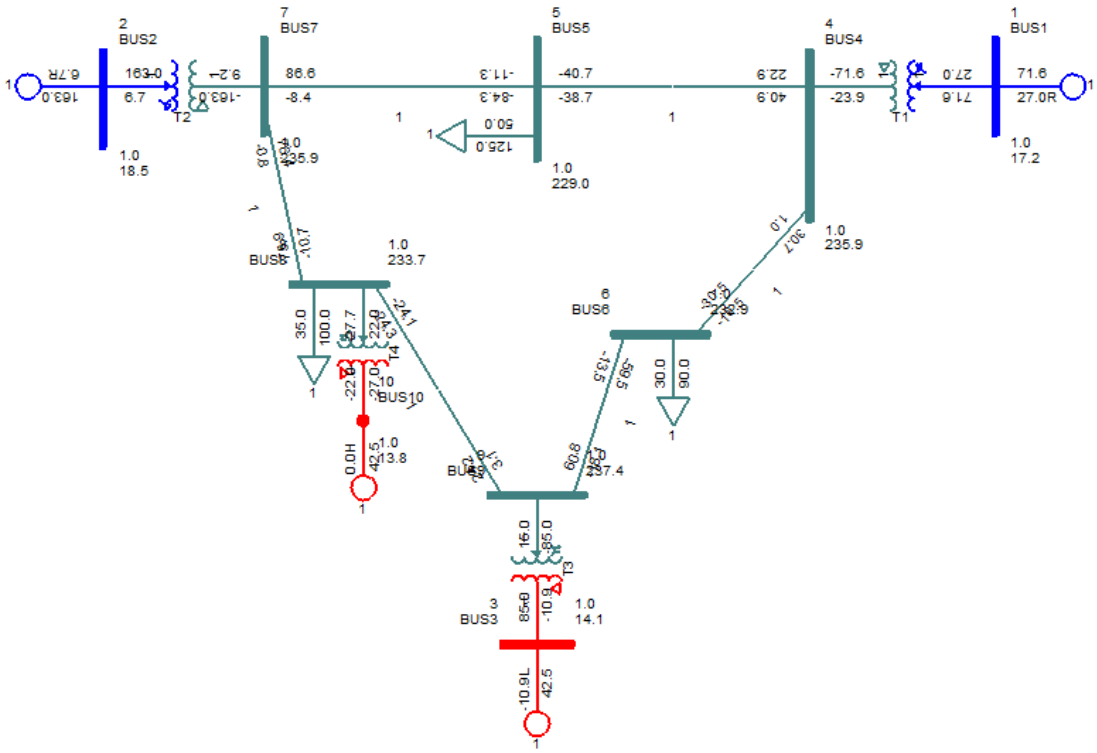

Figure 5. 72 : IEEE9 Bus System Wind Power Remodeled with the Partial Replacement (50%) of Generator 3 and the Addition of the other 50% at bus 8

Table 5. 15 Active and Reactive power generation of the IEEE9 Bus System Wind Power Remodeled with the Partial Replacement (50%) of Generator 3 and the Addition of the other 50% at bus 8

GENERATOR	Active Power (pu)	Reactive Power (pu)
BUS 1 (Swing Bus)	0.72	0.25
BUS 2	1.63	0.03
BUS 3 (Wind Power)	0.425	-0.1
BUS 10 (Wind Power)	0.425	0

5.3.1 Faults at Bus 2 of the IEEE9 Bus System Wind Power Remodeled with the Partial Replacement (50%) of Generator 3 and the Addition of the other 50% at bus 8

The introduction of the second wind turbine is expected to affect the fault clearing time in bus 2

5.3.1.1 Three-phase Symmetrical Fault at Bus 2 of the IEEE9 Bus System Wind Power Remodeled with the Partial Replacement (50%) of Generator 3 and the Addition of the other 50% at bus 8

There is an initial power flow for 1 sec, and then the fault is applied. The critical time was calculated at 0.2 sec, so the fault is cleared at 1.2 sec. Line 2-7 is tripped concurrently, and at 2.2 sec, it is connected again. The power flow is happening until 12 sec. This process can be seen in Table 5.16. Figures 5.73 -5.77 illustrate the power angle of generator 2 with respect to the power angle of the swing bus, the buses frequency, the real and active power of the generators, including the ones producing wind power, and the buses voltage when the fault is cleared at CFCT. Figure 5.78 shows the loss of synchronization of the power angle of generator 2 with respect to the power angle of the swing bus when the fault is cleared 0.05 sec after the CFCT. During the post-fault power flow, the buses 10 and 3, where the wind energy production is, have similar plots with few oscillations.

Table 5. 16 IEEE9 Wind Power 50% Replaced at Bus 3 and 50% Added at Bus 8 Three-phase symmetrical Fault at Bus 2

Action	Time (sec)
Steady State	0.00
Apply Fault	1.00
Clear Fault	1.2
Trip Line	1.2
Connect Line	2.2
Power Flow	12.00

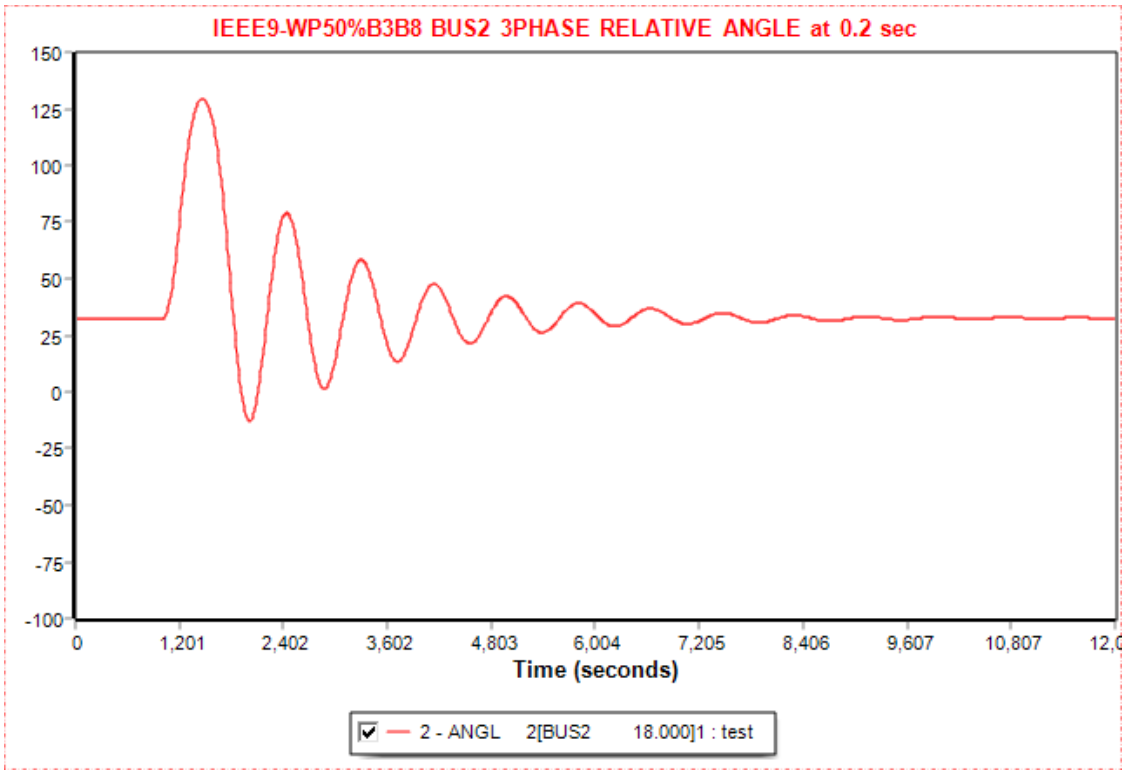

Figure 5. 73 Relative power angle plots of three-phase symmetrical fault at bus 2 when it is cleared at 1.2 sec at IEEE9 Wind Power Remodeled with 50% Replaced at Bus 3 and 50% Added at Bus 8

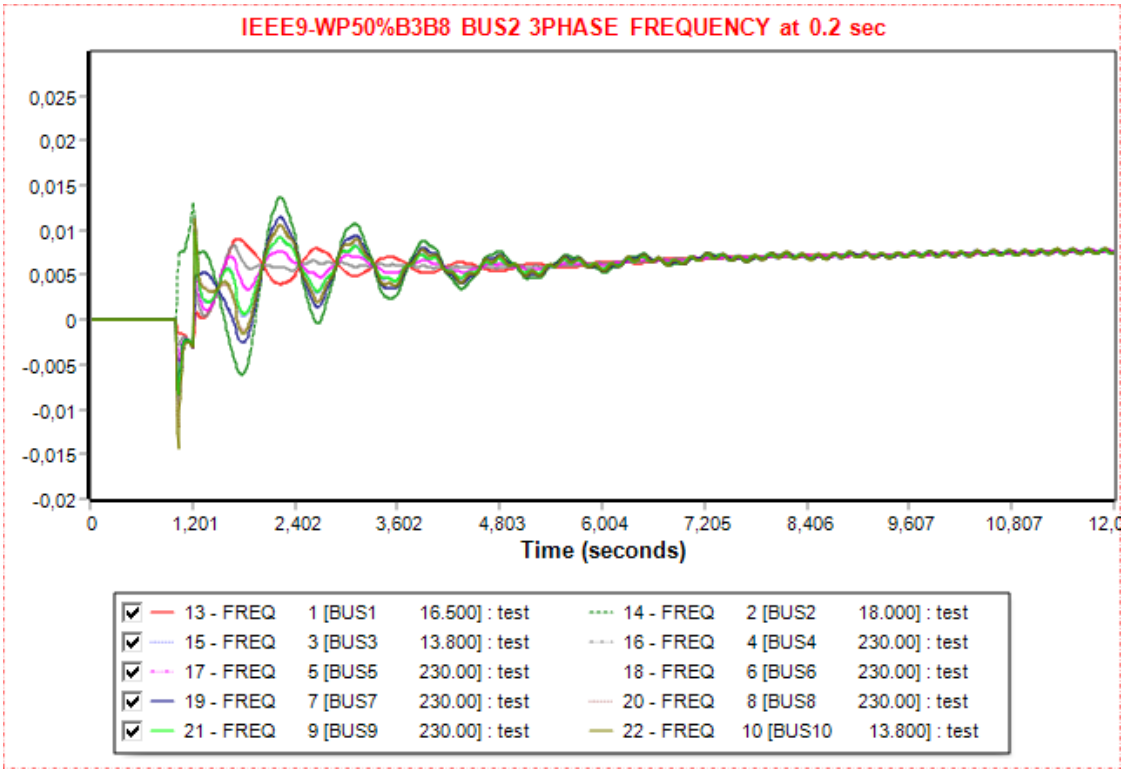

Figure 5. 74 Frequency plots of three-phase symmetrical fault at bus 2 when it is cleared at 1.2 sec at IEEE9 Wind Power Remodeled with 50% Replaced at Bus 3 and 50% Added at Bus 8

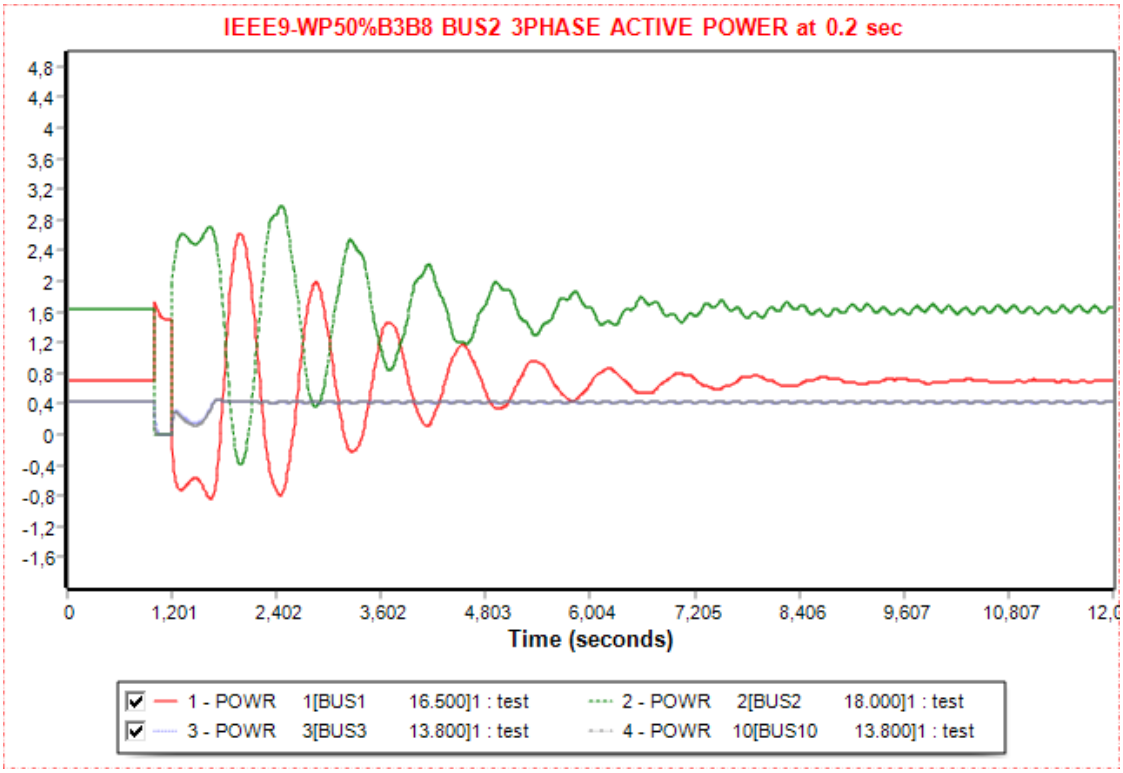

Figure 5. 75 Active Power plots of three-phase symmetrical fault at bus 2 when it is cleared at 1.2 sec at IEEE9 Wind Power Remodeled with 50% Replaced at Bus 3 and 50% Added at Bus 8

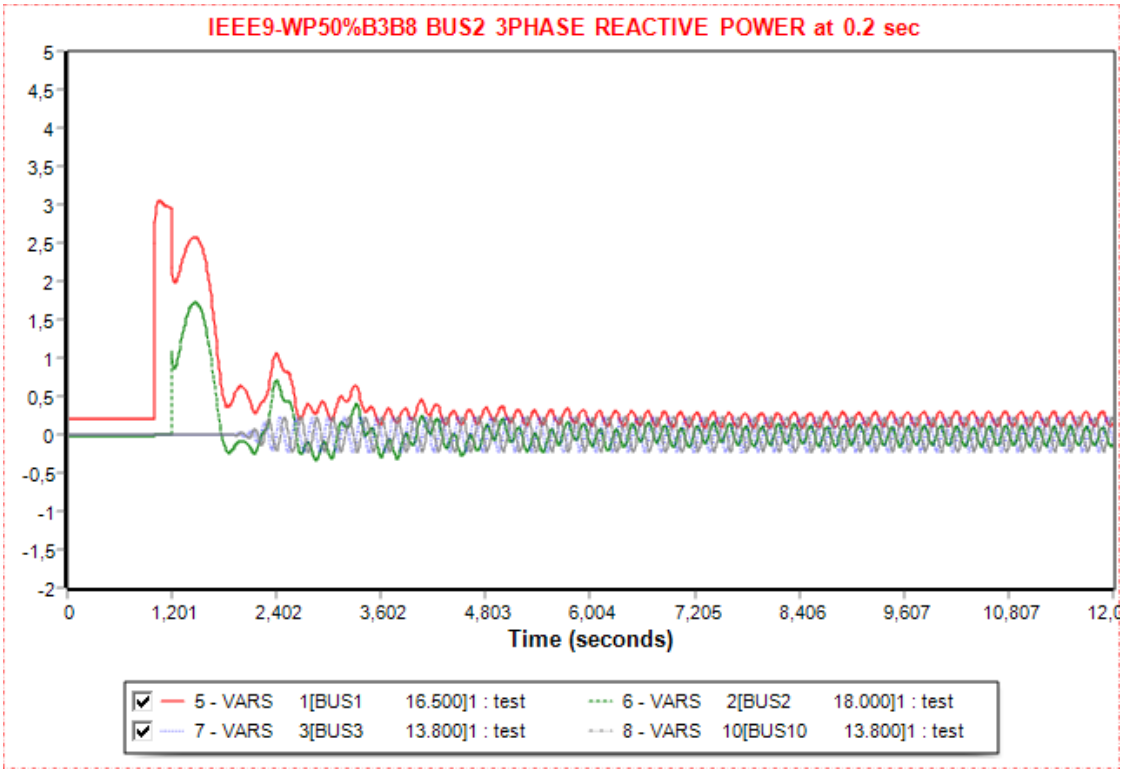

Figure 5. 76 Reactive Power plots of three-phase symmetrical fault at bus 2 when it is cleared at 1.2 sec at IEEE9 Wind Power Remodeled with 50% Replaced at Bus 3 and 50% Added at Bus 8

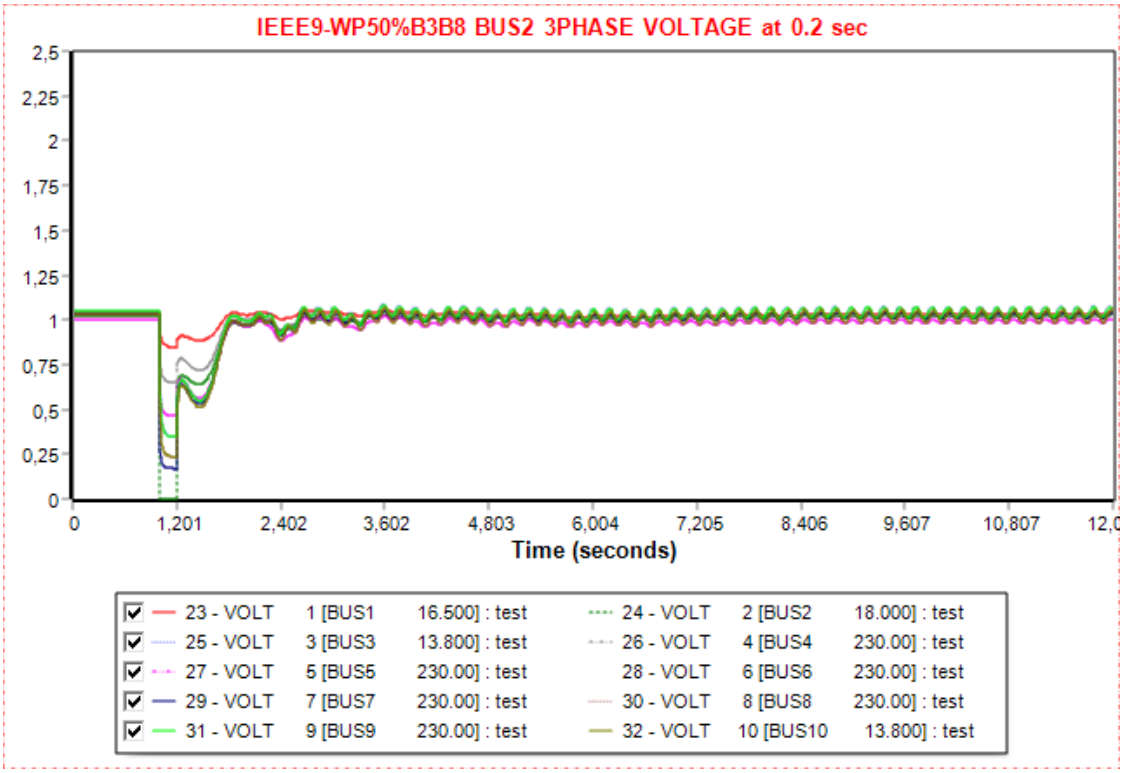

Figure 5. 77 Voltage plots of three-phase symmetrical fault at bus 2 when it is cleared at 1.2 sec at IEEE9 Wind Power Remodeled with 50% Replaced at Bus 3 and 50% Added at Bus 8

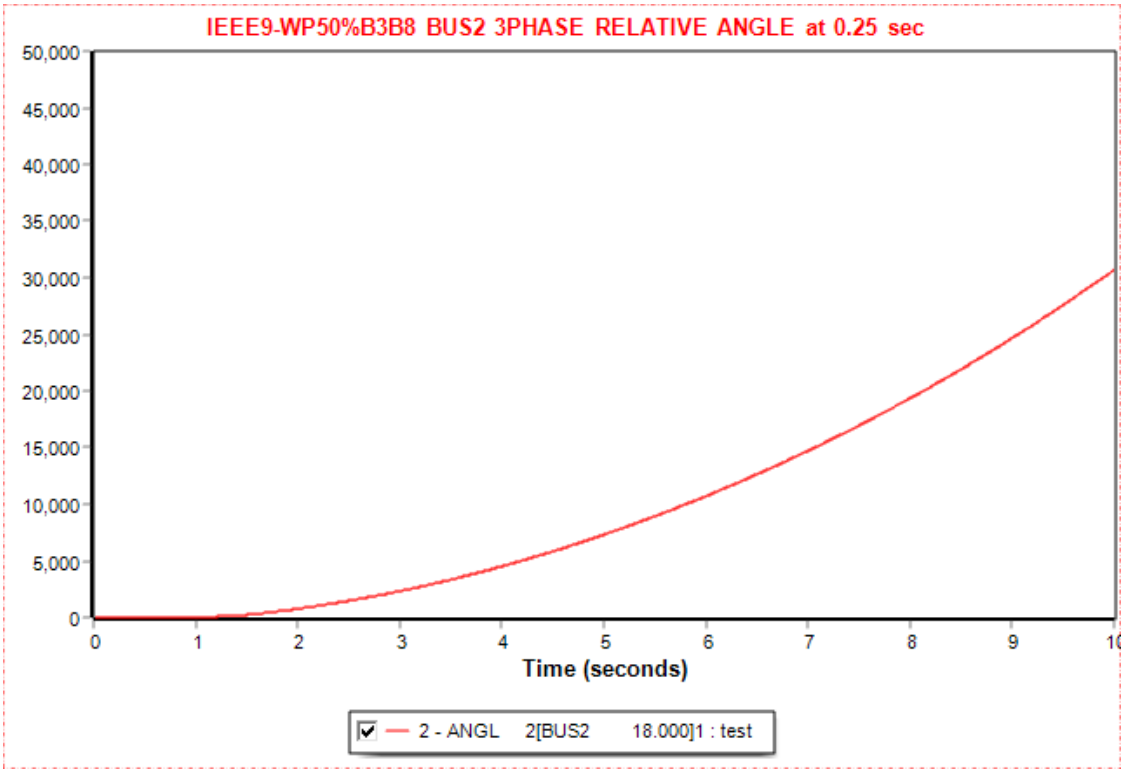

Figure 5. 78 Relative power angle plots of three-phase symmetrical fault at bus 2 when it is cleared at 1.25 sec at IEEE9 Wind Power Remodeled with 50% Replaced at Bus 3 and 50% Added at Bus 8

5.3.1.2 SLG Fault at Bus 2 of the IEEE9 Bus System Wind Power Remodeled with the Partial Replacement (50%) of Generator 3 and the Addition of the other 50% at bus 8

The difference from the simulation of section 5.3.1.1 is the SLG fault. The clearing time was calculated at 0.75 sec. After the initial load flow, an SLG fault with a duration of 0.75 sec is applied at 1 sec. For its clearance line 2-7 is tripped immediately and is connected again after 1 sec at 2.75 sec, resuming the load flow until 12 sec. The process is presented in Table 5.17. Figures 5.79-5.83 depict the power angle of generator 2 with respect to the power angle of the swing bus, the buses frequency, the real and active power of the generators, including the ones producing wind power, and the buses voltage when the fault is cleared at CFCT. Figure 5.84 shows the loss of synchronization of the power angle of generator 2 with respect to the power angle of the swing bus when the fault is cleared 0.05 sec after the CFCT. Like previous sections, the oscillations continue to appear.

Table 5. 17 IEEE9 Wind Power Remodeled with 50% Replaced at Bus 3 and 50% Added at Bus 8 SLG Fault at Bus 2

Action	Time (sec)
Steady State	0.00
Apply Fault	1.00
Clear Fault	1.75
Trip Line	1.75
Connect Line	2.75
Power Flow	12.00

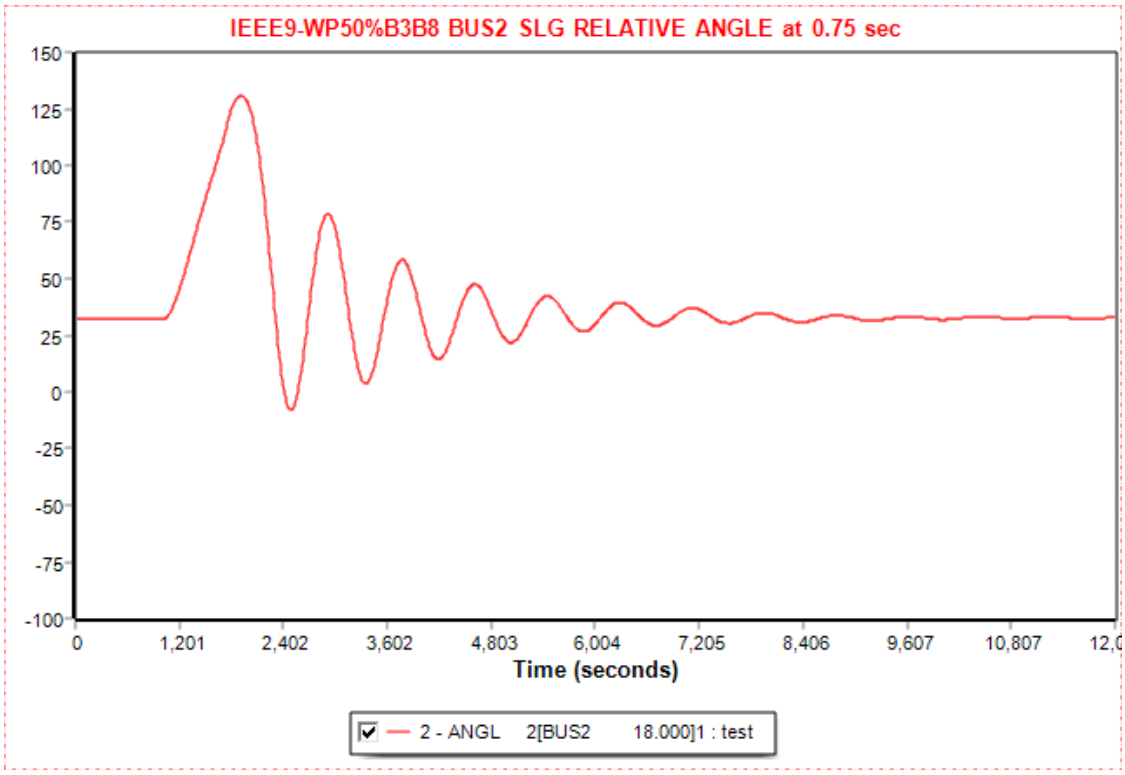

Figure 5. 79 Relative power angle plots of SLG fault at bus 2 when it is cleared at 1.75 sec at IEEE9 Wind Power Remodeled with 50% Replaced at Bus 3 and 50% Added at Bus 8

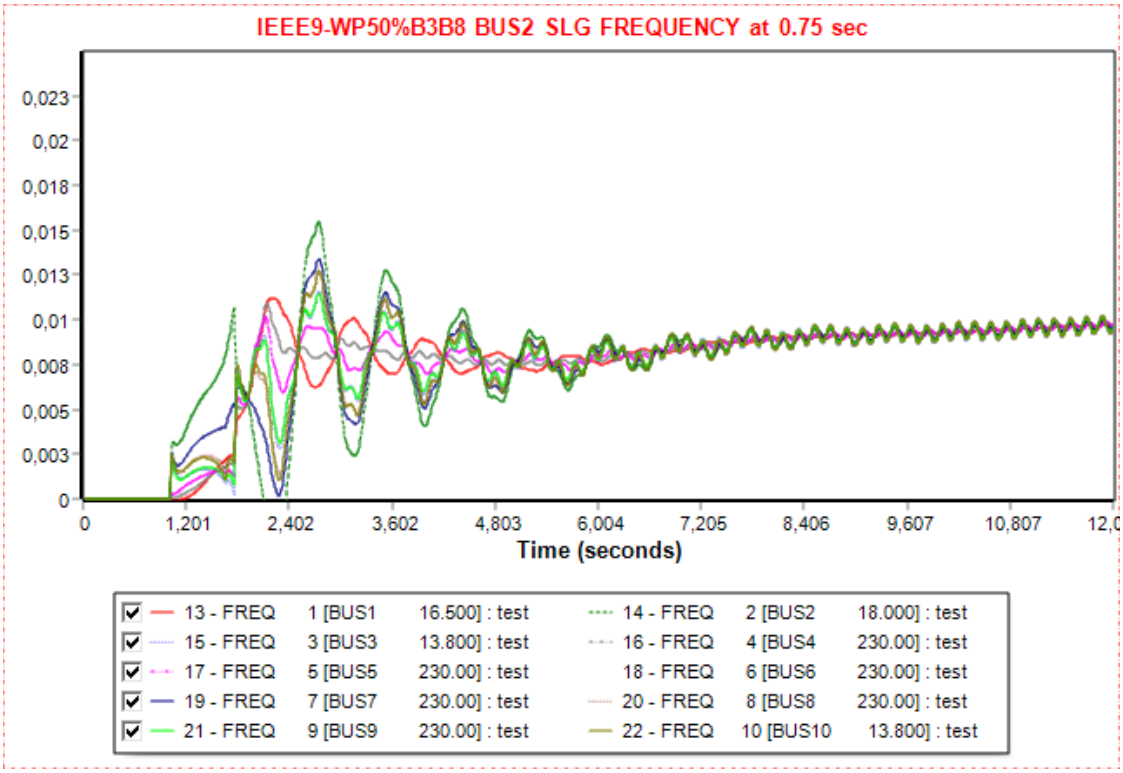

Figure 5. 80 Frequency plots of SLG fault at bus 2 when it is cleared at 1.75 sec at IEEE9 Wind Power Remodeled with 50% Replaced at Bus 3 and 50% Added at Bus 8

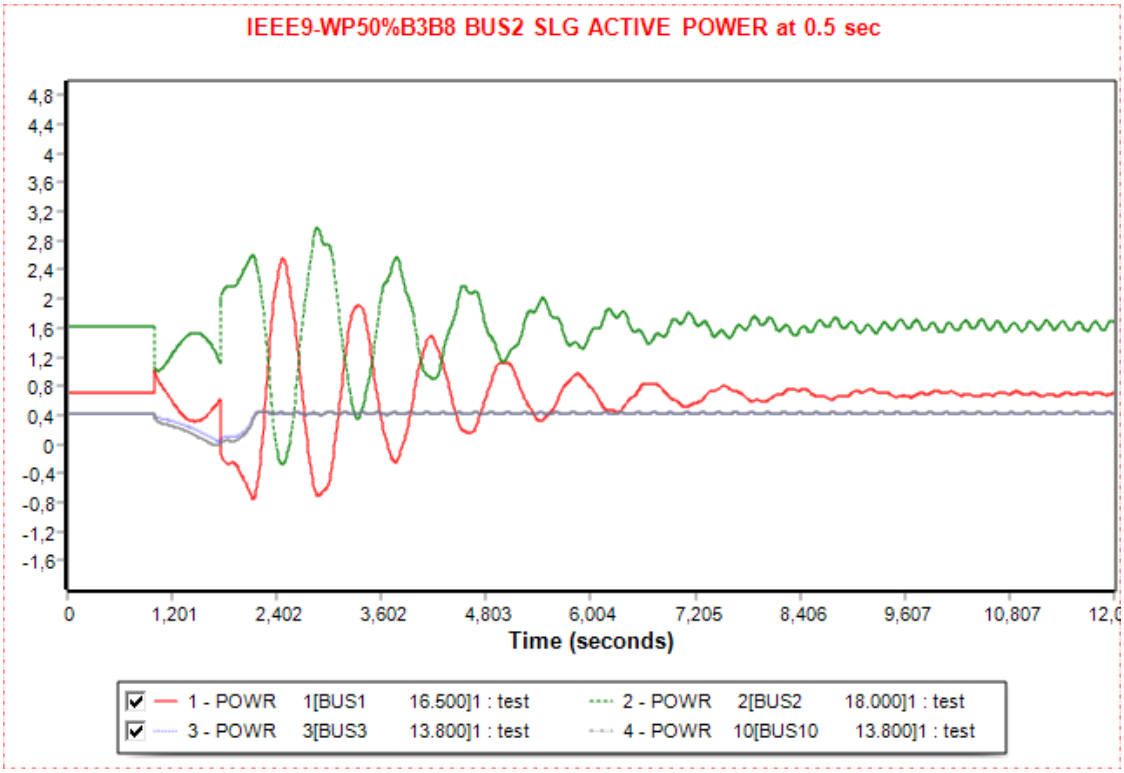

Figure 5. 81 Active Power plots of SLG fault at bus 2 when it is cleared at 1.75 sec at IEEE9 Wind Power Remodeled with 50% Replaced at Bus 3 and 50% Added at Bus 8

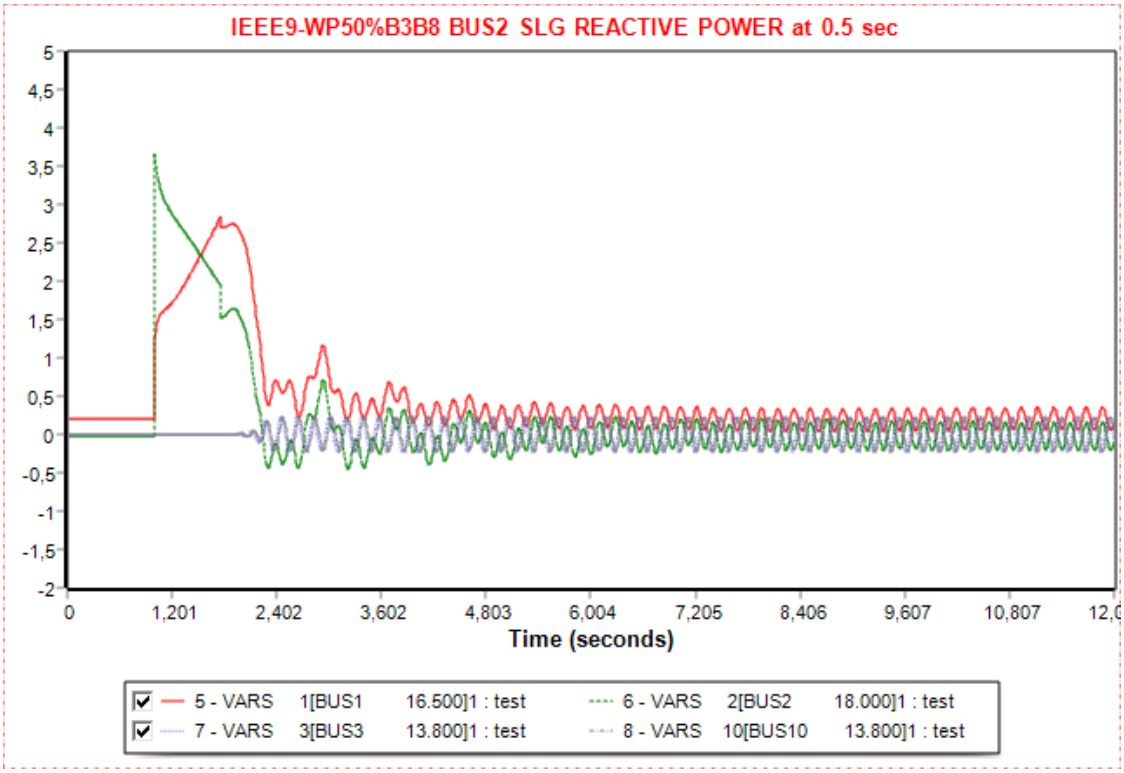

Figure 5. 82 Reactive Power plots of SLG fault at bus 2 when it is cleared at 1.75 sec at IEEE9 Wind Power Remodeled with 50% Replaced at Bus 3 and 50% Added at Bus 8

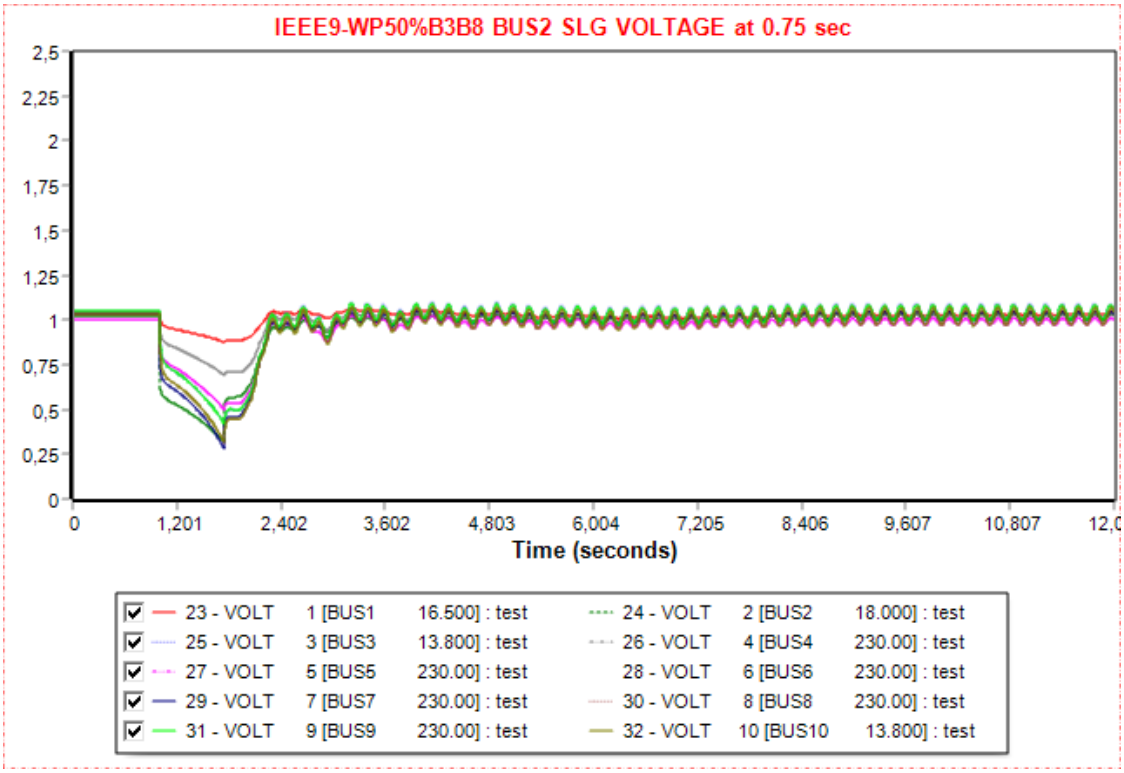

Figure 5. 83 Voltage plots of SLG fault at bus 2 when it is cleared at 1.75 sec at IEEE9 Wind Power Remodeled with 50% Replaced at Bus 3 and 50% Added at Bus 8

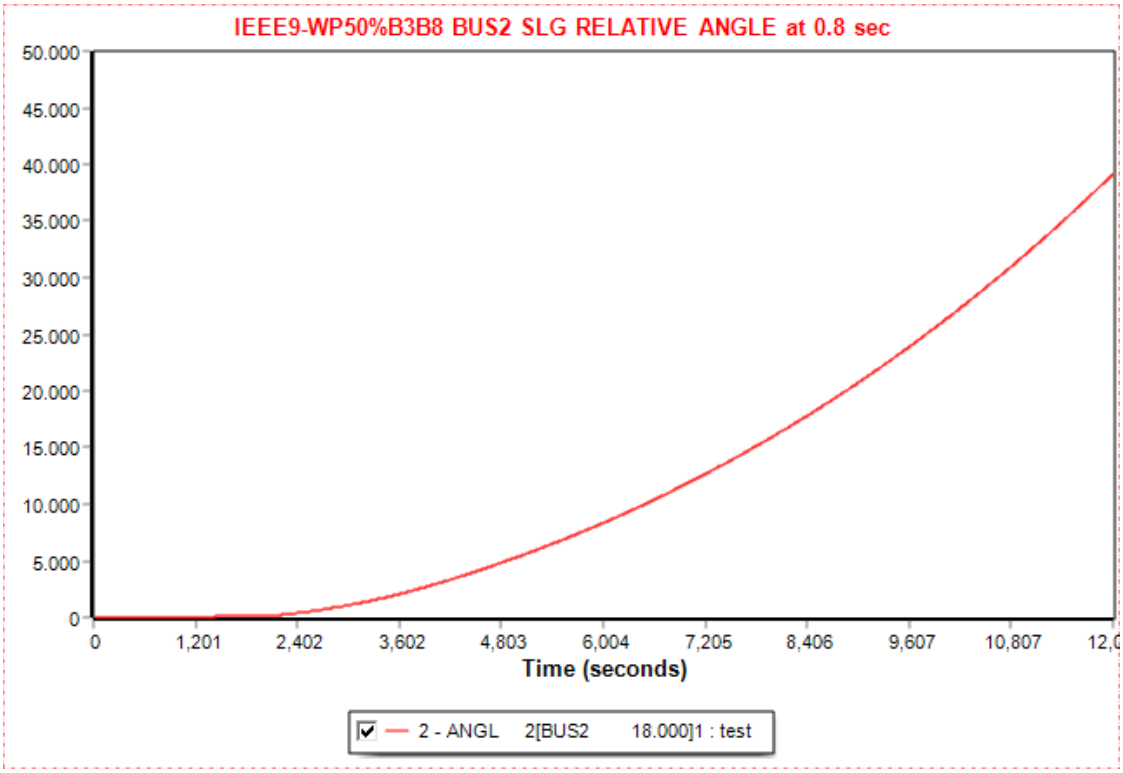

Figure 5. 84 Relative power angle plots of SLG fault at bus 2 when it is cleared at 1.8 sec at IEEE9 Wind Power Remodeled with 50% Replaced at Bus 3 and 50% Added at Bus 8

5.3.2 Faults at Bus 7 of the IEEE9 Bus System Wind Power Remodeled with the Partial Replacement (50%) of Generator 3 and the Addition of the other 50% at bus 8

The location of the fault in the following sections is the bus 7, which is a neither generation nor load bus.

5.3.2.1 Three-phase Symmetrical Fault at Bus 7 of the IEEE9 Bus System Wind Power Remodeled with the Partial Replacement (50%) of Generator 3 and the Addition of the other 50% at bus 8

The simulation starts with an initial load flow at 1 sec. The critical time was calculated to be 0.2 sec, so that is the duration of the three-phase symmetrical fault that is applied. When the disturbance is cleared at 1.2 sec, line 7-8 is tripped and after 1 sec is connected to the network again. This can be seen in Table 5.18. Figures 5.85 -5.89 illustrate the power angle of generator 2 with respect to the power angle of the swing bus, the buses

frequency, the real and active power of the generators, including the ones producing wind power, and the buses voltage when the fault is cleared at CFCT. Figure 5.90 shows the loss of synchronization of the power angle of generator 2 with respect to the power angle of the swing bus when the fault is cleared 0.05 sec after the CFCT.

Table 5. 18 IEEE9 Wind Power Remodeled with 50% Replaced at Bus 3 and 50% Added at Bus 8 Three-phase symmetrical Fault at Bus 7

Action	**Time (sec)**
Steady State	0.00
Apply Fault	1.00
Clear Fault	1.2
Trip Line	1.2
Connect Line	2.2
Power Flow	12.00

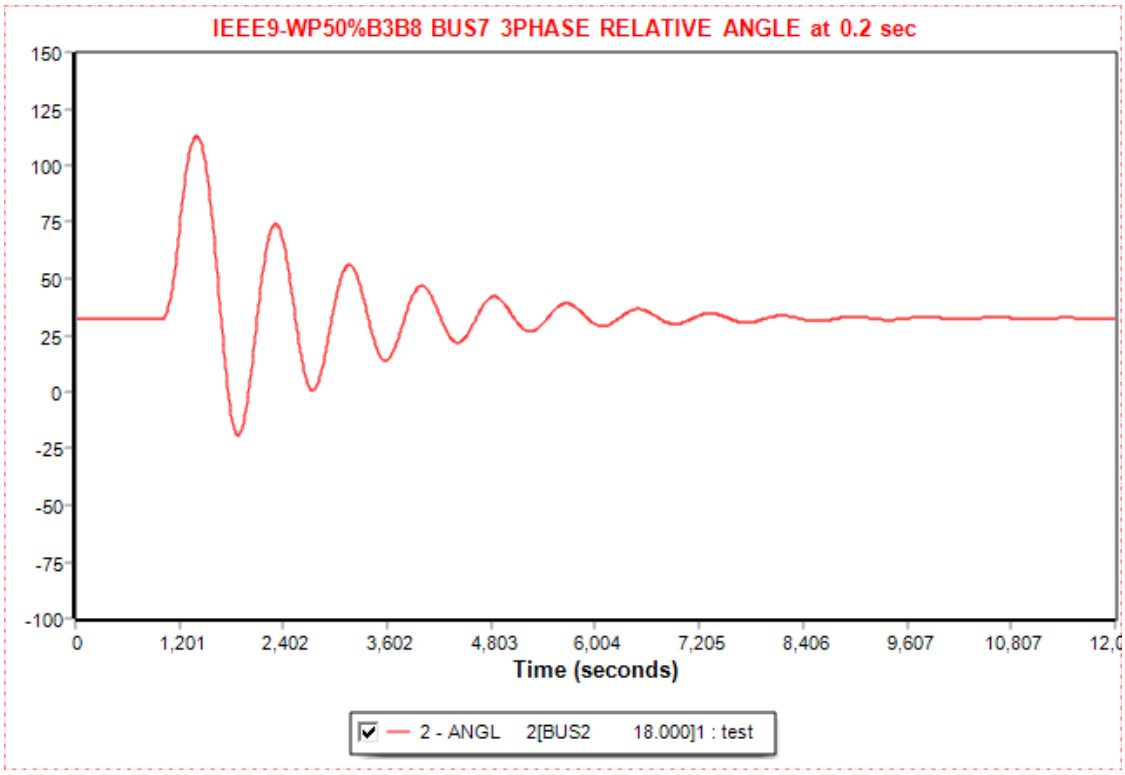

Figure 5. 85 Relative power angle plots of three-phase symmetrical fault at bus 7 when it is cleared at 1.2 sec at IEEE9 Wind Power Remodeled with 50% Replaced at Bus 3 and 50% Added at Bus 8

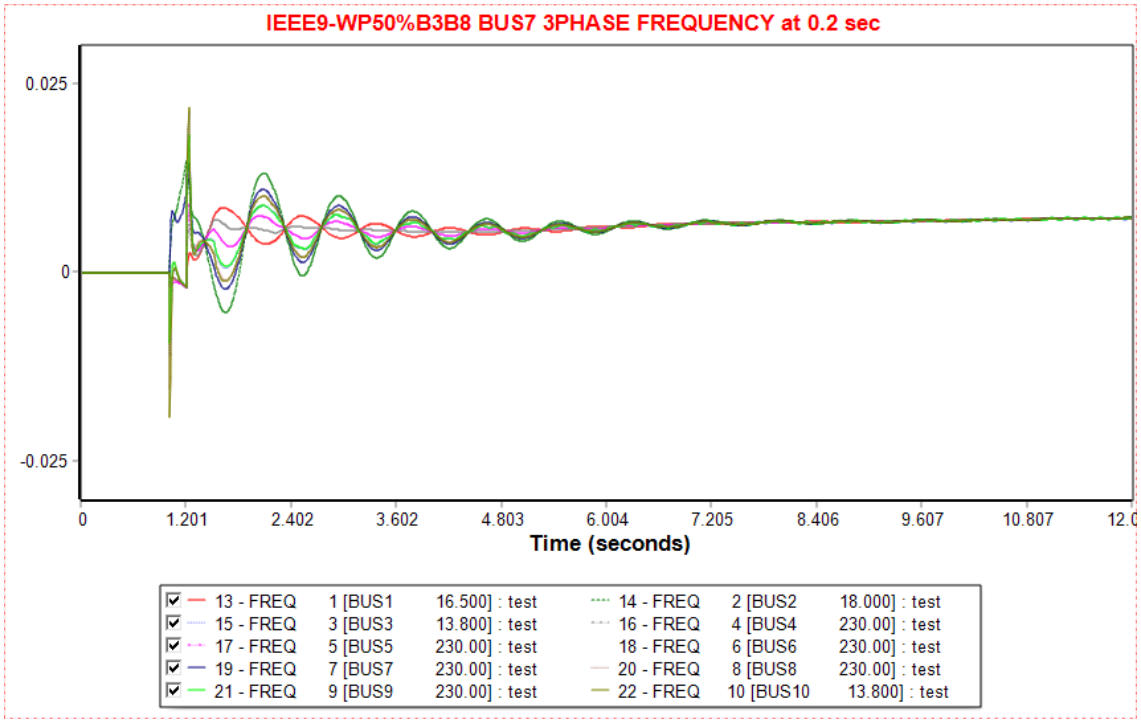

Figure 5. 86 Frequency plots of three-phase symmetrical fault at bus 7 when it is cleared at 1.2 sec at IEEE9 Wind Power Remodeled with 50% Replaced at Bus 3 and 50% Added at Bus 8

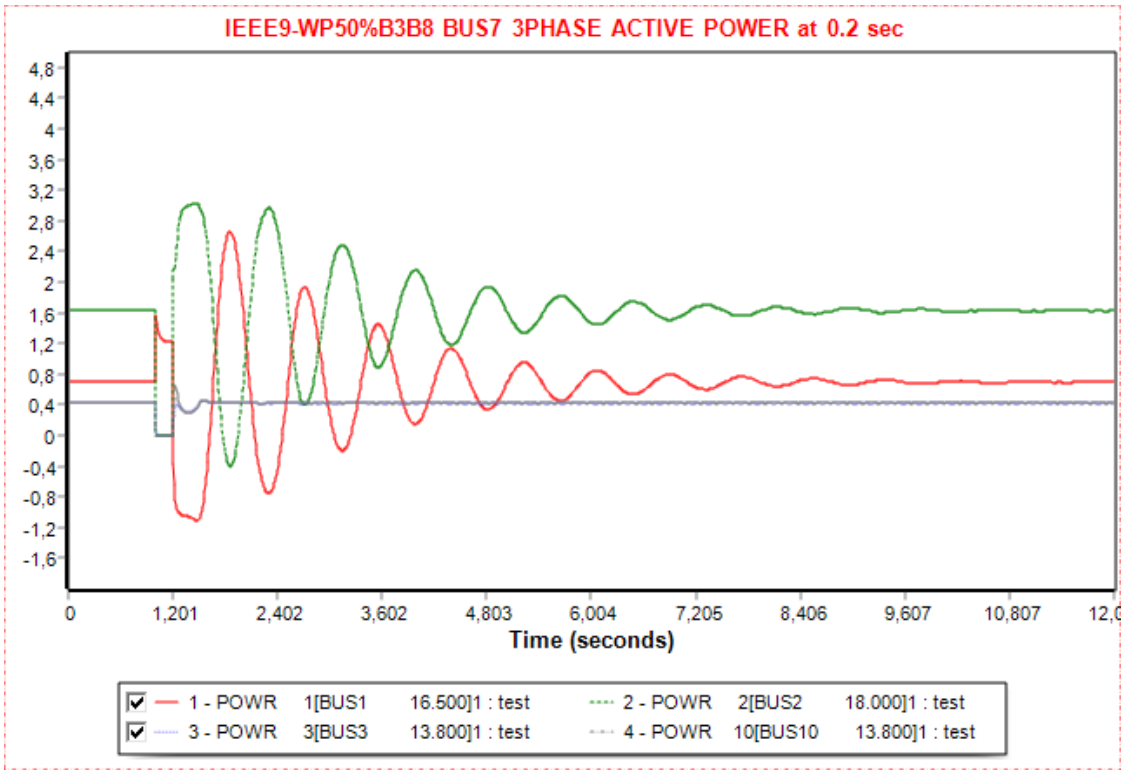

Figure 5. 87 Active Power plots of three-phase symmetrical fault at bus 7 when it is cleared at 1.2 sec at IEEE9 Wind Power Remodeled with 50% Replaced at Bus 3 and 50% Added at Bus 8

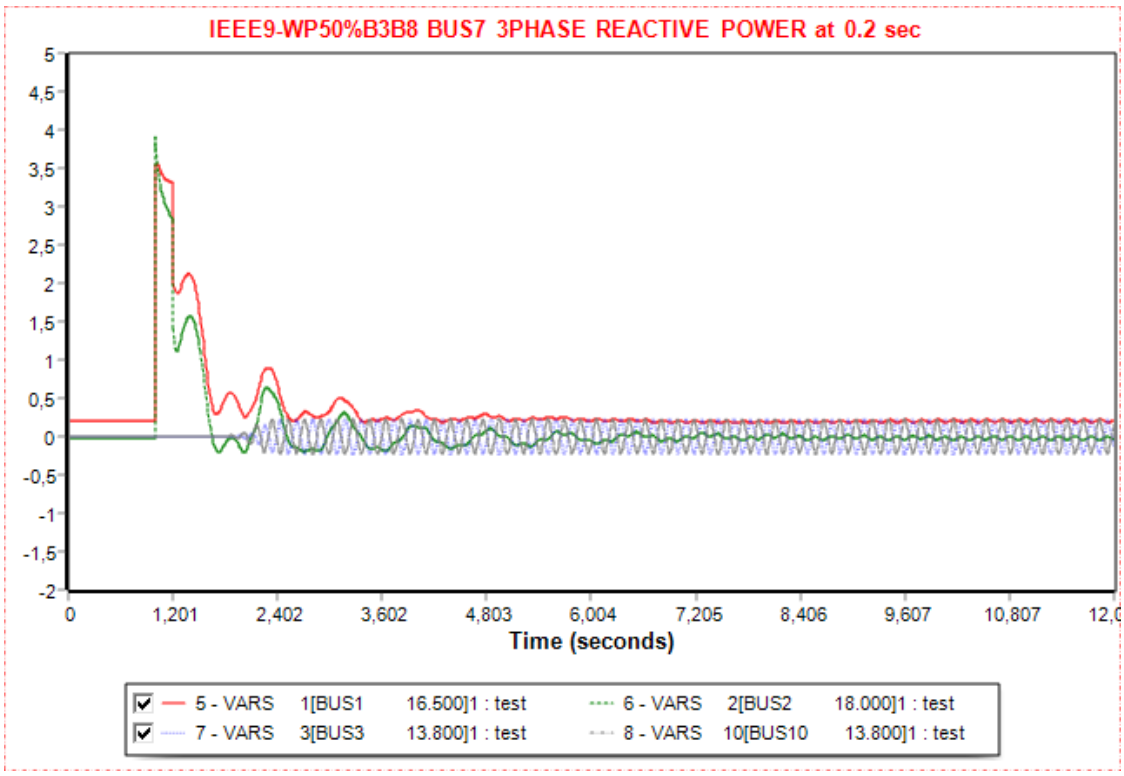

Figure 5. 88 Reactive Power plots of three-phase symmetrical fault at bus 7 when it is cleared at 1.2 sec at IEEE9 Wind Power Remodeled with 50% Replaced at Bus 3 and 50% Added at Bus 8

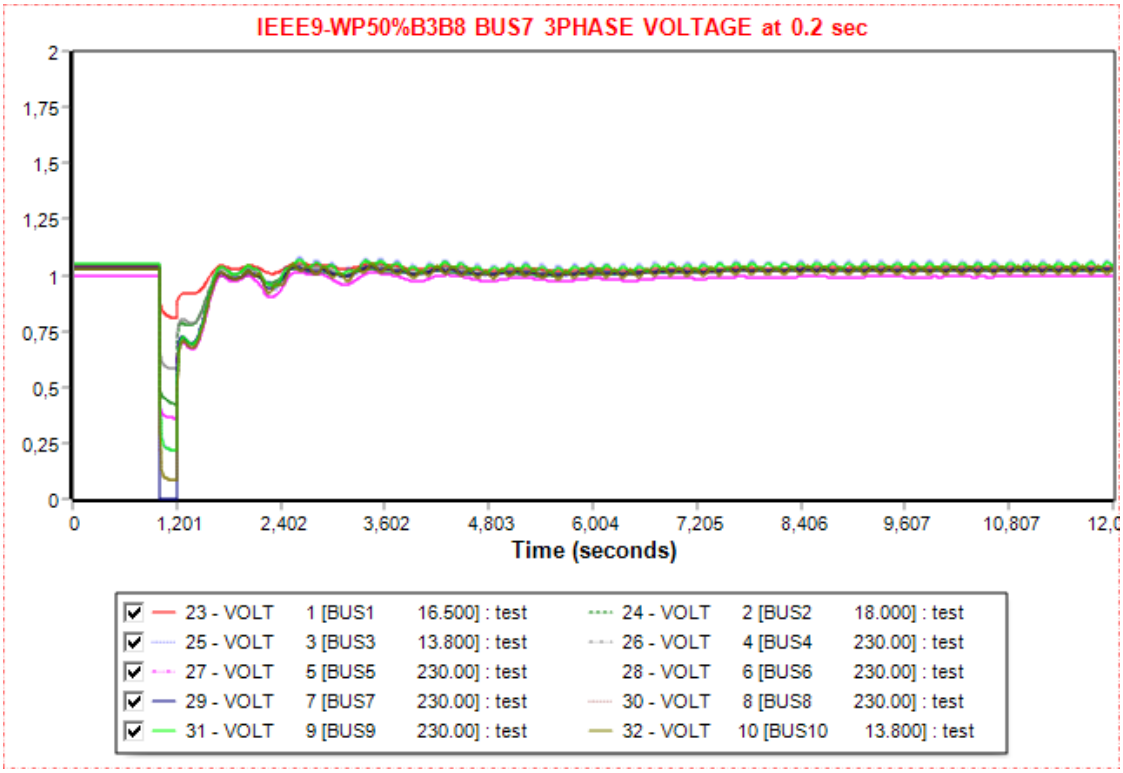

Figure 5. 89 Voltage plots of three-phase symmetrical fault at bus 7 when it is cleared at 1.2 sec at IEEE9 Wind Power Remodeled with 50% Replaced at Bus 3 and 50% Added at Bus 8

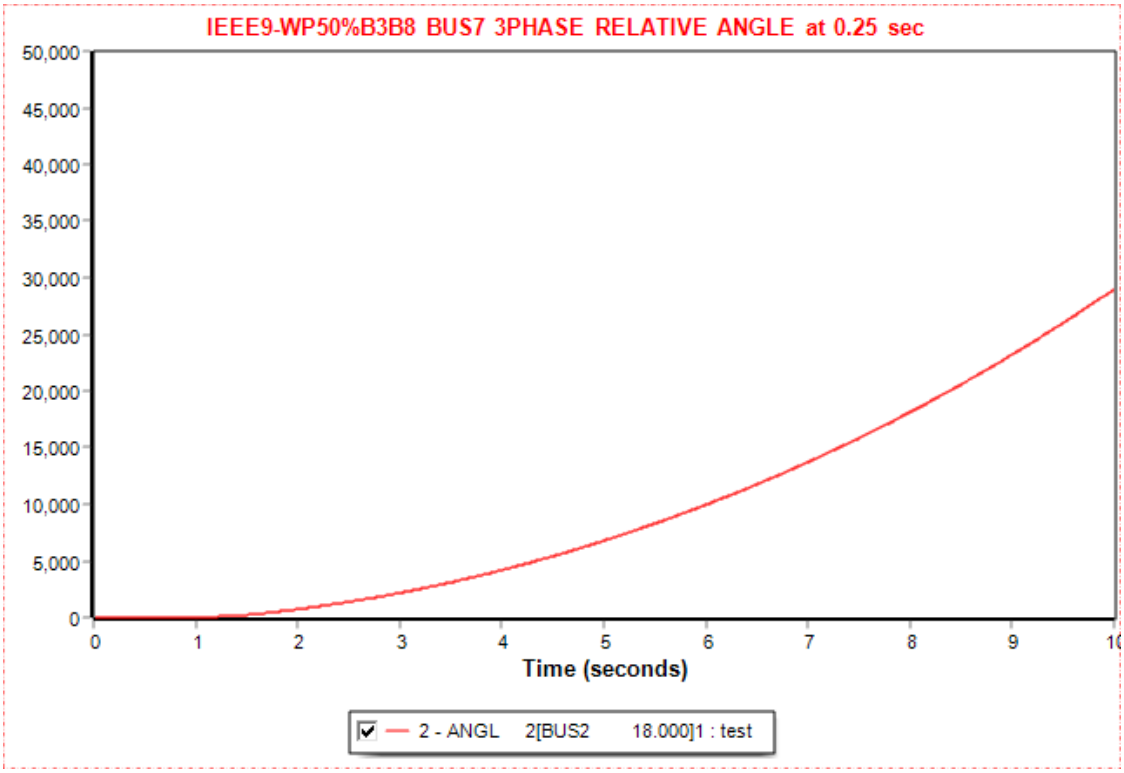

Figure 5. 90 Relative power angle plots of three-phase symmetrical fault at bus 7 when it is cleared at 1.25 sec at IEEE9 Wind Power Remodeled with 50% Replaced at Bus 3 and 50% Added at Bus 8

5.3.2.2 SLG Fault at Bus 7 of the IEEE9 Bus System Wind Power Remodeled with the Partial Replacement (50%) of Generator 3 and the Addition of the other 50% at bus 8

In this simulation, the fault is an SLG, and the network can remain stable despite the duration of the fault. Like in other sections, since there is no CFCT, the fault duration is 0.5 sec in order to see the transient behavior of the system. Firstly, there is an initial power flow for 1 sec, and then the disturbance is applied for 0.5 sec. At the same time, for the fault clearance, the line 7-8 is tripped, and after 1 sec, at 2.5 sec, it is connected to the network. As seen from Table 5.19, the simulation lasts for 12 sec. Figures 5.91-5.95 present the power angle of generator 2 with respect to the power angle of the swing bus, the buses frequency, the real and active power of the generators, including the ones producing wind power, and the buses voltage when the fault is cleared at 0.5 sec.

Table 5. 19 IEEE9 Wind Power Remodeled with 50% Replaced at Bus 3 and 50% Added at Bus 8 SLG Fault at Bus 7

Action	**Time (sec)**
Steady State	0.00
Apply Fault	1.00
Clear Fault	1.5
Trip Line	1.5
Connect Line	2.5
Power Flow	12.00

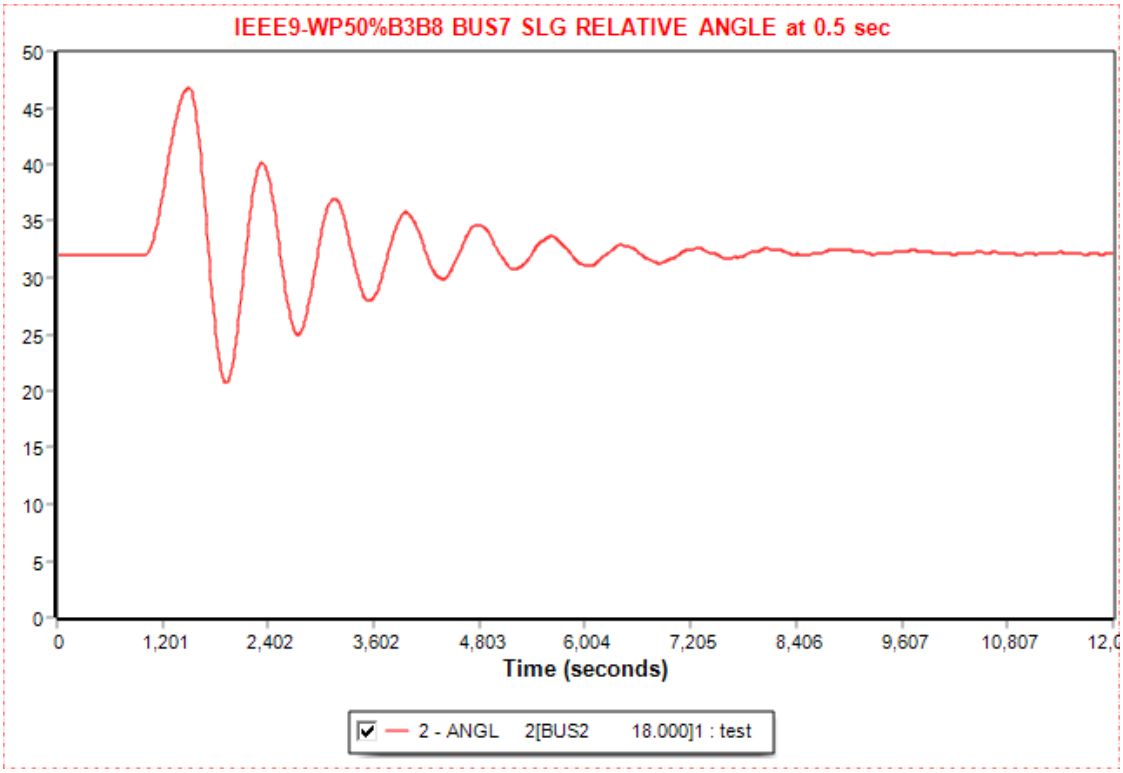

Figure 5. 91 Relative power angle plots of SLG fault at bus 7 when it is cleared at 1.5 sec at IEEE9 Wind Power Remodeled with 50% Replaced at Bus 3 and 50% Added at Bus 8

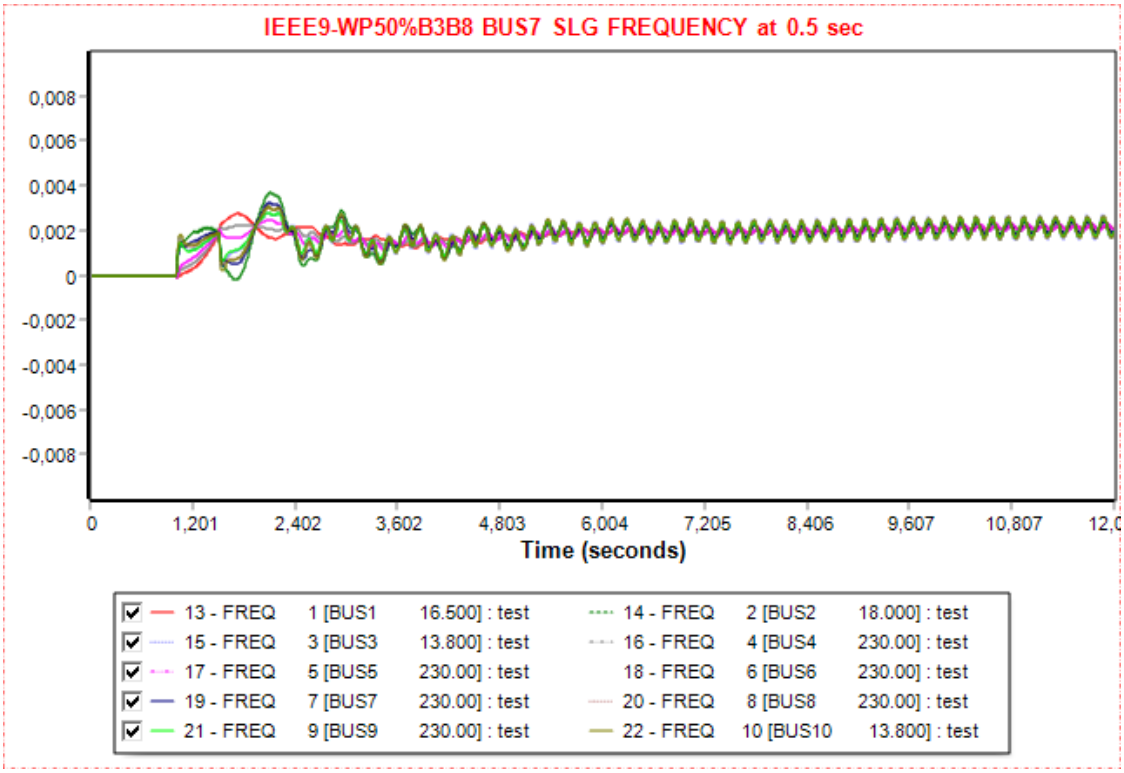

Figure 5. 92 Frequency plots of SLG fault at bus 7 when it is cleared at 1.5 sec at IEEE9 Wind Power Remodeled with 50% Replaced at Bus 3 and 50% Added at Bus 8

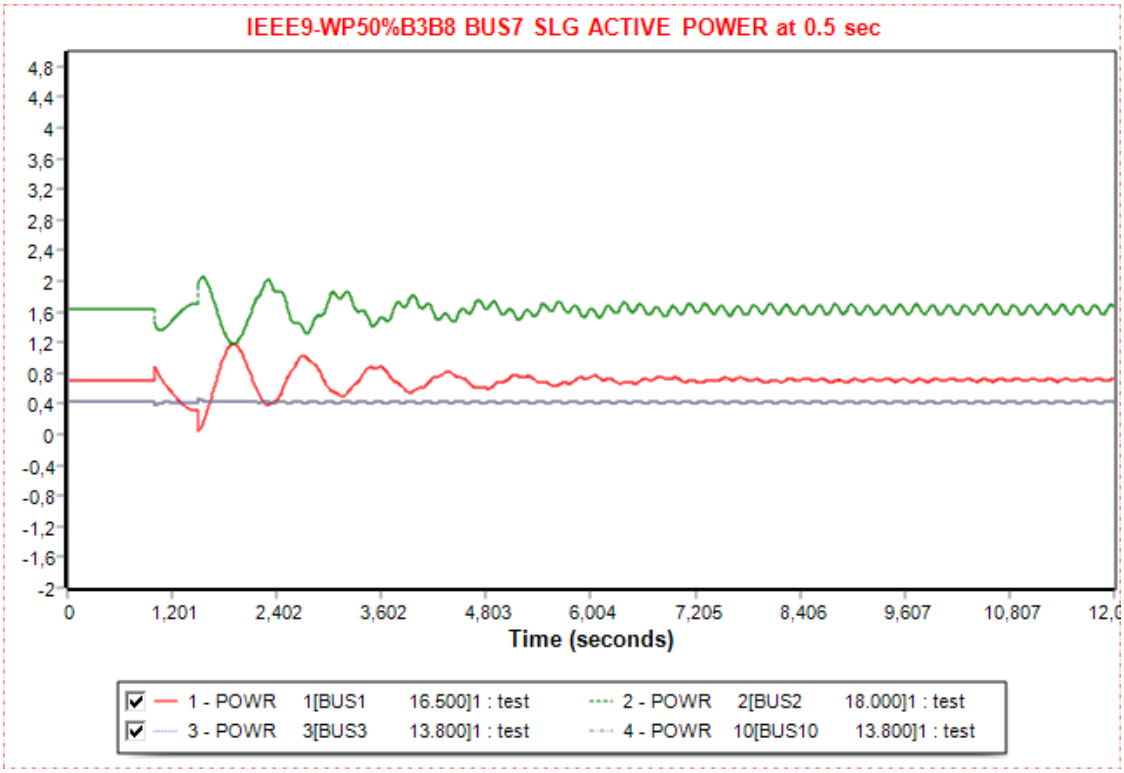

Figure 5. 93 Active Power plots of SLG fault at bus 7 when it is cleared at 1.5 sec at IEEE9 Wind Power Remodeled with 50% Replaced at Bus 3 and 50% Added at Bus 8

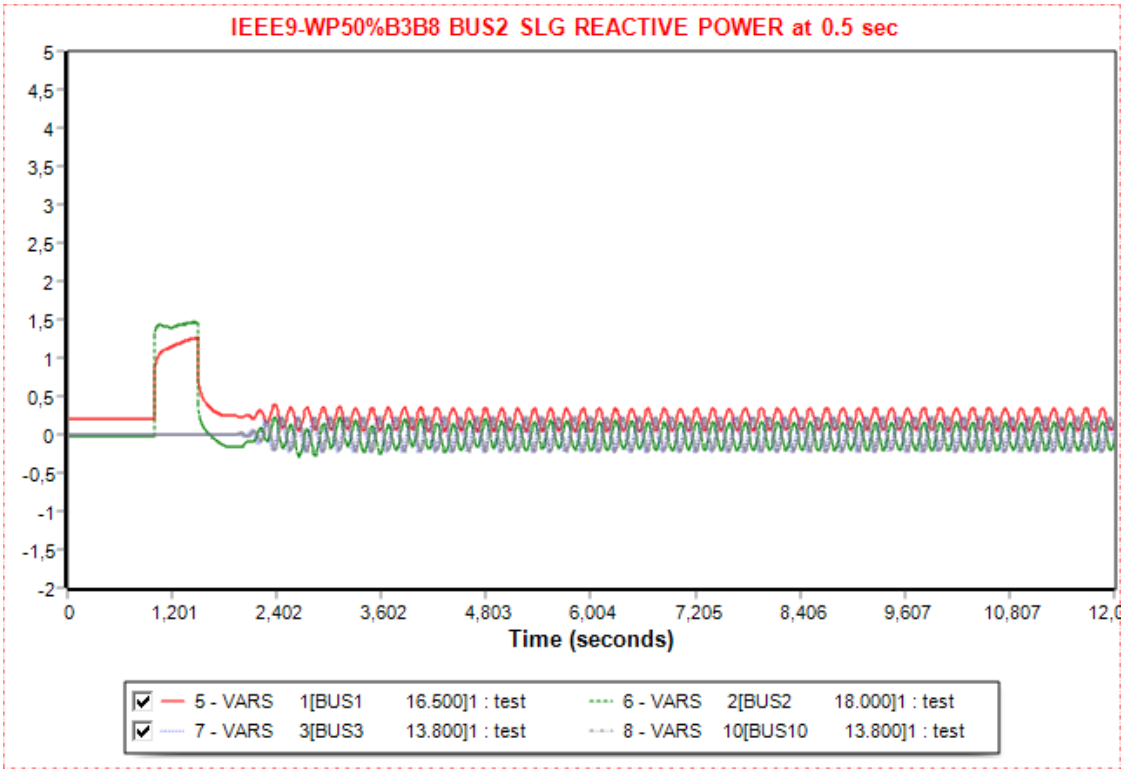

Figure 5. 94 Reactive Power plots of SLG fault at bus 7 when it is cleared at 1.5 sec at IEEE9 Wind Power Remodeled with 50% Replaced at Bus 3 and 50% Added at Bus 8

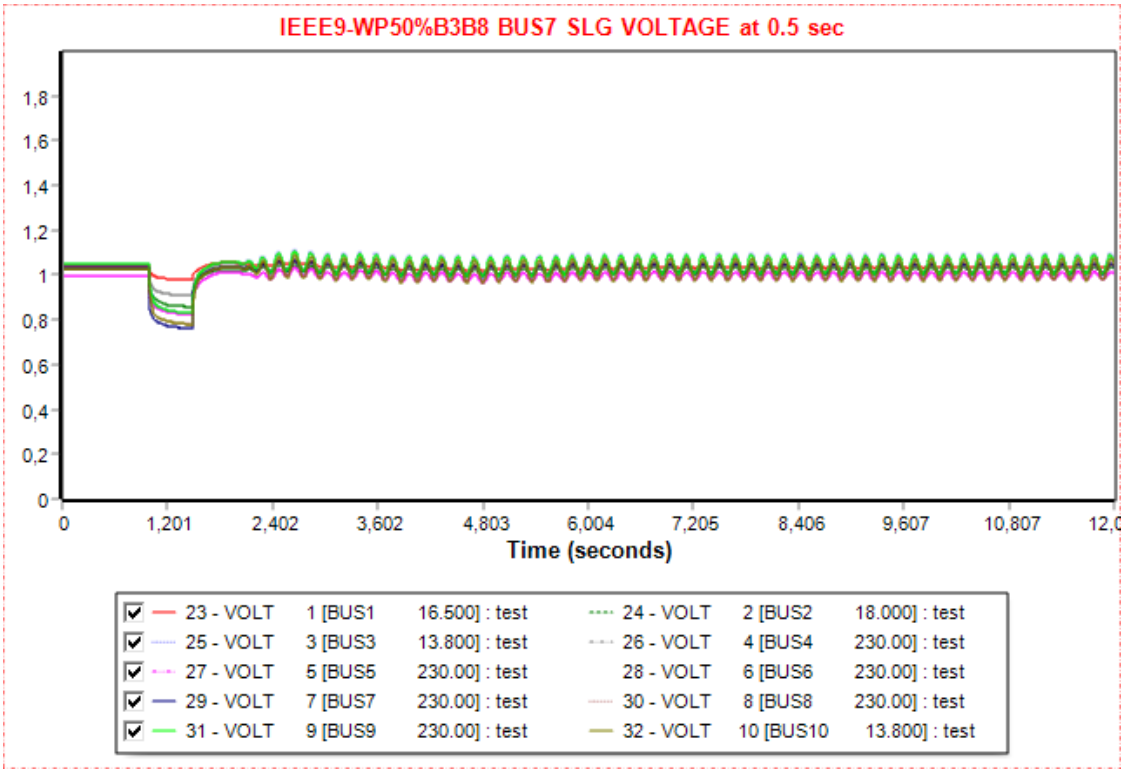

Figure 5. 95 Voltage plots of SLG fault at bus 7 when it is cleared at 1.5 sec at IEEE9 Wind Power Remodeled with 50% Replaced at Bus 3 and 50% Added at Bus 8

5.3.3 Faults at Bus 8 of the IEEE9 Bus System Wind Power Remodeled with the Partial Replacement (50%) of Generator 3 and the Addition of the other 50% at bus 8

In this scenario/case the bus 8 is not only connected to a 100 MW load but it is directly connected to a bus linked with a 42.5 MW wind farm.

5.3.3.1 Three-phase Symmetrical Fault at Bus 8 of the IEEE9 Bus System Wind Power Remodeled with the Partial Replacement (50%) of Generator 3 and the Addition of the other 50% at bus 8

The simulation starts with the network at the steady-state condition for 1 sec. The duration of the three-phase symmetrical fault is 0.35, which is also the CFCT. When the disturbance is cleared at 1.35 sec, line 8-7 is tripped and after 1 sec is connected to the network again. The process is presented in Table 5.20. Figures 5.96-5.100 illustrate the power angle of generator 2 with respect to the power angle of the swing bus, the buses

frequency, the real and active power of the generators, including the ones producing wind power, and the buses voltage when the fault is cleared at CFCT. Figure 5.101 shows the loss of synchronization of the power angle of generator 2 with respect to the power angle of the swing bus when the fault is cleared 0.05 sec after the CFCT. It is worthy of mentioning that in the frequency plot in Figure 5.97, there is a dense oscillation with significant limits. This may be due to the coexistence of a load and a generator.

Table 5. 20 IEEE9 Wind Power Remodeled with 50% Replaced at Bus 3 and 50% Added at Bus 8 Three Phase Fault at Bus 8

Action	Time (sec)
Steady State	0.00
Apply Fault	1.00
Clear Fault	1.35
Trip Line	1.35
Connect Line	2.35
Power Flow	12.00

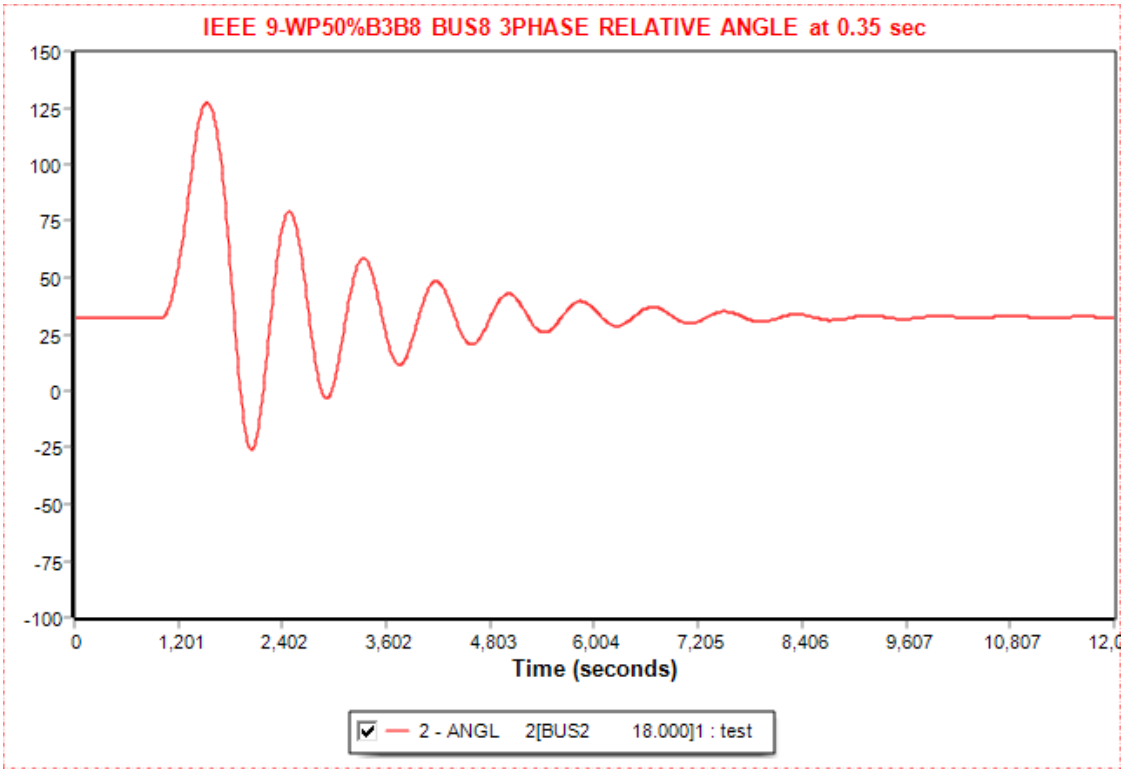

Figure 5. 96 Relative power angle plots of three phase fault at bus 8 when it is cleared at 1.35 sec at IEEE9 Wind Power Remodeled with 50% Replaced at Bus 3 and 50% Added at Bus 8

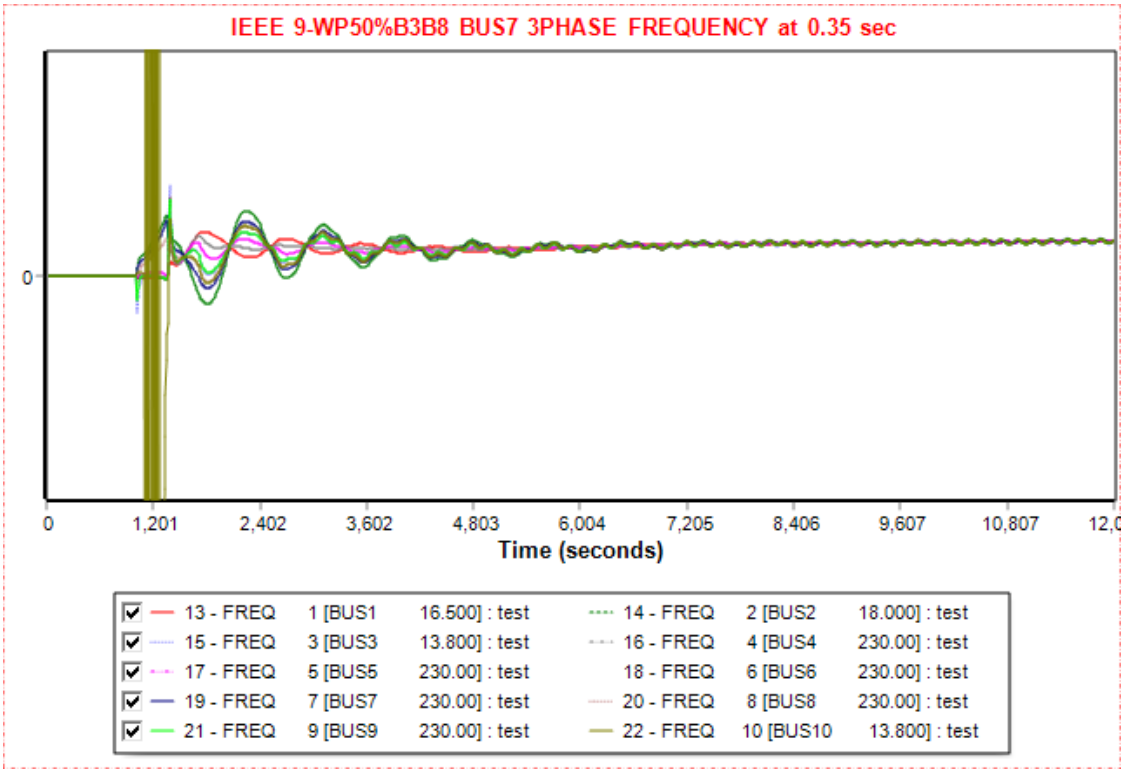

Figure 5. 97 Frequency plots of three phase fault at bus 8 when it is cleared at 1.35 sec at IEEE9 Wind Power Remodeled with 50% Replaced at Bus 3 and 50% Added at Bus 8

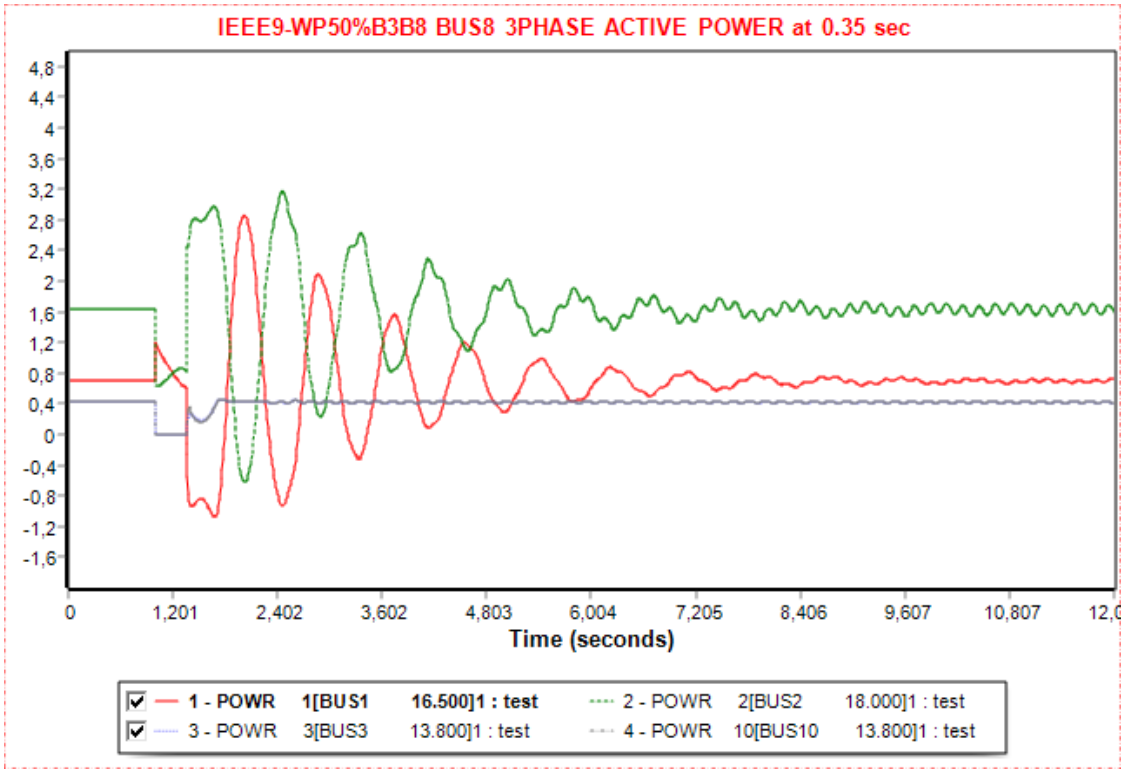

Figure 5. 98 Active Power plots of three phase fault at bus 8 when it is cleared at 1.35 sec at IEEE9 Wind Power Remodeled with 50% Replaced at Bus 3 and 50% Added at Bus 8

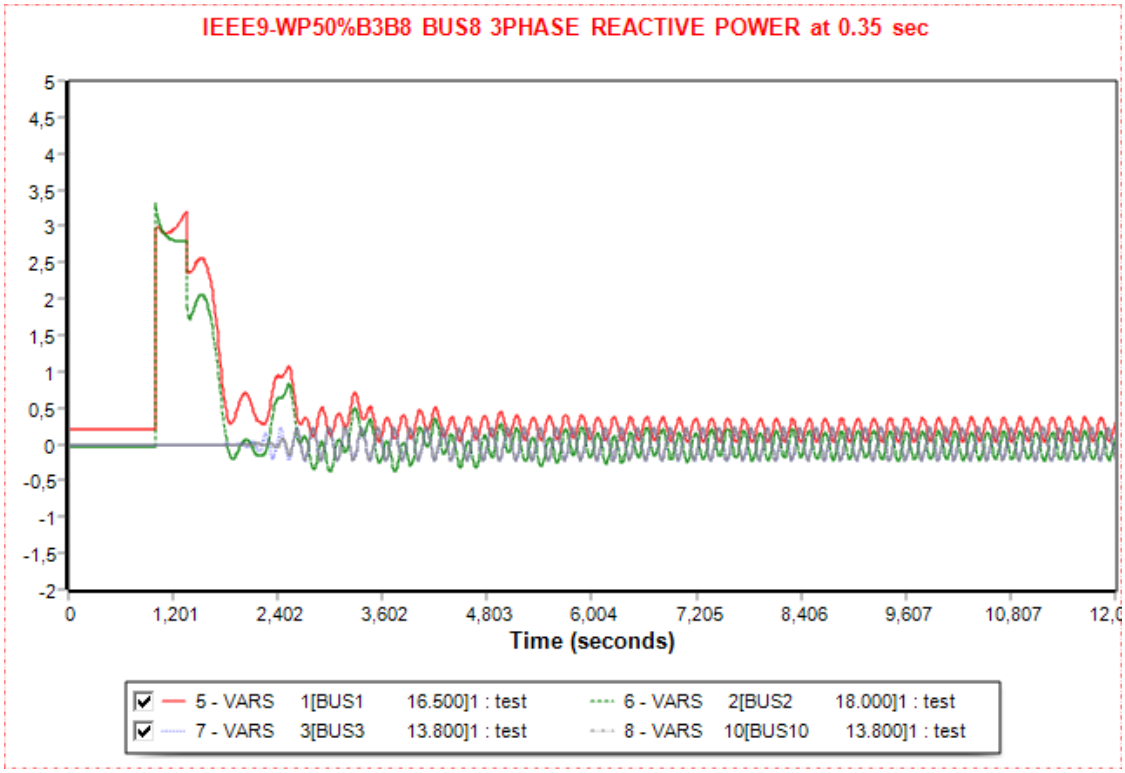

Figure 5. 99 Reactive Power plots of three phase fault at bus 8 when it is cleared at 1.35 sec at IEEE9 Wind Power Remodeled with 50% Replaced at Bus 3 and 50% Added at Bus 8

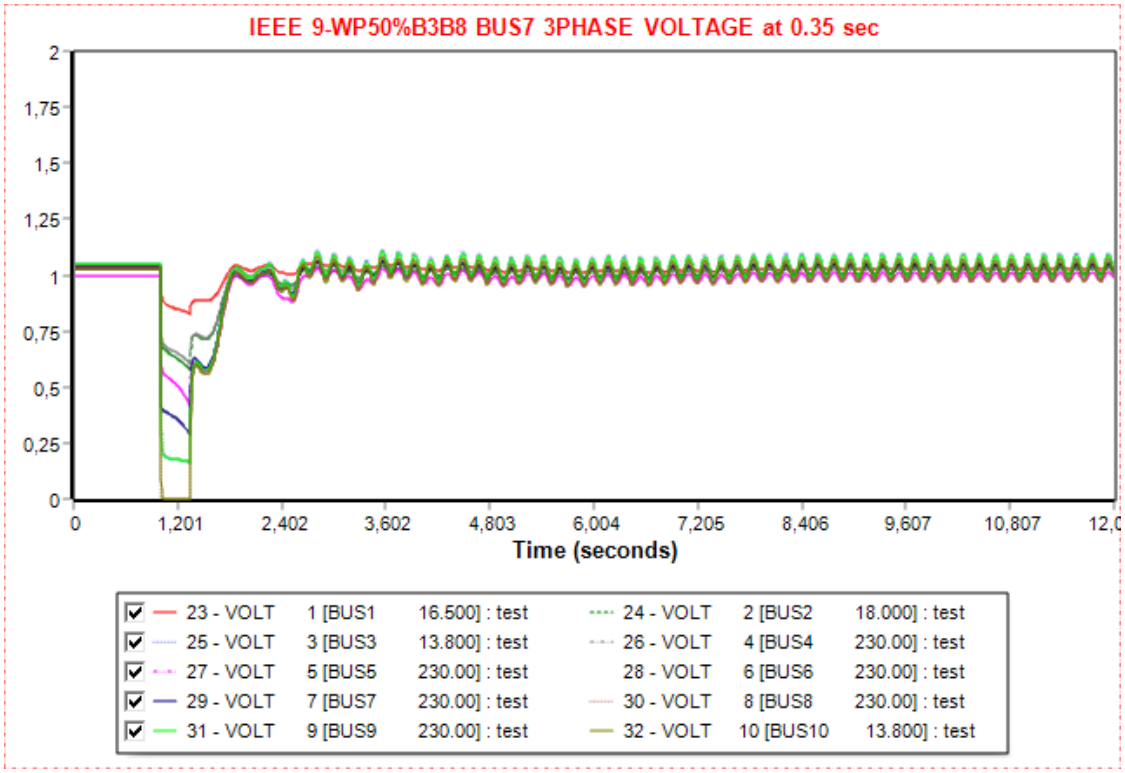

Figure 5. 100 Voltage plots of three phase fault at bus 8 when it is cleared at 1.35 sec at IEEE9 Wind Power Remodeled with 50% Replaced at Bus 3 and 50% Added at Bus 8

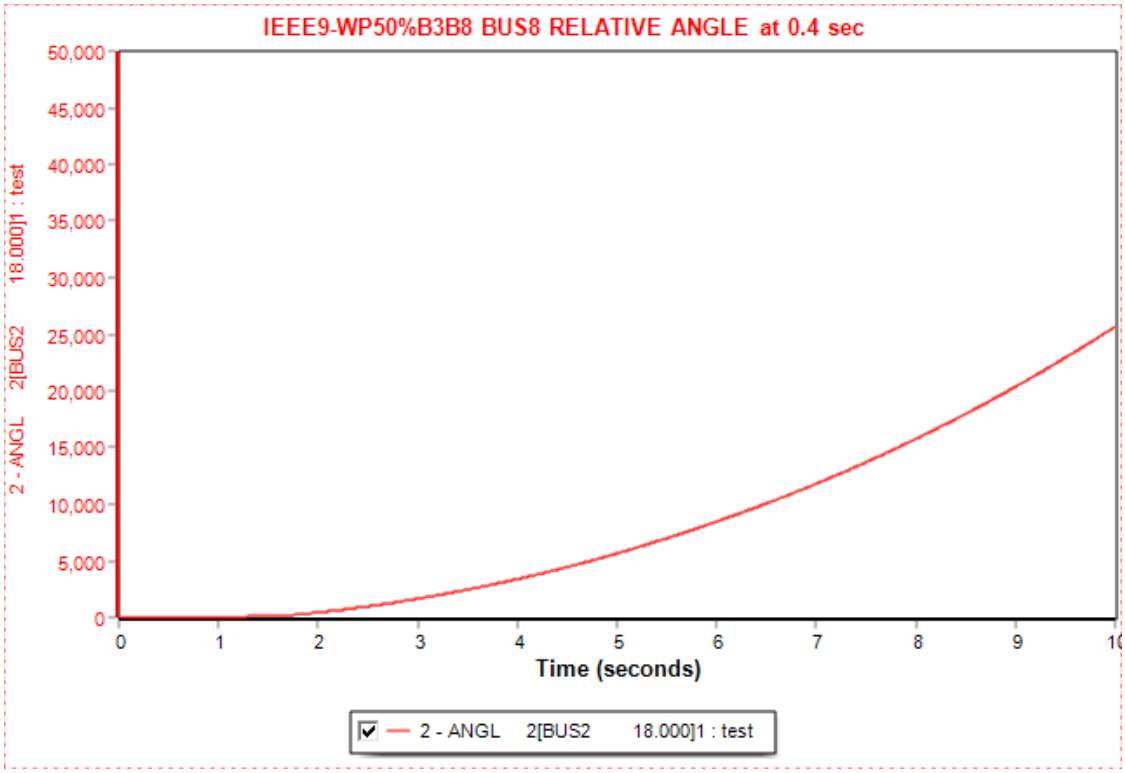

Figure 5. 101 Relative power angle plots of three phase fault at bus 8 when it is cleared at 1.4 sec at IEEE9 Wind Power Remodeled with 50% Replaced at Bus 3 and 50% Added at Bus 8

5.3.3.2 SLG Fault at Bus 8 of the IEEE9 Bus System Wind Power Remodeled with the Partial Replacement (50%) of Generator 3 and the Addition of the other 50% at bus 8

The network can maintain its stability despite the duration of the SLG fault. The fault is cleared at 0.5 sec to study the transient behavior of the system, as there is no CFCT. Firstly, there is an initial power flow for 1 sec, and then the disturbance is applied for 0.5 sec. Simultaneously, for the fault clearance the line 8-7 is tripped and after 1 sec, at 2.5 sec, it is connected to the network. As seen from Table 5.21, the simulation lasts for 12 sec. Figures 5.102-5.106 depict the power angle of generator 2 with respect to the power angle of the swing bus, the buses frequency, the real and active power of the generators, including the ones producing wind power, and the buses voltage when the fault is cleared at 0.5 sec. From Figure 5.103, the rapid change in the frequency that was noticed in the three-phase symmetrical is not appearing here.

Table 5. 21 IEEE9 Wind Power Remodeled with 50% Replaced at Bus 3 and 50% Added at Bus 8 SLG Fault at Bus 8

Action	Time (sec)
Steady State	0.00
Apply Fault	1.00
Clear Fault	1.5
Trip Line	1.5
Connect Line	2.5
Power Flow	12.00

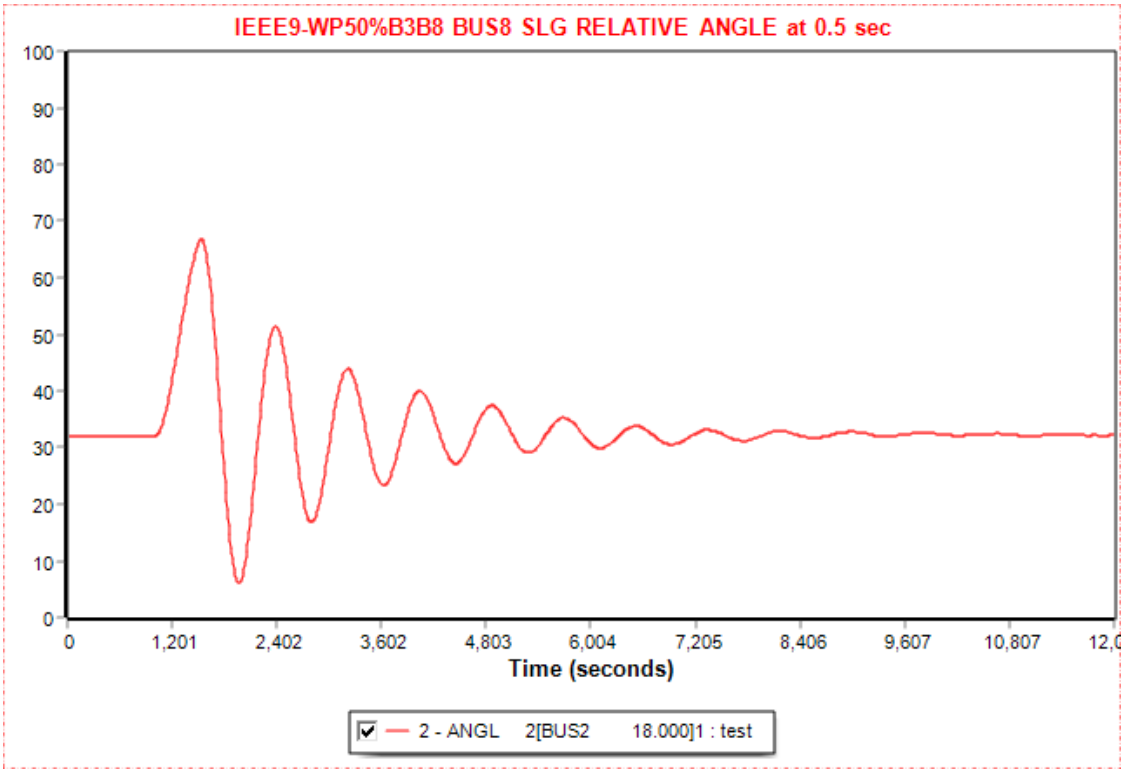

Figure 5. 102 Relative power angle plots of slg fault at bus 8 when it is cleared at 1.5 sec at IEEE9 Wind Power Remodeled with 50% Replaced at Bus 3 and 50% Added at Bus 8

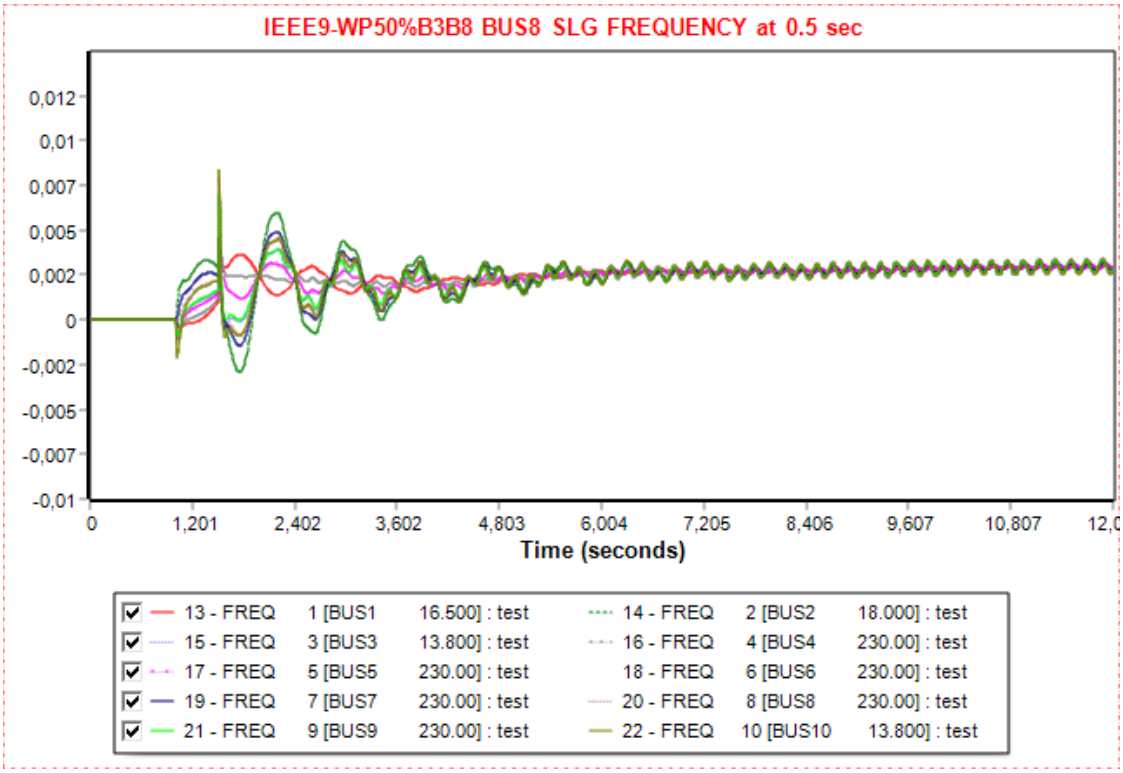

Figure 5. 103 Frequency plots of slg fault at bus 8 when it is cleared at 1.5 sec at IEEE9 Wind Power Remodeled with 50% Replaced at Bus 3 and 50% Added at Bus 8

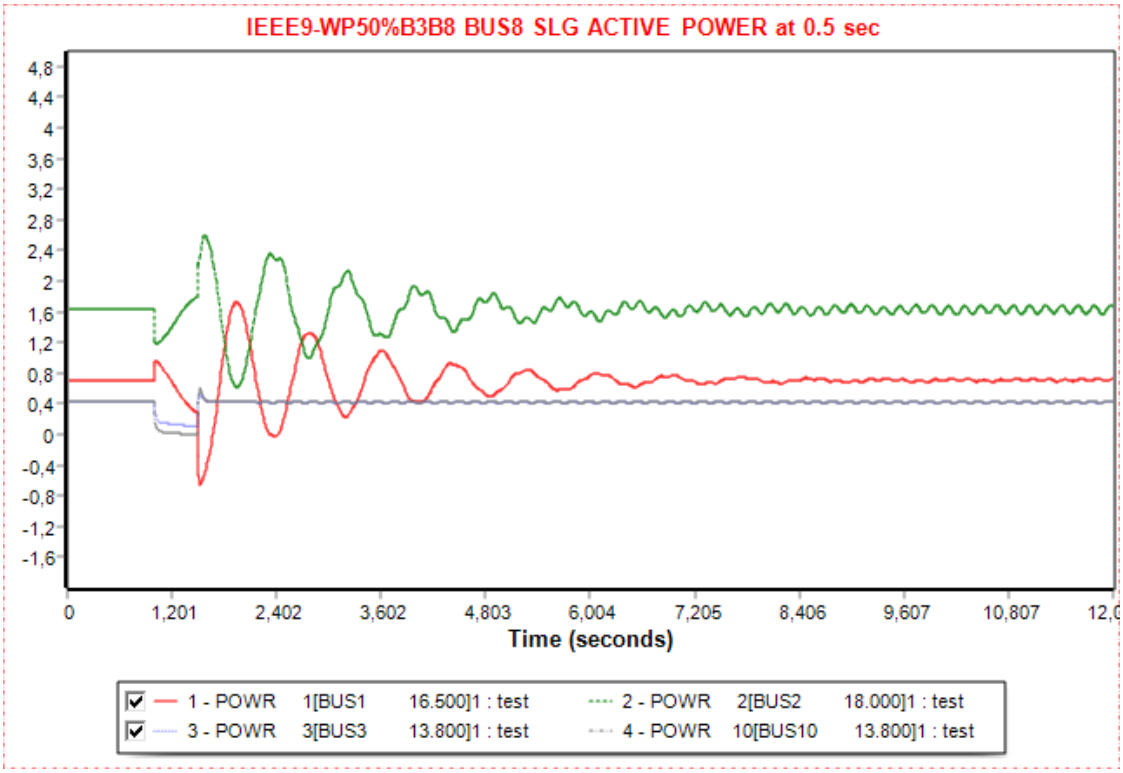

Figure 5. 104 Active Power plots of slg fault at bus 8 when it is cleared at 1.5 sec at IEEE9 Wind Power Remodeled with 50% Replaced at Bus 3 and 50% Added at Bus 8

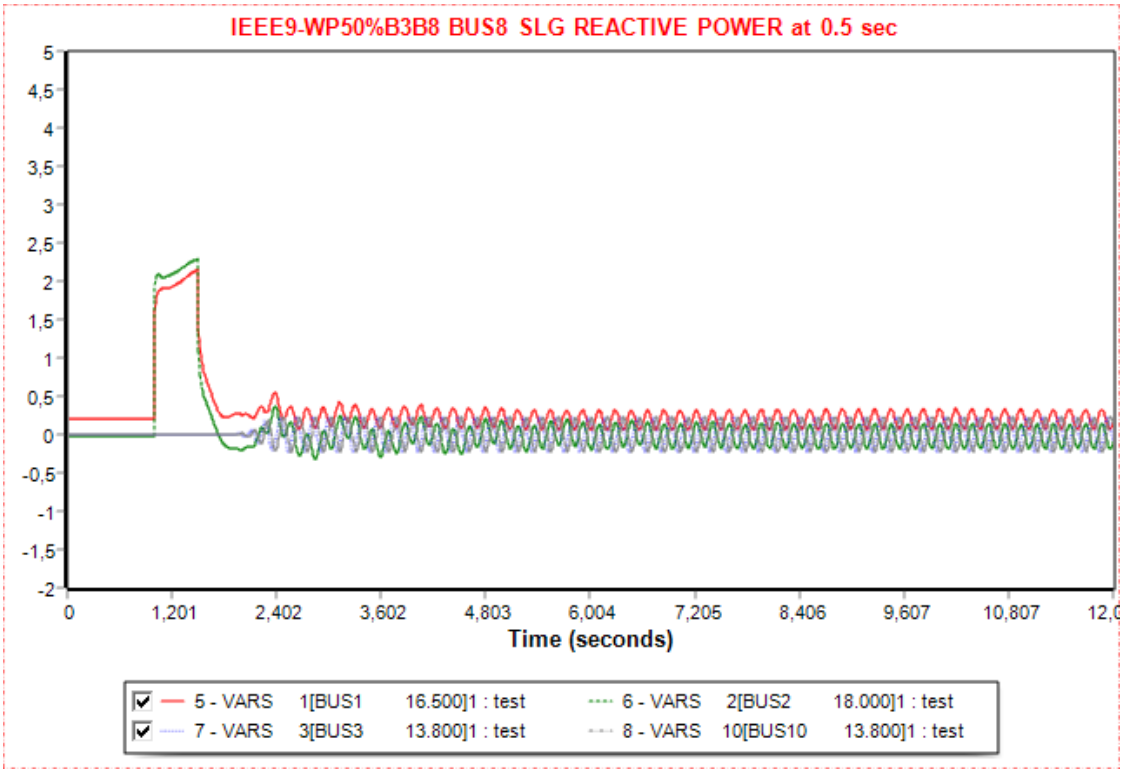

Figure 5. 105 Reactive Power plots of slg fault at bus 8 when it is cleared at 1.5 sec at IEEE9 Wind Power Remodeled with 50% Replaced at Bus 3 and 50% Added at Bus 8

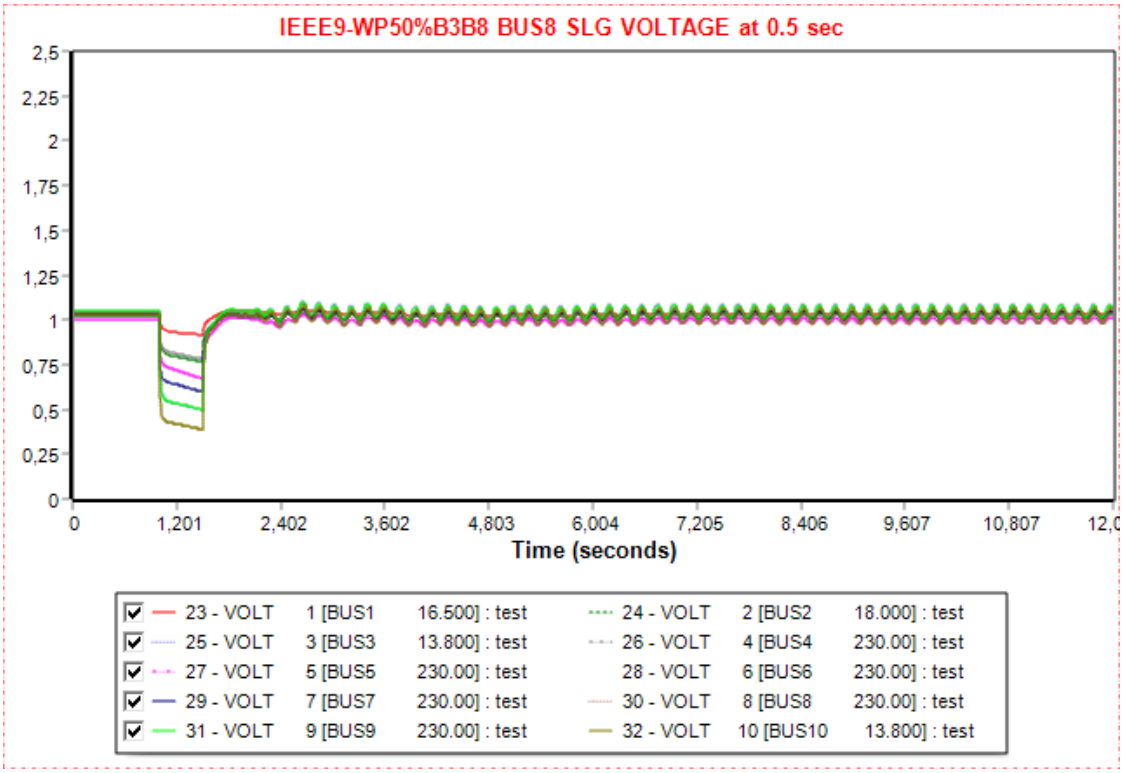

Figure 5. 106 Voltage plots of slg fault at bus 8 when it is cleared at 1.5 sec at IEEE9 Wind Power Remodeled with 50% Replaced at Bus 3 and 50% Added at Bus 8

5.3.4 Diagram Analysis of the IEEE9 Bus System Wind Power Remodeled with the Partial Replacement (50%) of Generator 3 and the Addition of the other 50% at bus 8

The relative power angle of generator 2 with respect to swing bus' power angle plot diagrams, in this scenario, are like the previous ones. Generator 2 is the one examined for desynchronization, as generator 1 is the swing bus with the two wind farms being asynchronous. The three-phase symmetrical fault diagrams (Figure 5.73, 5.85, 5.96) and the SLG diagrams (Figure 5.79, 5.91, 5.102) are similar to the other two because generator 2 in all scenarios has the same dynamic data and the fault locations are similar.

The frequency presents similarities in all three-phase symmetrical faults (Figures 5.74, 5.86, 5.97) and all SLG faults (Figures 5.80, 5.92, 5.103). Moreover, in this scenario, there is a tenth plot representing bus 10, which is necessary for the connection of the wind turbine. In the three faults graphs, there is, in the beginning, a decrease in the buses frequencies, apart from generator 2, and then they arise. In all three plots and the SLG

ones, the frequencies stabilize a little above 0 Hz with nearly zero oscillations. In the three-phase symmetrical fault at bus 8 (Figure 5.97), there is a massive deviation in the wind turbine's frequency that may be the result of the existence of a load and a generator in a single bus during a strong fault's occurrence.

There is one more plot in the active plot diagrams because there is a fourth generator, a wind farm connected at bus 10. The three-phase symmetrical fault diagrams (Figure 5.75, 5.87, 5.98) and the SLG faults (5.81, 5.93, 5.104) have many similarities with the previous cases. The new wind farm active power has similar values as the wind farm in bus 3 with a small decrease and a recovery a few sec after the fault clearance. The fluctuations of the two synchronous generators are like the previous scenarios.

A fourth plot is appearing in the reactive power plots. The same applies here to the reactive power plots as the three-phase symmetrical fault diagrams (Figure 5.76, 5.88, 5.99) and the SLG faults (5.82, 5.94, 5.105). In all plots, the oscillations of the wind turbine buses (3 and 10) are larger than the other buses. The synchronous machines' reactive power's initial increase is because the system tries to maintain its stability.

The voltages in all the diagrams in both three-phase symmetrical faults (Figure 5.77, 5.89, 5.100) and the SLG faults (5.83, 5.95, 5.106) have similar behavior during the simulation. The only difference is the voltage drop to 0 pu in the three-phase symmetrical faults at the bus where the fault is applied. The wind farm’s voltage at bus 3 drops at 0.75 pu in all three-phase diagrams, and the one in bus 8, where the second wind farm is, drops at 0.25 pu. When the fault occurs at bus 8 the connected wind farm voltage drops at 0 pu (Figure 5.100). When the SLG occurs at bus 2 (Figure 5.83), the voltage of bus 3 is 0.75 pu and the voltage of bus 10 is 0.25. The difference in the voltage plot between other scenarios can be observed in the SLG fault at bus 8, where the wind turbine's existence makes the SLG fault stronger. In that disturbance’s Figure (5.106), the voltage of bus 3 is 0.75 pu during the fault, and the one at bus 10 is 0.4 pu. [4][6][9-17][19][20][22][23][38][41]

5.4 SCENARIO 4: IEEE9 Bus System Wind Power Remodeled with the Partial Replacement (50%) of Generator 2 and the Addition of the other 50% at bus 8

This scenario is not like previous ones as bus 2 is partially replaced at 50% by a wind farm with a capacity of 81.5MW, and the other 50% is added as a new wind farm at bus 10, which is connected to bus 8. In this scenario, just like 5.3, the distributed generation by wind energy is examined. The generator in bus 3 is examined for loss of synchronization since generator 1 is in the swing bus and the other are asynchronous wind generators. It is important to see how the system reacts because synchronous generators' total power is decreased by 50% from the previous scenario. The remodeled system created in PSS/E is presented in Figure 5.107. In Table 5.22, the initial load flow can be seen in pu with 100 MVA as base. In the diagrams, there is going to be one more plot that is bus 10 because the creation of this bus was necessary for the addition of a wind farm at bus 8.

Table 5. 22 Active and Reactive power generation of the IEEE9 Bus System Wind Power Remodeled with the Partial Replacement (50%) of Generator 2 and the Addition of the other 50% at bus 8

GENERATOR	Active Power (pu)	Reactive Power (pu)
BUS 1 (Swing Bus)	0.78	0.2
BUS 2 (Wind Power)	0.815	0.08
BUS 3	0.815	-0.18
BUS 10 (Wind Power)	0.815	0

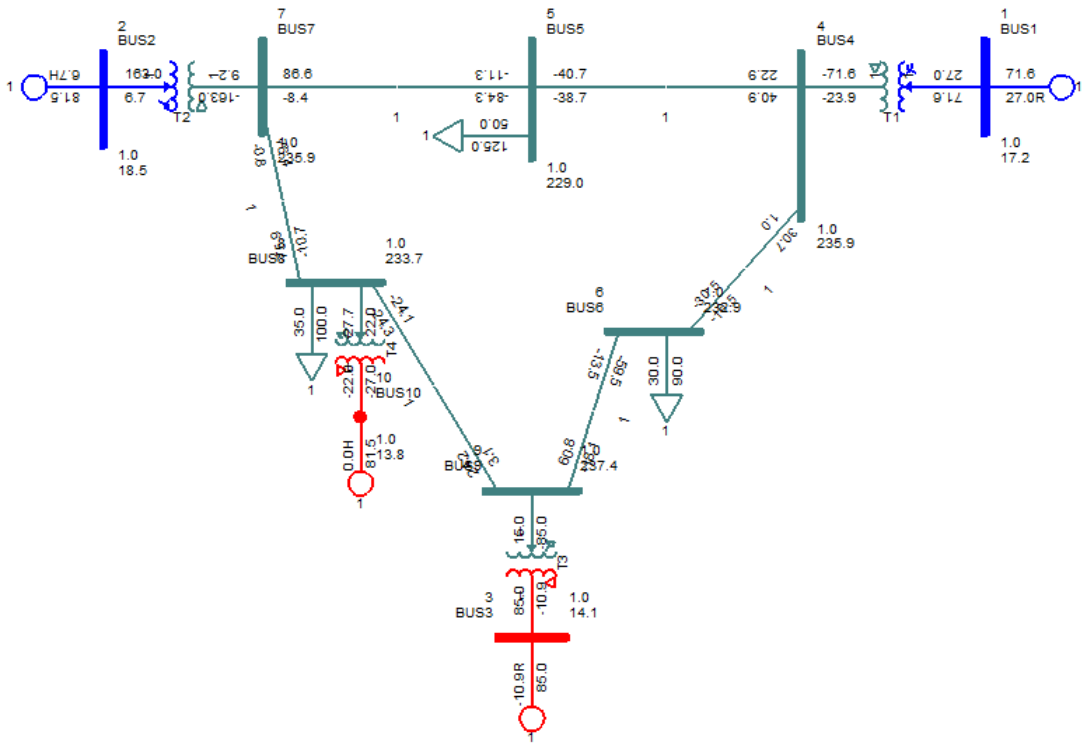

Figure 5. 107 IEEE9 Bus System Wind Power Remodeled with the Partial Replacement (50%) of Generator 2 and the Addition of the other 50% at bus 8

5.4.1 Faults at Bus 2 of the IEEE9 Bus System Wind Power Remodeled with the Partial Replacement (50%) of Generator 2 and the Addition of the other 50% at bus 8

The disturbance in this bus is expected to influence the critical clearing time compared with the original IEEE 9 Bus System because the grid has now two wind farms. But the bus 2 is now connected to a wind turbine so the fault in an asynchronous generator may have little effect on the grid's stability.

5.4.1.1 Three-phase Symmetrical Fault at Bus 2 of IEEE9 Bus System Wind Power Remodeled with the Partial Replacement (50%) of Generator 2 and the Addition of the other 50% at bus 8

The network can maintain its stability despite the duration of this balanced three-phase fault. The disturbance is cleared at 0.5 sec for the grid's transient behavior analysis, as there is no CFCT. Firstly, there is a power flow for 1 sec, and then the fault is applied for 0.5 sec. Simultaneously, for the fault clearance the line 2-7 is tripped and after 1 sec, at 2.5

sec, it is connected to the network. As seen from Table 5.23, the simulation lasts for 12 sec. Figures 5.108-5.112 present the power angle of generator 3 with respect to the power angle of the swing bus, the buses frequency, the real and active power of the generators, including the ones producing wind power, and the buses voltage when the fault is cleared at 0.5 sec. Despite the previous simulations, replacing the generator at bus 2 with a wind farm severely affects the CFCT.

Table 5. 23 IEEE9 Bus System IEEE9 Wind Power Remodeled with 50% Replaced at Bus 2 and 50% Added at Bus 8

Action	Time (sec)
Steady State	0.00
Apply Fault	1.00
Clear Fault	1.5
Trip Line	1.5
Connect Line	2.5
Power Flow	12.00

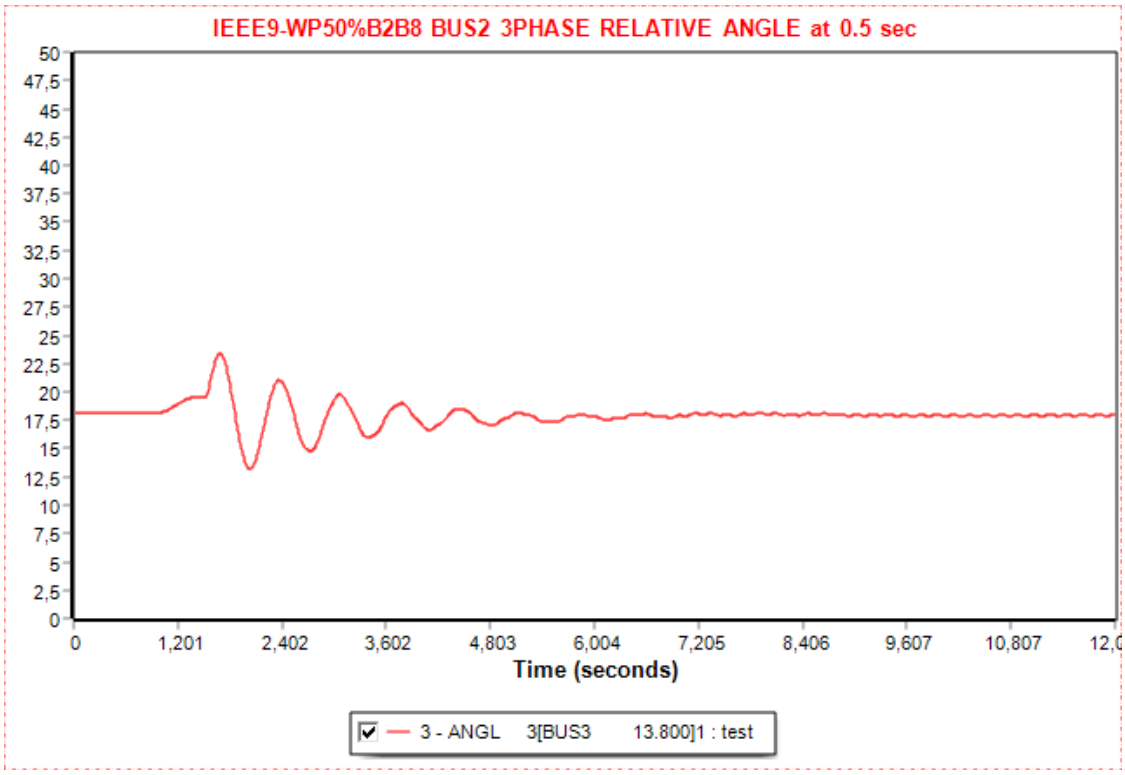

Figure 5. 108 Relative power angle plots of three-phase symmetrical fault at bus 2 when it is cleared at 1.5 sec at IEEE9 Wind Power Remodeled with 50% Replaced at Bus 2 and 50% Added at Bus 8

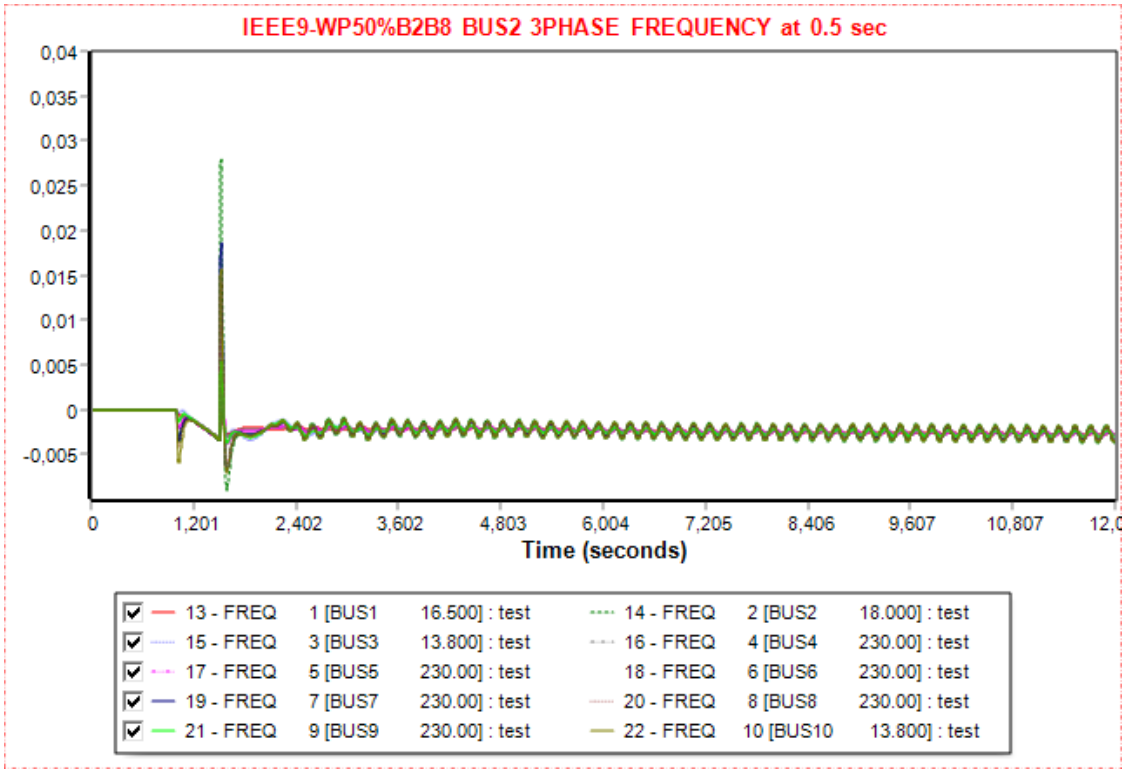

Figure 5. 109 Frequency plots of three-phase symmetrical fault at bus 2 when it is cleared at 1.5 sec at IEEE9 Wind Power Remodeled with 50% Replaced at Bus 2 and 50% Added at Bus 8

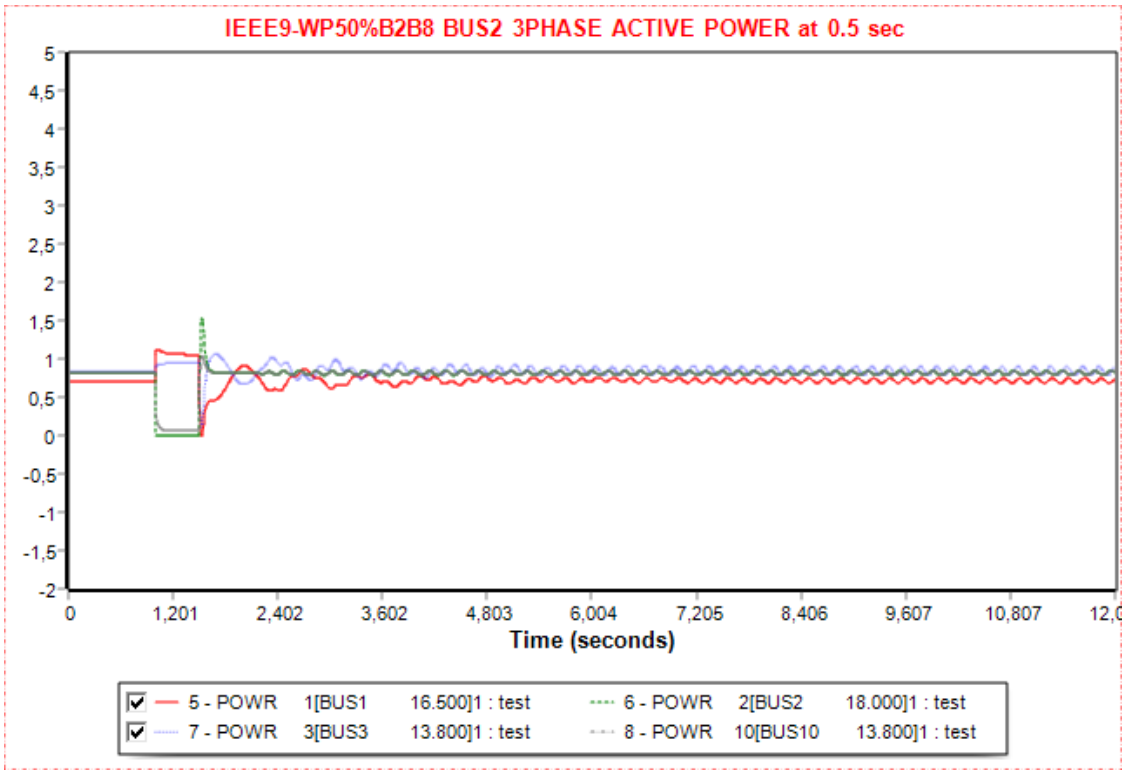

Figure 5. 110 Active Power plots of three-phase symmetrical fault at bus 2 when it is cleared at 1.5 sec at IEEE9 Wind Power Remodeled with 50% Replaced at Bus 2 and 50% Added at Bus 8

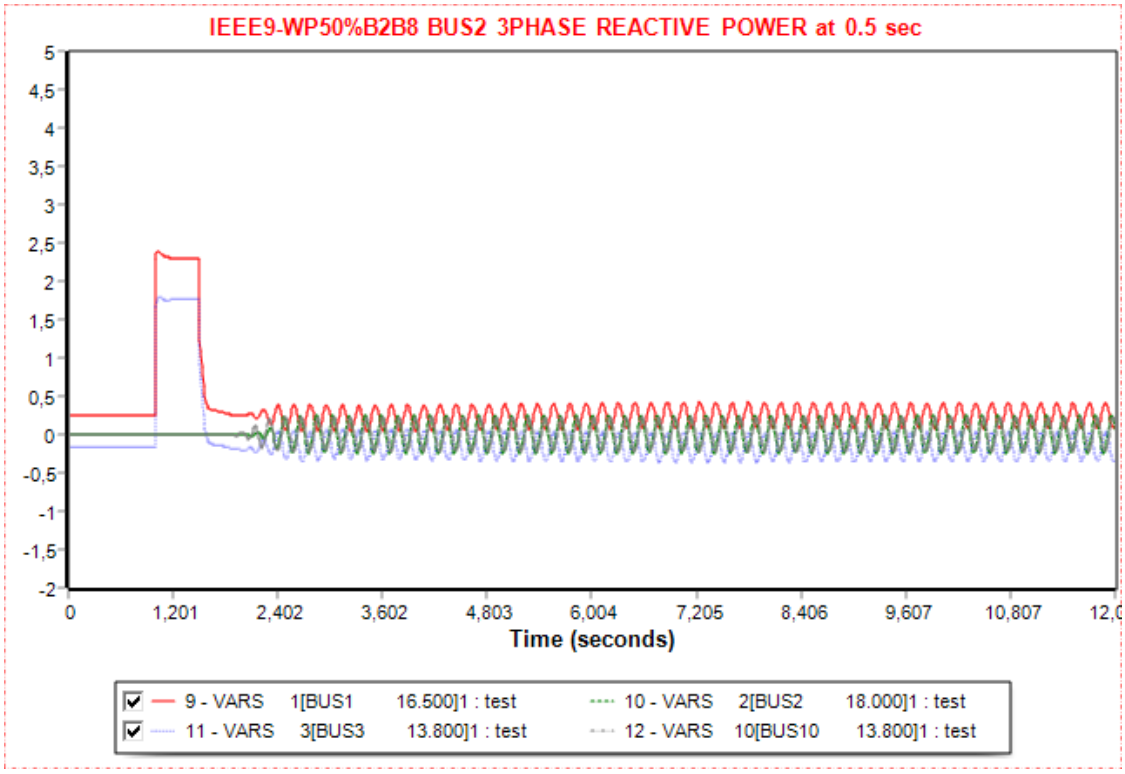

Figure 5. 111 Reactive Power plots of three-phase symmetrical fault at bus 2 when it is cleared at 1.5 sec at IEEE9 Wind Power Remodeled with 50% Replaced at Bus 2 and 50% Added at Bus 8

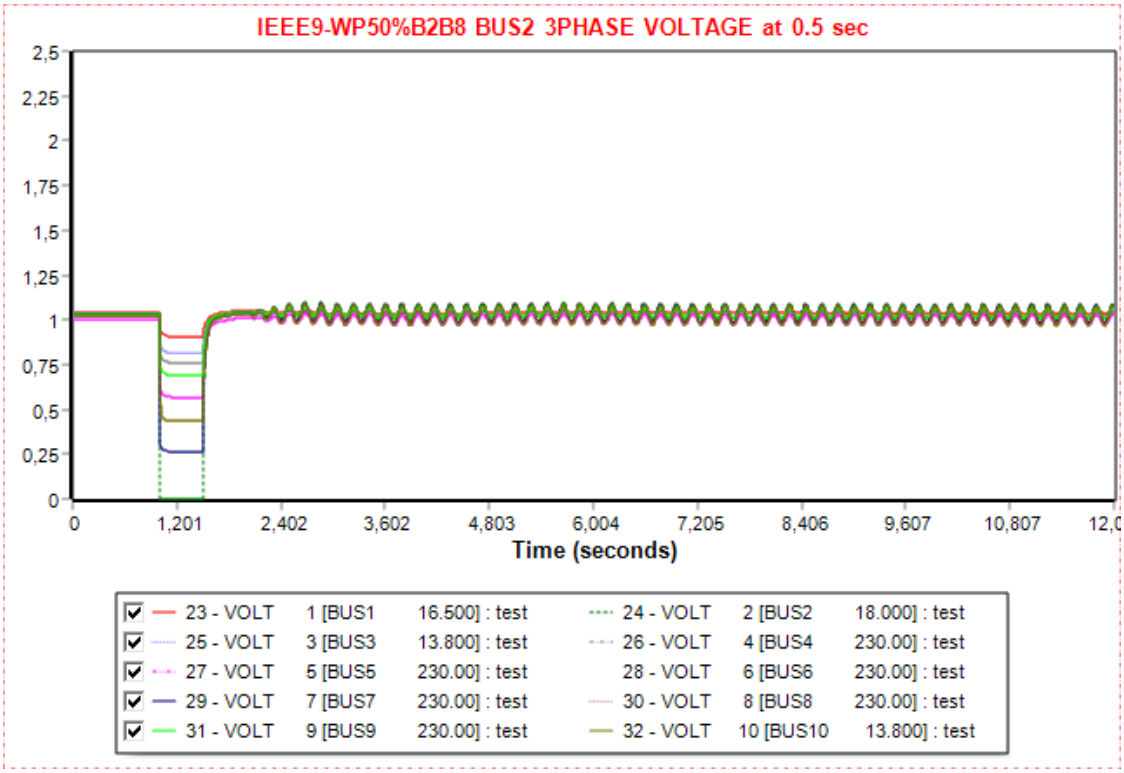

Figure 5. 112 Voltage plots of three-phase symmetrical fault at bus 2 when it is cleared at 1.5 sec at IEEE9 Wind Power Remodeled with 50% Replaced at Bus 2 and 50% Added at Bus 8

5.4.1.2 SLG Fault at Bus 2 of IEEE9 Bus System Wind Power Remodeled with the Partial Replacement (50%) of Generator 2 and the Addition of the other 50% at bus 8

In this simulation, the fault is an SLG, and the network can remain stable despite the duration of the fault. Like the three-phase symmetrical fault of section 5.4.1.1, there is no CFCT, so the disturbance duration is 0.5 sec in order to see the transient behavior of the system. Firstly, there is a power flow for 1 sec, and then the fault is applied for 0.5 sec. At the same time, for the fault clearance, the line 2-7 is tripped, and after 1 sec, at 2.5 sec, it is connected to the network. As seen from Table 5.24, the simulation lasts for 12 sec. Figures 5.113-5.117 present the power angle of generator 3 with respect to the power angle of the swing bus, the buses frequency, the real and active power of the generators, including the ones producing wind power, and the buses voltage when the fault is cleared at 0.5 sec.

Table 5. 24 IEEE9 Wind Power Remodeled with 50% Replaced at Bus 2 and 50% Added at Bus 8 SLG Fault at Bus 2

Action	Time (sec)
Steady State	0.00
Apply Fault	1.00
Clear Fault	1.5
Trip Line	1.5
Connect Line	2.5
Power Flow	12.00

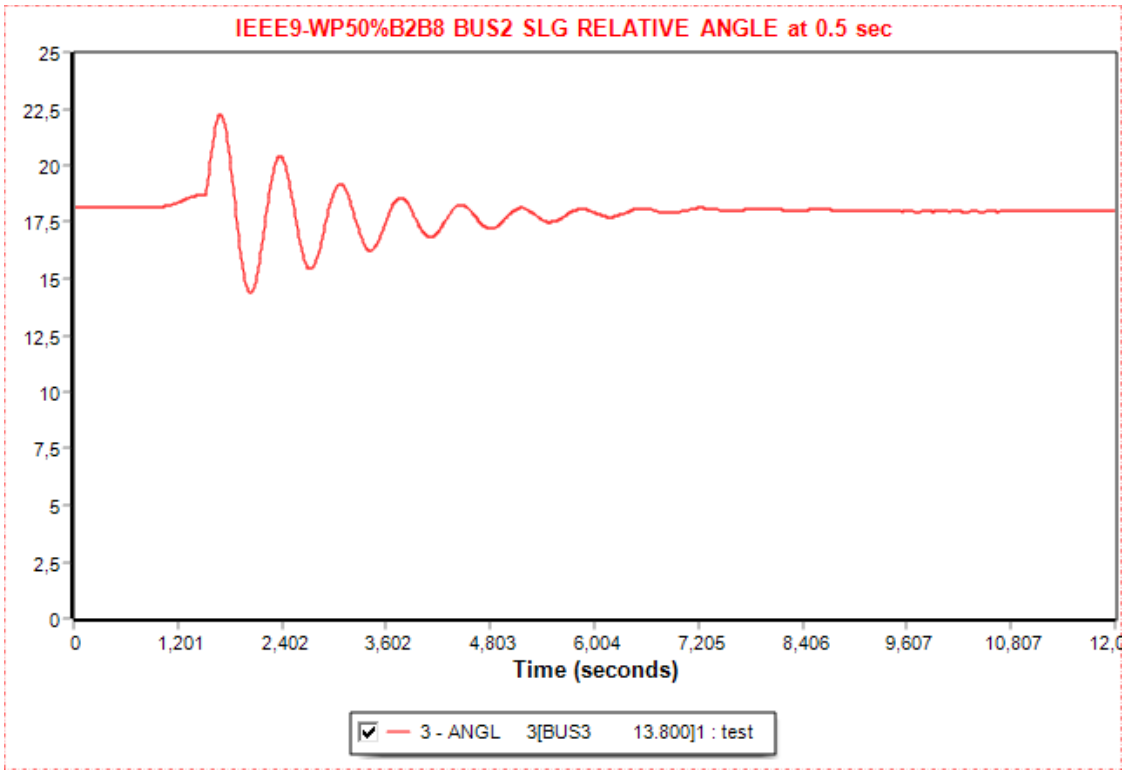

Figure 5. 113 Relative power angle plots of SLG fault at bus 2 when it is cleared at 1.5 sec at IEEE9 Wind Power Remodeled with 50% Replaced at Bus 2 and 50% Added at Bus 8

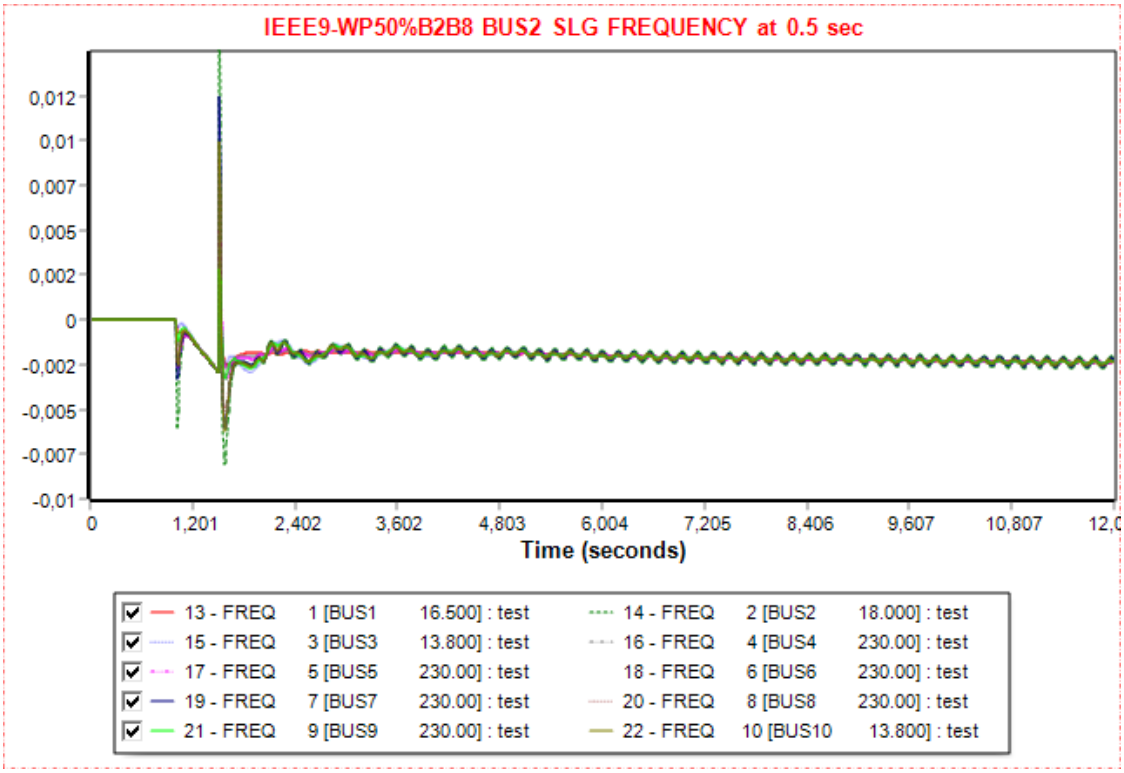

Figure 5. 114 Frequency plots of SLG fault at bus 2 when it is cleared at 1.5 sec at IEEE9 Wind Power Remodeled with 50% Replaced at Bus 2 and 50% Added at Bus 8

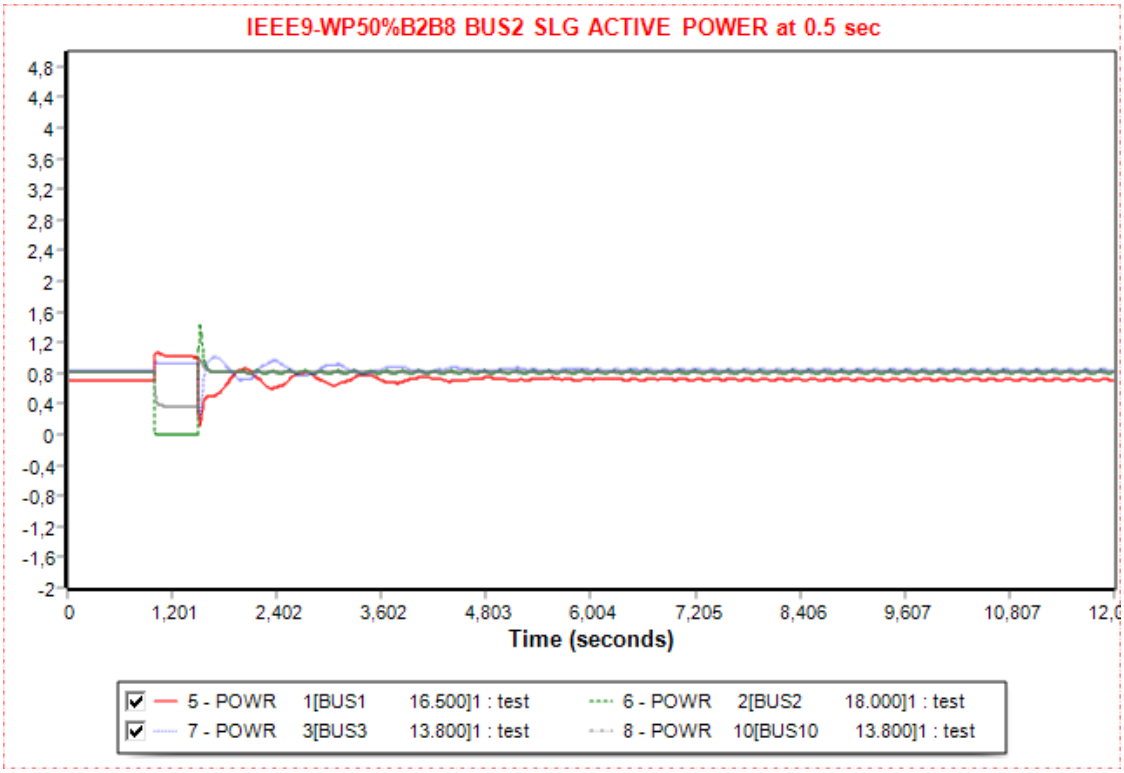

Figure 5. 115 Active Power plots of SLG fault at bus 2 when it is cleared at 1.5 sec at IEEE9 Wind Power Remodeled with 50% Replaced at Bus 2 and 50% Added at Bus 8

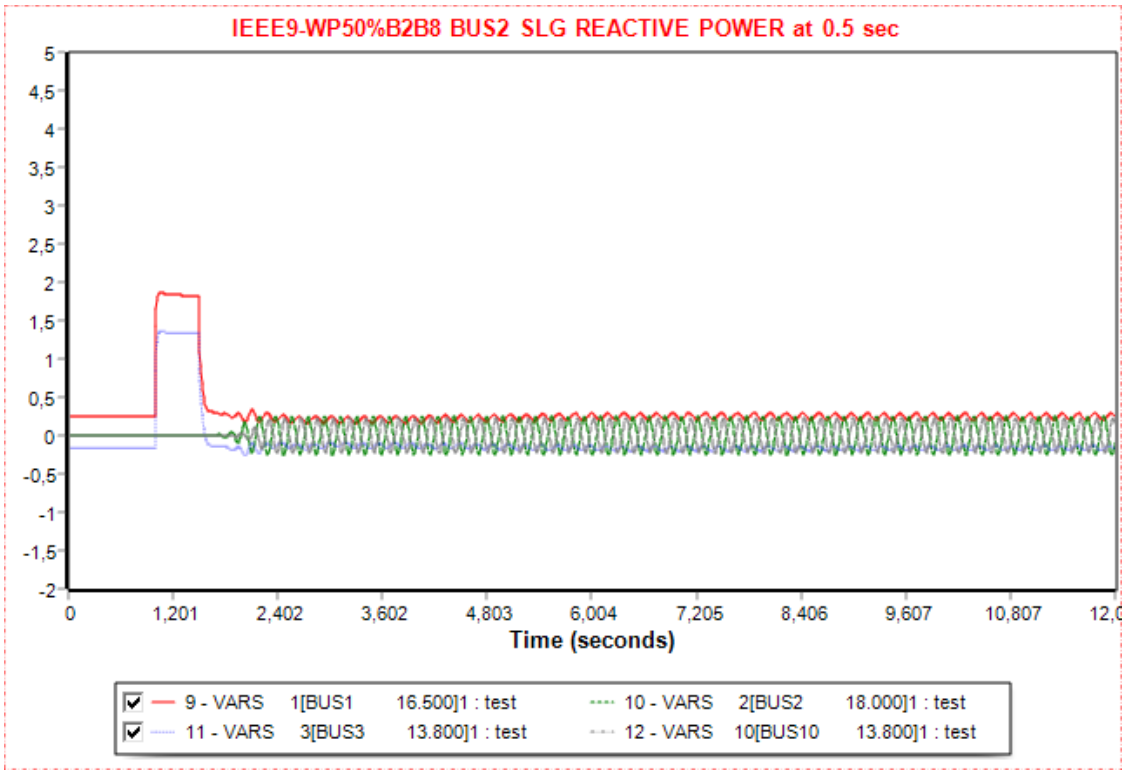

Figure 5. 116 Reactive Power plots of SLG fault at bus 2 when it is cleared at 1.5 sec at IEEE9 Wind Power Remodeled with 50% Replaced at Bus 2 and 50% Added at Bus 8

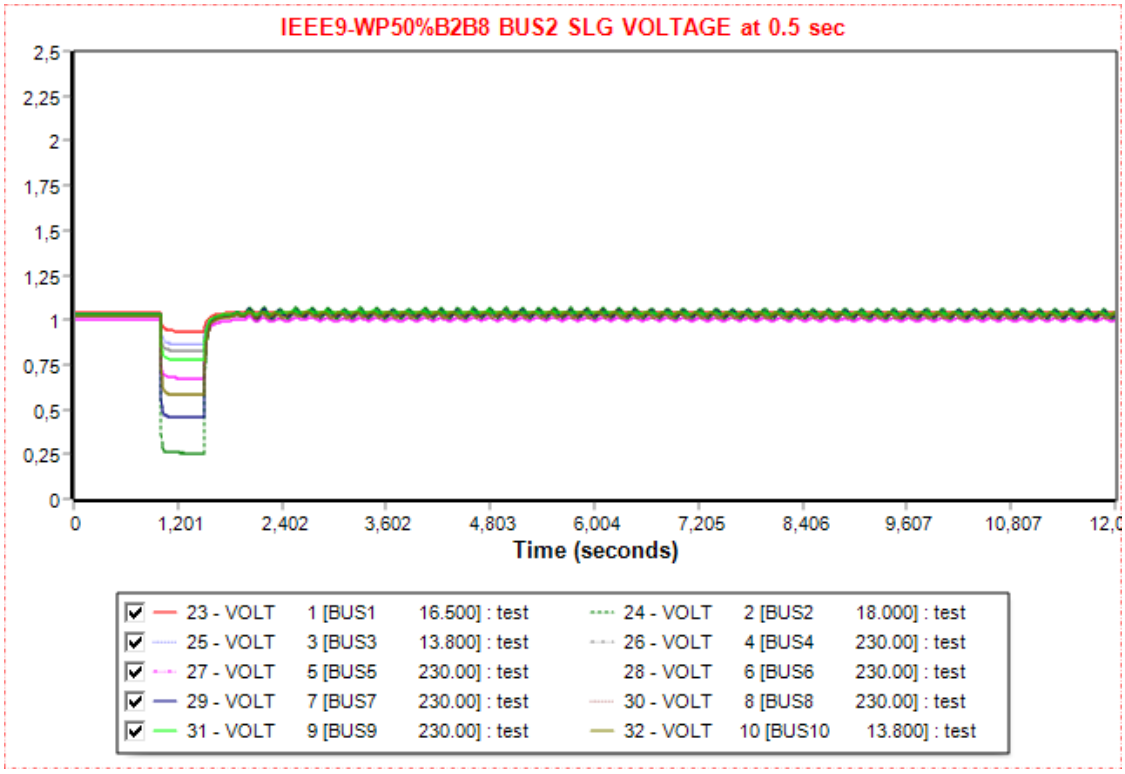

Figure 5. 117 Voltage plots of SLG fault at bus 2 when it is cleared at 1.5 sec at IEEE9 Wind Power Remodeled with 50% Replaced at Bus 2 and 50% Added at Bus 8

5.4.2 Faults at Bus 7 of the IEEE9 Bus System Wind Power Remodeled with the Partial Replacement (50%) of Generator 2 and the Addition of the other 50% at bus 8

Due to the distance of the generator connected at bus 3 with bus 7 it is expected for the fault to not have a severe effect to the grid just like in previous scenarios.

5.4.2.1 Three-phase Symmetrical Fault at Bus 7 of IEEE9 Bus System Wind Power Remodeled with the Partial Replacement (50%) of Generator 2 and the Addition of the other 50% at bus 8

In this simulation, the fault is not capable of making the grid unstable, so there is no CFCT. For transient stability analysis, the fault is applied for 0.5 sec in order to see the transient behavior of the system. In the beginning, there is a power flow for 1 sec, and then a symmetrical three-phase fault happens at bus 7. The clearing of the fault is done at 1.5 sec with the instant tripping of line 7-8. After 1 sec, the line is again connected to the grid at 2.5 sec, and the load flow continues until 12 sec. The described process is presented in Table 5.25. Figures 5.118-5.122 depict the power angle of generator 3 with respect to the power angle of the swing bus, the buses frequency, the real and active power of the generators, including the ones producing wind power, and the buses voltage when the fault is cleared at 0.5 sec. Comparing the Figures with the ones from section 5.4.1.1, the impact of this disturbance is not as mild.

Table 5. 25 IEEE9 Wind Power Remodeled with 50% Replaced at Bus 2 and 50% Added at Bus 8 Three-phase symmetrical Fault at Bus 7

Action	Time (sec)
Steady State	0.00
Apply Fault	1.00
Clear Fault	1.5
Trip Line	1.5
Connect Line	2.5
Power Flow	12.00

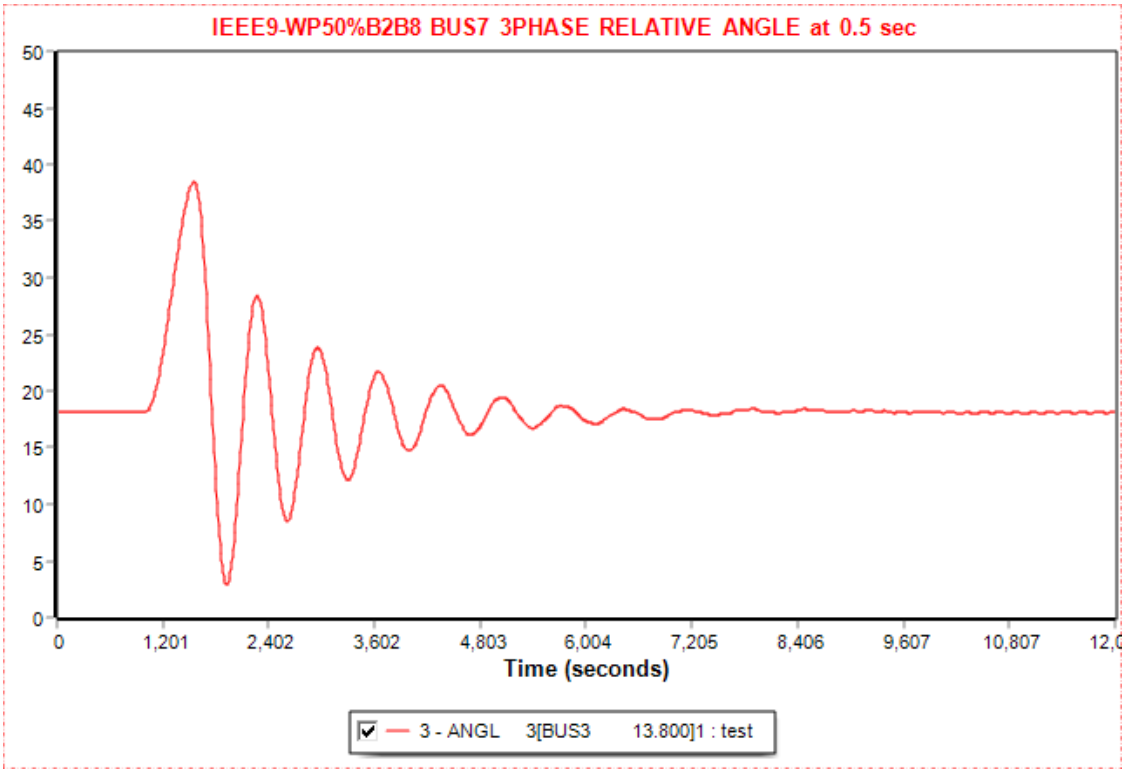

Figure 5. 118 Relative power angle plots of three-phase symmetrical fault at bus 7 when it is cleared at 1.5 sec at IEEE9 Wind Power Remodeled with 50% Replaced at Bus 2 and 50% Added at Bus 8

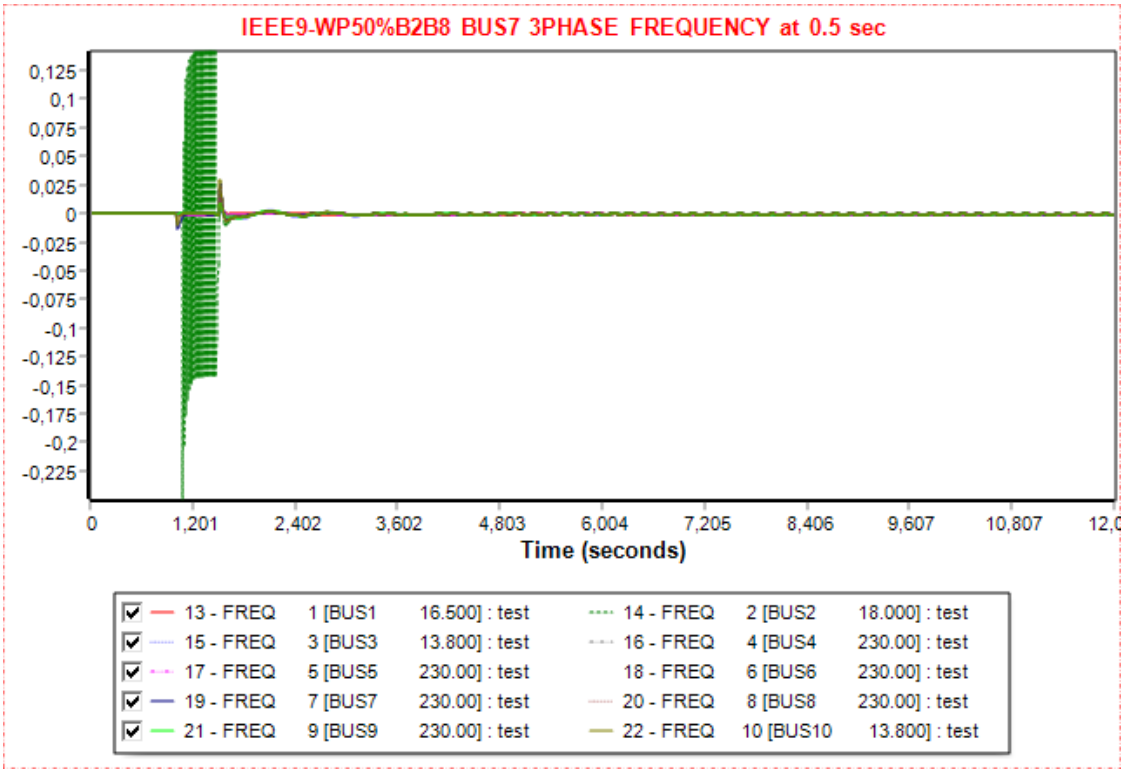

Figure 5. 119 Frequency plots of three-phase symmetrical fault at bus 7 when it is cleared at 1.5 sec at IEEE9 Wind Power Remodeled with 50% Replaced at Bus 2 and 50% Added at Bus 8

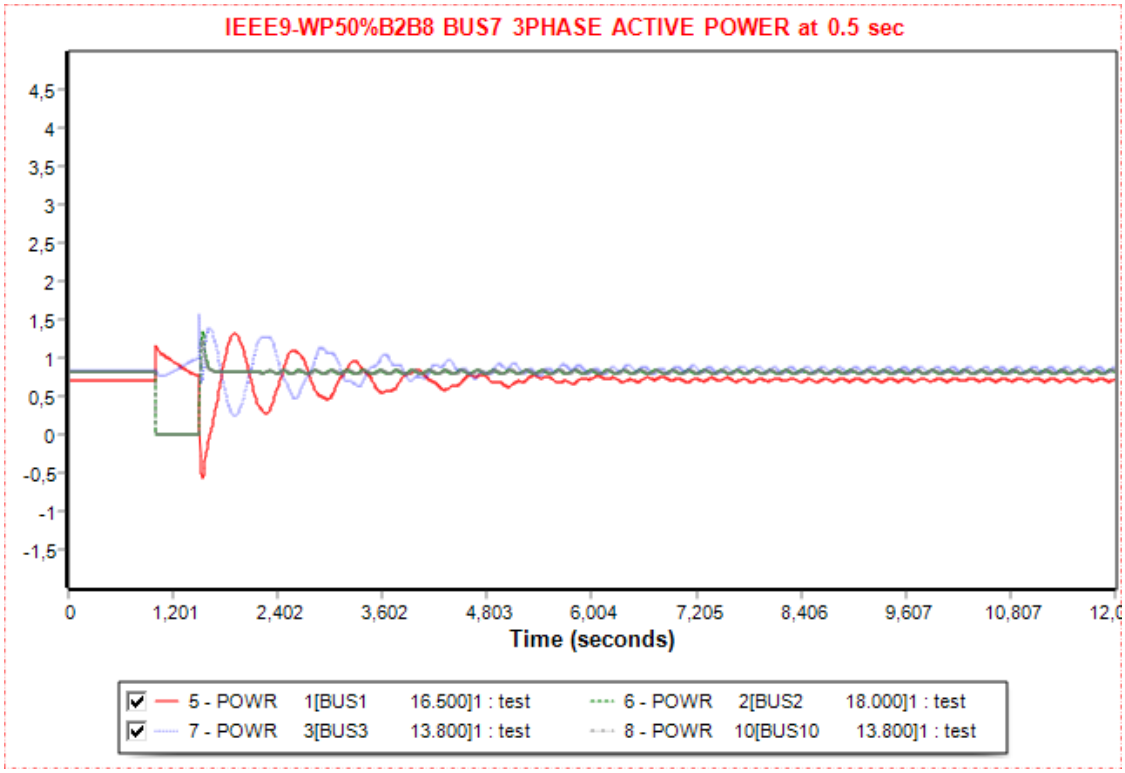

Figure 5. 120 Active Power plots of three-phase symmetrical fault at bus 7 when it is cleared at 1.5 sec at IEEE9 Wind Power Remodeled with 50% Replaced at Bus 2 and 50% Added at Bus 8

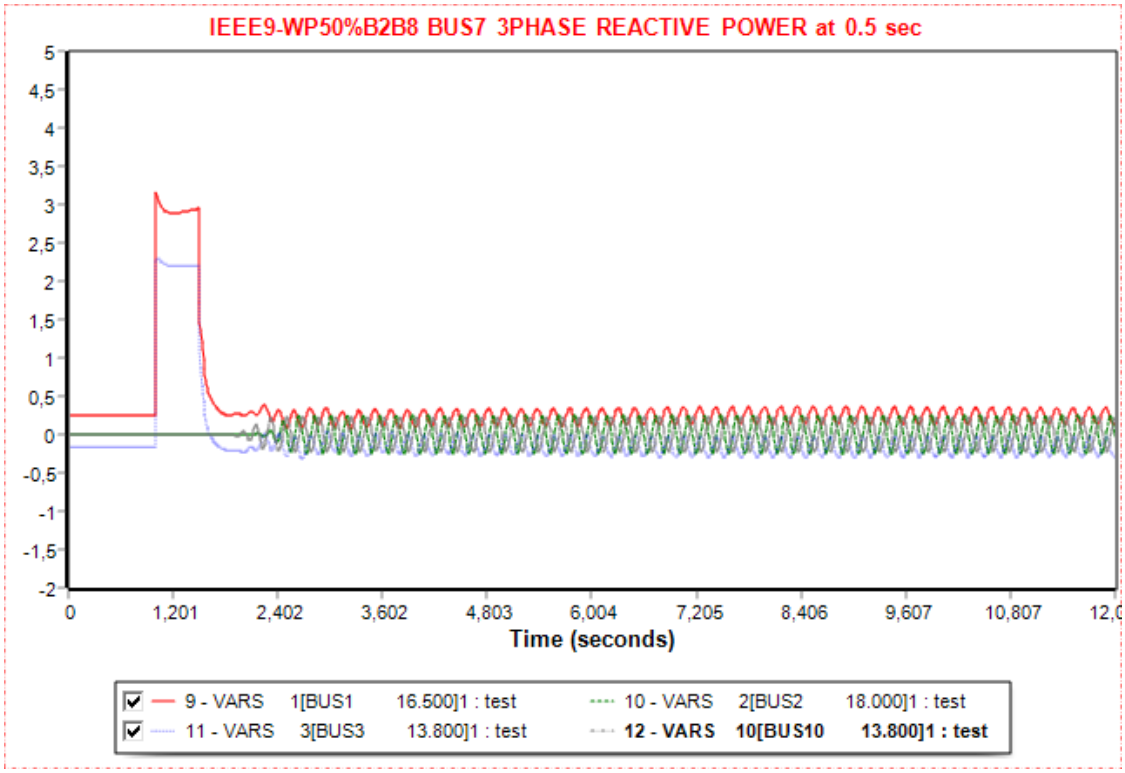

Figure 5. 121 Reactive Power plots of three-phase symmetrical fault at bus 7 when it is cleared at 1.5 sec at IEEE9 Wind Power Remodeled with 50% Replaced at Bus 2 and 50% Added at Bus 8

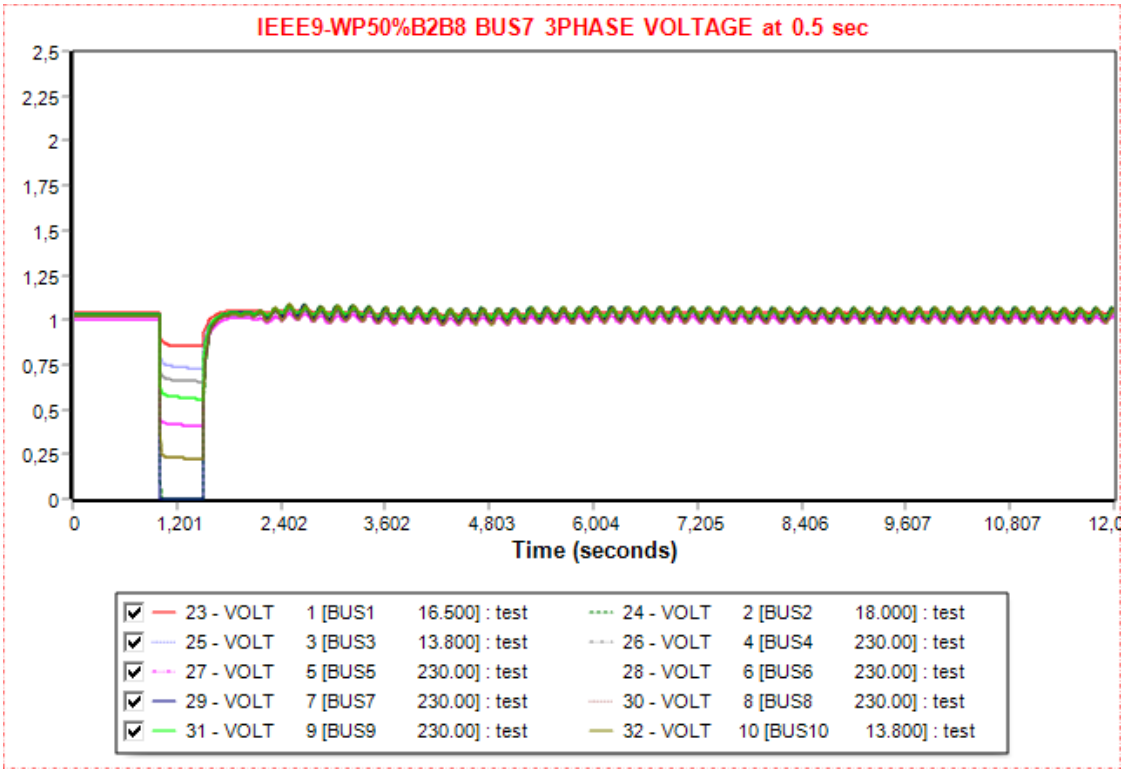

Figure 5. 122 Voltage plots of three-phase symmetrical fault at bus 7 when it is cleared at 1.5 sec at IEEE9 Wind Power Remodeled with 50% Replaced at Bus 2 and 50% Added at Bus 8

5.4.2.2 SLG Fault at Bus 7 of IEEE9 Bus System Wind Power Remodeled with the Partial Replacement (50%) of Generator 2 and the Addition of the other 50% at bus 8

The network can maintain its stability despite the duration of the SLG fault. The fault is cleared at 0.5 sec to study the transient behavior of the system, as there is no CFCT. There is an initial power flow for 1 sec, and then the disturbance is applied for 0.5 sec. Simultaneously, for the fault clearance line 7-8 is tripped, and after 1 sec, at 2.5 sec, it is connected to the network. As seen from Table 5.26, the simulation lasts for 12 sec. Figures 5.123-5.127 present the power angle of generator 3 with respect to the power angle of the swing bus, the buses frequency, the real and active power of the generators, including the one producing wind power, and the buses voltage when the fault is cleared at 0.5 sec.

Table 5. 26 IEEE9 Wind Power Remodeled with 50% Replaced at Bus 2 and 50% Added at Bus 8 SLG Fault at Bus 7

Action	Time (sec)
Steady State	0.00
Apply Fault	1.00
Clear Fault	1.5
Trip Line	1.5
Connect Line	2.5
Power Flow	12.00

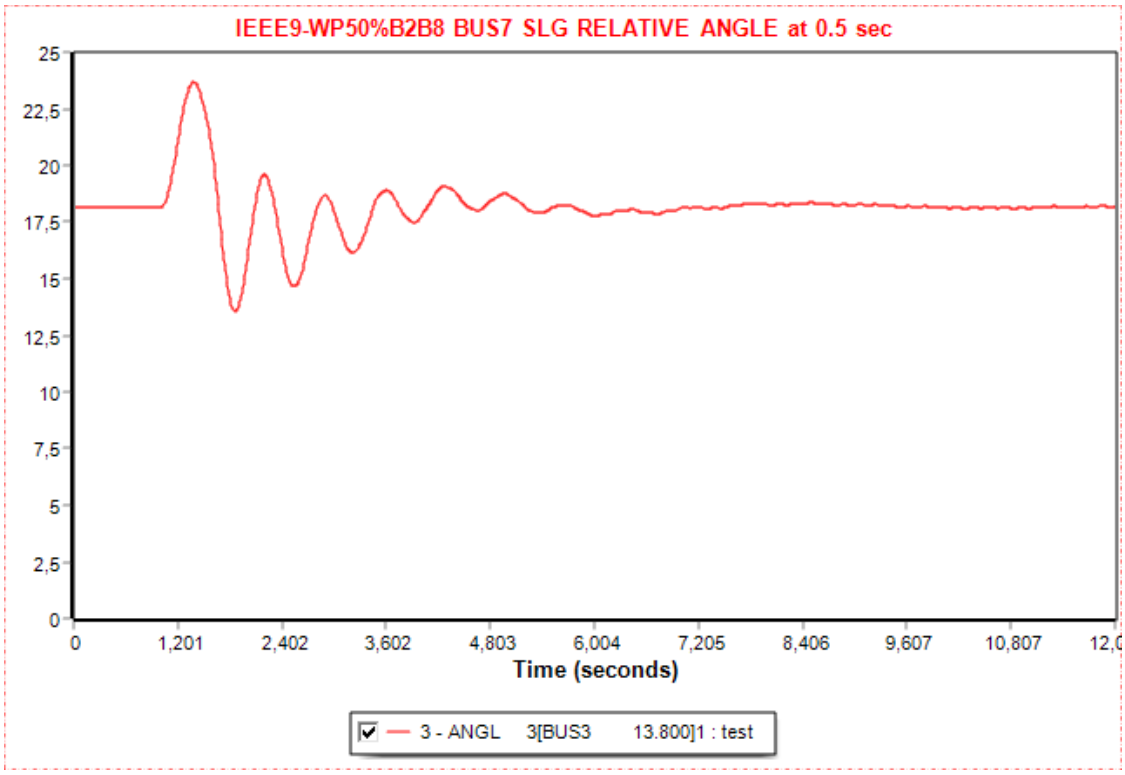

Figure 5. 123 Relative power angle plots of SLG fault at bus 7 when it is cleared at 1.5 sec at IEEE9 Wind Power Remodeled with 50% Replaced at Bus 2 and 50% Added at Bus 8

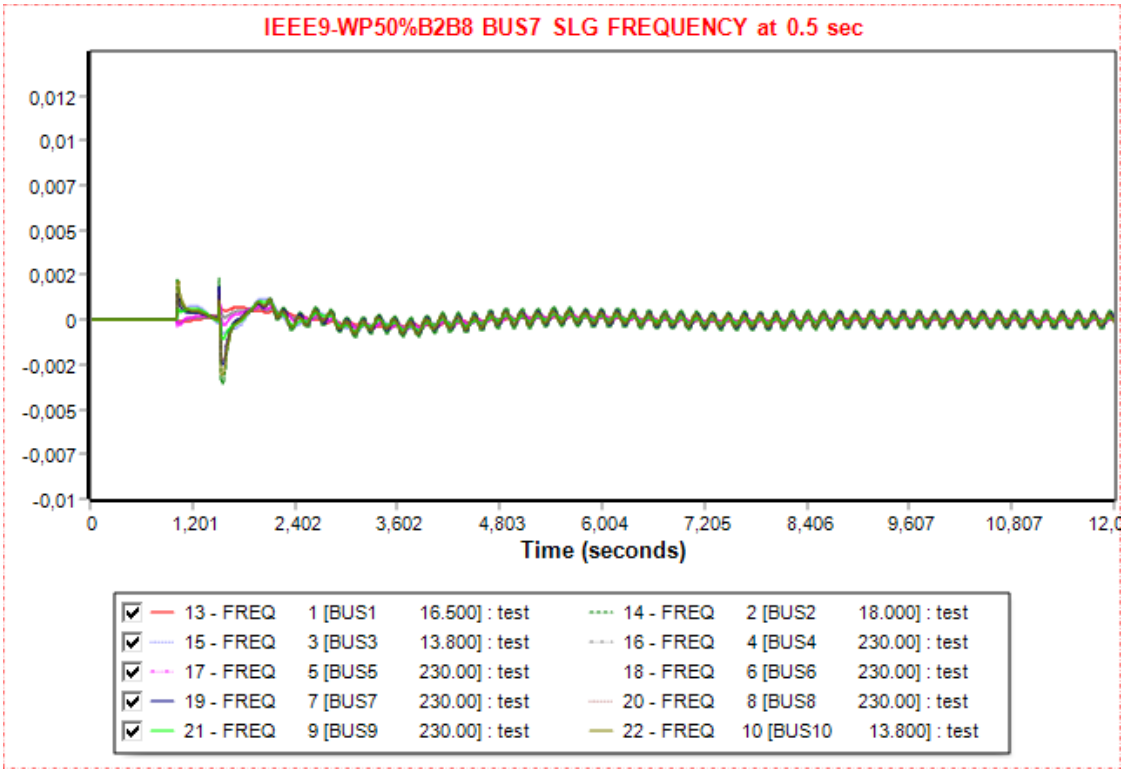

Figure 5. 124 Frequency plots of SLG fault at bus 7 when it is cleared at 1.5 sec at IEEE9 Wind Power Remodeled with 50% Replaced at Bus 2 and 50% Added at Bus 8

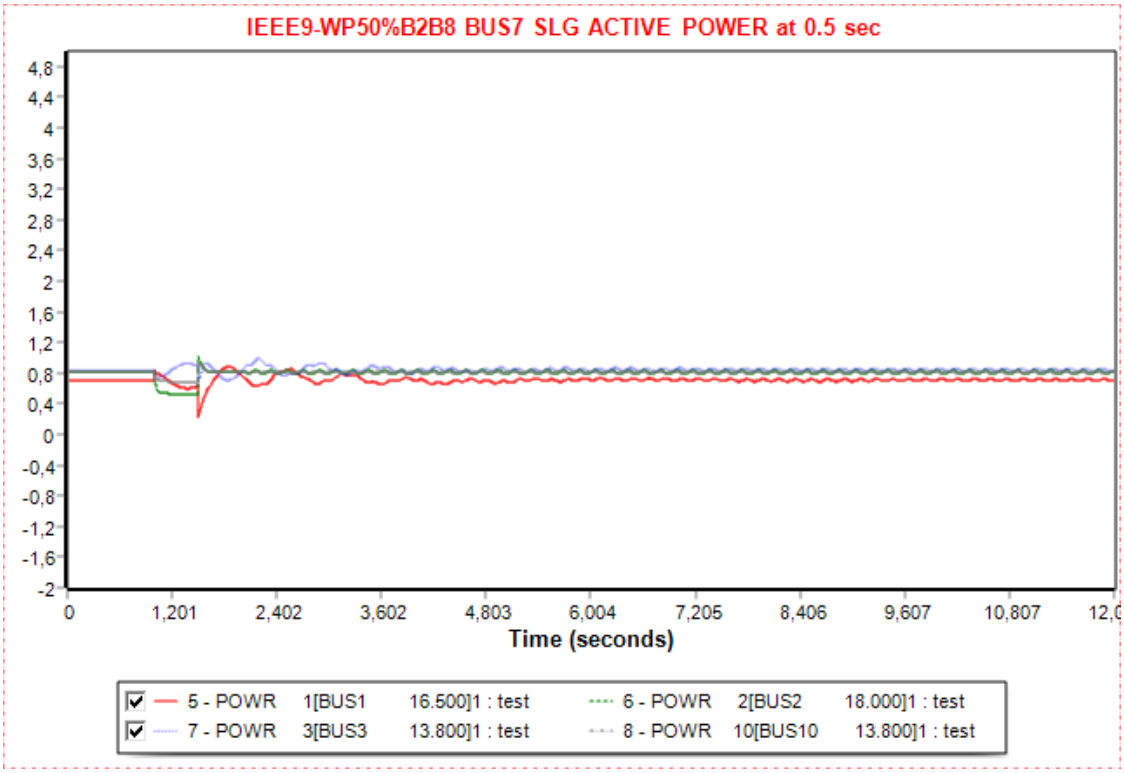

Figure 5. 125 Active Power plots of SLG fault at bus 7 when it is cleared at 1.5 sec at IEEE9 Wind Power Remodeled with 50% Replaced at Bus 2 and 50% Added at Bus 8

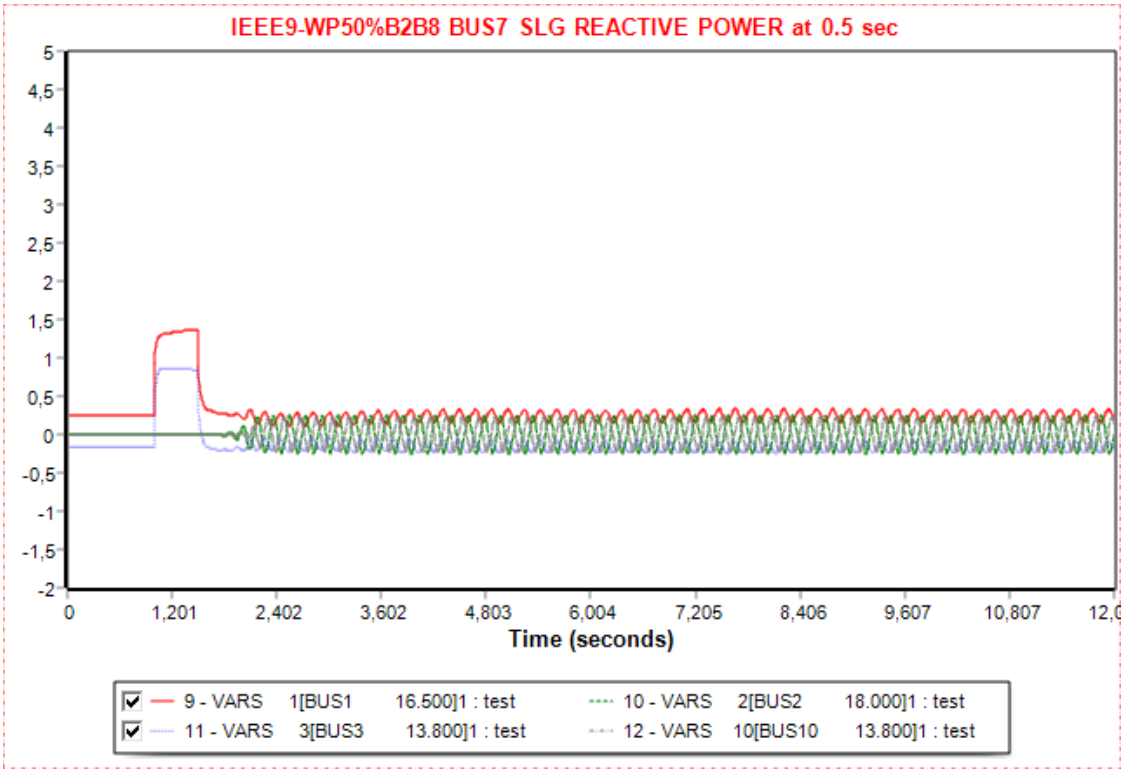

Figure 5. 126 Reactive Power plots of SLG fault at bus 7 when it is cleared at 1.5 sec at IEEE9 Wind Power Remodeled with 50% Replaced at Bus 2 and 50% Added at Bus 8

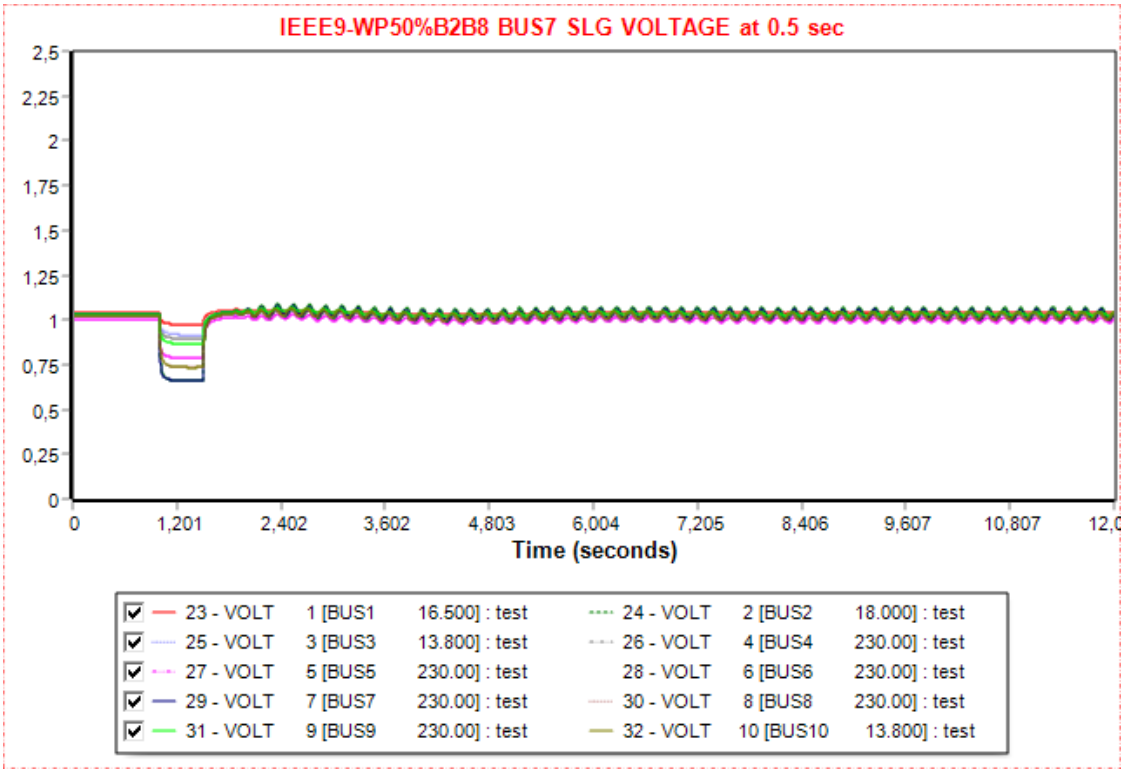

Figure 5. 127 Voltage plots of SLG fault at bus 7 when it is cleared at 1.5 sec at IEEE9 Wind Power Remodeled with 50% Replaced at Bus 2 and 50% Added at Bus 8

5.4.3 Faults at Bus 8 of the IEEE9 Bus System Wind Power Remodeled with the Partial Replacement (50%) of Generator 2 and the Addition of the other 50% at bus 8

Bus 8 in the IEEE 9 Bus System is connected to 100MW and 35 MVAR load. In this case, there is a modification, which is the bus 10, which is connected to a 81.5 MW wind farm.

5.4.3.1 Three-phase Symmetrical Fault at Bus 8 of IEEE9 Bus System Wind Power Remodeled with the Partial Replacement (50%) of Generator 2 and the Addition of the other 50% at bus 8

The simulation's critical fault clearing time was calculated to be 2.05 sec, which is relatively high. At first, there is an initial load flow for 1 sec, and then a symmetrical three-phase fault occurs until 3.05 sec. When the fault is cleared, at the same time the line 8-7 opens for the fault to be cleared internally. Then it closes again after 1 sec, at 4.05 sec, and the system runs until 12 sec (Table 5.27). Figures 5.128-5.132 present the power angle of generator 3 with respect to the power angle of the swing bus, the buses frequency, the real and active power of the generators, including the one producing wind power, and the buses voltage when the fault is cleared at CFCT. From power angle Figure 5.128, 1 sec post-fault, the system begins to lose synchronization as there is a rise in the power angle and a few oscillations in the other diagrams but recovers back after the clearance. Figure 5.90 shows the loss of synchronization of the power angle of generator 3 with respect to the power angle of the swing bus when the fault is cleared 0.05 sec after the CFCT.

Table 5. 27 IEEE9 Wind Power Remodeled with 50% Replaced at Bus 2 and 50% Added at Bus 8 Three-phase symmetrical Fault at Bus 8

Action	Time (sec)
Steady State	0.00
Apply Fault	1.00
Clear Fault	3.05
Trip Line	3.05
Connect Line	4.05
Power Flow	12.00

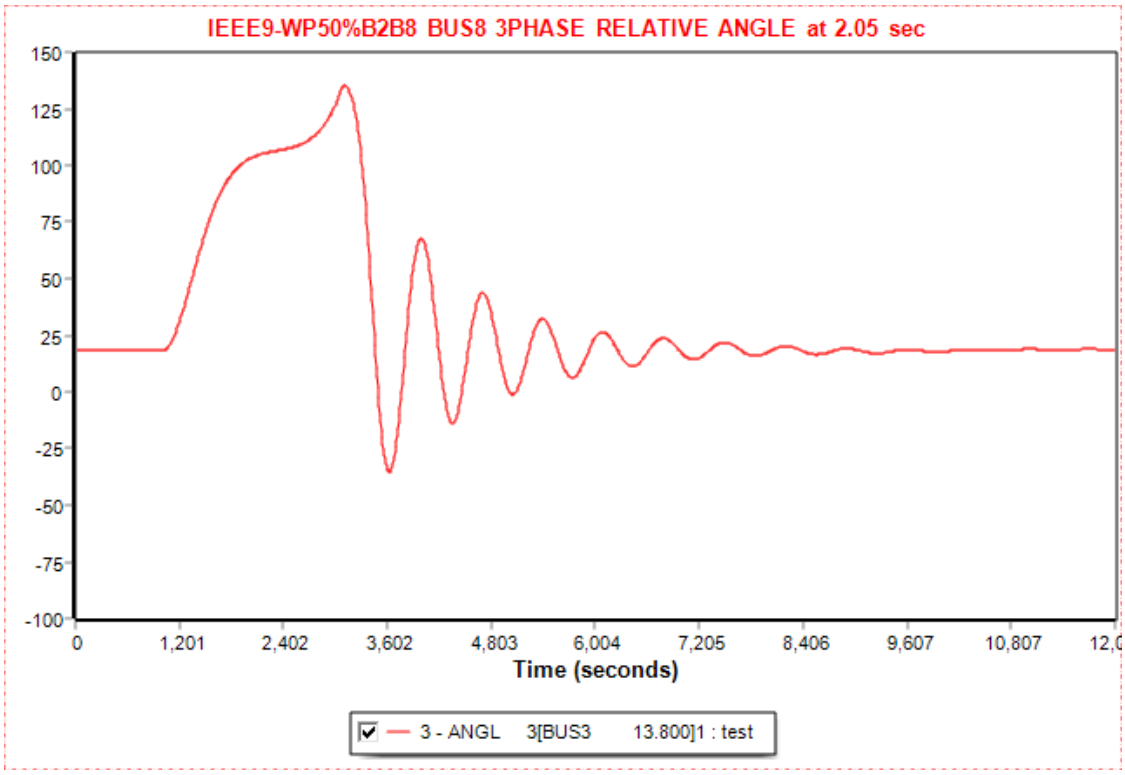

Figure 5. 128 Relative power angle plots of three-phase symmetrical fault at bus 8 when it is cleared at 3.05sec at IEEE9 Wind Power Remodeled with 50% Replaced at Bus 2 and 50% Added at Bus 8

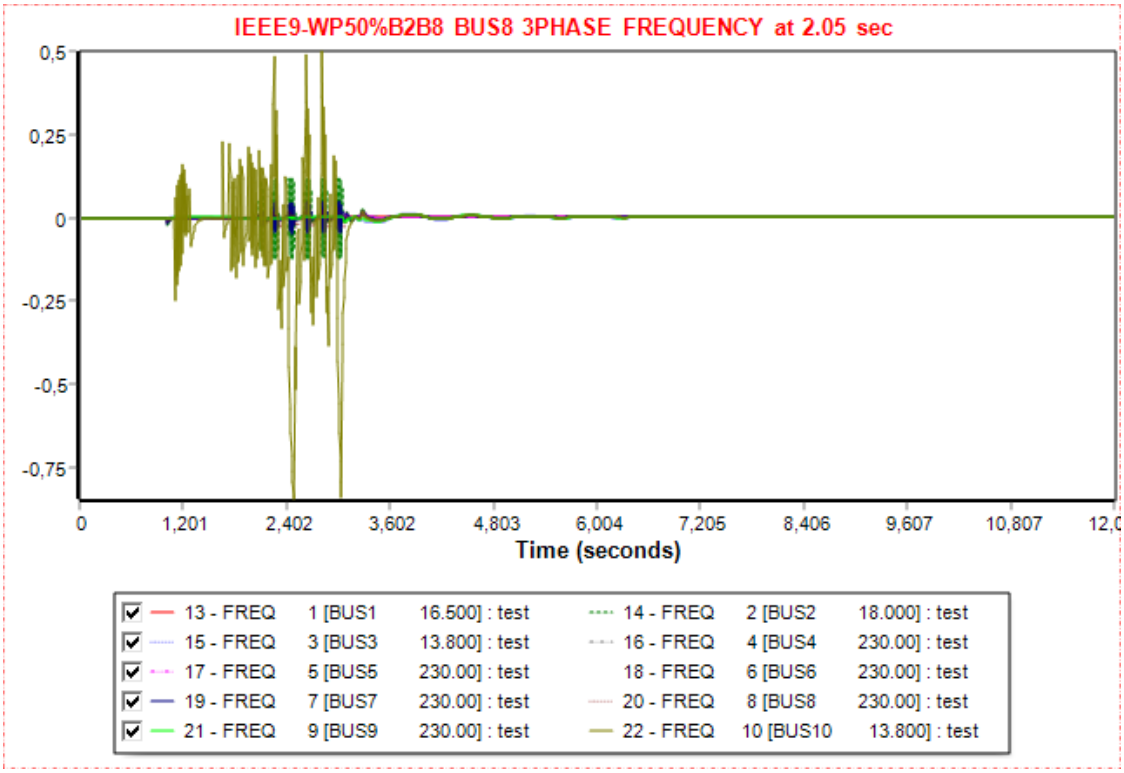

Figure 5. 129 Frequency plots of three-phase symmetrical fault at bus 8 when it is cleared at 3.05 sec at IEEE9 Wind Power Remodeled with 50% Replaced at Bus 2 and 50% Added at Bus 8

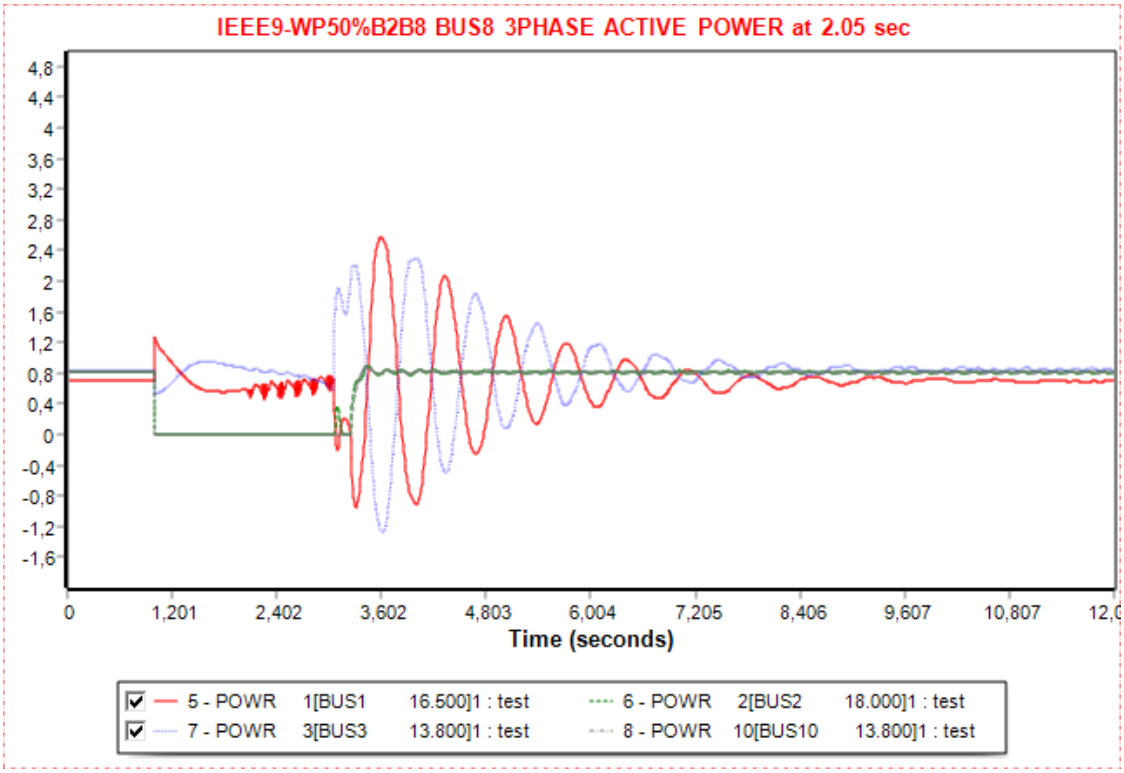

Figure 5. 130 Active Power plots of three-phase symmetrical fault at bus 8 when it is cleared at 3.05 sec at IEEE9 Wind Power Remodeled with 50% Replaced at Bus 2 and 50% Added at Bus 8

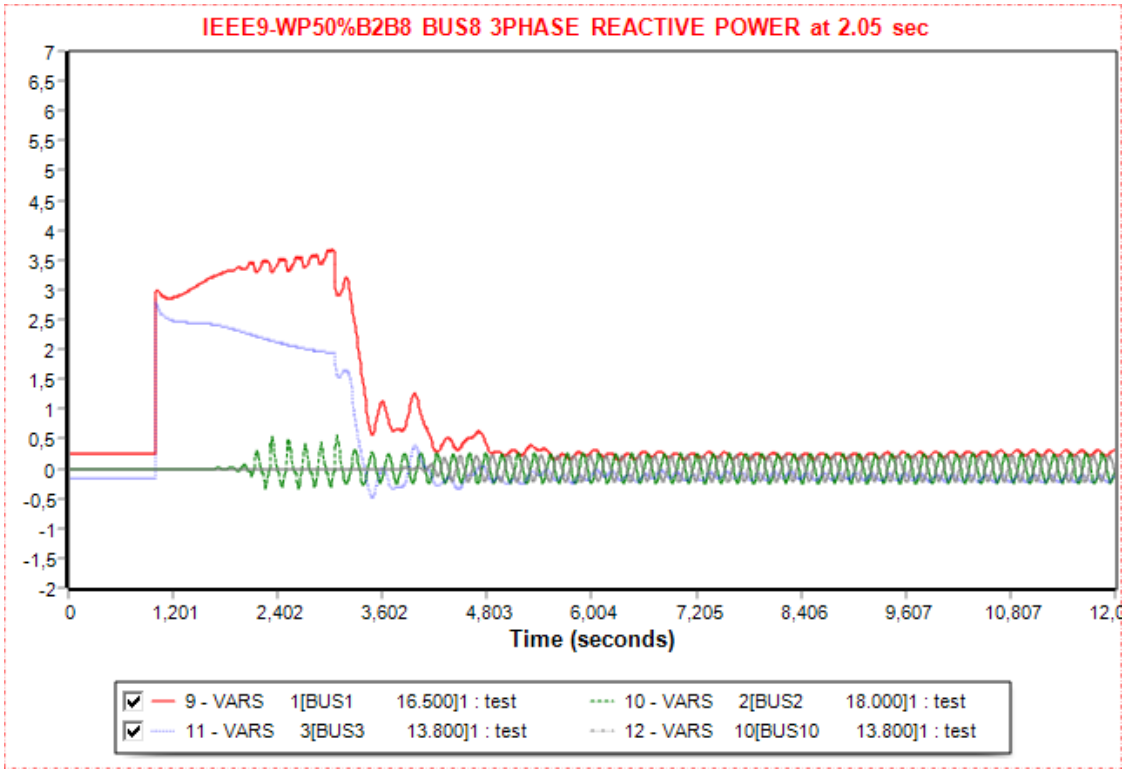

Figure 5. 131 Reactive Power plots of three-phase symmetrical fault at bus 8 when it is cleared at 3.05 sec at IEEE9 Wind Power Remodeled with 50% Replaced at Bus 3 and 50% Added at Bus 8

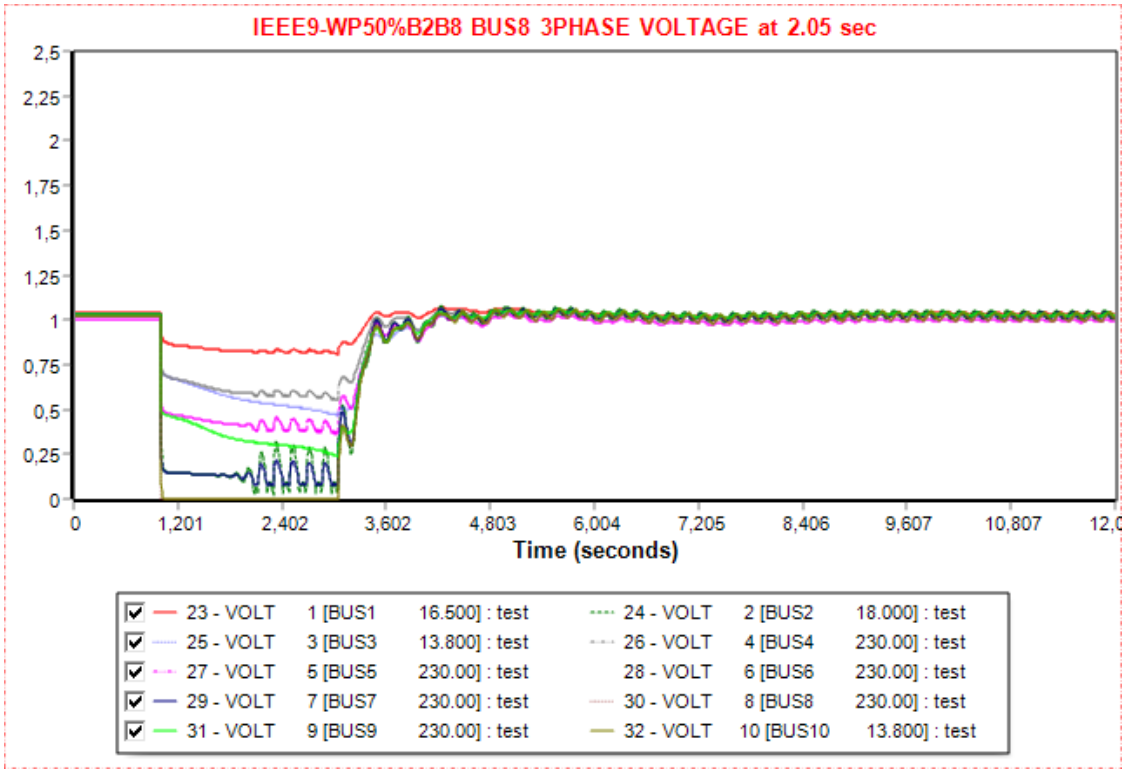

Figure 5. 132 Voltage plots of three-phase symmetrical fault at bus 8 when it is cleared at 3.05 sec at IEEE9 Wind Power Remodeled with 50% Replaced at Bus 2 and 50% Added at Bus 8

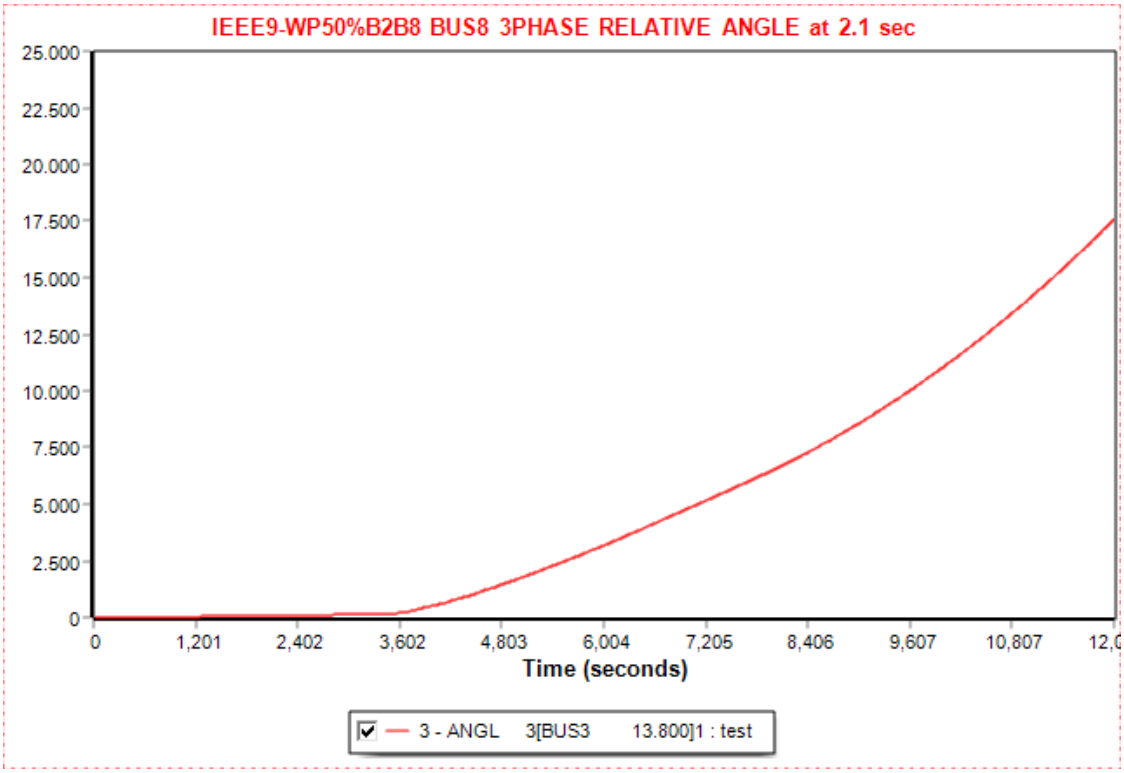

Figure 5. 133 Relative power angle plots of three-phase symmetrical fault at bus 8 when it is cleared 3.1 sec at IEEE9 Wind Power Remodeled with 50% Replaced at Bus 2 and 50% Added at Bus 8

5.4.3.2 SLG Fault at Bus 8 of IEEE9 Bus System Wind Power Remodeled with the Partial Replacement (50%) of Generator 2 and the Addition of the other 50% at bus 8

The grid can sustain its stability no matter how long the SLG fault duration at bus 8 is. Since there is no CFCT, the fault is applied for 0.5 sec in order to see the transient behavior of the system. There is an initial load flow for 1 sec, and then the disturbance occurs for 0.5 sec. or the fault clearance concurrently line 8-7 is tripped, and after 1 sec, at 2.5 sec, it is connected to the network. As seen from Table 5.28, the simulation lasts for 12 sec. Figures 5.133-5.137 present the power angle of generator 3 with respect to the power angle of the swing bus, the buses frequency, the real and active power of the generators, including the one producing wind power, and the buses voltage when the fault is cleared at 0.5 sec.

Table 5. 28 IEEE9 Wind Power Remodeled with 50% Replaced at Bus 2 and 50% Added at Bus 8 SLG Fault at Bus 8

Action	Time (sec)
Steady State	0.00
Apply Fault	1.00
Clear Fault	1.5
Trip Line	1.5
Connect Line	2.5
Power Flow	12.00

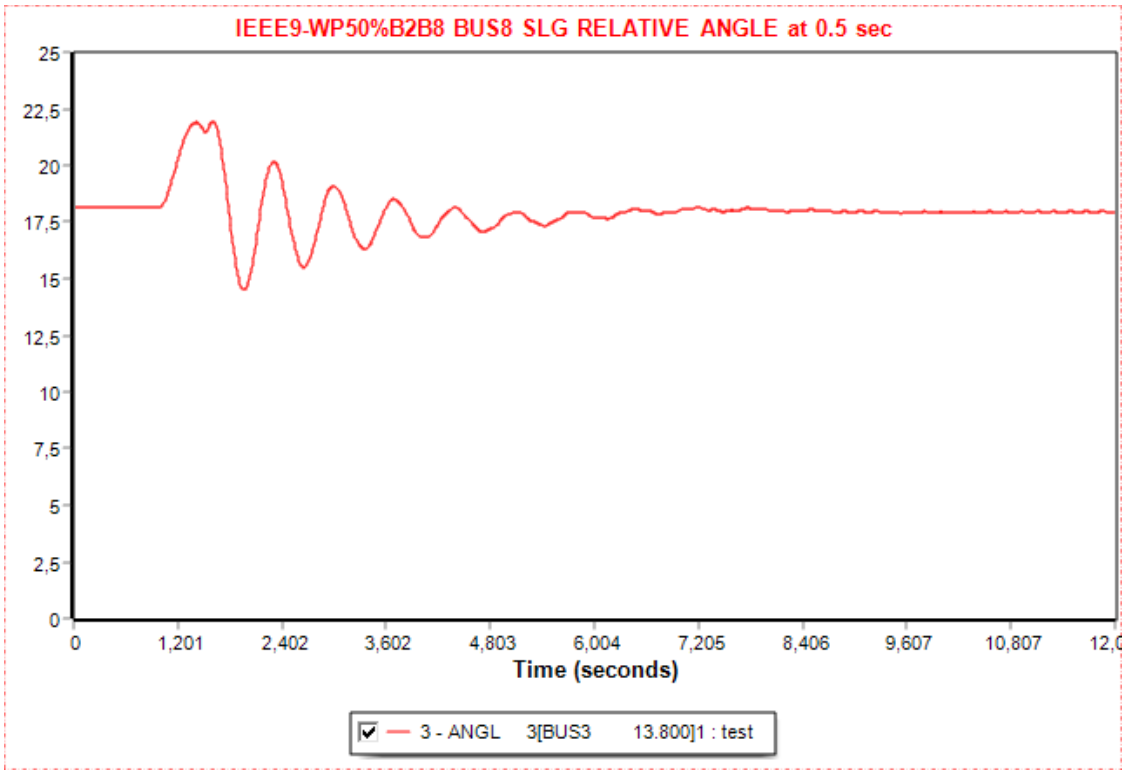

Figure 5. 134 Relative power angle plots of SLG fault at bus 8 when it is cleared at 1.5 sec at IEEE9 Wind Power Remodeled with 50% Replaced at Bus 2 and 50% Added at Bus 8

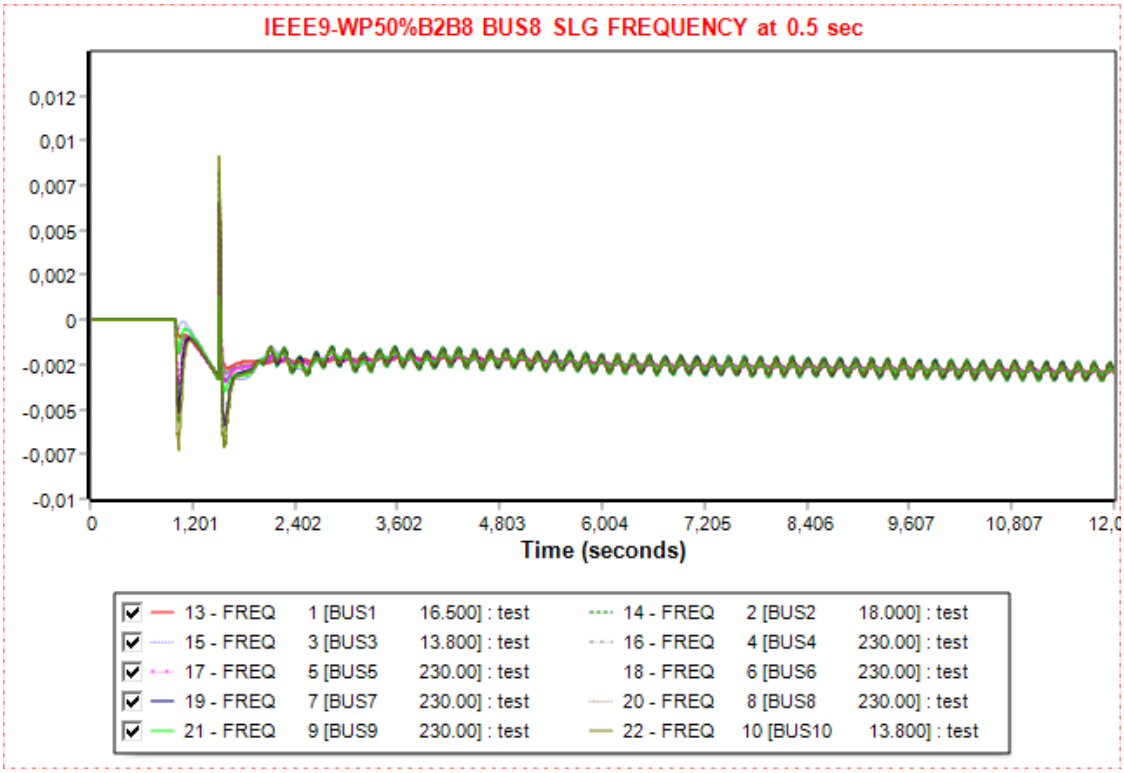

Figure 5. 135 Frequency plots of SLG fault at bus 8 when it is cleared at 1.5 sec at IEEE9 Wind Power Remodeled with 50% Replaced at Bus 2 and 50% Added at Bus 8

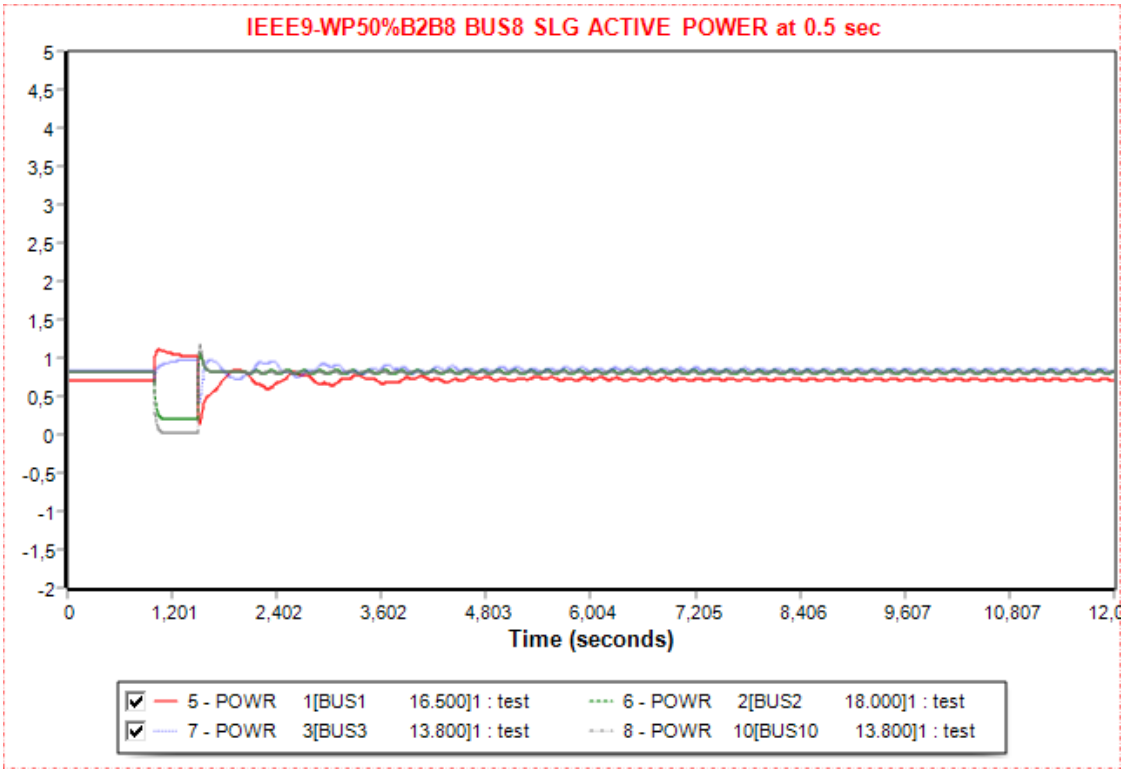

Figure 5. 136 Active Power plots of SLG fault at bus 8 when it is cleared at 1.5 sec at IEEE9 Wind Power Remodeled with 50% Replaced at Bus 2 and 50% Added at Bus 8

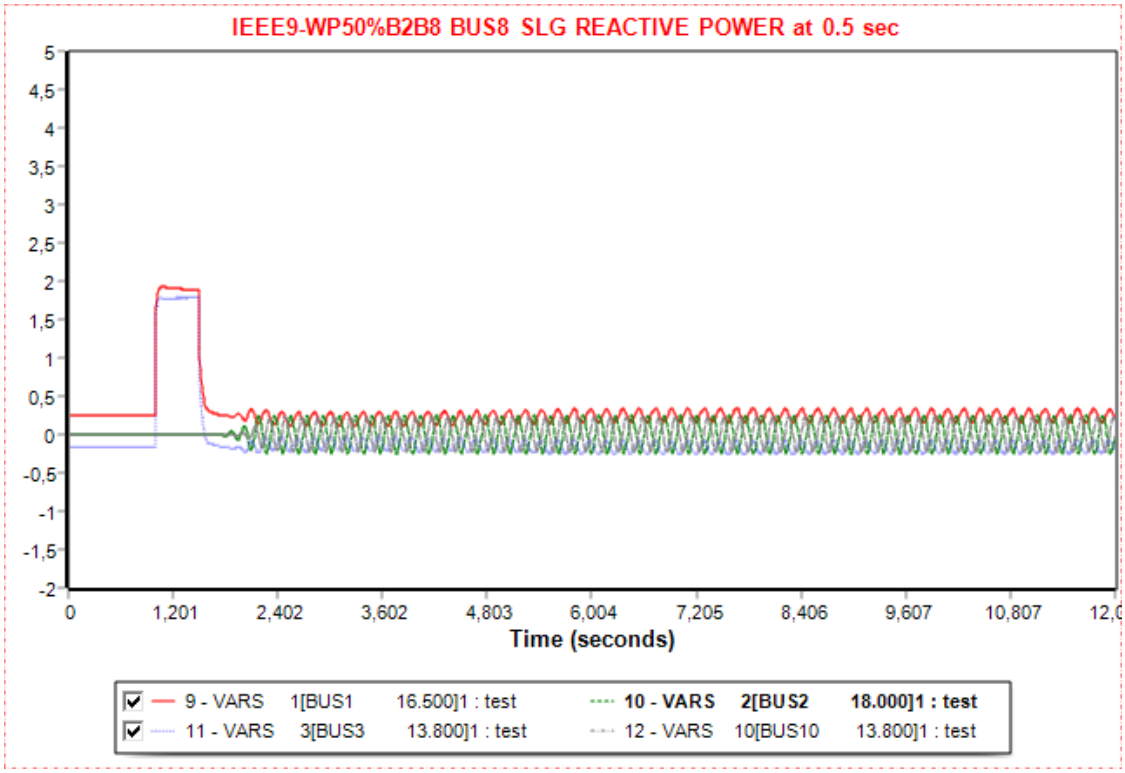

Figure 5. 137 Reactive Power plots of SLG fault at bus 8 when it is cleared at 1.5 sec at IEEE9 Wind Power Remodeled with 50% Replaced at Bus 2 and 50% Added at Bus 8

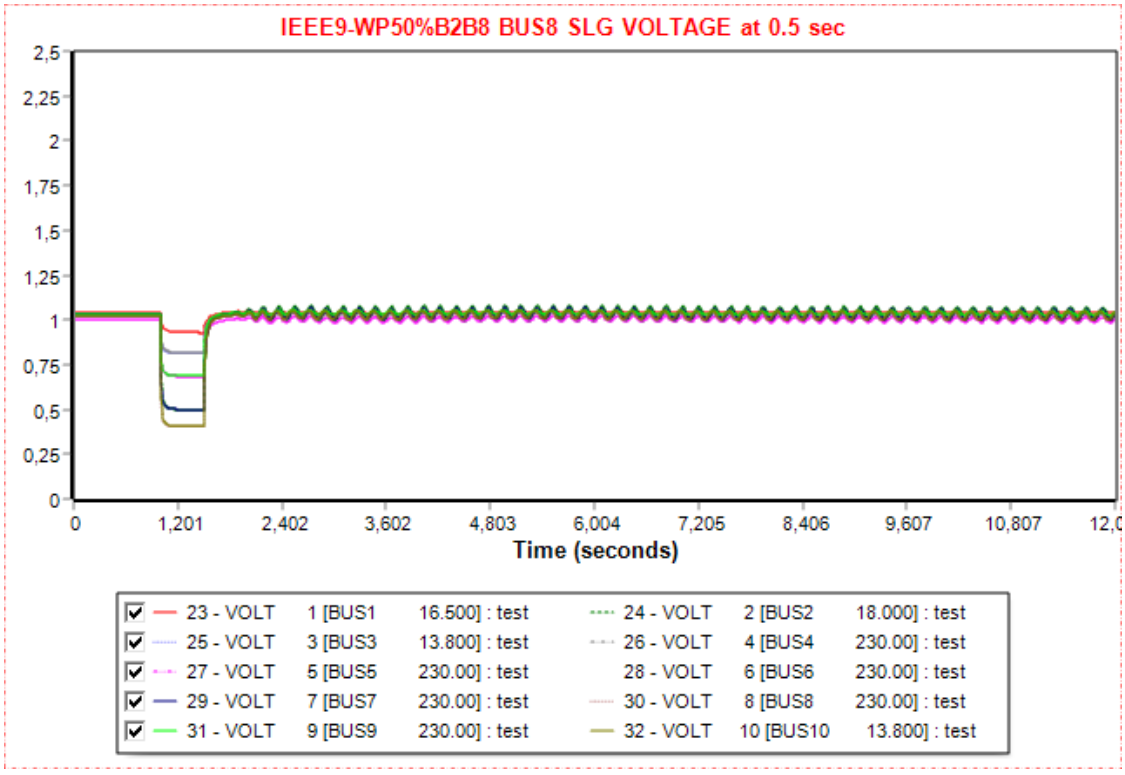

Figure 5. 138 Voltage plots of SLG fault at bus 8 when it is cleared at 1.5 sec at IEEE9 Wind Power Remodeled with 50% Replaced at Bus 3 and 50% Added at Bus 8

5.4.4 Diagram Analysis of the IEEE9 Bus System Wind Power Remodeled with the Partial Replacement (50%) of Generator 2 and the Addition of the other 50% at bus 8

The relative power angle diagrams in this scenario are different than the previous ones because the generator that is now examined is the one connected in bus 3. It can be observed that the three-phase symmetrical fault at bus 2 (Figure 5.108) and the SLG faults (Figure 5.113, 5.123, 5.134) have no significant effect as the width of the total oscillation is around 10 – 12.5 degrees. The three-phase symmetrical faults at the other two buses are more substantial as the total width is 35 degrees at bus 7 (Figure 5.118) and around 100 degrees at bus 8 (Figure 5.128).

In the frequency plots, despite the system's different structures, the frequencies are quite similar as in the other scenarios. There are three facts noticed in the three-phase symmetrical fault diagrams (Figure 5.109, 5.119, 5.129) and the SLG diagrams (Figure 5.114, 5.124, 5.135). Secondly, when a three-phase symmetrical fault occurs at buses 7 and 8, the frequencies have rapid fluctuations (Figure 5.119, 5.129). In all the diagrams, the frequencies at bus 2 and bus 10, which are linked with wind farms, have the biggest fluctuations. Finally, the frequencies tend to stabilize a little lower of 0 pu instead of higher like in the previous scenarios.

The active power plots of the three-phase symmetrical fault diagrams at bus 2 (Figure 5.110) and the SLG at all buses (Figure 5.115, 5.125, 5.136) are quite similar. The two wind turbines' active power have opposite behavior when the fault occurs. The wind farm at bus 3 slightly increases, during the disturbance, in contrast to bus 10, where the active power decreases, and in three-phase symmetrical Figures 5.125 and 5.136, it nearly reaches 0 pu. When the system becomes stable, there are small oscillations due to the wind turbine model.

In the three-phase symmetrical fault diagrams (Figure 5.111, 5.121, 5.131) and the SLG reactive diagrams (Figure 5.116, 5.126, 5.137), the reactive power post-fault behavior is similar with different oscillation widths. In the three-phase symmetrical fault at bus 2 (Figure 5.109) and all the SLG diagrams, there is a rise of the reactive power for generator 1 around 2 – 2.5 pu and generator 3 around 1 to 1.5 pu. The three-phase symmetrical

reactive power diagram at bus 7 (Figure 5.119) is around 2.5 pu for generator 1 and 3.2 pu for generator 3. The last reactive power diagram, the three-phase symmetrical fault at bus 8, has a rise of 3 pu for bus 3 and 4 pu for the swing bus. What is interesting here is that after 1 sec of the fault the generator 3 decreases its reactive power and the swing bus is rising.

The post-fault voltage behavior is similar in three-phase symmetrical faults (Figure 5.112, 5.122, 5.132) and the SLG diagrams (Figure 5.117, 5.127, 5.138). The only difference lies in the voltage drop depending on the location of the fault. When a three-phase symmetrical fault occurs at bus 2 (Figure 5.112), the wind turbine' voltage at this bus becomes 0 pu and the one at bus 10, where the second wind farm is, becomes 0.5 pu. In the SLG fault at bus 2 (Figure 5.117), the post-fault voltage is 0.25 pu and 0.5 pu for bus 10. For a three-phase symmetrical fault at bus 7 (Figure 5.122), the voltage's value during the fault is around 0 pu for bus 2 and 0.25 pu for bus 10. Likewise, for SLG (Figure 5.127), the voltage is around 0.75 pu for both wind farm buses. When a three-phase symmetrical occurs at bus 8, the wind farm's voltage connected to bus 10 is 0 pu, and the other wind farm's voltage is 0.25 pu. For SLG at bus 8 (Figure 5.138), both wind farm voltages dropp around 0.5 pu. [4][6][9-17][19][20][22][23][38][41]

5.4 Comparison of the Scenarios

In the previous sections, there were four simulations with wind energy penetration on a system and different distribution of it. In Table 5.29 the critical fault clearing time of each scenario is presented, where the columns are the buses in which the fault is happening, and the rows are the type of fault and the remodeled system with wind power. The time is represented in seconds and the NS means that the fault is not severe for the power system. The replacement of generator 3 with 100% of wind power gives low clearing time and makes the system quite prone to faults. Similar results can be seen in the partial replacement of plant 3 by 50% and addition of 50% at bus 8. The difference can be seen in the SLG CFCT, where the system is less tolerant of the fault in scenario 3 with 0.75 sec, and in scenario 1 it can only sustain it for 0.9 sec. A little greater result can be seen in case 2, the partial replacement of gen 3. In this case, the 41.5 MW of the wind turbine brings a

little more stability, but it can not cover the load. For that reason, the swing bus increases its generation. Finally, significantly greater results can be seen in the last case, where it can withstand the fault for a longer time. It is necessary to say that the replacement of generation 2 is the main reason for that result, as the generator 3 that is examined is 81.5 MW, the same as the wind turbine plants. It is calculated, also, that in scenario 4, as the fault location closes to bus 3 the system can not sustain the fault for too long and the results are similar to the previous cases when bus 2 was tested. It is not in this thesis but to justify the previous statement, the CFCT appears to be 0.25 sec when the fault occurs on bus 3 and 0.4 sec on bus 9 for scenario 4. Apart from the small oscillations, which are normal for the WTG type 4 as seen in [20], the wind turbines have similar behavior as the traditional synchronous generators. Finally, as the level of integration is growing (scenario 1,3,4 in contrast to 2) the oscillations are greater.

Table 5. 29 The CFCT of the simulations

CASE	BUS 2	BUS 7	BUS 8
WP 100% - three-phase symmetrical	0.2	0.2	0.35
WP 100% - SLG	0.9	NS	NS
WP 50% - three-phase symmetrical	0.2	0.25	0.4
WP 50% - SLG	1.75	NS	NS
WP 50%B3B8 - three-phase symmetrical	0.2	0.2	0.35
WP 50%B3B8 - SLG	NS	NS	NS
WP 50%B2B8 - three-phase symmetrical	NS	NS	2.05
WP 50%B2B8 - SLG	NS	NS	NS

CHAPTER 6

CONCLUSION

In this thesis, there was a comparison of four different wind integrated systems. In the first scenario, there was a replacement of a generator with a wind farm. It was deduced that the system could operate and recover from the disturbance if cleared within time. Similar results were presented in the second scenario, where there was a partial replacement of a generator at 50% of the maximum output by a wind farm. The other two cases were a replacement of a generator at 50% by a wind farm and the addition of the other 50% by a wind farm in another bus. After the occurrence of a three-phase symmetrical and an SLG, the transient behavior was similar and non-problematic for many cases. The turbines that were used were the type 4 as inductors. In the diagrams, aside from some near zero oscillations during the system's stabilization, the results were quite similar to the academic research introduced in the first chapter. For the scenarios, the fourth had better CFCTs than the others and the second smaller oscillations during stabilization. It can be concluded that there was no negative impact, and the integration was smooth, without problems in the transient stability.

For future research suggestions, many things can be done. Firstly, the same simulation can be made with real-time location and data. Specifically, the wind turbines' accurate positions in the farm and actual wind data can be taken into account. Another research suggestion is using the IEEE 14 Bus System, IEEE 39 Bus System, or another power system with the same turbine and the same faults. Moreover, the scenarios presented in this thesis can be used for transient stability analysis, with the disturbance being the other two types of fault, a line-line or a double-lined ground one. Finally, a complete stability analysis can be made. In parallel with transient stability, small signal, voltage stability using PV and QV curves, and frequency stability can be examined.

REFERENCES

[1] *Kabouris, John & Kanellos, Fotis. (2009). Impacts of Large Scale Wind Penetration on Energy Supply Industry. Energies. 2. 10.3390/en20401031.*

[2] *H. Zhang and L. L. Lai, "Research on wind and solar penetration in a 9-bus network," 2012 IEEE Power and Energy Society General Meeting, San Diego, CA, 2012, pp. 1-6, doi: 10.1109/PESGM.2012.6345218.*

[3] *H. Ibrahim, M. Ghandour, M. Dimitrova, A. Ilinca, J. Perron, "Integration of Wind Energy into Electricity Systems: Technical Challenges and Actual Solutions", Energy Procedia, Volume 6,2011,Pages 815-824,ISSN 1876-6102*

[4] *M. Katsivelakis, D. Bargiotas and A. Daskalopulu, "Transient Stability Analysis in Power Systems Integrated with a Doubly-Fed Induction Generator Wind Farm," 2020 11th International Conference on Information, Intelligence, Systems and Applications (IISA, Piraeus, 2020, pp. 1-7, doi: 10.1109/IISA50023.2020.9284361.*

[5] *Asija, Divya & Choudekar, Pallavi & Singla, Ruchira & Chouhan, Malvika. (2015). Performance Evaluation and Improvement in Transient Instability of IEEE 9 Bus System Using Exciter and Governor Control. Procedia Computer Science. 70. 733-739. 10.1016/j.procs.2015.10.111.*

[6] *Edrisian, Ashkan & Hajian, Mohsen & Kermani, Mostafa & Ebadian, Mahmoud. (2015). Impact of Reactive Power on Stable Production of Wind Farms. Majlesi Journal of Energy Management. 4. 1-9.*

[7] *Kamdar, Renuka & Kumar, Manoj & Agnihotri, Ganga. (2014). Transient Stability Analysis and Enhancement of IEEE- 9 Bus System. Electrical & Computer Engineering: An International Journal. 3. 41-51. 10.14810/ecij.2014.3204.*

[8] *Kaur, Gurpreet, and Navneet Singh Bhanga. "Transient stability analysis of ieee 9 bus system using power world simulator." International Journal of Advanced Research in Electric Electronics & Instrumentation Engineering 5.4 (2016).*

[9] *Jaikumar Pettikkattil Radhakrishnan (2014). Transient Stability Analysis of Grid with DFIG Wind Power Plant. Msc Thesis for California State University, Northbridge*

[10] *Christian Ekstrand, Farsad Mansori (2020). Stability Related Issues for High Wind Power Penetration. Thesis for Department of Physics and Electrical Engineering Faculty of Technology Linneuniversitetet.*

[11] *Syahputra, Ramadoni & Robandi, Imam & Ashari, Mochamad. (2014). Performance Analysis of Wind Turbine as a Distributed Generation Unit In Distribution System. International Journal of Computer Science and Information Technology. 6. 39-56. 10.5121/ijcsit.2014.6303.*

[12] *Mohammad Seyedi (2009). Evaluation of the DFIG Wind Turbine Built-in Model in PSS/E. MSc Thesis for Division of Electric Power Engineering Department of Environment and Energy of CHALMERS UNIVERSITY OF TECHNOLOGY.*

[13] *Soued, Salah, H. S. Ramadan, and Mohamed Becherif. "Effect of Doubly Fed Induction Generator on Transient Stability Analysis under Fault Conditions." Energy Procedia 162 (2019): 315-324.*

[14] *Kabashi, Gazmend & Kadriu, Kadri & Gashi, Ali & Kabashi, Skender & Komoni, Vjollca. (2011). Wind Farm Modeling for Steady State and Dynamic Analysis. World Academy of Science, Engineering and Technology. 50.*

[15] *Ameur, Arechkik, Khalid Loudiyi, and Mohammed Aggour. "Steady state and dynamic analysis of renewable energy integration into the grid using pss/e software." Energy Procedia 141 (2017): 119-125.*

[16] *Akhmatov, Vladislav. "System stability of large wind power networks: A Danish study case." International Journal of Electrical Power & Energy Systems 28.1 (2006): 48-57.*

[17] *L. Wang, M. Hsieh and C. Chang, "Transient analysis of an offshore wind farm connected to Taiwan power system using PSS/E," OCEANS 2014 - TAIPEI, Taipei, 2014, pp. 1-5, doi: 10.1109/OCEANS-TAIPEI.2014.6964539.*

[18] *Mohamad, Arfah & Hashim, Norazlan & Hamzah, Noraliza & Ismail, Nik & Latip, M.F.. (2011). Transient stability analysis on Sarawak's Grid using Power System Simulator for Engineering (PSS/E). 521-526. 10.1109/ISIEA.2011.6108766.*

[19] *Anup, Sunitha, Ashu Verma, and T. S. Bhatti. "Transient stability study in solar photovoltaic-wind plant based multimachine system." 2017 IEEE International Conference on Smart Grid and Smart Cities (ICSGSC). IEEE, 2017.*

[20] *Chen, Wuhui, et al. "Small-Signal Performance of Type 4 Wind Turbine Generator-Based Clusters in Power Systems." Energies 11.6 (2018): 1486.*

[21] *Iyambo, P. K., and Raynitchka Tzoneva. "Transient stability analysis of the IEEE 14-bus electric power system." AFRICON 2007. IEEE, 2007.*

[22] *Abdelhalim, Hussein M., et al. "Transient stability of power systems with different configurations for wind power integration." 2013 IEEE PES Innovative Smart Grid Technologies Conference (ISGT). IEEE, 2013.*

[23] *Youssef, Erhab, Rasha M. El Azab, and Amr M. Amin. "Comparative study of voltage stability analysis for renewable energy grid-connected systems using PSS/E." SoutheastCon 2015. IEEE, 2015.*

[24] *Muñoz, J. C., and C. A. Cañizares. "Comparative stability analysis of DFIG-based wind farms and conventional synchronous generators." 2011 IEEE/PES Power Systems Conference and Exposition. IEEE, 2011.*

[25] *Kundur, Prabha, et al. "Definition and classification of power system stability IEEE/CIGRE joint task force on stability terms and definitions." IEEE transactions on Power Systems 19.3 (2004): 1387-1401.*

[26] *ALShamli, Yaqoub, et al. "A review of concepts in power system stability." 2015 IEEE 8th GCC Conference & Exhibition. IEEE, 2015.*

[27] *Kundur, P. "Power System Stability And Control by Prabha Kundur. pdf." Electric Power Research Institute (1993).*

[28] *Sulistiawati, Irrine Budi, et al. "Critical clearing time prediction within various loads for transient stability assessment by means of the extreme learning machine method." International Journal of Electrical Power & Energy Systems 77 (2016): 345-352.*

[29] *PSS/E 33.4 Programm Operation Manual (2013). Siemens PTI*

[30] *www.new.siemens.com*

[31] *www.psspy.org*

[32] *www.powerworld.com*

[33] *Demetriou, Panayiotis, et al. "Dynamic IEEE test systems for transient analysis." IEEE Systems Journal 11.4 (2015): 2108-2117.*

[34] *Ahmed, Mahmoud & Abdel Gawad, Ahmed. (2016). Utilization of Wind Energy in Green Buildings.*

[35] *Pao, Lucy Y., and Kathryn E. Johnson. "A tutorial on the dynamics and control of wind turbines and wind farms." 2009 American Control Conference. IEEE, 2009.*

[36] *https://www.britannica.com/technology/wind-turbine*

[37] *Jay Senthil and Yuriy Kazachkov (2014). 2nd Generation Models for Modeling of Renewable Sources (Wind & PV) in PSS®E. Renewable Energy Modeling task Force (REMTF) Workshop, Siemens PTI.*

[38] *Pourbeik, P., et al. "Generic stability models for type 3 & 4 wind turbine generators for WECC." 2013 IEEE Power & Energy Society General Meeting. IEEE, 2013.*

[39] *Chen, Bing, et al. "Addressing protection challenges associated with Type 3 and Type 4 wind turbine generators." 2015 68th Annual Conference for Protective Relay Engineers. IEEE, 2015.*

[40] *www.esig.energy/wiki-main-page/type-4-generic-wind-turbine-generator-model-phase-ii. WECC REMTF, EPRI.*

[41] *WAQAS ALI MEMON, NEELESH KUMA, UMAR MEMON, JITENDER KUMAR, KHAMISO KHAN, ALEEM-UL-HAQUE. LOADFLOW STUDIES OF A GRID INTERFACED WINDFARM USING PSS/E (2015). Bsc Thesis for Department of Electrical Engineering at Mehran University, Jamshoro.*